Recovery of seabed habitat from the impact of prawn trawling in the far northern section of the Great Barrier Reef Marine Park

CSIRO Marine and Atmospheric Research
CSIRO Mathematical and Information Sciences
Final Report to GBRMPA

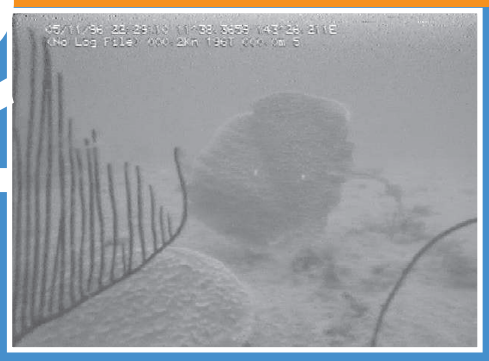

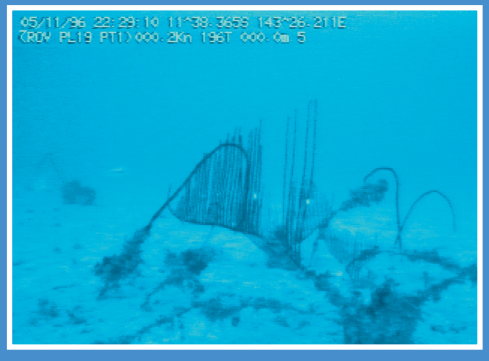

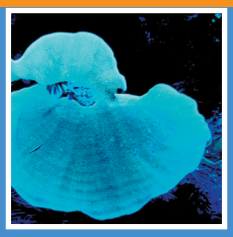

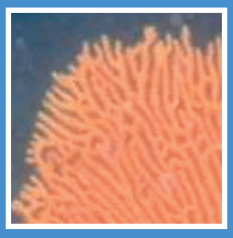

C. R. Pitcher
M. Austin
C. Y. Burridge
R. H. Bustamante
S. J. Cheers
N. Ellis
P. N. Jones
A. G. Koutsoukos
C. H. Moeseneder
G. P. Smith
W. Venables
T. J. Wassenberg

CSIRO

Australian Government
Great Barrier Reef
Marine Park Authority

National Library of Australia Cataloguing-in-Publication entry:

Title: Recovery of seabed habitat from the impact of prawn trawling in the far northern section of the Great Barrier Reef Marine Park : CSIRO final report to GBRMPA / C.R. Pitcher ... [*et al*.].

ISBN: 9781921424267 (pbk.)
9781921424281 (CD-ROM)
9781921424274 (pdf)

Notes: Includes index.
Bibliography.

Subjects: Benthos--Queensland--Great Barrier Reef Marine Park.
Shrimp fisheries--Environmental aspects--Queensland--Great Barrier Reef Marine Park.

Other Authors/Contributors:
Pitcher, C. R. (Clifford Roland)
CSIRO. Marine and Atmospheric Research.
Great Barrier Reef Marine Park Authority.

Dewey Number: 577.7709943

Citation:
Pitcher C.R., Austin M., Burridge C.Y., Bustamante R.H., Cheers S.J., Ellis N., Jones P.N., Koutsoukos A.G., Moeseneder C.H., Smith G.P., Venables W., Wassenberg T.J., (2008) Recovery of Seabed Habitat from the Impact of Prawn Trawling in the Far Northern Section of the Great Barrier Reef Marine Park. CSIRO Final Report to GBRMPA, pp. 189

Published: April 2008 by CSIRO Marine and Atmospheric Research

April 2008

Recovery of Seabed Habitat from the Impact of Prawn Trawling in the Far Northern Section of the Great Barrier Reef Marine Park

CSIRO Final Report to GBRMPA

C.R. Pitcher
M. Austin
C.Y. Burridge
R.H. Bustamante
S.J. Cheers
N. Ellis
P.N. Jones
A.G. Koutsoukos
C.H. Moeseneder
G.P. Smith
W. Venables
T.J. Wassenberg

Marine and Atmospheric Research
Mathematical and Information Sciences
Marine Laboratories
P.O. Box 120
Cleveland QLD 4163

ISBN 978-1-921424-26-7

This report gives the results and conclusions of CSIRO research to measure the recovery of seabed habitat fauna after intensive repeated trawling. The project activities included the results from fieldwork conducted in November, 1994, April, 1995 (pre-impact), to January 1996, Oct–Nov 1996, Nov–Dec 1997 and February 2001 (5+ years post-impact) to record the number, size and condition of benthos *in situ*, by using non-extractive remote video observations and laboratory measurements of benthos recorded on video.

Acknowledgements

This project was funded by the Great Barrier Reef Marine Park Authority and CSIRO Marine Research. We are indebted to many people who helped us to obtain a successful conclusion to this project. Don Battersby and Marc Lennard, the willing and helpful crew of the research vessel James Kirby. Sue Cheers and Anthea Koutsoukos did much of the video analysis. Ian McLeod helped with the spaital analyses. Louise Bell designed the report covers. Toni Cannard coordinated the contributions from multiple authors, collated and formatted the drafts of this report; Alan Butler and Nic Bax reviewed earlier drafts; Vivienne Mawson edited the final draft and Meredith Prendergast implemented her edits. Two external reviewers provided comments that improved the final version of the report.

Contents

Figures

Tables

SUMMARY

The project has assessed the recovery of seabed habitat fauna after a previous experiment involving intensive repeated trawling. The project's activities included field observations of recovery, laboratory quantification of video recordings, analyses and reporting. This project has achieved each of the three objectives specified by the Great Barrier Reef Marine Park Authority (GBRMPA); it has:

1. documented the recovery of living seabed habitat one, two and five years after the depletion experiment by assessing attributes of the sessile megafaunal community.
2. estimated recovery rates, identified taxa that recovered within the five-years and estimated the possible time frames for others.
3. identified which of the measured taxa are vulnerable with respect to trawling.

For this project, it was essential to use non-extractive sampling tools so as not to interfere with the recovery of the study area. Therefore video recordings, from a Remotely Operated Vehicle (ROV) and a towed video Sled, were made of the seabed habitat fauna of the study area. The video Sled could rapidly cover long, reasonably straight transects, while the ROV could be positioned with much greater accuracy and could examine seabed fauna in more detail.

Six 2.8 km long tracks that were each trawled 13 times in December 1995 during a repeated-trawl depletion experiment of a previous project, were each re-surveyed by the ROV and video Sled in Oct–Nov 1996, Oct–Nov 1997 and Jan–Feb 2001. At the same time, six un-trawled control tracks were also re-surveyed. The Sled was towed one or more times along the full length of each impact track and control track. The ROV was deployed on 2 or 3 sites along each of the Sled tracks to measure and monitor specific discrete patches of benthos. Two parallel laser beams on the ROV were used for scaling video images for measurement.

An acoustic underwater tracking system and differential GPS, in conjunction with the ship's gyro compass heading, allowed the position of the remote cameras to be tracked and recorded to facilitate later analysis. The video, position and sonar data from the video Sled and ROV were acquired with a computer logging system.

Images of benthos recorded on the video tapes were later captured and measured to provide a record of the megabenthos species, position coordinates, size and condition of all identifiable sessile megabenthos at each site. A semi-automated computerised video analysis system facilitated capture and measurement of megabenthos. Sled videos from tows made over the same tracks during an earlier experiment in 1994–1995 were also analysed.

This report outlines the accumulated progress and results from the 1994–2004 research to measure the recovery of seabed habitat fauna after intensive repeated trawling. Data extracted from earlier video Sled tows (Poiner *et al.* 1998 Effects of Trawling Report) were combined with data from video acquired during this current project. Over the six surveys, images of ~57,000 benthic organisms were captured. These images were quantified to provide data on the numbers, size and condition of species for statistical analyses to isolate and test for any impact and recovery signals after trawling. About 20 species were sufficiently abundant for analysis although the sample sizes for many of these were small and gave more uncertain results. Recovery rates were estimated with specification of their uncertainty, and taxa that would be vulnerable if exposed to trawling, were identified.

The first, and most emphatic result was that the variability in the natural composition and dynamics of these sessile faunal assemblages was found to be substantial throughout the study. Differences in the assemblages of shallow and deep sites were also significant. Nonetheless, despite larger changes due

to other processes, there were overall patterns of impact and recovery apparent to varying extents for most of the 20 species and for the multispecies composition of the assemblages.

Impacts on numbers ranged from none, or possibly even positive (weed-like) responses, through negligible for some resilent seawhips and gorgonians, moderate for some sponges and other gorgonians, to high for some hard corals and other sponges. Recovery rates varied similarly, from rapid for some soft corals and ascidians, moderate for a range of sponges, gorgonians and hard corals, to slow for some other sponges and gorgonians.

Most species tended to show size-selective impacts on larger individuals, and many of these showed some degree of recovery trend such that effects typically disappeared by the end of the study. Similarly, although some impacted individuals were in noticeably poor condition, at the population level any impacts on condition typically were relatively small and in virtually all cases, their condition appears to have recovered during the study — at least for the individuals remaining on the seabed.

The recovery time frames estimated by this project were independent of the extent of the initial impact due to the form of statistical model used. The number of species estimated to have recovered during the study ranged from about 20% to 75% between the ROV and Sled data, with the remaining species estimated to recover after several more years to several decades. However, there was considerable uncertainty in these estimates of recovery time, which varied from a factor of two, to as much as zero to infinity. Further, in reality, recovery may depend on the intensity of trawling and take longer where higher trawl intensity had caused greater depletions and be faster where lower trawl intensity had caused less depletion.

The total physical structure provided by these living seabed habitat fauna appeared to have been affected to some extent by the trawling, but from video Sled evidence also appeared to have largely recovered by the last survey. The species that contributed most to the physical structure also appear to be among the more resilient. Nevertheless, the multi-species composition of these seabed assemblages was changed by the trawling, though less so in the more variable shallow sites. By the last survey, the assemblage composition showed signs of recovery, particularly in shallow sites and where trawl intensity had been lower. Conversely, there were fewer signs of assemblage recovery on deep sites and where trawl intensity had been higher, as a number of individual species had not recovered.

The vulnerability of seabed fauna to trawling is a combination of the rate of their removal (or mortality) per trawl and their subsequent rate of recovery. It is also subject to wide confidence intervals due to the uncertainties in both rates. The vulnerability of animals with rapid recovery rates is relatively insensitive to their depletion rate. Conversely, the vulnerability of animals with slow recovery rates is critically sensitive to their depletion rate. The vulnerability of species was estimated and the animals ranked in approximate order of vulnerability. A number of sponges, hard corals and gorgonians were most vulnerable, with a range of mostly gorgonians and a few other sponges having intermediate vulnerability, and several soft corals, ascidians and a few gorgonians were least vulnerable.

These estimates of trawl impact rates, recovery rates, and faunal vulnerability provide objective information that can be expected to facilitate progress towards sustainable multiple use of the seabed in the region. Model-based approaches such as the Trawl Scenario MSE (management strategy evaluation; Ellis & Pantus 2001) have used information from this project to assist with assessments of sustainability and comparing the environmental benefits of a range of alternative management options. Knowledge of the distribution and abundance of the seabed fauna has recently become available (Pitcher *et al.* 2007) and was also critical for such evaluations. Management measures that prevent co-location of human activities that may have impact on these fauna, through zoning of habitats for appropriate sustainable use, can be expected to have the greatest environmental benefits.

1 INTRODUCTION

The objectives of this Recovery of Seabed Habitat project were to document the recovery of sessile seabed fauna (alcyonarians, gorgonians, sponges & corals) after a previous repeat-trawling experiment had depleted these fauna (Poiner *et al.* 1998, Burridge *et al.* 2003). The approach taken was to assess the attributes of the vulnerable species or taxa, the physical structure and the community complexity, and then to measure the status of these attributes at years one, two and four after impact. Subsequently, a review of the results would indicate whether longer-term measurements are required.

For this project, non-extractive sampling tools, such as quantitative observation, were essential so as not to interfere with the recovery of the study area. As half of the study sites were too deep for diving, video recordings, from a video Sled and a Remotely Operated Vehicle (ROV), of the seabed habitat of the study area were used. The ROV could be positioned with greater accuracy and could examine the aggregated patches of seabed fauna and measure them in more detail, whereas the video Sled could rapidly cover long, reasonably straight, transects that passed through the patches of fauna and also covered the sparsely covered seabed between patches.

1.1 Background

The research described in this report on the Recovery of Seabed Habitat follows on from a five-year study on the environmental effects of prawn trawling (Poiner *et al.* 1998), conducted by the CSIRO Division of Fisheries (now CSIRO Marine & Atmospheric Research, CMAR) and the Queensland Department of Primary Industries & Fisheries (QDPIF), in the Far Northern Section of the Great Barrier Reef (GBR), Australia, during 1991–1996.

The CSIRO-QDPIF study provided a factual basis for the GBR Marine Park Authority (GBRMPA), industry and managers to assess the impacts of prawn trawling, and for GBRMPA and other management agencies to draw on when considering marine park zoning and other management options. The study had three main components: (1) a description of the seabed communities in the study area and an estimate of the impact that prawn trawling has on them; (2) a description of the composition of prawn trawl bycatch; and (3) a study of the fate of discards, including the effect of trawling on seabird populations.

The effect of trawling on seabed communities was examined in three ways:

- by surveying a cross-shelf area closed to trawling and comparing the species composition and abundance with that in adjacent areas north and south open to trawling (Burridge *et al.* 2006).
- by conducting a Before-After-Control-Impact (BACI) experiment in the mid-shelf part of the area closed to trawling (see in Poiner *et al.* 1998)
- by conducting a repeat-trawling depletion experiment on selected tracks in the mid-shelf part of the area closed to trawling (Burridge *et al.* 2003).

The experimental context for the current project was established by the earlier study's repeat-trawl depletion experiment on six tracks ~2.8 km long × ~35 m wide in the mid-shelf section of the cross-

shelf closure in the northern GBR, in November 1995. It was estimated that this experiment removed 70–95% of the biomass of attached seabed fauna from the six tracks (Burridge *et al.* 2003).

It remained to measure the rates of recovery of the seabed after this known intensity of trawling in order to be able to quantitatively evaluate various alternative management options for trawling (eg. see Ellis and Pantus 2001). This report describes the results of a five-year field study (1996 – 2000), followed by laboratory analysis of those and earlier observations extending back to 1994, to measure the recovery of seabed habitat fauna that was subjected to intensive repeated trawling, effectively building on the previous study's results and recommendations.

1.1.1 Estimated impact of trawling

The results of the five-year CSIRO-QDPIF study (Poiner *et al.* 1998), in relation to trawl impacts on seabed habitat, are summarised briefly here. The differences in seabed communities between the areas open and closed to trawling were small: few significant differences were detected, even though the survey was able to detect medium effect-sizes of -60% and allow for cross-shelf trends in the community composition.

In 1993-94, a BACI experiment was set up in the Far Northern Cross-Shelf Closure to examine the impact of a single-prawn-trawl per unit area on the benthic invertebrate and fish communities. The experiment was conducted in 24 plots (each ~3.4 km^2), 12 of which were trawled once-over completely and the other 12 were reserved as untrawled control plots. Although the treatment removed ~38 t of benthos and the analysis was powerful enough to detect a ~3-fold change, the results of this experiment indicated that trawling of intensity 1× per unit area does not cause the substantial impact on benthic communities that had been expected (in the order of 10-fold).

The repeat-trawl depletion experiment in 1995 was carried out to provide a more precise estimate of the depletion rate per trawl, place in perspective the results of the single-trawl per unit area BACI experiment, and determine the intensity of trawling that would cause a substantial impact on the non-mobile organisms of the seabed community.

In this experiment, a 12-fathom trawl net (a swept path of about 15 m) was hauled 13 times along each of six tracks, within six of the 12 plots that were trawled once-over by the BACI. Each track was ~2.8 km long and known from previous surveys to contain several relatively dense patches of sessile megabenthos. Using differential GPS and careful navigation, a high degree of overlap was achieved between successive trawls. For all tracks, there was a central area between 10 and 15 m wide that was trawled at least 10 times, and the full width of the coverage by the 13 additional trawls was contained within a swathe about 35 m (less than 40 m) wide.

Analysis of the sessile benthos catch data by method of Leslie-Davis regression indicated that each trawl depleted 5–20% of the total available biomass of sessile benthos, a rate of depletion that may be undetectable in areas that are trawled infrequently or sparsely. However, if such vulnerable benthos occur in an area where trawling is more intensive, the cumulative effect of frequent trawls is likely to be substantial both in terms of organisms directly affected by trawling and indirectly due to removal of habitat for fish and other organisms. In the repeat-trawling experiment, 13 trawls appeared to remove 70-95% of the initial biomass, but the possibility of damage to biota left on the seabed could not be examined. Subsequently, *in situ* observations reported in the first phase of the current project (Year 1

Recovery Final Report, Pitcher *et al.* 2000) found that some fauna were more resilient, and some less resilient, than was indicated by the Leslie-Davis regression analysis of fauna brought up to the vessel.

The results for a single-trawl impact and for an intensive repeated-trawl impact were both highly relevant to understanding the overall impact of trawling. It has recently become clear that trawl grounds are not subjected to a uniform intensity of trawling. Logbook data that could be resolved at 6 minute grid resolution showed that trawling effort in the Far Northern Section of the GBRMP was most intense near the coast, with some small areas of highly concentrated effort, and progressively less intense offshore. Thus, large areas of the marine park open to trawling may never be trawled or perhaps only sparsely once every few years, whereas fewer small areas may be trawled many times in a year. GPS position records from working trawlers has shown that trawling is also further aggregated within 6 minute grid at scales of tens to hundreds of metres. The introduction of a satellite-based vessel monitoring system (VMS) to the Queensland East Coast Prawn Fishery in 2001 has subsequently made available much more reliable information on the distribution and intensity of trawling; this information will be invaluable to managing of the environmental impacts of prawn trawling.

1.2 Needs

While it was important to determine the impact of trawling on the non-mobile seabed communities, it was equally important to know their recovery after trawling. Different fauna will have different recovery rates and will sustain different population levels in 'balance' with the amount removed by trawling. This balance depends on the vulnerability of the fauna and the intensity of trawling — the more vulnerable the fauna and the higher the trawling intensity, the greater the likelihood of localised extinction. What was needed was an understanding of the likely recovery rates for the range of vulnerabilities of seabed fauna, to make it possible to estimate the levels of effort that different fauna can sustain as well as estimate the fishery-wide impacts of trawling over time. The environmental performance of different scenarios for managing trawling can then be evaluated, with the aim of achieving environmental sustainability. These were the objectives of a related "Trawl Scenario Modelling Project" (Ellis and Pantus, 2001) that modelled both impact dynamics and recovery dynamics, as well as trawl effort dynamics — the outcomes of this recovery project have provided and will continue to provide crucial input to such models.

The trawl scenario management strategy modelling project (Ellis and Pantus, 2001) was conducted under the guidance of a stakeholder steering committee (with representation from GBRMPA, QDPIF, Queensland Seafood Industry Association (QSIA), Australian Marine Conservation Society (AMCS), Australian Fisheries Management Authority (AFMA), Environment Australia (EA) and CSIRO) and funded by CSIRO and GBRMPA. The Trawl Scenario Model has since adopted the results of recovery reported here and benefited GBRMPA and GBR stakeholders, the Queensland trawl fishery, their managers and the community. Benefits will be in the form of a factual biological and ecological basis for management decisions, for the development of operational environmental sustainability indicators for use under State and Commonwealth fishery and environmental legislation. Managers will be able to respond objectively and effectively to community concerns and provide objective balance to competing pressures. The community will have accurate and independent information on the environmental sustainability of trawling.

1.3 Research objectives

There were three main objectives for this Recovery of Seabed Habitat project:

(1) Document the recovery of living seabed habitat one, two and four years after the repeat-trawling experiment by assessing the following attributes of the sessile megafaunal community:

- density of each sessile megafauna species
- size distributions of each sessile megafauna species
- condition (proportion missing or dead) of sessile megafauna individuals, by species
- physical structure (as an index of habitat complexity for other species)
- assemblage complexity (composition and relative abundance of species).

Recovery could be considered complete when the sessile megafauna in the intensively trawled tracks has returned to a state whereby the relative composition of taxa, abundance, size and condition of organisms is indistinguishable from the pre-impact state and trends are indistinguishable from those on control tracks. In consultations with GBRMPA managers, it was deemed that "recovery" will have occurred when the attributes of populations and assemblages of impact tracks are within detectable limits of the pre-impact state and/or the current state of control tracks. In analyses, both the pre-impact state and the state and trend of controls were used together to estimate the reference state against which changes in trawled tracks were assessed.

It was conceivable that monitoring surveys may need to continue at progressively longer intervals if "recovery", as defined, was to be observed. Nevertheless, information on the "rate" of recovery obtained within the current scope of the project will be of considerable value (see Section 1.2 Needs). In practice, it is possible that the precision with which "recovery rates" can be estimated will determine when sufficient monitoring surveys have been conducted. In either case, the results will be reviewed at the end of the current Project to assess whether recovery has occurred or whether recovery rates have been estimated with sufficient precision, and to decide whether longer term measurements are required.

(2) Estimate recovery rates, identify taxa that recover within the four-year period and estimate the possible time frames for others. Recovery time frames will be predicted with uncertainty ranges based on estimated recovery rates. For example, it may be possible to state recovery timeframes such as 5–10 years for species showing some recovery in 4 years; 10–50 years for those showing little recovery in 4 years.

(3) Identify which of the measured taxa are vulnerable with respect to trawling. Taxa that are potentially vulnerable, as individuals, are those that are:

- easily removed
- not removed, but suffer significant observable damage
- slow to recover, or do not recover.

These taxa will be vulnerable, as populations, to trawl impact if:

- they are slow-growing
- the recruitment rates are low
- the animals are slow to reach maturity.

1.4 Project activities

A summary of project-related activities leading up to this final report is given below. For plots referred to, see Figure 2-1 on page 2-10:

- **March 1994 and April 1995:** Previous monitoring of plots during the BACI experiment (see in Poiner *et al.* 1998) involved towing a single transect of the video Sled over known patches of megabenthos identified from earlier exploratory video surveys.

- **November–December 1995:** Repeat trawls (13) were made along the same track in each of 6 plots (see in Poiner *et al.* 1998). Preliminary video Sled images were collected before and during the trawling with a handycam in a waterproof housing.

- **January 1996:** The video Sled was towed along the 6 repeat trawl tracks and 6 control tracks and the ROV was deployed on several benthos patches on trawled tracks.

- **October–November 1996:** The first field trip of the current project surveyed 34 ROV sites and 12 video Sled tracks (with 2 replicate runs each) one year after the repeat trawl experiment. The preliminary report on this Year-1 phase, which was submitted in November 1997, assessed the *in situ* impact and feasibility of measuring recovery in phase 2 of the project. A revised final version of that Year-1 Recovery Report was submitted in June 2000 (Pitcher *et al* 2000).

- **November-Decmber 1997:** The Year-2 field-trip re-surveyed the same set of ROV sites and video Sled tracks (with 3 replicate runs on each trawled track) .

- **September 1999:** The second phase of the project formally commenced, enabling a start on measurement of epibenthos recorded on video tapes, a task that took over two years to complete.

- **November-Decmber 1999:** The Year-4 field survey was conducted, but due to equipment failure had to be repeated in January 2001 (see next sub-section).

- **2002–2004:** The final phase was the analysis of the data to identify the species and their number and heights, to estimate recovery from the impact of different intensities to trawling, identify the vulnerable taxa and to prepare the written report to GBRMPA.

1.4.1 Issues affecting the project's activities

During the project, various issues arose that affected the planned activities. They included software and hardware advances and new methods of incorporating technology to improve and ensure data integrity, and issues arising in the field.

1. The phase 2 of the Project was not formally approved until September 1999; analysis of videos and further fieldwork could only begin from this date rather than earlier, as had been planned.

2. The field work for the Year-4 recovery monitoring survey was conducted during November-December 1999. On this survey, video was recorded from 30 video Sled runs on the 6 impacted and 6 control tracks. However, new power supplies that had been installed on the ROV overheated and subsequently leaked. Consequently, this survey was not completed until January-

February 2001 after the manufacturer had rebuilt the ROV. However, continued ROV thruster brush problems meant that about a third of ROV patches could not be surveyed in Year-4.

3. The video Sled recordings made during the previous effects of trawling project (Poiner *et al.* 1998) had not been intended for quantitative measurement. In order to make use of their valuable information in this recovery project, significant development of post-hoc calibration techniques was required to measure the size of epibenthos from the earlier Sled tows.

4. During 2001-2002, analysis of the video tapes continued. Initial hardware problems with early-model computer video capture cards and analogue video tape recorders made capture of video images and measurement data unreliable and caused delays. This was resolved by the purchase and use of professional digital video tape recorders that improved the speed of analysis and the stability of captured images. To ensure reliability and consistency, all previously measured analogue tapes were copied to the digital format and re-measured, using the new digital system.

1.5 Sampling overview

The six tracks that were each trawled 13 times during the depletion experiment in December 1995 were re-surveyed by the ROV and video Sled (Oct-Nov 1996, Oct-Nov 1997 and Jan-Feb 2001). At the same time, six un-trawled tracks were also re-surveyed in six of the BACI control plots. Video, position and sonar data from the video Sled and ROV were acquired with the same computer logging system. An acoustic underwater tracking system and differential GPS, in conjunction with the ship's gyro compass heading, allowed the position of the remote camera to be tracked, navigated and recorded to facilitate later analysis. Two parallel laser beams on the ROV were used for scaling and ranging.

The Sled was towed along the full length of each impact track and control track. In January 1996 and previously, each track had been surveyed once by the Sled; in November 1996, the Sled was towed twice along each impact and control track; subsequently, the Sled was towed three times along each impact and twice on control tracks. The ROV was deployed on 3 or 2 sites along each of the Sled tracks to measure and monitor specific patches of benthos that had been identified during the earlier BACI experiment.

Benthos recorded on the video tapes were later measured to provide a record of the megabenthos species, position coordinates, and size and condition of all identifiable sessile megabenthos at each site. A semi-automated computerised video analysis system, involving custom software, facilitated measurement of megabenthos.

1.6 Scope of this Report

Previous research (Effects of Trawling Report – Chapter 5 Depletion Experiment in Poiner *et al.* 1998; and the Year 1 Recovery Final Report, Pitcher *et al.* 2000) showed that, for many of the sessile taxa, if the sample size was adequate, a significant effect of trawling was apparent in at least one or more of the measured attributes in analyses with different intensities of trawling (Table 1-1). The Year 1 Recovery Report (Pitcher *et al.* 2000) compared the data on fauna remaining on the seabed in the repeat-trawl tracks with the data on fauna that were brought to the surface in the 'standard' 12 fathom

"Florida Flyer" prawn net used in the repeat-trawl experiment (Ch.5 in Poiner *et al.* 1998). For those benthos taxa analysed, the average estimated rate of decrease in density with trawl intensity corresponded to ~12% per trawl (range 0%-39%), so that in areas trawled 13 times, their density was only ~20% of that in un-trawled areas (range 100%-1%). This conclusion is close to the overall average estimate of removal (~11% per trawl, range 4%-20%) obtained from analysing of the catch of sessile organisms during the repeat-trawl experiment. However, there were some important differences for some types of fauna. For example, in the repeat-trawl catch, the sponges tended to have lower rates of depletion, whereas the gorgonians tended to have higher rates. The *in situ* observations, however, tended to indicate the opposite, with relatively more gorgonians and seawhips remaining (even though their condition may have deteriorated). A possible explanation for this apparent contradiction is likely to be that catchability changed with subsequent trawls.

The results from the first year of the project (Table 1-1) indicated the ways in which trawl impact was manifested in different organisms with different structures and morphologies. Red sea whips (*Junceella juncea*) appeared to be relatively resilient to removal, as did some gorgonians, although many of those remaining had been damaged and were in poor condition. Sponges, soft corals and some gorgonians were relatively easily removed and hard corals were easily broken. Some species showed size dependent effects, with larger individuals being affected more (eg. fan sponge, *Ianthella flabelliformis*. Most gorgonians were intermediate in resilience. The interaction between these differences and trawl impact caused a marked change in the community composition of the seabed habitat.

Given that the previous reports have examined in detail the direct effect of the repeat-trawl experiment, this report has focused on attempting to identify the post-impact changes with time in experimental areas by comparing them with changes in control areas, and to distinguish the changes from the high natural variability that appears to be characteristic of these sessile seabed assemblages.

Table 1-1: Summary of Year 1 results for measured attributes against trawl intensity for *in situ* sessile benthos. All tracks from the October 1996 survey were used in the analysis of video Sled measurements of density, height and width. All patches from the October 1996 survey were used in the analysis of ROV measurements of nearest-neighbour distance, height, width, area and condition. Data from two impact tracks (19 and 21) before and after the repeat-trawl experiment were also used in the analysis of ROV measurements of condition (percent alive). 🡻 = detrimental effect where $p < 0.25$, 🡻NS = ($0.10 < p \leq 0.25$), + = ($0.05 < p \leq 0.10$), * = ($0.01 < p \leq 0.05$), ** = ($0.001 < p \leq 0.01$), *** = ($p < 0.001$). Grey with ? = test probably compromised by low numbers at higher trawl intensities. Source: *EoT Recovery Year 1 Final Report* (Pitcher *et al.* 2000).

Species	Type	Sled Count	ROV Count	Sled Density	ROV NND	Sled Height	Sled Width	ROV Height	ROV Width	ROV Area	ROV % complete	ROV % alive	Before vs After
Alertigorgia orientalis	Gorgonian	210	26	NS	NS	🡻 *	🡻 +	🡻 NS	NS	🡻 NS	NS	NS	NS
Bebryce sp.	Planar gorgonian	–	27	–	NS	–	–	NS	NS	NS	NS	NS	–
Ctenocella pectinata	Planar gorgonian	324	828	🡻 **	🡻 **	🡻 NS	🡻 *	NS	🡻 **	🡻 ***	🡻 ***	🡻 ***	🡻 ***
Cymbastella sp.	Prostrate sponge	70	27	🡻 ***	NS ?	NS ?	🡻 NS ?	NS ?	NS ?	NS ?	NS ?	NS ?	–
Dichotella divergens	Gorgonian	–	492	–	🡻 ***	–	–	NS	🡻 +	🡻 +	NS	🡻 **	🡻 **
Ellisella sp.	Planar gorgonian	–	434	–	NS	–	–	🡻 **	🡻 **	🡻 **	NS	🡻 **	🡻 ***
Ianthella basta	Fan sponge	–	46	–	🡻 *** ?	–	–	NS ?	NS ?	NS ?	NS ?	NS ?	–
Ianthella flabelliformis	Fan sponge	199	355	🡻 ***	🡻 **	NS	NS	🡻 ***	🡻 ***	🡻 ***	NS	NS	NS
Junceella fragilis	White sea whip	66	685	🡻 **	🡻 ***	–	–	–	–	–	–	🡻 **	–
Junceella juncea	Red sea whip	2059	2448	🡻 NS	NS	–	–	–	–	–	–	🡻 ***	🡻 ***
Nephtheidae sp.7	Soft coral	–	65	–	🡻 **	–	–	NS	NS	NS	NS	NS	–
Nephtheidae sp.s	Soft coral	475	–	🡻 *	–	NS	NS	–	–	–	–	–	–
Sarcophyton sp	Soft coral	–	57	–	🡻 NS ?	–	–	NS ?	NS ?	NS ?	NS ?	NS ?	–
Subergorgia suberosa	Fan gorgonian	–	113	–	🡻 ***	–	–	🡻 *	🡻 *	🡻 *	NS	NS	–
Turbinaria frondens	Hard coral	38	114	–	🡻 * ?	–	–	NS ?	NS ?	NS ?	🡻 ***	🡻 ***	–
Turbinaria sp.	Hard coral	–	49	–	🡻 NS+?	–	–	NS ?	NS ?	NS ?	🡻 NS ?	🡻 * ?	–
Xestospongia sp	Barrel sponge	56	47	🡻 *	NS ?	NS ?	🡻 NS ?	NS	NS	NS ?	NS ?	NS ?	NS ?

2 METHODS

2.1 Overview

For this project, development and deployment of non-extractive sampling tools, such as quantitative observation, was essential so that recovery of the seabed fauna in the study area was not compromised. Further, because the study sites were too deep for diving, data were extracted from remote video recordings of the sessile seabed fauna of the study area. These were made from a video Sled and a remotely operated vehicle (ROV).

The advantage of the video Sled is that it can cover long, straight transects rapidly; the disadvantage is that it cannot stop for detailed observation and cannot be placed in precisely pre-determined positions (only to within about ±20 m of them). The ROV can be positioned with much greater accuracy, but takes longer to deploy, and so was used to examine several discrete patches of epibenthic fauna on each transect in more detail. The data obtained by Sled and ROV are therefore complementary.

2.1.1 Tracks surveyed

The locations of the tracks surveyed are shown in Figure 2-1 on page 2-10. Six tracks (one on each of shallow ~20 m plots numbered 4, 18, 21 and deep ~35 m plots numbered 12, 15, 19) were each trawled 13 times during the repeat-trawl experiment in December 1995, and once during the earlier BACI experiment. Another six tracks from within the randomly selected control plots of the BACI experiment (shallow plots numbered 3, 17, 22 and deep plots numbered 1, 11, 20) were un-trawled controls. For each trawled track, the control track chosen had a megabenthos assemblage as similar as possible to that of the benthos composition and density of the trawled track before it had been repeatedly trawled. This information came from video Sled and ROV surveys of the plots made for the BACI experiment in 1993–1995. With four surveys completed after the repeat-trawl experiment, we were able to compare recovery trends and variability on trawled tracks with trends and variabilty on untrawled control tracks.

2.1.2 Sampling schedule

From a biological perspective, we had recommended that surveys be conducted 1, 2 and 4 years after the repeat-trawling — in Oct-Nov 1996, Oct-Nov 1997, and Oct-Nov 1999. However, logistics and other issues arising during the project resulted in surveys being conducted at intervals of 10, 23 and 61 months. We recognised that monitoring surveys may be required at progressively longer intervals until "recovery" has occurred, or until recovery rates are estimated with sufficient precision to estimate the ultimate recovery times with adequate confidence.

Recovery rates were expected to differ among species: some might recover in less than a year, whereas others would undoubtedly take many years, as was estimated for large sponges on the North West Shelf of Australia (Sainsbury *et al.* 1996). There would also be organisms that would take an intermediate length of time to recover. The proposed timetable for monitoring surveys was intended to enable us to identify and document fauna with fast and intermediate recovery rates and estimate their recovery time. Sampling needed to be sufficiently frequent in the early years for this to be possible.

For organisms that take longer to recover, regression-type methods are an appropriate way to detect trends and make forecasts. Initially, three time points are the minimum for estimating recovery rates and time frames and would become an important component of any future longer time series, with the later sampling taking place at progressively longer intervals. This strategy is the most cost-effective for obtaining the required information on recovery in the shortest time.

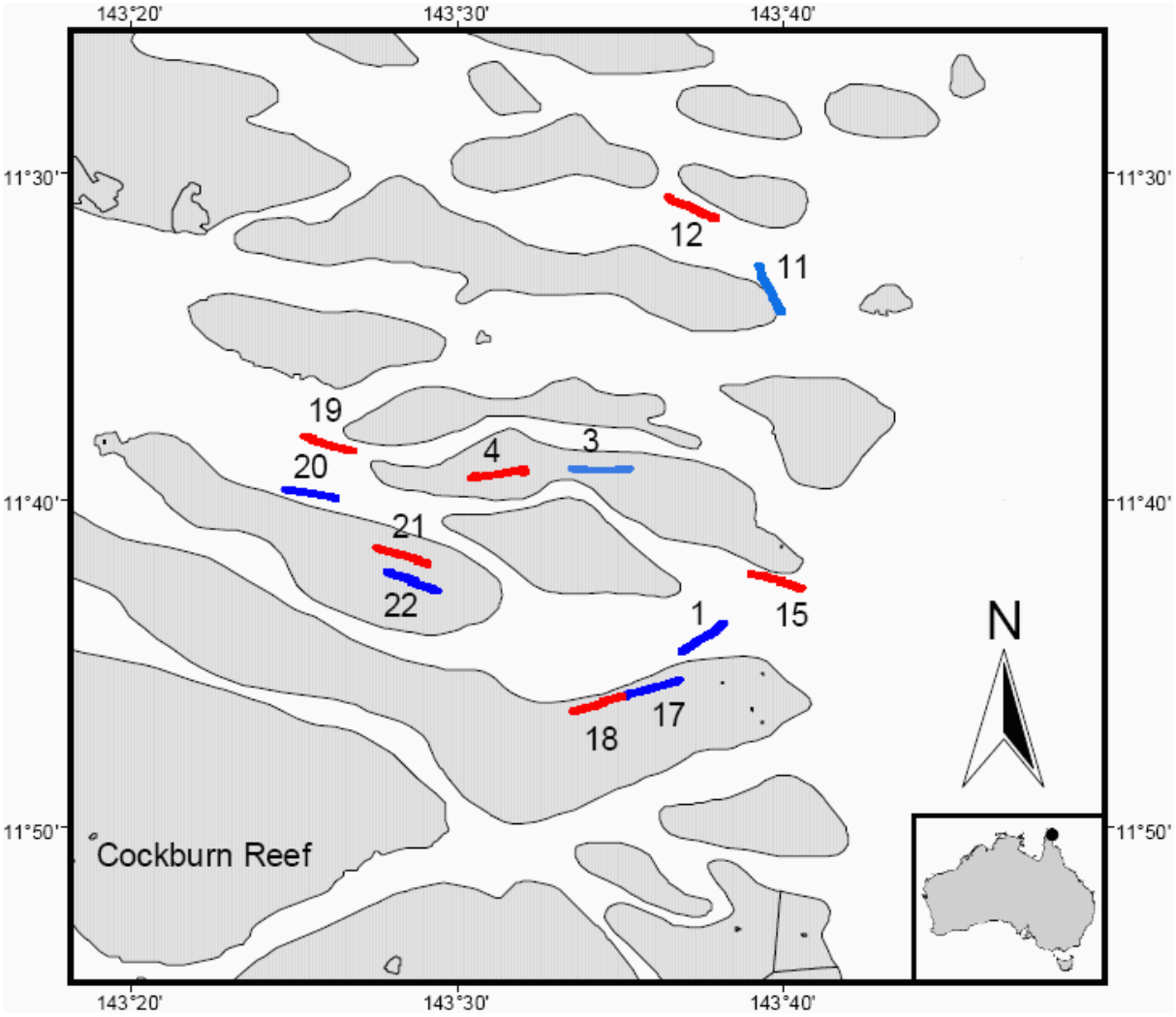

Figure 2-1: Map of the shallow (~20 m) shoals (shaded) and deeper (30-50 m) channels indicating the study area and trawl tracks (numbered) where the video Sled was run in the far northern section of the Great Barrier Reef (red line = treatment, blue line = control).

2.2 Sampling methods and data handling

2.2.1 Video data collection for recovery monitoring

Video, position and sonar data from the video Sled and ROV were acquired with the same logging system. An acoustic tracking system (ORE LXT, incorporating a transceiver hydrophone mounted under the vessel and a multibeacon model 4330A mounted on the video Sled or ROV) with an accuracy of ± 1 m was used to locate the position of the video Sled or ROV (Hydrovision Offshore

Hyball) relative to the vessel's position. A DGPS (Differential Global Positioning System) was used to locate the position of the vessel. The GPS differential corrections were transmitted to the vessel's DGPS receiver from a reference base station that was set up at the beginning of the survey on Sir Charles Hardy Island. The differential base station initially comprised a Navstar XR5M DGPS system, transmitting SC104 DGPS correction data via VHF radios (Midland) and packet modems (Kantronics KPC3). A mirror-image set-up on the vessel received and processed the differential corrections, giving average vessel positioning precision of ±1–1.5 m. The Navstar DGPS was later replaced by a Trimble DMS 12, which provided average vessel positioning precision of <1 m. The LXT and DGPS, in conjunction with the ship's gyro compass heading, allowed the position of the tracked remote camera to be calculated in real time, with average accuracy and precision better than 2 m (Pitcher *et al.* 2000), and displayed on a navigation plotter and overlaid on the video recording. Waypoint positions of benthos patches were displayed in the navigation plotter window.

Both the Sled and ROV video systems used a colour camera mounted in a waterproof housing. The video Sled camera was a Panasonic with a 2.1 mm auto-iris lens and the ROV camera was a JVC with a 3.5 mm lens. The video image was transmitted to the vessel along an umbilical cable through a data encoder (C-Systems "Screen Writer"), which continuously overlaid the UTC time/date from the GPS and positional data on the video images, into two computer-controlled video recorders (Panasonic AG5700 SVHS VCR's initially and later Panasonic AJ-D230H DVC Pro digital video recorders) and then to high-resolution video monitors.

The acquired data were logged into an MS Access database table by a customised tracking-navigating-logging software application running on a Windows NT4 Pentium PC. The data recorded were from GPS (UTC date, time, latitude, longitude, speed, track), Sounder (depth), Gyro (heading), LXT (acoustic target bearing, slant-range, depression angle), VCRs (tape frame positions), Operator (Site number, seabed habitat code, 0–9).

To facilitate the measurement of the sessile seabed fauna, two diode lasers (Laserex 5 mW) were mounted either side of the ROV video camera. The angles of the lasers were set to account for refraction of the light beams through the perspex housing to give two parallel beams that projected onto objects as two points 100 mm apart, for scaling and ranging. The lasers were checked for accuracy in water and were confirmed to be 100 mm apart at distances ranging from 0 to 4 m. Most benthos images were captured at ranges of 0.3–0.6 m.

Occasionally, if the lasers overheated, or when the object to be measured was very small, other methods were used to scale the size of the animals. For example, a wire rod was attached to the ROV, extending forward with the tip bent at right angles; the length of the tip was set at 100 mm so that the ROV could be driven up to an object and the wire rod tip be placed against the object as a scale in lieu of the lasers. Where the object to be measured was very small, the ROV was driven up to the animal and the ROV's manipulator was placed beside the animal and the dimensions of a stainless steel bolt in the claw was used as the scale.

2.2.2 Sampling strategy

The Sled was towed once or twice along the full length of each control track and up to three times along each impact track. Although the Sled's movements could not be controlled precisely in advance, the Sled's position was recorded, and when image frames (~1.3 m wide) were captured from the video-tape for measurement, the Sled's position at that instant was linked to the benthos data.

Every second, the field observer watching the video monitor entered the seabed habitat type with a single digit numeric code. The code was recorded into the position-logging database. As the substratum changed, the observer entered one of the code numbers (1 = sand; 2 = rubble; 3 = algae; 4 = *Pinctada* shell beds; 5 = whips and gorgonians; 6 = gorgonians and sponges; 7 = sponge and corals; 8 = rock, 9 = reef — Figure 2-2).

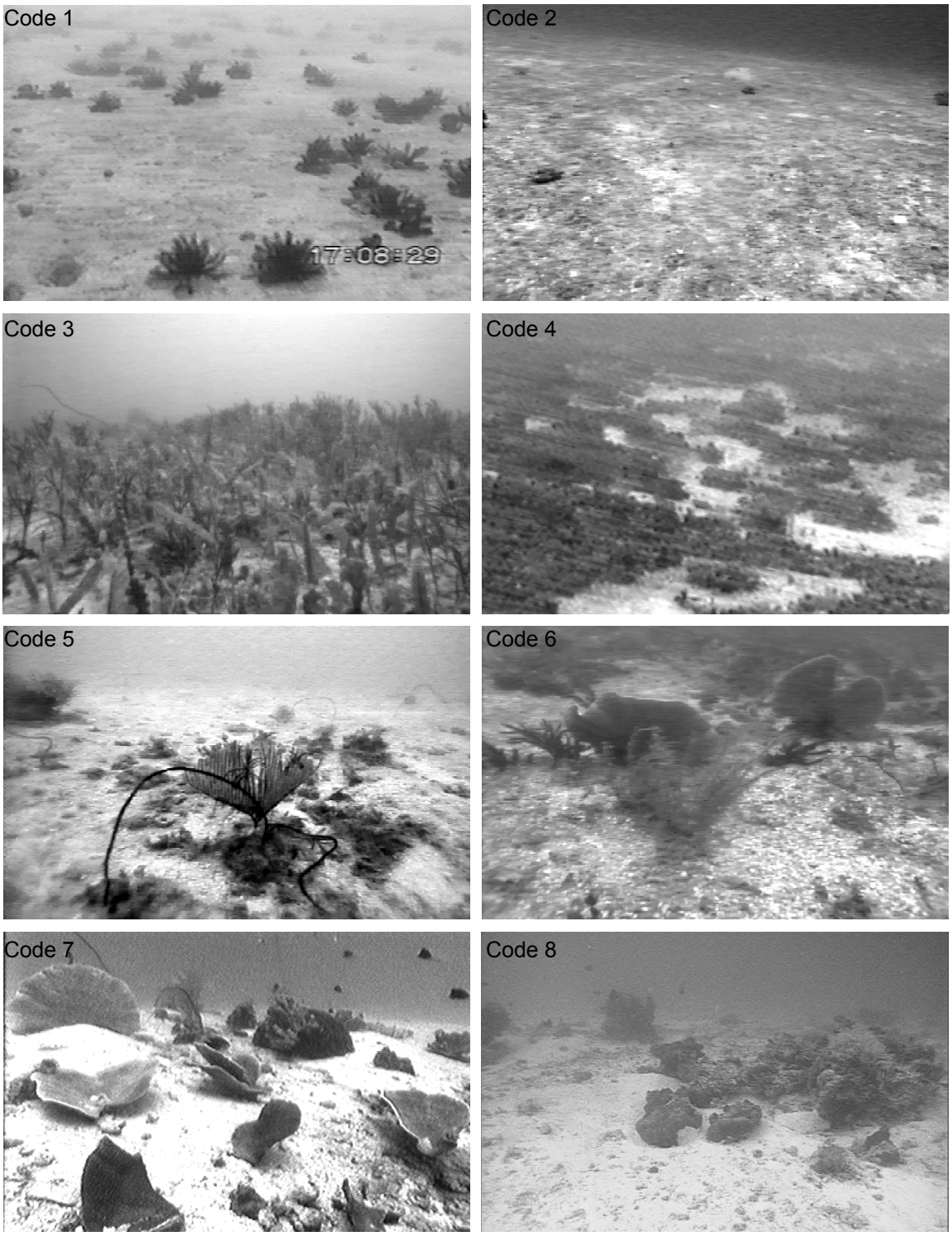

Figure 2-2: Typical habitat types observed on the seabed in the study area: code 1: bare sandy substratum, in this instance with many crinoids; code 2: bare rubbly substratum; code 3 substratum of sand with algae (mostly *Caulerpa* sp); code 4: substratum with beds of *Pinctada* shells in depressions; code 5: small garden patch with whips & gorgonians on rubbly substratum; code 6: larger garden with gorgonians and fan sponges (*Ianthella* sp); code 7: garden of hard corals (*Turbinaria* sp.) with gorgonians and sponges; code 8: rocky habitat with other benthos.

These data provided a general overview of the changing substrata or habitat along the video Sled paths before repeat trawling and during subsequent recovery surveys by graphically comparing the proportions of broad substratum and habitat types along the trawl paths over time.

The ROV was deployed on three (occasionally two) specific sites along each of the 12 Sled tracks, a total of 34 sites, to measure and monitor sessile benthos in discrete patches, surrounded by sand. These patches had been identified in previous Sled surveys prior to the depletion experiment and had been used to determine the path of the depletion tracks. A 500 kg clump-weight was deployed adjacent to each patch to anchor the vessel and tether the ROV. The ROV was able to survey a 30–40 m radius around the clump-weight. Within each of these patches, sessile benthos were observed carefully and recorded on video. The ROV was driven up to each sessile benthic organism and positioned so that the object was centred and filled about half to two-thirds of the field of view. For planar growth-forms, it was positioned perpendicular to the growth-plane, so that height and width of could later be measured. The position of each organism was logged at the same time so that the distribution of individuals within the sites could be determined for analysis, as well as for use as navigation waypoints for subsequent surveys. The aim was to achieve sufficiently accurate position information to yield absolute data on species composition, abundance and size of sessile megabenthic organisms in patches at sites that were re-visited in each subsequent survey. Parallel scaling lasers were used to determine distance to, and size of, megabenthos.

Benthos recorded on the Sled and ROV video tapes were later identified, to the extent possible, and measured to provide data for statistical analyses of the megabenthos species, position coordinates, and size and condition of all identifiable sessile megabenthos at each site. These data were also used to construct maps showing the position and size of identifiable species at each site. The types of fauna measured included ascidians, soft corals, sea whips and gorgonians, sponges, and hard corals — all of various morphologies.

2.2.3 Video tape analysis system and protocols

The video tapes were analysed with a semi-automated image measurement system comprising a computer-controlled digital video recorder (Panasonic DVC Pro AJ-D230H) connected to a monitor and a Pentium computer running Windows NT4, a Flashpoint™ video capture card and the Optimus 6.5 video analysis software. The control software was a custom-written application that accepted operator inputs to control the VCR frame position, maintained DDE links between the original tracking database and the video frames, pause the VCR at selected images (i.e. for the ROV when the laser points were visible on the object), pass control and instructions to the Optimus software to capture the selected frame and execute a macro that allowed the operator to digitise a scale, and the height, width and area of the object. These data were then passed back to the control software, where the user verified the measurements, species selection and entry of condition information (i.e. % missing, % dead, % encrusted) before the data were saved to the database together with matching position data from the field tracking database. There were uncertainties with the identity of the epibenthic fauna — identifications were made to species wherever possible, other taxa were identified to genera, and yet others to higher taxonomic levels, such order or even phylum. Captured images were saved to disk before and after the measurement lines were overlaid on the image. In the field, the date and time (nearest second) were recorded onto the video tape and database and used for subsequent checking of the synchronisation with the tracking–position database.

For the Sled, the video tapes were paused at each sessile benthic organism. The height was digitised from an image captured after the video tape was advanced until the attached base of the organism coincided with a "ground-line" displayed across the bottom of the screen to correspond to a position directly below a horizontal bar fixed across the front of the video Sled. This bar, 50 cm above the plane of the base of the video Sled, served as a reference scale for the height of fauna. It was marked at 100 mm intervals and so also served as a scale for measuring the width of fauna. Subsequently, each animal was assigned to the lowest putative taxon, and any damage or encrusting organisms were recorded.

The heights of all fauna observed by the Sled, except sea whips, were calculated with photogrammetric techniques, based on the digitised Sled reference scales. Sophisticated photogrammetric techniques were developed specifically for this project (see Appendix 7.1) because changes to camera, housings and Sled-setups between surveys meant that the simple ground-line approach would have introduced between-survey biases. There was also uncertainty in determining the position of the ground-line that was resolved by the photogrammetric techniques, and further, the video frame rate and tow speed meant that it was rarely possible to pause the video exactly on the ground-line; the nearest frame could have been up to several cm in front or behind the line. The precision and accuracy of the photogrammetric techniques and ground-line placement were checked in tanks by imaging a 5 cm grid with each available Sled camera and housing combination, as described for the ROV below. The Sled was also checked in the field by attaching the 5 cm grid to the bar-plane and suspending it in the water while images were captured.

The ROV was fitted with lasers 100 mm apart (or 100 mm wire rod, or 12 mm manipulator bolt) to be used as a scale to measure the animals. If an animal could be viewed only by looking down from above, the sequence of measurements was lasers, the short axis at right angle to the long axis, then the long axis, then area; and "above" was entered. If an animal was vertically digitate or finely branched (like *Ctenocella pectinata*), the lasers could not always be placed on the animal. However, one laser was always visible and could be used as a scale to measure the animal because the lasers were aligned so that there was a fixed relationship between the position of each laser to the other opposite the centreline of the image.

The precision and accuracy of the ROV measurements were checked in a salt-water tank by imaging a 1.9 m square base, accurately marked with reference lines 5 cm apart to form a grid. A frame was attached to the gridded base, and the ROV was held rigidly in this frame at distances of 0.5, 1.0 and 1.5 m. Tests comprised repeatedly measuring 15 sets of square grid targets of known size and distance from the ROV. The typical precision and accuracy for height and width was about 1–2%, and for area ~2–4%. Details of these methods and results were provided in the Year 1 Recovery Report (Pitcher *et al.* 2000).

The protocols for the operators analysing all the video tapes were on a template placed on the digitising board. When digitising the animals after image capture, the following sequence of actions was followed in accordance with the macro programmed in the Optimus video analysis software: • digitise the scale (lasers, bar, rod or bolt), • digitise the width, • digitise the height, • digitise the area (outline). If any of these parameters was not measurable, the operators had to simulate the digitising on the screen away from the animal and record in the comments only the parameter that was measurable. The animal was otherwise recorded as "locate only". For example, if the animals were whips, which could not be measured, the operators would check "locate only" and enter an estimate of the whip's length. If the vertical plane of the animal was not at right angles to the camera, it would not be possible to measure the width, so only the height was measured. If an animal was lying flat, the

"locate only" button was checked and "flat" was entered. Where all or part of an animal ran off the edge of the video screen, the height only was recorded, or it was recorded as "locate only" if the height was not measurable.

2.2.4 Filtering the acoustic tracking system data

In all sampling surveys the positioning information for the boat, ROV and Sled was sometimes inaccurate and needed to be corrected. Occasionally, the GPS positions of the boat were incorrect due to eg. change of satellites. The acoustic tracking system sometimes failed to measure slant range to the ROV correctly when the noise from the ROV's thrusters caused spurious pings from the transponder and other interference sometimes caused similar problems with the Sled. Rough weather caused the boat to pitch, roll and yaw which resulted in the gyro compass swinging excessively, and the GPS antenna and the tracking pole pitching and yawing through greater angles. This movement, combined with timing differences between the data output from the gyro compass, the tracking system and the GPS, contributed to occasional spurious data. Also, an occasional computer hang in the field resulted in a number of missing records.

An application was developed to graph the time sequence of acquired raw positioning data, including the vessel's GPS latitude and longitude, the tracker slant range, bearing and depression angle, in order to identify and manually remove obviously invalid points. Each input variable was processed separately and independently. Such removed points and missing values were then automatically interpolated from surrounding values. A smoothing algorithm was then applied to the data, based on averaging five points and stepping two points. All ROV and Sled positions on the seabed were recalculated from the filtered GPS and tracker data. On occasions when a computer hang occurred during a Sled track, VCR counter data were also interpolated and matched with the position information to synchronise the data. The corrected data were then graphically examined to check whether the tracks for both the video Sled and the ROV repeatedly covered the same ground during each survey of the five years of the monitoring experiment.

2.3 Data Analysis Methods

Understanding and quantifying the intensity of experimental trawling that the benthic fauna measured in this project had been subjected to were basic requirements for the data analyses. In the BACI experiment of 1993–1994, twelve of 24 plots were trawled so that there was a coverage of one trawl per unit area. The other 12 plots were reserved as un-trawled controls. Subsequently, in November 1995, one track on each of six of the 12 treatment plots was then trawled repeatedly. The repeat trawling covered a swathe ~35 m wide and the trawl intensity across the swathe ranged from 1 to 13 trawls, plus 1 trawl from the BACI experiment. A central strip, roughly 10–15 m wide, in each track was trawled 10 or more times. A position-referenced trawl intensity database was constructed from records of the trawler's differential GPS position, logged during the repeat-trawl experiment, and from the swept path of the trawl net (~18 m). The position-referenced trawl-intensity data from the repeat-trawl experiment was cross-referenced with the position-referenced data for each individual organism from the video tapes, so that the trawl intensity corresponding to every measured benthos organism could be estimated. This enabled maps to be constructed showing the species, position and size of all identifiable benthic fauna at each site and statistical analyses made of attributes in relation to trawl intensity.

2.3.1 Trawl intensity on impact plots

Even with the best navigation, it was not possible to guarantee that repeated trawls on a given track would sweep exactly the same path. Therefore, the intensity of repeated trawling on the six impact tracks in December 1995 could be expected to vary from zero (plus 1 trawl from the BACI) at the edge of repeat-trawling operations up to thirteen (+1) for any ground in the path of all trawls. Unfortunately, we were not able at that time to track directly the path of the trawl net itself for each ~ 3 km tow. We did, however, record the position of the boat at two-second intervals with D-GPS while trawls were being carried out. By making some assumptions about the position of the net relative to the boat and the width of the net opening, it was possible to build a map of expected trawl intensity and an associated measure of precision.

For the centre of the net, one possible approach was to assume that this followed exactly the same track as the boat. Given the winds and tidal currents in the Far Northern GBR, we considered this assumption unrealistic. Instead, we used a probabilistic approach to assigning a position for the centre of the net at any particular time. The net centre could be displaced some distance to port or starboard of the boat's line of travel, although a displacement of more than 5 degrees to either side seemed unlikely, as there was no noticeable offset of the trawl net. Deployment of several pairs of marker buoys on one plot demonstrated that trawling was confined to a corridor less than 60 m wide.

We assumed the net's centre could be displaced up to 30 m either side of the boat's line of travel, and assigned a probability to each displacement, as shown in Figure 2-3. Having no data on whether trawls were systematically offset to one side, we chose a normal distribution with a mean of zero so that the most likely position for the net centre was close to the boat's line of travel. We set the standard deviation of this "uncertainty" distribution to 3 m for trawls in shallow plots (~30 m) and 5 m for trawls in deep plots (~50 m), equivalent to a maximum offset angle of about 5 degrees.

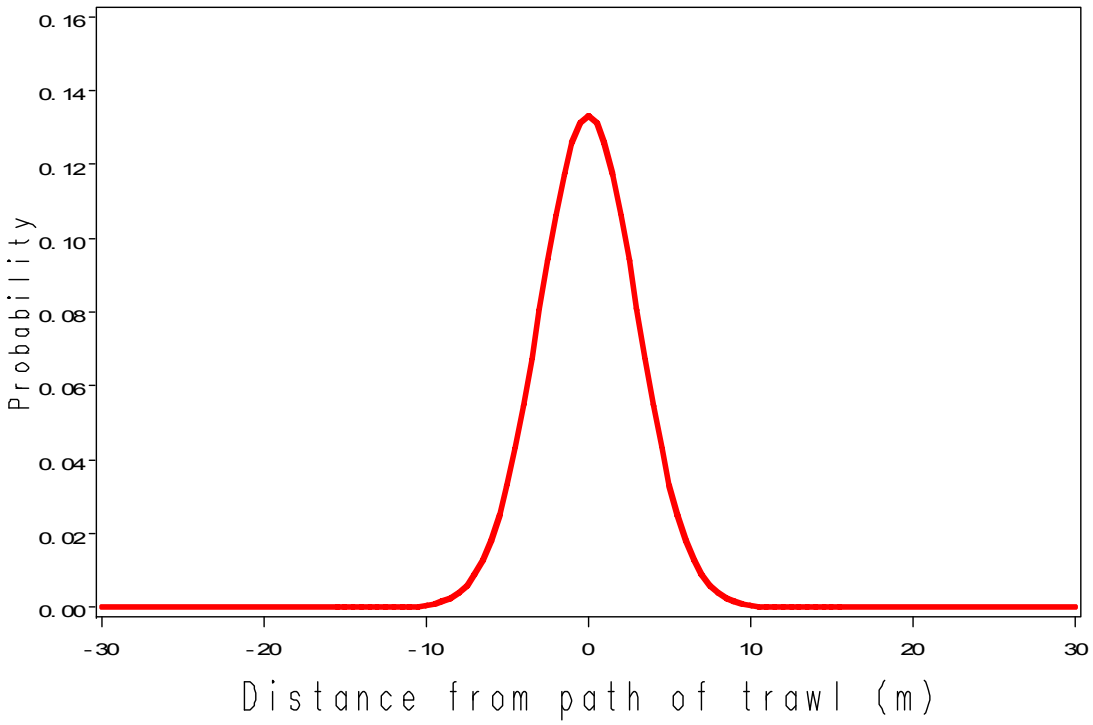

Figure 2-3: Probability density of displacement of centre of net relative to boat track.

Before evaluating trawl intensity, it is convenient to change from latitude and longitude to a rotated coordinate system (x, y) where x represents distance along the plot and y represents distance across the plot, perpendicular to x. This coordinate conversion was carried out separately for each plot, as plots are not all parallel to each other. The first step in this process was to convert position data from degrees to distances in metres. First, longitude was multiplied by the cosine of latitude. Then both coordinates were converted to arc-minutes before being multiplied by 1852. Using the full suite of boat transit records for a given plot, we then obtained the x/y coordinates as the first and second principal component scores of the centred latitude–longitude data for that plot. Boat positions are shown as latitude–longitude in Figure 2-4 and x/y in Figure 2-5.

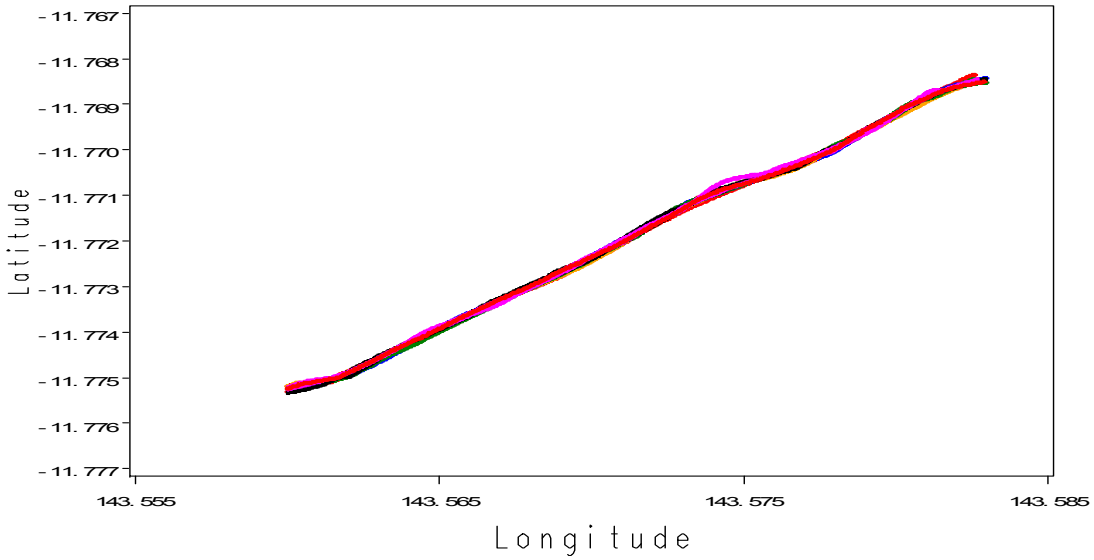

Figure 2-4: All 13 trawl tracks for Plot 18 in latitude-longitude coordinates.

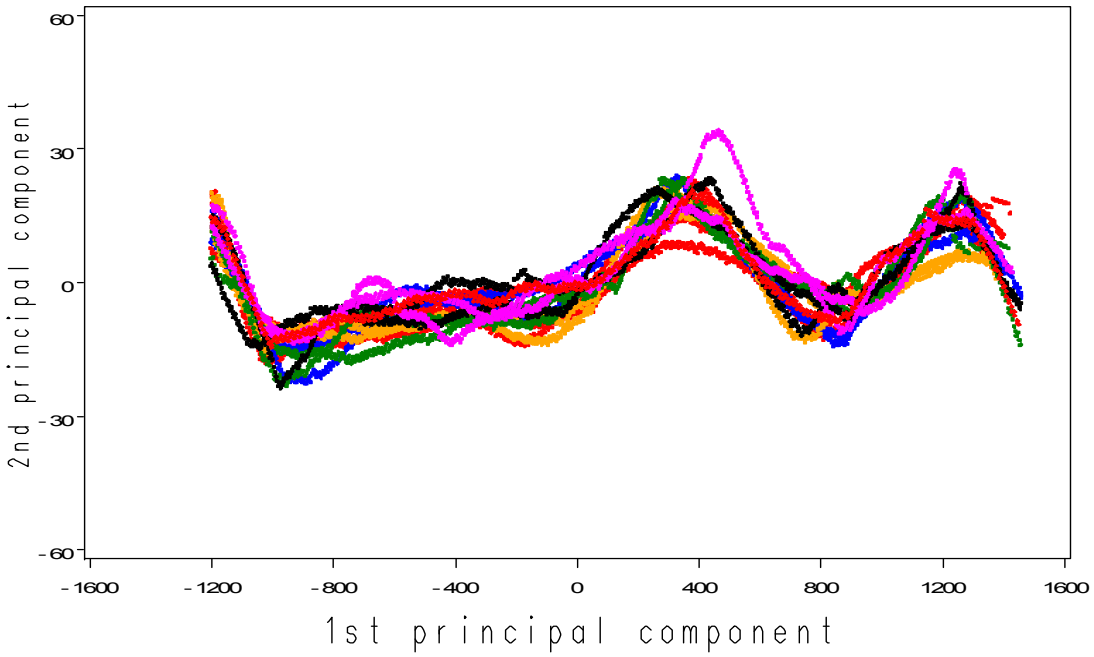

Figure 2-5: All 13 trawl tracks for Plot 18 in rotated coordinates. Note exaggerated vertical scale.

At a selected point X along the x-axis of the plot, we can represent the intensity of trawling caused by the passage of the i^{th} trawl, in a direction perpendicular to its line of travel (the y-axis). This intensity

has a "top hat" shape with a value of 1 for the path swept by the trawl (assumed to be 15 m wide in our case) and a value of 0 otherwise, as shown in Figure 2-6. The "top hat" is centred on Y_{bi}, this being where the boat cuts the y-axis at this point during the i^{th} trawl.

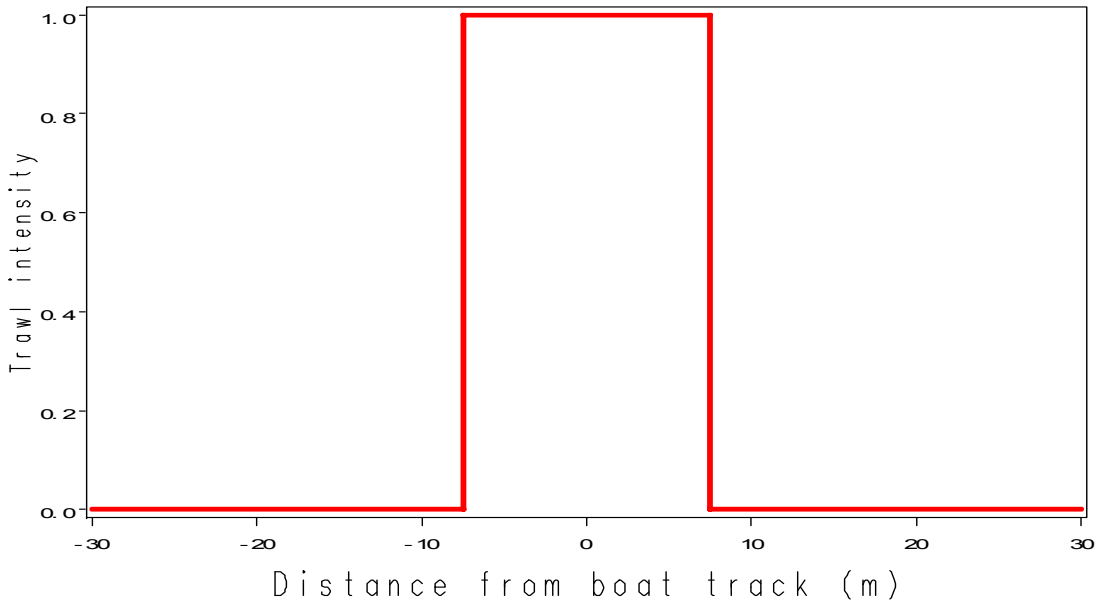

Figure 2-6: Intensity of trawling for a single trawl if the net is centred on the boat track.

Once we model uncertainty in the position of the centre of the net, we obtain a broader, flatter "rounded top hat" distribution for trawl intensity such as that shown in Figure 2-7. Since the probabilities from the normal distribution sum to 1, the area under the "top hat" and the "rounded top hat" is the same. However, the profile now represents the expected value of trawl intensity, and has an associated standard deviation. Mathematically, the expected trawl intensity for the i^{th} trawl at a selected point Y on the y-axis is expressed as follows:

$$E(t_i(Y \mid Y_{bi})) = \int_{-\infty}^{(Y-Y_{bi}-w/2)/\sigma} \frac{\exp(-\frac{z^2}{2})}{\sqrt{2\pi}} dz \quad - \quad \int_{-\infty}^{(Y-Y_{bi}+w/2)/\sigma} \frac{\exp(-\frac{z^2}{2})}{\sqrt{2\pi}} dz \tag{1}$$

where w is the width of the swept path (15 m) and σ is the standard deviation of the uncertinty in the position of the centre of the net (3 m or 5 m, depending on the depth of the plot). The standard deviation of trawl intensity is expressed mathematically as follows:

$$SD(t_i(Y \mid Y_{bi})) = \sqrt{E(t_i(Y \mid Y_{bi}))(1 - E(t_i(Y \mid Y_{bi})))} \tag{2}$$

This is shown in Figure 2-8. The standard deviation is highest near the edge of the net, when the net is located at the centreline.

We can expect thirteen different values of Y_{bi} for the position of the boat at a selected point X on the plot's main axis. An example is illustrated in Figure 2-9, for a randomly generated (but typical) set of Y_{bi} values for the 13 trawls. The total expected trawl intensity is given by:

$$E(t(Y(X))) = \sum_{i=1}^{13} E(t_i(Y(X) \mid Y_{bi}(X))) \tag{3}$$

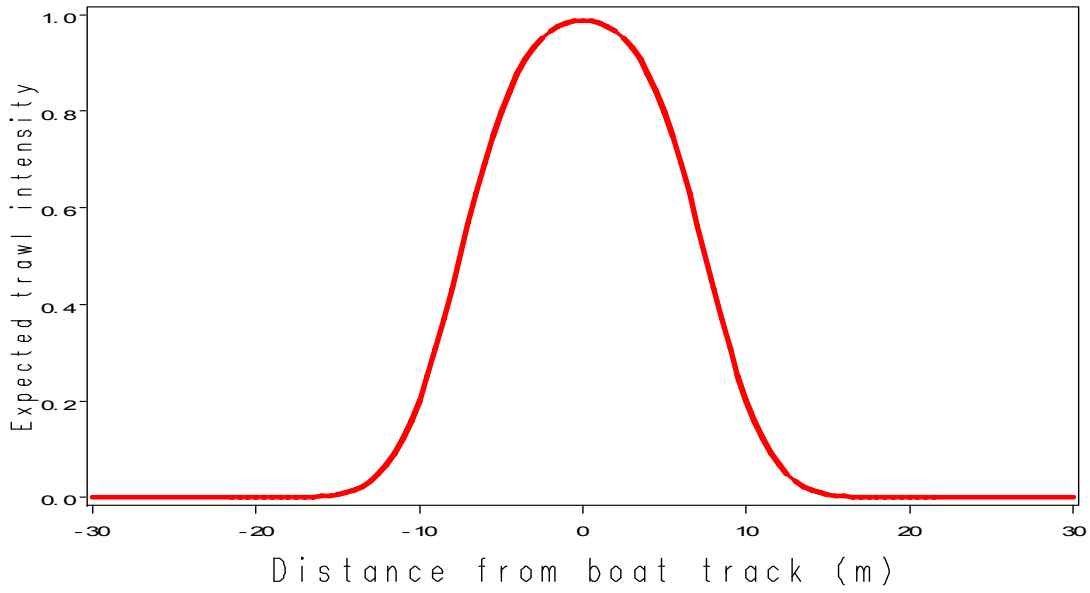

Figure 2-7: Expected intensity of trawling for a single trawl if the net position is uncertain.

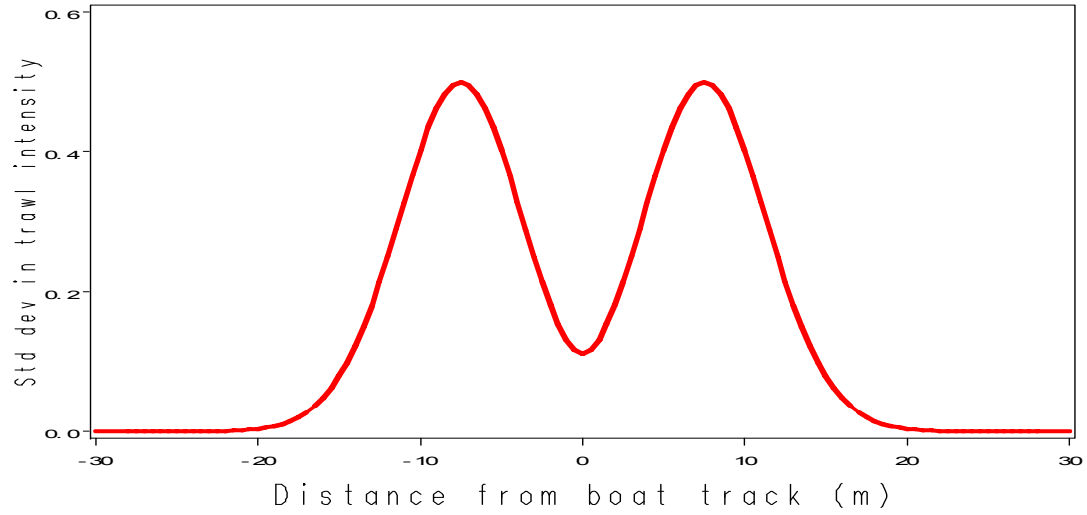

Figure 2-8: Standard deviation in intensity of trawling for a single trawl if the net position is uncertain.

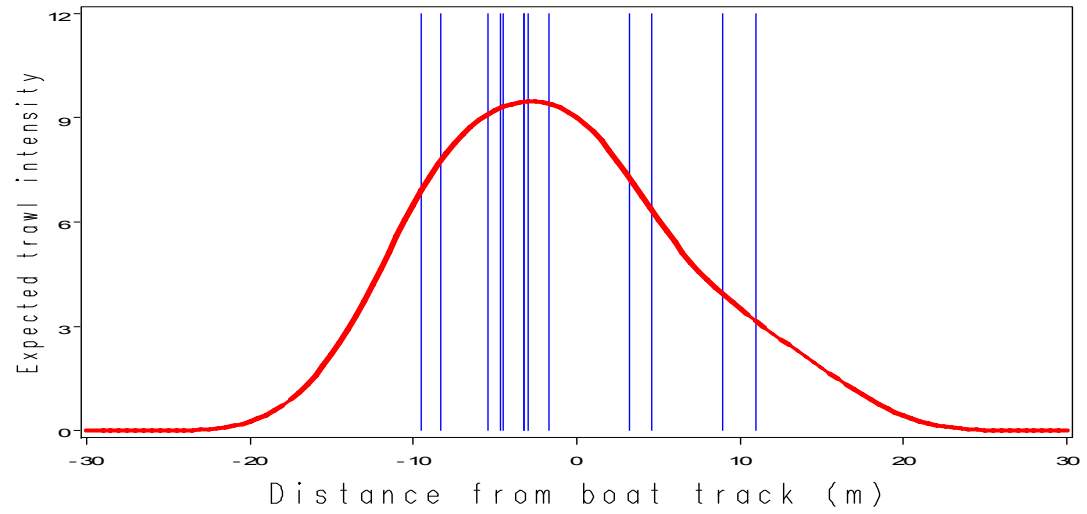

Figure 2-9: Expected intensity of trawling for 13 random boat-track positions.

2.3.2 Predicting for trawl intensity

The trawl intensity needed to be evaluated for any arbitrary position within the continuous "domain" of the plot – not merely at the set of discrete, irregular points represented by the set of ship positions. For example, we needed to assign trawl intensity to the positions of animals viewed by the ROV or the video Sled over six surveys. We might also want to construct a map of the trawl intensity for each plot using a regular grid of x/y values. A procedure to do this was implemented in S-plus as follows:

1. Convert the latitude–longitude coordinates of the new data set to the rotated coordinate system for that plot, producing a set of x/y values.
2. Generate the Y_{bi} for all 13 boat tracks for each x. This is done by linear interpolation of y on x for each boat track.
3. Compute the expected (total) trawl intensity for all values of Y recorded at each X.

The results of this procedure for selected plots are shown in Figure 2-10. The trawled region was effectively the region with expected intensity 0.1 or higher. This region tended to be slightly wider for the deep plots than for the shallow plots (Figure 2-10). For most of the plots there was a central strip with expected intensity of at least 9 trawls. In Plot 4, the navigation was particularly consistent, given the high-intensity strip was fairly wide along most of the length of the track. Also shown are tracks of some video transects made during the November 1996 survey. The transects sampled not only the high-intensity trawl areas but also some of the medium and low-intensity areas.

Figure 2-10 also shows the standard deviation of trawl-intensity. This tended to be highest in a pair of bands either side of the track centre, as expected from Figure 2-8. Overall, the standard deviation was higher for the deeper tracks, since these were assumed to have a greater uncertainty in net position due to the longer tow-wire required.

2.3.3 Analyses of Sled data

The Sled could not be towed over exactly the same ground at each survey or replicate and on impact tracks, the number of trawls along and across each Sled run varied from one (from the BACI) in areas that were not trawled in the repeat-trawl experiment to more than 10 near the middle of the repeat-trawled tracks. However, the positional information available for each second of the Sled replicates was used to assign estimates of trawl intensity to the observed seabed. After each organism observed by the Sled video was measured, and before data analysis, this position information was also used to assign an estimated trawl-intensity value to each organism. The value was the best available estimate of the trawl intensity for the position, as estimated in Section 2.3.2. Accordingly, fauna on impact tracks could have a trawl impact value in the range 1–14, depending on their position relative to the paths of the repeat-trawls. Fauna on control tracks had a trawl-impact value of zero.

For species observed by the Sled with adequate frequency of occurrence, uni-variate analyses were carried out for three variables: population density, height and condition of organisms. Animal width and area were measured, but in the case of the Sled were not analysed because it was not possible to ensure that planar animals were perpendicular to the field of view. For analyses of species density over time, trawl intensity was included as a covariate in terms of the average intensity on all seabed observed on each Sled replicate on impact tracks — this avoided segmentation of each Sled replicate into units of differing area, which would have occurred if replicates had been stratified by trawl intensity. Further, because the field of view of the Sled camera system changed over time, the swept area of each Sled replicate was included as a weighting covariate. Analyses of species population

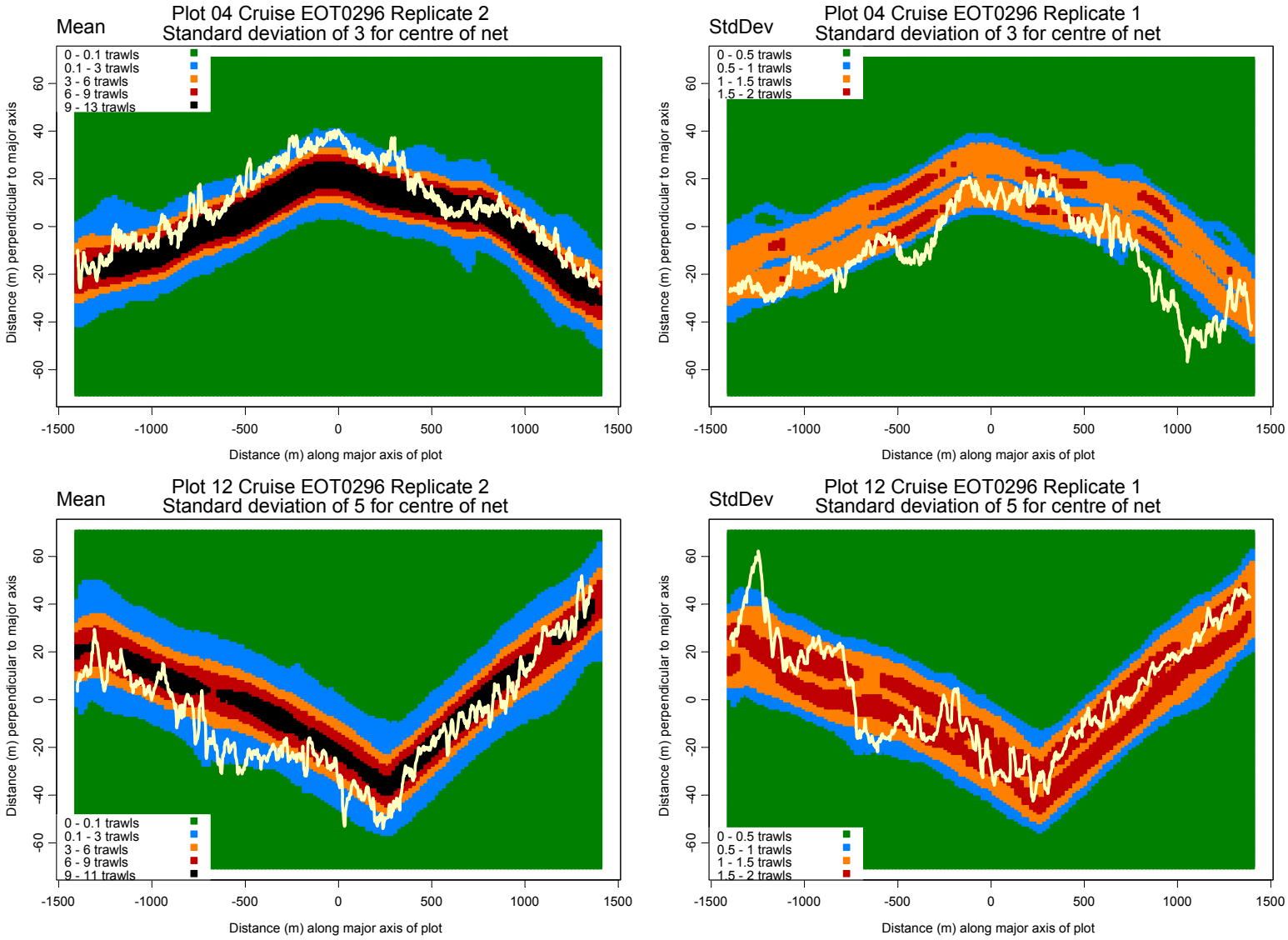

Figure 2-10: Expected trawl intensity and standard deviation for shallow plot 4 and deep plot 12, assuming a centre-of-net uncertainty standard deviation of 3 m and 5 m respectively. Overlaid are Sled video tracks for survey EOT0296 with replicate 2 in the left panel and replicate 1 in the right. The plots are in rotated coordinates with exaggerated across-track scale.

condition index and physical habitat structure by Sled replicate included the trawl intensity covariate in the same way. In contrast, for the analyses of Sled species individual height data, the trawl intensity assigned to individual organisms was included as a continuous explanatory variable.

Analyses of the composition of multi-species assemblages aimed to assess whether the relative mix of Sled-recorded species, by trawl intensity, changed over time as well as in overall abundance. Due to the data matrix required by such analyses, it was necessary to aggregate these species into the following trawl-intensity strata: Controls = 0; Impacts: 1 to 5 trawls, >5 to 9 trawls, and >9 to 14 trawls. These strata were denoted by the labels: (0,0], (1,5], (5,9] and (9,14] respectively. On impact replicates, each stratum included about a third of the data overall.

2.3.3.1 Size distributions

The "Sled" species targeted for analysis were selected largely by examining frequency of occurrence data and size distributions. Size distributions, constructed at 10 cm intervals, provided indications of changes in size structure, including possible recruitment, to assist interpretation of analysis results. Taxa had to be sufficiently abundant to produce a size-frequency distribution. The selected species were the more abundant, structurally dominant sessile benthic fauna, most with potential to grow larger than ~20–30 cm high. These comprised between 18 and 20 taxa (depending on the attribute being analysed) of the 36 that were observed, identified and measured during quantification of the Sled video.

2.3.3.2 Abundance analyses

Analyses of the "Sled" species density used a model-based approach to examine whether changes with time in numbers per Sled replicate were consistent with an impact and subsequent recovery on impact tracks relative to changes on control tracks.

For these analyses, Sled tracks were characterised by the average trawl intensity of the path they covered. The numbers of organisms of each species observed along the track was then modelled conditionally as a Poisson random variable with log-mean given by the following split formula. Let Y_{dmj} be the count of a particular taxon from a Sled track in depth stratum d, Survey m and plot j. Let $\mathrm{E}[Y_{dmj}] = \mu_{dmj}$ be the mean count. Also let A be the "swept area" of the Sled track on that occasion. Firstly for control plots, as well as impact plots before impact, we propose:

$$\log \mu_{dmj} = \mu_0 + \tau_d + C_m + P_j + \phi \log A$$

For impact plots post-impact the formula has additional terms:

$$\log \mu_{dmj} = \mu_0 + \tau_d + \gamma_1 i + \gamma_2 ti + \gamma_3 t^2 i + \gamma_4 ti^2 + C_m + P_j + \log A$$

where i is the average trawl intensity for the sled track and t is the time after impact, in months. Time t is zero for control plots and for impact plots pre- repeat-trawl. In both cases the random terms have distributions:

$$C_m \sim \mathrm{N}(0, \sigma_C^2), \quad P_j \sim \mathrm{N}(0, \sigma_P^2), \quad \text{independently.}$$

The term in swept area $\log A$ is included as offset in the equation with coefficient one. The effect was equivalent to considering the number of organisms per unit area, or density.

Several sub-models of the fixed effects were considered.

1. The random terms were present to allow for uncontrolled influences due to the particular survey and plot-survey combinations, hopefully allowing underlying fixed effects of trawling and recovery to be more easily uncovered and estimated. There was some degree of confounding between fixed and random effects, however, which could not be avoided because of the experimental imbalance.
2. The model parameters, coefficients and variance components, were estimated by the marginal PQL method, suggested by Breslow and Clayton, 1993, as implemented by the function `glme` of the `correlatedData` library in S-PLUS.

Individual terms in the fixed-effect part of the model were informally tested with an approximate Wald's test, and models were more formally compared by likelihood-ratio test analogues, although the accuracy of these methods is open to some question. However, these were the only methods available with this class of model, so options were limited.

2.3.3.3 Size (height) analyses

Analyses of height of the "Sled" species aimed to examine whether changes with time in the relationship between mean height and trawl-intensity were consistent with an impact (eg. reduction in mean height with higher trawl-intensity due to selective removal of larger individuals) and subsequent recovery on impact tracks relative to changes in mean height on control tracks.

The models were somewhat similar to those used in the analysis of densities for the Sled, but used ordinary normal linear mixed models rather than conditional Poisson GLMMs. The heights of organisms of each species observed along the track were then modelled as a normal random variable, with mean given by the following split formula. Let Y_{dmj} be the height of an organism in a particular taxon seen on a Sled track in depth stratum d, Survey m and plot j. Let $\mathrm{E}[Y_{dmj}] = \mu_{dmj}$ be the mean height. Firstly for control plots, as well as impact plots before impact, we propose:

$$\log \mu_{dmj} = \mu_0 + \tau_d + C_m + (CP)_{mj}$$

For impact plots after-impact, the formula has additional terms:

$$\log \mu_{dmj} = \mu_0 + \tau_d + \gamma_1 i + \gamma_2 ti + \gamma_3 t^2 i + \gamma_4 t i^2 + C_m + (CP)_{mj}$$

where i is the estimated trawl intensity for the animal's location and t is the time after impact, in months. Time t is zero for control plots and for impact plots pre- repeat-trawl. In both cases the random terms have distributions:

$$C_m \sim \mathrm{N}(0, \sigma_C^2), \quad (CP)_{mj} \sim \mathrm{N}(0, \sigma_{CP}^2), \quad \text{independently.}$$

Information was only available where the organisms were observed, and this was sometimes quite sporadic for some of the less commonly observed taxa. Several sub-models of the fixed effects were considered.

The model parameters, coefficients and variance components, were estimated by the standard maximum likelihood method, as implemented by the standard function `lme` in S-PLUS.

Individual terms in the fixed-effect part of the model were informally tested by Wald's test, and models were more formally compared by likelihood-ratio tests.

2.3.3.4 Condition analyses

During quantification of the Sled video, staff estimated the percentage to which each organism was complete (*C*) relative to its characteristic morphology (if appropriate), and of the observable part the percentage apparently dead (*D*) and the percentage of its skeleton encrusted (*E*) by other organisms. These attributes were combined to provide a single indicator of condition for each individual:

$$C\left(1-\left(D+E\right)/100\right)$$

Analyses of condition were based on the average for each Sled replicate of the indicator for all individuals of a given species, i.e.

$$\text{Condition Index} = I_c = 100 \text{ - Average(individual condition)}$$

Condition indices were investigated by random effects models similar to those adopted for density above, but using normal linear mixed-effects models rather than Poisson conditional GLMMs. The index was first mapped to an open-ended scale using a logistic transformation, slightly adjusted to accommodate zeros:

$$t(I_c) = \log\left(\frac{I_c + 0.5}{100 - I_c + 0.5}\right)$$

Let $t(I_c)_{dmj}$ be the transformed condition indes of a particular taxon from a sled track in depth stratum d, Survey m and plot j. Let $\mathrm{E}[t(I_c)_{dmj}] = \mu_{dmj}$ be the mean count. Firstly, for control plots (as well as impact plots before impact), we propose:

$$\mu_{dmj} = \mu_0 + \tau_d + C_m + (CP)_{mj}$$

For impact plots after impact the formula has additional terms:

$$\mu_{dmj} = \mu_0 + \tau_d + \gamma_1 i + \gamma_2 ti + \gamma_3 t^2 i + \gamma_4 ti^2 + C_m + (CP)_{mj}$$

where i is the average trawl intensity for the sled track and t is the time after impact, in months. Time t is zero for control plots and for impact plots pre- repeat-trawl. In both cases the random terms have distributions:

$$C_m \sim \mathrm{N}(0, \sigma_C^2), \quad P_j \sim \mathrm{N}(0, \sigma_P^2), \quad (CP)_{mj} \sim \mathrm{N}(0, \sigma_{CP}^2), \quad \text{independently.}$$

Several sub-models of the fixed effects were considered. Tests and estimation were done with standard Wald's test and likelihood-ratio results.

After analysis, predictions were back-transformed onto the original scale, using a slightly modified back-transformation:

$$I_c = \max\left(0, \min\left(100, \frac{101e^t}{1+e^t} - 0.5\right)\right)$$

The transformation was partly to provide a scale in which a normal analysis is reasonable, and partly to ensure the natural constraint that, after back-transformation, the condition index could not extend further than its natural range of [0,100].

2.3.3.5 Physical habitat structure

Analyses of the structure of the physical habitat, created by the sessile fauna, were based on the measured area of all individual animals summed for each Sled replicate, because total vertical cross-sectional area was considered the single attribute measured that would be most closely related to the physical structure available as habitat for other animals such as fishes. However, it was recognised that this approach would ignore a habitat quality aspect: a few large individual areas may total the same as many small individual areas but were not necessarily ecologically equivalent. Nevertheless, the approach is analogous to topographic complexity methods applied in, for example, intertidal areas.

Where the area was unavailable or invalid for "Sled" animals (in ~21,000 of ~37,000 cases), an estimate was made from Area=α.Height$^{\beta}$ relationships developed from the ROV dataset. Where height was also unavailable or invalid (~4,000 of ~37,000), the mean height for "Sled" taxa for that combination of main factors was substituted, and area was estimated from the ROV relationship. Hence, in these cases the contribution to habitat structure was largely a function of numbers.

The structure index was swept-area standardised within the analyses in a similar manner as Sled species abundance analyses.

The models for physical structure were very similar to the Sled numbers analyses, but used a normal linear mixed-effects model rather than a Poisson conditional model. The same random structure was used. The response was $\mathrm{Area}^{0.35}$, where the power, 0.35, was selected as most effective, after some initial informal investigations and later diagnostic checks confirmed.

For analysis the response was taken as:

$$Y = \frac{\text{Estimated total exposed area}}{\text{Total swept area for the sled track}}.$$

Random effects models were considered to be of the same form as those considered for the transformed condition indices above, with the additional feature that the variances of the standardised index were assumed to be inversely proportional to swept area, and hence the analysis used swept area as a weighting factor. A range of simpler models were considered. Estimation was by maximum likelihood and tests were done with either Wald's tests or likelihood ratio tests.

2.3.4 Analyses of ROV data

Observations made by the ROV before the start of the Recovery of Seabed Habitat Project provided the locations of discrete patches of benthic fauna surrounded by sand. These were re-surveyed as sites to monitor recovery. The aim of the project was to census all individuals of conspicuous taxa of sessile megafauna within each discrete patch.

The intensity of trawling within each of the impact patches ranged from areas that were not trawled by the repeat-trawl experiment to areas that were trawled more than 10 times. For analyses of the trawl

impact, each measured organism for which position data was available was subsequently assigned a trawl-intensity attribute based on the distribution of trawl intensities during the repeat-trawl experiment. The value of this attribute was the best available estimate of the intensity of trawling for that position (see Section 2.3.2). Accordingly, fauna on impact patches could have a trawl impact value in the range 1–14 (including the 1 trawl per unit area applied during the impact phase of the BACI experiment), depending on their position relative to the paths of the repeat-trawls. Fauna on control patches had a trawl impact value of zero. For analyses of change in the numbers or composition of fauna, individual organisms were aggregated into the following trawl intensity strata: Controls = 0; Impacts: 1 to 5 trawls, >5 to 9 trawls, and >9 to 14 trawls — and were denoted by the labels: (0,0], (1,5], (5,9] and (9,14]. On impact ROV patches, each stratum included about a third of the data overall.

For ROV surveys conducted during this recovery monitoring project, data analyses were able to take advantage of a high degree of precision and repeatability in positioning, together with captured images of benthos that can be measured accurately through the use of scaling lasers and digital image measurement. The data available for analyses included: species, numbers, position, height, width, area, %missing, %dead, and %encrusted of the benthos animal. The full attribute set was available for most of the selected structural sessile benthic taxa. However, it was not always possible to obtain the full attribute set for each individual. For example, seawhips could not be scaled with the lasers, so for seawhips the data available were species, numbers, position, %dead, and %encrusted. In the case of ROV video available from observations made before this project (e.g. April 1995), the ROV was deployed only opportunistically and sampling methods were still under development; consequently, few benthos were quantified pre-impact and ROV analyses were largely restricted to months 10, 23 and 61.

2.3.4.1 Size distributions

The ROV species were selected for analyses, as with those in the Sled video, largely by examining frequency of occurrence data and size distributions. ROV size distributions were also constructed at 10 cm intervals and provided indications of changes in size structure, including possible recruitment, to assist interpretation of analysis results. Taxa had to be sufficiently abundant to produce size-frequency distributions. The selected ROV species were the more abundant, structurally dominant, sessile benthic fauna, most with potential to grow larger than ~20–30 cm high. These comprised about 22-26 taxa (depending on the attribute being analysed) of the 34 that were observed, identified and measured during quantification of the ROV video.

2.3.4.2 Abundance surrogate analyses

Direct estimates of the true density of fauna were not really available from the ROV patches because the ROV's deployment aimed to census all individuals in the patch for measurement, and so were deliberately targeted measurements unlike the Sled transect. However, three abundance-related attributes were available from the ROV data.

The first attribute was raw census numbers by species for patches that were reliably and consistently censused from survey to survey. From these, examination of change with time in within-patch numbers and among patch relative-numbers was possible. However, absolute comparisons between patches and treatments were difficult, as patches differed in size. Three patches in the month 61

survey were not censused completely due to technical problems with the ROV; these were excluded from density-sensitive analyses. Six other patch–time combinations included satellite subpatches of animals that were not censused in all years; these satellite subpatches were also excluded from density-sensitive analyses. The animals remaining after these exclusions were termed 'core' animals. Also, survey month 1 pre-dated this project and the ROV was deployed only opportunistically to develop methods; these were also excluded from quantitative analyses.

The second attribute was patch–area standardised densities by species, in order to attempt quantitative comparisons between patches and treatments. This involved estimating the area of the footprint of all animals in each patch at each time. The footprint was estimated by a spatial approach, where each animal was buffered by a circle of half the overall median nearest-neighbour distance between all located animals, then the circles were intersected and overlapping areas were removed and the remaining areas were summed. Patch–area densities were then estimated as raw census numbers by species divided by respective patch–area. This was obviously a biased estimate, which would de-emphasise differences in density, although equally so for all treatment–time combinations.

The third attribute was calculated individual nearest-neighbour distances (NND), by species, as an (inverse) surrogate for density. The NND of each species within each ROV patch was estimated for each benthos individual by calculating the distance between the latitude–longitude position of all pairs of the same species and retaining the smallest distance. This is also obviously a biased estimate, but again equally so for all treatment–time combinations. However, NND cannot be calculated for single occurrences and absences cannot be represented by NND. Consequently, NND was inverted to infer individual densities by assuming animals would be hexagonally packed at NND apart, i.e:

$$\text{Individual Density} = 1/\left(NND^2 \sin\left(60^{\circ}\right)\right)$$

This again is a biased estimate, but allowed absences to be included in the dataset as an instance of zero density for that species, and single occurrences were included as 1/patch-area.

Another approach applied in the multi-species assemblage analyses (see Section 2.3.5 below) involved standardising each patch by overall numbers of animals observed to examine relative changes in species mixtures with time.

For most species nearest-neighbour density had a distribution very much skewed to the right. It has a non-negative range, but zero is a legitimate and frequently occurring value. To produce a scale in which normal modelling assumptions are reasonable, some transformation was needed. We adopted a power transformation, $t(d) = d^{0.125}$. With a small fractional power the effect is very similar to a log-transformation but does not require any special treatment to accommodate zero values. For most species this transformation seemed to produce a scale with roughly constant variance and simplified the mean structure in a similar way to what we might expect a log-transformation to achieve. Nevertheless, for many species the data remained extremely patchy and with frequent clumps.

We considered random-effects models of the standard form, as per the Sled, for transformed nearest-neighbour densities, but generally with a somewhat simpler mean structure than usual. The random effects were also simpler and only included a random effect for plot and patch-within-plot. Trials of models with Survey random effects as well were difficult to fit, and where they succeeded the results were not appreciably different to those with the simpler models.

2.3.4.3 Size (height/width/area) analyses

Analyses of the height, width and area of ROV species, as with those from the Sled video, aimed to examine whether changes with time in the relationship between the mean of size attributes and trawl intensity were consistent with an impact (reduction in mean size with higher trawl-intensity) and subsequent recovery on impact tracks relative to changes in mean size on control tracks.

Size responses for the ROV data were all analysed in the same way, using a linear normal random-effects model with random terms for survey, plot and patch-within-plot and fixed effect terms for topography, intensity and time after impact. In effect the control plots were all considered to be observed at time zero, and the impact plots were at times greater than zero, as appropriate.

Height and width were taken as the response directly, but area was transformed by taking the square root. This transformation was suggested as useful by simple preliminary analyses and confirmed later by diagnostic plots.

2.3.4.4 Condition analyses

During quantification of the ROV video, staff estimated three attributes of animal condition in the same manner as for the Sled animals. Again, these attributes were combined to provide a single indicator of condition for each individual. For the ROV data, analyses of condition were based on the average of the individual species indicators for each patch/time/trawl-intensity strata combination, i.e. Condition Index = 100 – Average(individual condition).

The ROV condition index data were analysed with a similar transformation and model as those used for the Sled condition index described above. In this case, however, the trawl intensity was taken as a categorical variable with four classes, namely 0, 0+ to 5, 5+ to 9 and 9+ trawls. Again the extremely clumpy nature of the data militated against very detailed models, so only very simple models were considered. The random effect terms were, as usual, survey, plot and patch-within-plot.

2.3.4.5 Physical habitat structure

In the ROV dataset, analyses of physical habitat structure, due to the presence of sessile fauna, were based on the measured area of all individual animals in an analogous manner to the Sled data. However, while Sled transects could be swept-area standardised, ROV patches were censused; consequently, vertical cross-sectional areas of individuals were summed for each reliably censused patch/time/trawl-intensity strata combination. Again, as with Sled animals, where cross-sectional area was unavailable or invalid for ROV animals (in ~13,000 of ~20,000 cases, mostly seawhips), an estimate was made from Area = α.Height$^{\beta}$ relationships. Where height was also unavailable or invalid (~12,000 of ~20,000, again mostly seawhips), the mean height for ROV taxa for that combination of main factors was substituted, and area was estimated from the area:height relationship. However, in the case of sea whips, the mean height for Sled whips for that combination of main factors was substituted. Given the large number of seawhips, it was important to recognise their possible contribution to habitat structure, even though they are narrow; this approximate method was largely a rescaling of their numbers.

Models for physical structure were very similar to ROV numbers analyses, but using a normal linear mixed-effects model rather than a Poisson conditional model. The same random structure was used.

The response was $\mathrm{Area}^{0.35}$, where the power, 0.35, was chosen after some initial informal investigations and confirmed by later diagnostic checks as useful.

2.3.5 Analyses of assemblage composition

The similarity of assemblages of sessile seabed fauna among and between treatment factors was analysed for both the ROV and Sled data sets. The data used in these analyses included: (a) the total number of individuals of each taxa, (b) the number of taxa, and (c) the estimated total volume per taxa (expressed in cm^3, as a proxy for total taxon biomass). Estimated volume was developed as a proxy for assemblage biomass because many similarity metrics are scale-sensitive, and while some of the small fauna were very numerous, some large fauna were uncommon. Thus, the volume proxy was an attempt to account for these discrepancies by taking size (such as individual height, width and area) as well as abundance into account. In all analyses within the experimental monitoring plots, the spatial units monitored were *patches* for the ROV and *tracks* for the Sled, with constant locations across time (in months) before or after experimental trawl impact. All data in patches and tracks were classified into four categories according to the trawl intensity experienced during the repeated-trawl experiment: controls = 0 trawls, low impact = 1–4 trawls, medium impact = 4–8 trawls, and high impact = 8–13 trawls. For assemblage composition, the data were then pooled up to the next experimental level of *plots* as the base analysis unit.

The analyses of assemblage composition included general univariate descriptions and multivariate ordinations. Common univariate community indices such as k-dominance curves were used, where species abundance or biomass are summarised to extract information on assemblage patterns, and presented graphically, without reducing the information to a single summary statistic such as species richness or diversity (Clarke and Warwick 1994). This analysis is independent of the species or taxa present and extracts common features of the assemblage structure. The total number of individuals (abundance) and the proxy for total biomass (total estimated volume), were used as the basis for these analyses for both ROV and Sled data sets.

Over the monitoring period, the survey area of each ROV patch and the swept area of each Sled track was not constant, as described above. Because abundances and total volumes of the taxa were correlated with patch size and swept area, the assemblage abundance and volume data of each experimental patch and track were standardised by area to provide density data. Thus the response variables used in the multivariate analyses were the number of individuals and the volume per square metre (NI m^2 and cm^3/m^2, respectively). While the density standardisation of the Sled data by Sled swept area was relatively simple, in the case of the ROV patches, estimation of patch area was not straightforward or absolute (see next section), consequently relative abundance was also examined for ROV patches (below).

2.3.5.1 ROV patch area estimation

The area of each ROV patch was approximated by the following spatial method, based on the position of each discrete observation of an animal on an ROV patch. A Voronoi polygon coverage (or Delaunay triangulation, Legendre and Legendre 1998) was created that placed each individual in its own polygon. The resulting Voronoi polygon coverage for each patch has the property that any location within a polygon is closer to the polygon centroid than to the centroid of any other polygon. A 0.25 m buffer was created around each animal position and used to clip the Voronoi polygons so that

the maximum radius was 0.25 m. The value of 0.25 m was selected because it was half the median value of the nearest neighbour distance between individual biota. The summed clipped polygon areas for each surveyed patch through time was then used to standardise the volume and abundance. Although this method did produce absolute densities, it was a biased approximation that would reduce sensitivity to real changes in abundance, hence relative abundances were also examined.

2.3.5.2 Relative abundance

Due to the uncertainty in estimating ROV patch area, relative abundance was also calculated in order to remove the weighting effect of surveyed area. First, for each patch, the number of individuals observed of all taxa for all surveys was totalled and divided by the number of times the patch was surveyed (usually 3, but sometimes 2) — this was the patch average abundance. Second, for taxa on each patch at each survey occasion, the number of individuals was divided by the patch average abundance — this was the taxon relative abundance. The sum of taxon relative abundances for a given patch at a given survey time could be greater or less than one, depending on trends in total numbers. Over the entire monitoring period, the sum of taxon relative abundances for a given patch would be either 3 (or 2) depending on the number of times the patch had been surveyed. Third, because multivariate analyses were conducted at the plot level, for each taxon, the average taxon relative abundance was calculated for each survey across all patches located within each plot (usually 3, but sometimes 2).

2.3.5.3 Total volume as a proxy for biomass

The non-intrusive nature of the ROV and Sled monitoring did not provide direct measurements of biomass, although individual biomass would have been a highly desirable metric for assessing the overall impact and recovery of the benthos after trawling. However, several individual metrics were determined for each taxon: individual height, width and area. Table 2-1 lists the combined total number of observations in the ROV and Sled data sets for each individual taxon. Between 1994/5 and 2001, the monitoring and assessments of the effects of trawling on benthos yielded a substantial number of individual observations across 36 taxa, totalling 56,803 individual measurements, with 20,026 for the ROV and 36,777 for the Sled respectively (Table 2-1).

Based upon these substantial sources of quantitative individual metrics, an approximation for the volume of individuals was developed as a proxy for their biomass. Table 2-2 lists for each taxon the total number of observations, the geometric form, the respective geometric equations to estimate the volume, the relation between individual height (the most frequently available metric) and volume, the regression coefficient, the total number of observations and the total estimated volume. We commenced by first assigning a general shape to each taxa, using known and estimated geometric figures such as cylinder, cone, rod, fan, disc, bottle, vase, parallelepiped (a 3D parallelogram), mushroom, or feather (Table 2-2). The next step was to estimate volumes using the taxon-specific geometric equations. In this step we managed to estimate the volume of nearly 43% of the total observations for the ROV and seld data sets. Estimates for an additional 24% of observations were added by using those observations that had only the height. This was achieved by determining the relationship between the individual height and individual volume using combined data sets that was best described by a power relationship – that is, $Volume = a*Height^b$.

Thus, this two-step procedure enabled us to estimate the volume of 38,277 observations that accounted for 67% of the total data set (Table 2-2). The remaining identified animals could not be measured, but were considered in the total counts per taxon. The resulting estimated volume for each track, patch and plot, was then standardised by dividing by the sampled area of each individual plot and each monitoring time and expressed in cubic centimetres (cm^3) per square metre (m^2).

Table 2-1: List of taxa and total number of individuals and their percentage (%) contribution to each benthic assemblage of the ROV, and Sled and total data sets.

Taxa	ROV	%	Sled	%	Total	%
Acabaria sp.	1	0.005			1	0.002
Alcyonacea	1 511	7.545	1 951	5.305	3 462	6.095
Alcyoniidae	5	0.025	32	0.087	37	0.065
Amphimedon sp.			1	0.003	1	0.002
Annella reticulata	170	0.849	118	0.321	288	0.507
Ascideacea	74	0.370	25	0.068	99	0.174
Bebryce sp.	202	1.009	3	0.008	205	0.361
Cirrhipathes sp.	51	0.255	39	0.106	90	0.158
Ctenocella pectinata	2 496	12.464	2 142	5.824	4 638	8.165
Cymbastela coralliophila	51	0.255	147	0.400	198	0.349
Dichotella divergens	2 118	10.576	1 948	5.297	4 066	7.158
Echinogorgia sp.	58	0.290	72	0.196	130	0.229
Ellisella sp.	101	0.504	3	0.008	104	0.183
Hippospongia elastica	1	0.005	4	0.011	5	0.009
Hydroid	178	0.889	38	0.103	216	0.380
Hypodistoma deeratum	71	0.355	433	1.177	504	0.887
Ianthella basta	124	0.619	61	0.166	185	0.326
Ianthella flabelliformis	858	4.284	919	2.499	1 777	3.128
Junceella fragilis	2 693	13.448	1 523	4.141	4 216	7.422
Junceella juncea	5 590	27.914	13 525	36.776	19 115	33.651
Lobophytum sp.	13	0.065	10	0.027	23	0.040
Mopsella sp.	3	0.015	1	0.003	4	0.007
Nephtheidae	993	4.959	10 676	29.029	11 669	20.543
Pennatulacea			2	0.005	2	0.004
Plumigorgia sp.	28	0.140	1	0.003	29	0.051
Porifera	601	3.001	268	0.729	869	1.530
Pteroeides sp.	3	0.015	31	0.084	34	0.060
Sarcophyton sp.	187	0.934	332	0.903	519	0.914
Scleractinia	238	1.188	616	1.675	854	1.503
Semperina brunea	57	0.285	31	0.084	88	0.155
Solenocaulon sp.	449	2.242	1 019	2.771	1 468	2.584
Subergorgia sp.	178	0.889	48	0.131	226	0.398
Subergorgia suberosa	372	1.858	81	0.220	453	0.797
Turbinaria frondens	501	2.502	596	1.621	1 097	1.931
Virgularia sp.			10	0.027	10	0.018
Xestospongia testudinaria	50	0.250	71	0.193	121	0.213
36 taxa	**20 026**	**100**	**36 777**	**100**	**56 803**	**100**

Table 2-2: Total number of observations for each taxon, the geometric form, the volume equation, and the relation between individual height and volume. N = number; ht = height; w = width; π = pi; A = area; w x w= w^2, numbers are multipliers expressed in millimetres.

Taxa	Total	Height	Width	Area	Geometric Form	Volume Equations	Volume in 1st evaluation	Height - Volume Equations	r^2	N	Volume in 2nd evaluation
Acabaria sp.	1	1	1	1	Fan	ht × w/4 × 3	*1*				*1*
Alcyonacea	3,460	1,907	1,798	1,798	Mushroom	ht × w × w	*1859*	Volume = 0.848*Height$^{3.1236}$	r^2 = 0.7614	559	*1,798*
Alcyoniidae	37	34	31	31	Mushroom	ht × w × w	*33*	Volume = 5.1653*Height$^{2.548}$	r^2= 0.8084	31	*31*
Amphimedon sp.	1	1	1	1	Parallelepiped	ht × w × w	*1*				*1*
Annella reticulata	288	228	202	202	Fan	ht × w/2 × 4	*222*	Volume = 5.2636*Height$^{2.3891}$	r^2 = 0.9212	140	*202*
Ascideacea	99	72	68	68	Cylinder	ht × w × w	*68*	Volume = 0.1242*Height$^{1.9645}$	r^2 = 0.8499	53	*68*
Bebryce sp.	207	130	130	130	Fan	ht × w/3 × 3	*128*			125	*130*
Cirrhipathes sp.	90				Coil	ht × 16 × π	*0*	Volume = 0.2051*Height2$^{0.0942}$	r^2 = 0.8896		
Ctenocella pectinata	4,640	3,504	3,183	3,182	Fan	ht × w/2 × 5	*3370*	Volume = 8.7491*Height$^{1.2537}$	r^2 = 0.7114	1,806	*3,196*
Cymbastela coralliophila	200	171	115	114	Disc	a × 10	*113*	Volume = 0.1525*Height$^{1.9185}$	r^2 = 0.8515	46	*114*
Dichotella divergens	4,081	2,857	2,736	2,732	Fan	ht × w/5 × 5	*2807*	Volume = 0.0713*Height$^{2.0555}$	r^2 = 0.7788	1,312	*2,736*
Echinogorgia sp.	131	95	92	92	Fan	ht × w/3 × 3	*95*	Volume = 0.075*Height$^{2.0085}$	r^2 = 0.751	43	*92*
Ellisella sp.	104	89	89	89	Fan	ht × w/4 × 3	*89*	Volume = 0.0024*Height$^{4.9642}$	r^2 = 0.6496	86	*89*
Hippospongia elastica	5	4	4	4	Cone	ht × (w/2 × w/2 × π)/3	*4*	Volume = 1.3899*Height$^{1.9314}$	r^2 = 0.9164	4	*4*
Hydroid	216	45	43	43	Feather	ht × w	*44*	Volume = 21.88*Height$^{2.0018}$	r^2 = 0.5912	22	*1*
Hypodistoma deeratum	507	290	286	286	Bottle	ht × π × w × w	*289*	Volume = 0.4416*Height$^{1.8615}$	r^2 = 0.8568	42	*286*
Ianthella basta	185	149	120	120	Disc	a × 3	*120*	Volume = 1.0625*Height$^{1.9918}$	r^2= 0.9601	102	*120*
Ianthella flabelliformis	1,779	1,354	1,095	1,095	Disc	a × 10	*1352*			763	*1,095*
Junceella fragilis	4,221	1,525			Rod	ht × 25 × π	*0*				*1,525*
Junceella juncea	19,221	13,604	4	4	Rod	ht × 25 × π	*6*	Volume = 16.879*Height$^{2.1575}$	r^2 = 0.8193		*13,604*
Lobophytum sp.	23	20	19	19	Mushroom	ht × w × w	*19*			20	*19*
Mopsella sp.	4	1	1	1	Fan	ht × w/3 × 3	*1*	Volume = 1.236*Height$^{2.885}$	r^2 = 0.8641		*1*
Nephtheidae	12,021	10,415	10,258	10,254	Mushroom	ht × w × w	*10084*			774	*10,258*
Pennatulacea	2	2	2	2	Fan	ht × w × 10	*2*	Volume = 0.0571*Height$^{2.0526}$	r^2= 0.8937		*2*
Plumigorgia sp.	29	23	23	23	Fan	ht × w/4 × 2	*23*	Volume = 2.6391*Height$^{2.7836}$	r^2 = 0.8532	22	*23*
Porifera	869	655	631	631	Parallelepiped	ht × w × w	*637*			411	*9*
Pteroeides sp.	34	30	30	30	Fan	ht × w × 10	*30*	Volume = 6.6575*Height$^{2.608}$	r^2 = 0.8799		*30*
Sarcophyton sp.	520	429	352	351	Mushroom	ht × w × w	*361*	Volume = 2.0869*Height$^{2.9889}$	r^2 = 0.8793	140	*352*
Scleractinia	854	525	470	470	Parallelepiped	ht × w × w	*476*	Volume = 0.5442*Height$^{2.0341}$	r^2 = 0.934	128	*470*
Semperina brunea	88	74	69	69	Fan	ht × w/2 × 10	*73*			50	*69*
Solenocaulon sp.	1,475	737	275	274	Cylinder	ht × 4	*721*	Volume = 0.1697*Height$^{1.9401}$	r^2 = 0.9298	78	*737*
Subergorgia sp.	226	165	151	151	Fan	ht × w/4 × 4	*164*	Volume = 0.3366*Height$^{1.9396}$	r^2 = 0.8877	137	*151*
Subergorgia suberosa	453	292	281	281	Fan	ht × w/2 × 5	*288*	Volume = 1.2859*Height$^{1.9559}$	r^2 = 0.9413	221	*281*
Turbinaria frondens	1,105	910	671	671	Vase	ht × w × 8	*884*			406	*671*
Virgularia sp.	10	5	2	2	Cylinder	ht × w/2 × w/2 × π	*5*	Volume = 1.341*Height$^{2.8786}$	r^2 = 0.9343		*2*
Xestospongia testudinaria	121	112	109	109	Cylinder	ht × w/2 × w/2 × π	*111*			45	*109*
Total	**57,307**	40,501	23,379	23,367			*24,480*			7,566	*38,277*

2.3.5.4 Multivariate analyses

For the assemblage composition analyses, several symmetrical taxa-by-site data matrices were constructed, where the observations were the density (N/m²), the relative abundance and volume (cm^3/m^2) for the ROV data sets and the density and volume per plot for the Sled. All multivariate analyses were conducted separately for each depth and graphed, using symbols to indicate the trawl intensity and the survey time (months). All data for the relative abundance, density and volume were 4^{th} root transformed, a transformation suitable for highly skewed data and also appropriate for a balanced weighting of the influence of the common and uncommon taxa. Then the Bray-Curtis dissimilarity, a commonly metric used in ecology also known as percentage dissimilarity, was used to calculate from the taxa-by-site data matrix, four dissimilarity matrices among plots.

An ordination of the Bray-Curtis dissimilarity matrix was then performed using multidimensional scaling (MDS) as implemented in PRIMER v5 (Clarke and Gorley 2001). The purpose of multidimensional scaling was to provide a visual representation of the pattern of proximities (i.e. similarities or distances) among the plots. For example, given a matrix of similarities between plots for ROV data sets, MDS presents the plots on a two-dimensional (or higher) map such that those plots that are similar to each other are placed near each other on the map, and those patches that are different from each other are placed far away from each other on the map. That is, MDS finds a set of vectors in *p*-dimensional space such that the matrix of Euclidean distances among them corresponds as closely as possible to some function of the input Bray-Curtis dissimilarity matrix according to a criterion function called *stress*. This is the degree of correspondence between the distances among points implied by the MDS map and the input matrix is measured (inversely) by a *stress* function. This means that larger stress values lead to larger scatter in the plot (Clarke and Warwick 2001).

To assess statistically the differences among the resulting ordinations, analyses of similarities (ANOSIM) were conducted for each of the selected samples, using a general randomisation approach to the estimation of significance levels in the form of a Monte Carlo Permutation Test, again as implemented in PRIMER v5 (Clarke and Warwick, 1994). Based on the Bray-Curtis dissimilarity matrix, ANOSIM determines the corresponding rank similarities between samples in the underlying triangular matrix and calculates a statistic, *R*, which provides an absolute measure of how separated the treatment groups area, where 0 indicates that groups are indistinguishable, $R<0.25$ indicates that groups are barely separable, $R>0.5$ indicates that groups are clearly separable though overlapping, $R>0.75$ indicates that groups are well separated, and 1 indicates that all within groups samples are more similar than any between groups samples. The group labels are then randomly permuted many times to generate an empirical distribution for *R* against which the value of the *R*-statistic may be compared and its probability estimated (Clarke and Warwick 1994). When sample sizes are small and the number of permutation limited, the probability of the *R*-statistic is more limited and guidance should be taken from the value of *R* itself. The different trawl intensity categories (controls, low-medium-high trawl impact) were contrasted in this way, at the plot level. These multiple comparisons were conducted for each monitoring platform (ROV or Sled), depth (deep and shallow), and survey time (in months).

2.3.5.5 Rank dominance

For both Sled and ROV data sets, a series of cumulative(*k*) rank-dominance curves were calculated using PRIMER v5 (Clarke and Gorley 2001). Rank-dominance involves the ranking of taxa in

decreasing order of numerical or biomass abundance, and each ranked taxon abundance is expressed as percentage of the total abundance of all taxa. Typically, the cumulative (hence *k-)* percent abundance is plotted against the respective taxon rank, and the axis of ranks is expressed in a logarithmic scale to emphasise or down weight different sections of the resulting curve, enabling a better visualisation of the dominant taxa (Lambshead *et al.* 1983). The *most elevated* curves will have the lowest diversity, while the *least elevated* curves will have the most even diversity, thus a less dominated assemblage.

Again, matrices of sample-by-taxa data for both density (N/m²) and the volume (cm^3/m^2), aggregated up to the plot level, were used. The *k*-dominance curves were then calculated for each of the selected samples independently, and separately for monitoring platform (ROV or Sled), depth of each treatment plot (deep and shallow), and monitoring time (in months). The resulting cumulative dominance distribution curves was graphed.

2.4 Estimation of recovery time-frames

Recovery time-frames were considered for benthos numbers for Sled and ROV data as another study (Pitcher *et al.* 2004) had demonstrated that recovery was more dependent on the number of recruits than on the growth of individuals. Further, the statistical models' fit to the data were intended to identify recovery signals within the time-frame of the study, so may not behave reliably beyond this time. For this reason, simpler models of log(numbers) were fitted to the Sled data, involving only linear terms for the fixed effects of trawl intensity and the time*intensity interaction, with no higher order terms. The log coefficients simplified the estimation of impact and recovery rates. Given the uncertainty in the estimates, more complex approaches were unwarranted.

Due to the form of the model fitted, recovery time-frames thus estimated were independent of the extent of the initial impact, so simplifying the presentation of recovery time-frames. Nevertheless, estimates of the impact rate and population status under different trawl intensities of 2, 7 and 11 trawls were also summarized along with the recovery time-frame projections.

The average depleted state for each species in each intensity was estimated to provide the initial condition from which recovery time was estimated — this initial state was also presented in the output along with the average timeframe and confidence interval derived from uncertainty in the recovery rate. The depleted state was also estimated with uncertainty. The model for trawl depletion was:

$$N_i = N_0(1+d)^i$$

where N_i are numbers after i trawls, with initial numbers N_0 = 1 and depletion rate per trawl d (negative for depletion). The depletion rate was estimated by back-transformation of the model's trawl-intensity coefficient. The simple model for recovery was:

$$N_t = N_0(1+r)^t$$

where N_t are numbers after time t, with recovery rate r. The recovery rate was estimated by back-transformation of the model's time*intensity coefficient, and so is a function of trawl intensity; ie. recovery rate $r=(exp(a.i)-1)$, where a is the $t*i$ coefficent. Hence the numbers of years required for a population to recover from each depleted state N_i was:

$$t = \log(1/N_i)/\log(1+r)$$

Similary, the analyses of ROV log(census numbers) produced linear time*intensity coefficients that provided estimates of recovery rates in impact patches relative to controls. However, because the ROV patches were not randomised quadrats, it was difficult to estimate a reliable trawl-intensity coefficient. Consequently, the trawl-intensity coefficients of the nearest-neighbour density analyses were used as an approximation. These analyses were conducted on nearest-neighbour density^0.125, which approximates the log-transformation without the need for offsets to account for zeros, and the coefficient intensity/0.125 scaled to a mean density of 1, approximates the log-value and can be back-transformed to provide an estimate of the depletion rate.

Confidence intervals for recovery were estimated by substituting the ±standard errors of the models' time*intensity coefficients, multiplied by the value of the T-distribution for the 90% interval, into the above equations.

3 RESULTS

3.1 Field survey results

3.1.1 Sled tracks surveyed and evaluated

The project successfully conducted and evaluated 108 combinations of time, track and replicate video Sled tows (Table 3-1). Sled surveys made during previous projects were not deployed for the purpose of quantifying subsequent recovery, so significant method development (as discussed above) was required to calibrate these earlier surveys with those conducted during the current project, to provide an indication of the status of the tracks before and 1 month after the repeat-trawl experiment. Replicate Sled tows were introduced when this project began. After analysis of month 10 data for the Year 1 Report, a third replicate on impact tracks was introduced in survey month 23 to provide greater coverage of the trawl-intensity profile of the repeat-trawl tracks.

Table 3-1: Video Sled tracks surveyed, with number of animals observed, by time.

				Survey month				
Treatment	**Topography**	**SiteID**	**Replicate**	**-8**	**1**	**10**	**23**	**61**
Control	Deep	PL01TR01	1	595	1248	681	786	598
Control	Deep	PL01TR01	2			573	895	487
Control	Deep	PL11TR02	1	306	627	448	845	1605
Control	Deep	PL11TR02	2			839	748	1221
Control	Deep	PL20TR02	1	181	454	500	514	488
Control	Deep	PL20TR02	2			404	497	279
Control	Shallow	PL03TR01	1	212	198	164	158	403
Control	Shallow	PL03TR01	2			239	165	487
Control	Shallow	PL17TR03	1	56	63	160	105	121
Control	Shallow	PL17TR03	2			41	61	67
Control	Shallow	PL22TR03	1	153	139	125	203	538
Control	Shallow	PL22TR03	2			186	231	375
Impact	Deep	PL12TR03	1	103	199	230	120	318
Impact	Deep	PL12TR03	2			157	234	361
Impact	Deep	PL12TR03	3				256	762
Impact	Deep	PL15TR02	1	272	491	186	458	564
Impact	Deep	PL15TR02	2			270	303	870
Impact	Deep	PL15TR02	3				392	807
Impact	Deep	PL19TR02	1	140	130	176	202	296
Impact	Deep	PL19TR02	2			201	143	361
Impact	Deep	PL19TR02	3				168	238
Impact	Shallow	PL04TR01	1	181	225	281	249	613
Impact	Shallow	PL04TR01	2			221	187	598
Impact	Shallow	PL04TR01	3				185	424
Impact	Shallow	PL18TR03	1	184	115	170	253	178
Impact	Shallow	PL18TR03	2			113	132	222
Impact	Shallow	PL18TR03	3				168	184
Impact	Shallow	PL21TR03	1	125	106	106	149	755
Impact	Shallow	PL21TR03	2			121	216	496
Impact	Shallow	PL21TR03	3				121	221

3.1.2 ROV patches surveyed and evaluated

The project conducted and evaluated 95 combinations of time and track-patch ROV deployments (Table 3-2). However, ROV deployments conducted before this project began were only opportunistic, to develop methods. Lasers were not used until survey month 1, when a number of animals were measured on a few patches to test the patch survey and scaling methods. Technical failure of critical ROV components during the November 1999 survey meant an additional survey was made in January 2001, but continuing problems caused significant downtime and prevented some patches from being fully censused and others from being surveyed at all (Table 3-2). Consequently, 88 patch and time combinations were fully and successfully censused. The animals measured on these were included in quantitative analyses. Further, some satellite subpatches of animals that were surveyed were not censused in all years; these satellite subpatches were also excluded from quantitative analyses so that a consistent set of surveyed animals could be established.

3.1.3 Verifying the precision of revisiting video Sled and ROV tracks

Over a period of five years, the video Sled was repeatedly towed along the trawl-impacted and control tracks through specific waypoints, and the ROV visited specific sites to record information on the species composition, size and condition. The data giving the location of the Sled or ROV during each survey were overlaid for each track and patch across surveys to check the repeatability of positioning between surveys.

With the exception of some of the earlier video Sled tracks for the 1994–95 surveys (which were used to observe plots and patches for the previous BACI experiment and were not intended to monitor the subsequent repeated trawl path) all Sled tracks were very close to or overlay each other. The 1994-95 video Sled tracks were somewhat erratic on plots 4, 12 and 22, and on plot 12 did not align with the full length of later Sled runs, due to the different purpose of the earlier tows.

All subsequent tracks were used to monitor the impact of the repeat-trawling experiment. Although the path of the Sled could not be controlled exactly, the repeated Sled runs were deliberately towed along slightly different parts of the trawl track so that the ~1.5 m wide observed video path of the Sled would pass over different trawl intensity levels of the ~35-40 m wide trawl track of the repeat-trawl experiment. Plots of Sled tracks demonstrated that this was successfully achieved (eg. see Figure 2-10).

During January 1996, the ROV visited the patches only on repeat trawl tracks in the impacted plots (4, 12, 15, 18, 19 and 21). The spatial extent of the ROV trails in January 1996 were sometimes greater than for subsequent visits by the ROV, as the initial visit searched beyond the edge of the patches to be certain that the boundaries of the patches had been located.

Although not all patches could be visited by the ROV on all subsequent surveys (Table 3-2) due to weather, electro-mechanical problems, and time constraints, plots of ROV trails showed almost complete overlap of tracks for each patch for all surveys, indicating that the ROV clearly surveyed the same seabed from survey to survey. One exception was patch 1 in Plot 11. Initially (at month 10) two patches close to each other were surveyed; both patches had very large numbers of animals, but during subsequent surveys, time constraints meant that later only the larger western patch was repeatedly visited by the ROV.

Table 3-2: ROV Patches surveyed, with number of animals observed, by time. x = patches that could not be surveyed due to ROV technical issues; grey patches = not censused completely due to ROV technical issues; boxed = patch-time combinations included satellite sub-patches of animals that were not censused in all years, so satellite sub-patches at these sites were excluded from quantitative analyses.

			Survey months			
Treatment	**Topography**	**Site ID**	**1**	**10**	**23**	**61**
Control	Deep	PL01PT01		208	507	x
Control	Deep	PL01PT02		229	749	185
Control	Deep	PL01PT03		169	428	200
Control	Deep	PL11PT01		272	425	372
Control	Deep	PL11PT02		383	456	x
Control	Deep	PL11PT03		132	297	147
Control	Deep	PL20PT01	156	495	477	414
Control	Deep	PL20PT02		511	517	295
Control	Shallow	PL03PT01		262	310	243
Control	Shallow	PL03PT02		174	47	24
Control	Shallow	PL03PT03		109	60	x
Control	Shallow	PL17PT01		166	99	78
Control	Shallow	PL17PT02		x	29	x
Control	Shallow	PL17PT03		132	165	147
Control	Shallow	PL22PT01		169	238	x
Control	Shallow	PL22PT02		62	79	68
Control	Shallow	PL22PT03		x	219	116
Impact	Deep	PL12PT01		174	235	434
Impact	Deep	PL12PT03		130	225	249
Impact	Deep	PL15PT01		105	417	245
Impact	Deep	PL15PT02		287	547	x
Impact	Deep	PL15PT03		156	221	85
Impact	Deep	PL19PT01	218	102	167	209
Impact	Deep	PL19PT02	150	237	128	120
Impact	Deep	PL19PT03	65	89	80	204
Impact	Shallow	PL04PT01		135	157	104
Impact	Shallow	PL04PT02		76	36	91
Impact	Shallow	PL04PT03		90	74	x
Impact	Shallow	PL18PT01		127	283	213
Impact	Shallow	PL18PT02		94	94	x
Impact	Shallow	PL18PT03		262	312	371
Impact	Shallow	PL21PT01		297	156	197
Impact	Shallow	PL21PT02		154	137	x
Impact	Shallow	PL21PT03		47	81	198

3.2 Species for analyses

Almost 57,000 animals were observed and measured in this Project (Table 3-3). Of these, almost 37,000 were observed in the Sled video and the other 20,000 by the ROV. Overall, 36 taxa were identified, but the distribution of abundance was very uneven. A few species were numerous or very numerous — 9 taxa comprised ~90% of individuals — and dominated the physical structure of the sessile megabenthos assemblages in the area.

Some taxa were relatively more frequent in the ROV video (eg. *Ctenocella pectinata, Dichotella divergens, Ianthella flabelliformis, Turbinaria frondens*) and were indicative of patch-habitat fauna, whereas some other taxa (eg. Nephtheidae, *Solenocaulon, Hypodistoma deeratum*) were more frequently observed by the Sled between habitat patches.

Table 3-3: Frequency of taxa observed by the Sled and ROV

Rank	Benthos Taxa	Type	Sled	ROV	Total	Proportion
1	*Junceella juncea*	Red whips	13,525	5,590	19,115	33.65
2	Nephtheidae	Soft coral	10,676	993	11,669	20.54
3	*Ctenocella pectinata*	Gorgonian	2,142	2,496	4,638	8.16
4	*Junceella fragilis*	White whips	1,523	2,693	4,216	7.42
5	*Dichotella divergens*	Gorgonian	1,948	2,118	4,066	7.16
6	*Alcyonacea*	Soft coral	1,951	1,511	3,462	6.09
7	*Ianthella flabelliformis*	Fan sponge	919	858	1,777	3.13
8	*Solenocaulon* sp.	Gorgonian	1,019	449	1,468	2.58
9	*Turbinaria frondens*	Hard coral	599	502	1,101	1.94
10	Porifera	Sponge	268	601	869	1.53
11	Scleractinia	Hard coral	616	238	854	1.50
12	*Sarcophyton* sp.	Soft coral	332	187	519	0.91
13	*Hypodistoma deeratum*	Solitary ascidian	433	71	504	0.89
14	*Subergorgia suberosa*	Gorgonian	81	372	453	0.80
15	*Annella reticulata*	Gorgonian	118	170	288	0.51
16	*Subergorgia* sp.	Gorgonian	48	178	226	0.40
17	*Hydroid*	Hydroid	38	178	216	0.38
18	*Bebryce* sp.	Gorgonian	3	202	205	0.36
19	*Cymbastela coralliophila*	Sponge	147	51	198	0.35
20	*Ianthella basta*	Fan sponge	61	124	185	0.33
21	*Echinogorgia* sp.	Gorgonian	72	58	130	0.23
22	*Xestospongia testudinaria*	Sponge	71	50	121	0.21
23	*Ellisella* sp.	Gorgonian	3	101	104	0.18
24	Ascideacea	Colonial ascidian	25	74	99	0.17
25	*Cirrhipathes* sp.	Gorgonian	39	51	90	0.16
26	*Semperina brunea*	Gorgonian	31	57	88	0.15
27	Alcyoniidae	Soft coral	32	5	37	0.07
28	*Pteroeides* sp.	Sea pen	31	3	34	0.06
29	*Plumigorgia* sp.	Gorgonian	1	28	29	0.05
30	*Lobophytum* sp.	Soft coral	10	13	23	0.04
31	*Virgularia* sp.	Sea pen	10		10	0.02
32	*Hippospongia elastica*	Sponge	4	1	5	0.01
33	*Mopsella* sp.	Gorgonian	1	3	4	0.01
34	Pennatulacea	Sea pen	2		2	0.00
35	*Acabaria* sp.	Gorgonian		1	1	0.00
36	*Amphimedon* sp.	Sponge	1		1	0.00
	TOTAL		36,780	20,027	56,807	100.00

Analyses were attempted on species with a frequency of more than about 50 in either the Sled or ROV observations. For the Sled, analyses were attempted on 18-20 taxa (Table 3-4), and for the ROV 22-26 taxa (Table 3-5). However, analyses were not always successful for taxa with low frequency, particularly if they were not represented in all combinations of the main factors. Raw counts suggest

more animals were in low rather than high trawl-intensity strata (noting that the impact tracks were divided into three trawl-intensity strata whereas controls were not) (Table 3-4 & Table 3-5).

Table 3-4: Frequencies of taxa observed by the Sled video, by trawl-intensity strata.

Benthos Taxa	Deep				Shallow				Total
	(0,0]	(1,5]	(5,9]	(9,14]	(0,0]	(1,5]	(5,9]	(9,14]	
Junceella juncea	5378	1390	1493	774	1746	1487	653	604	13525
Nephtheidae	4406	1251	1291	679	1062	980	571	436	10676
Ctenocella pectinata	1301	203	252	107	111	92	50	26	2142
Alcyonacea	840	214	374	185	156	102	55	25	1951
Dichotella divergens	599	162	173	70	341	376	140	87	1948
Junceella fragilis	755	64	84	36	167	262	80	75	1523
Solenocaulon sp.	168	67	63	24	205	264	119	109	1019
Ianthella flabelliformis	720	71	65	17	19	15	7	5	919
Scleractinia	441	3	10		70	45	23	24	616
Turbinaria frondens	385	3	4	2	144	45	11	5	599
Hypodistoma deeratum	22	8	9	5	77	116	100	96	433
Sarcophyton sp.	249	5	5	5	43	14	5	6	332
Porifera	129	24	26	7	39	28	10	5	268
Cymbastela coralliophila	106	1			24	11	3	2	147
Annella reticulata	73	10	19	4	5	7			118
Subergorgia suberosa	22	2	18	15	8	10	4	2	81
Echinogorgia sp.	44	5	9	1	3	1	1	8	72
Xestospongia testudinaria	11	3	7	3	25	12	5	5	71
Ianthella basta	44	1	4		7	3	2		61
Subergorgia sp.	18	2	6		7	11	4		48

Table 3-5: Frequencies of taxa observed by the ROV, by trawl-intensity strata.

Benthos Taxa	Deep				Shallow				Total
	(0,0]	(1,5]	(5,9]	(9,14]	(0,0]	(1,5]	(5,9]	(9,14]	
Junceella juncea	2094	705	695	250	703	813	176	154	5590
Junceella fragilis	1173	90	72	24	635	475	120	104	2693
Ctenocella pectinata	1410	219	345	84	203	155	36	44	2496
Dichotella divergens	492	284	253	94	398	422	110	65	2118
Alcyonacea	624	324	227	75	81	119	42	19	1511
Nephtheidae	168	232	193	86	169	76	42	27	993
Ianthella flabelliformis	537	112	93	29	52	17	10	8	858
Porifera	247	51	93	20	117	44	17	12	601
Turbinaria frondens	206	3	6	1	218	58	6	4	502
Solenocaulon sp.	62	12	62	27	117	109	26	34	449
Subergorgia suberosa	221	34	35	19	17	34	8	4	372
Scleractinia	113	5	8	2	59	31	13	7	238
Bebryce sp.	67	60	30	14	2	25	4		202
Sarcophyton sp.	93	16	4		56	9	9		187
Hydroid	71	11	3	7	28	37	14	7	178
Subergorgia sp.	45	18	16	7	28	52	12		178
Annella reticulata	96	26	19	11	3	9	5	1	170
Ianthella basta	106	3	8		6	1			124
Ellisella sp.	23	28	14	1	21	11	3		101
Ascideacea	40	1	7		10	10	5	1	74
Hypodistoma deeratum	3	5	2		7	28	6	20	71
Echinogorgia sp.	6	11	33	5		3			58
Semperina brunea	27	8	9			10	3		57
Cirrhipathes sp.	45		2			3	1		51
Cymbastela coralliophila	10	1			30	6	3	1	51
Xestospongia testudinaria	3	10	3		20	11	2	1	50

Photographs of the some of the more common megabenthos species observed by the Sled and ROV, and images captured from video, are shown in Figure 3-1, Figure 3-2 and Figure 3-3 to accompany the following descriptions.

The sponges (Porifera) most commonly observed by both Sled and ROV were: *Ianthella flabelliformis*, *Cymbastella coralliophila, I. basta* and *Xestospongia testudinaria. I. flabelliformis* are large, regular, fan-shaped sponges up to 1.2 m high. They are several millimetres thick and have a relatively tough, fibrous, mesh-like skeleton, but can be torn. They are attached to the substrate at the base by a tough, fibrous stalk and are generally oriented with the large plane perpendicular to the currents, and bend over with the current. When these sponges are contacted by trawl gear, they are either detached from the substrate at the base or a portion may be torn off. If the trawl path and the current are in the same direction, the trawl may pass over some of these sponges without removing them. The structure and habitat of *I. basta* are similar, but it is thinner in cross-section and more irregular and rippled in shape. *Xestospongia* are solid, barrel-shaped sponges with fluted sides that grow up to about 0.5 m in diameter. If struck by the ground chain of a prawn net, they can be detached completely from the seabed or be broken into pieces. Several of these types of sponges have been observed, by a video camera mounted on the net, to be detached from the substratum by the net and then rolled under the net. *Cymbastella* are low, flat, firm, plate-shaped sponges up to about 0.5 m across. Their prostrate form is such that a chain from a prawn net might pass over them without causing much damage, or catch them under the edge causing damage or removal. Other sponges (usually lump-shaped) were not sufficiently abundant for individual analysis, so were grouped under Porifera.

The gorgonians observed by both Sled and ROV included: *Ctenocella pectinata*, *Dichotella divergens*, *Subergorgia* spp.s, *Annella reticulata*, *Semperina brunea*, *Bebryce* sp., *Echinogorgia* sp. *Ellisella* sp., and the sea-whips *Junceella juncea* (red) and *J. fragilis* (white). The largest gorgonian, *Ctenocella pectinata* grow up to 1 m high and 1.5 m across and, like the fan sponges, orient the plane of their growth form at right angles to the current. The other, smaller, fan gorgonians have a similar habit. *D. divergens* form is more 3-dimensional like a small bush. The rope-like sea-whips may grow more than 3 m long. All the gorgonians have a tough, fibrous skeleton with living tissue and polyps covering the outside like a sheath. They typically flex under the trawl gear, though the polyps may be damaged. *Solenocaulon* sp. forms hollow tubes, also with a tough fibrous structure and living tissue on the outside. They are often present as single stalks or as 3 to 4 stalks with a common base. They typically are thoroughly encrusted with hydroids and other zooanthids attached to the outside, forming a community of invertebrates.

The hard corals observed included *Turbinaria* sp. Often open vase-shaped, it is attached by a stalk at the base and may grow more than 1 m across. They are brittle and are generally broken by trawl gear. Other hard corals (Scleractinia) were free-standing lumps or encrusted over rocks. The soft corals observed included species of *Nephtheidae* (tree shaped) and *Alcyonacea* (cauliflower shaped), which may grow as high as 60-80 cm and have gelatinous bodies embedded with hard sclerites or spines, and the tough and fibrous *Sarcophyton* sp. (inverted toad-stool shaped).

The Ascidians observed were either solitary (eg. *Hypodistoma deerratum*) or in encrusting colonies. The colonial types could not be identified from video, so were all grouped under Ascidiacea. The solitary, free-standing *Hypodistoma deerratum* are bottle-shaped and can be up to 30 cm height with openings at the top about 2 cm in diameter. They are translucent, with a deeply sculptured exterior and a jelly-like texture, and are known to have a rapid, transient 1-2 year life cycle.

The hydroids observed had fine fibrous stems about 1 mm in diameter with several feather-like branches covered in fine, stinging polyps. They were usually colourless and translucent, except for a black stem, which bends with the current. These animals can grow to about 350 mm long.

Cymbastella coralliophila (sponge)

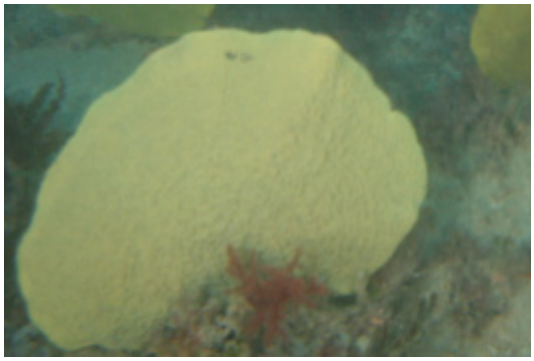

Ianthella flabelliformis (sponge)

Turbinaria frondens (hard coral)

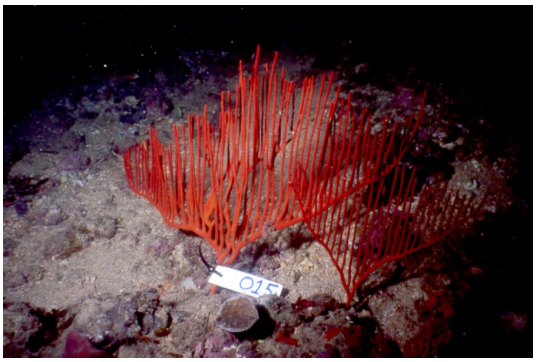

Ctenocella pectinata (gorgonian)

Dichotella divergens (gorgonian)

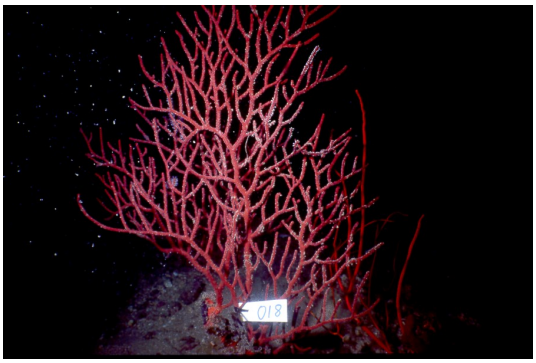

Subergorgia suberosa (gorgonian)

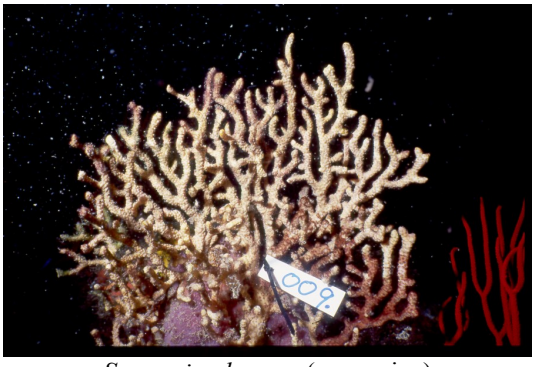

Semperina brunea (gorgonian)

Xestospongia testudinaria (sponge)

Figure 3-1: Photographs of some megabenthos species analysed

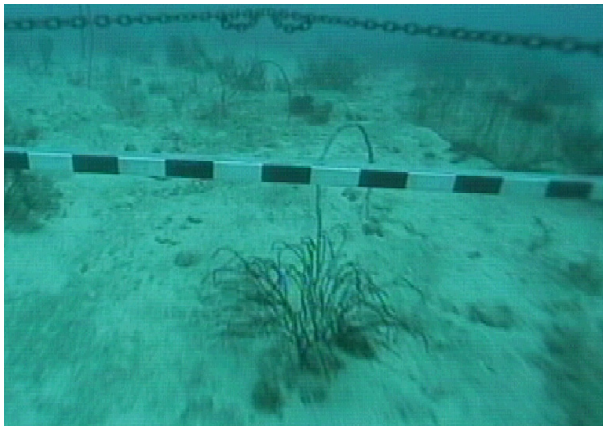

Junceella fragilis (whip) and
Dichotella divergens (gorgonian)

Junceella fragilis (whips) and
Turbinaria frondens (hard coral)

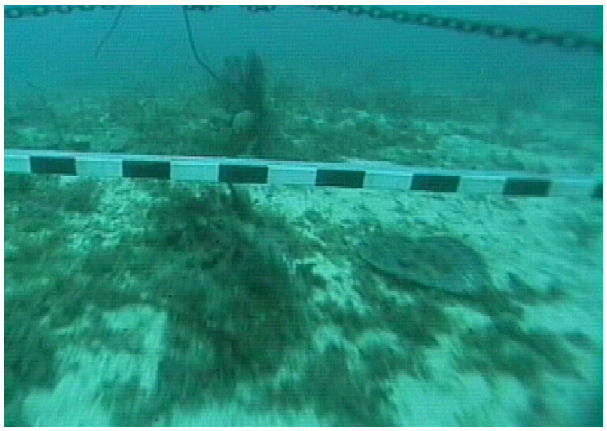

Cymbastella coralliophila (sponge)

Ctenocella pectinata (gorgonian) and whip

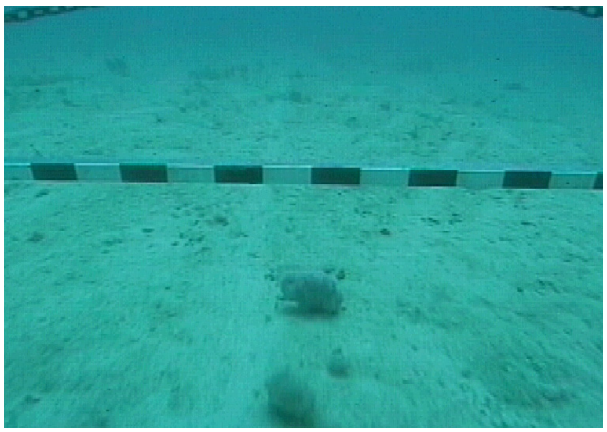

Alcyonacea (soft coral)

Hypodistoma deeratum (ascidian)

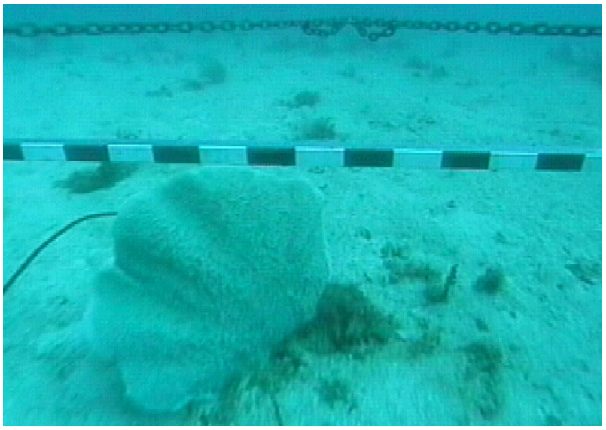

Ianthella flabelliformis (sponge)

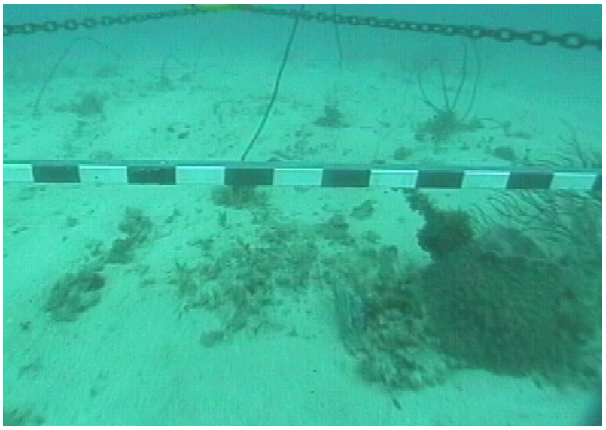

Xestospongia sp. (sponge)

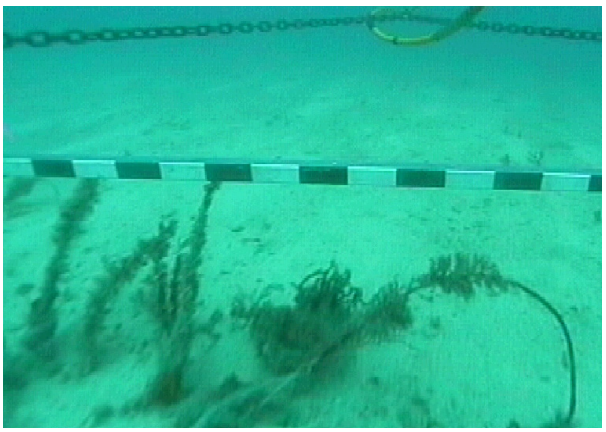

Solenocaulon sp (gorgonian)
and encrusted whip

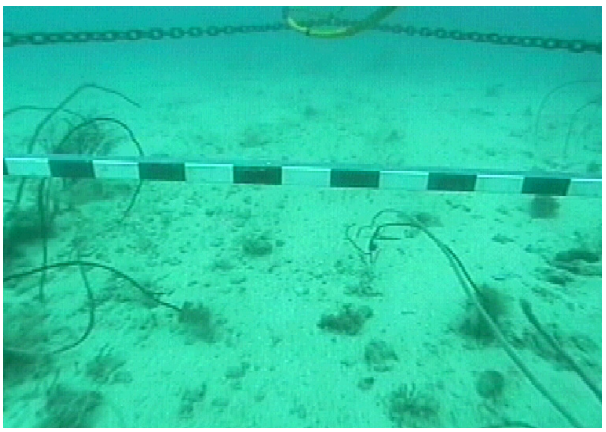

Junceella juncea (red whips)
and *J. fragilis* (white whips)

Porifera (sponge unidentified)

Nephtheidae (soft coral)

Figure 3-2: Sled video images of selected megabenthos species analysed

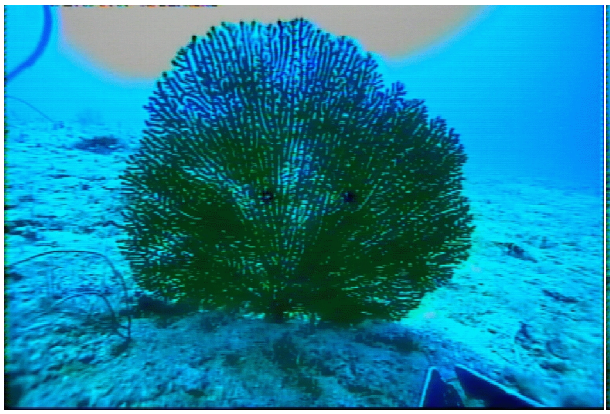

Annella reticulata

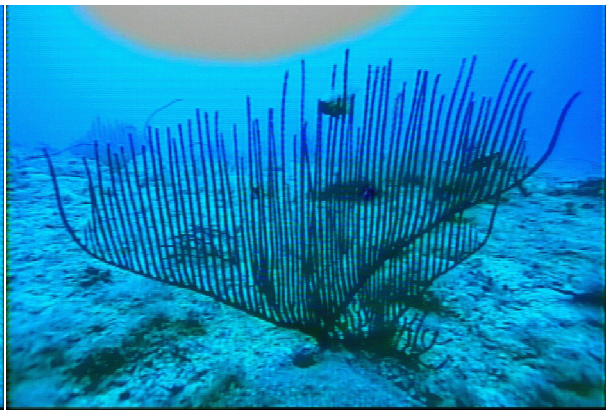

Ctenocella pectinata

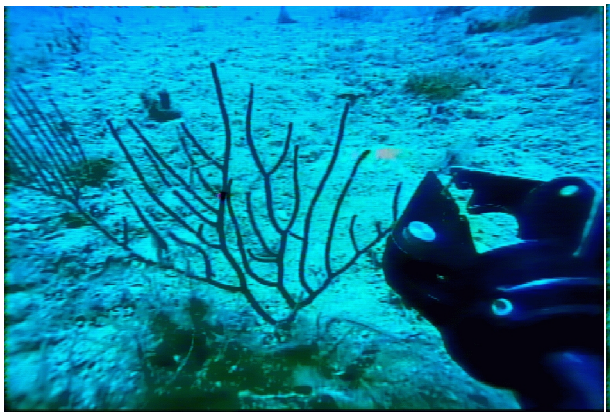

Subergorgia suberosa

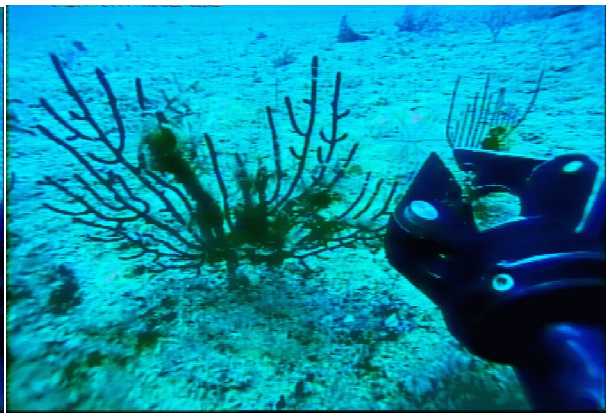

Echinogorgia sp.

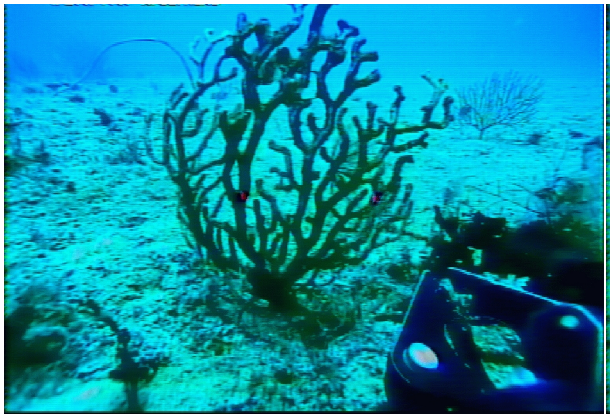

Semperina brunea

Junceella fragilis (whip) *Turbinaria* sp. (coral)

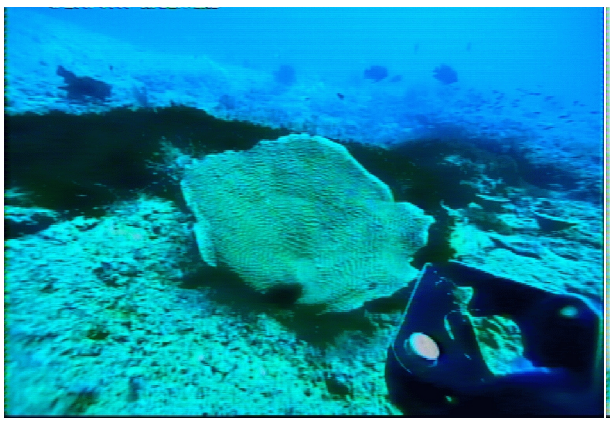

Turbinaria frondens

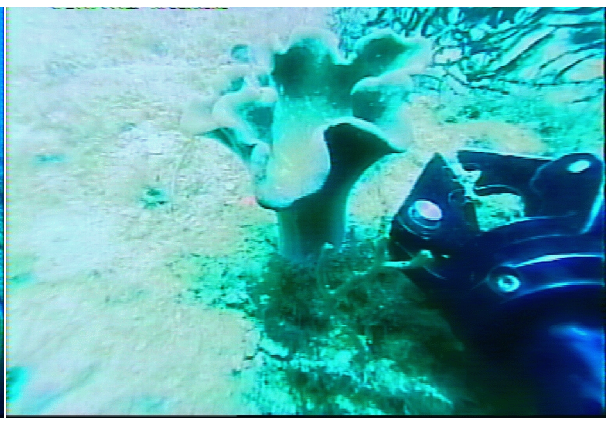

Sarcophyton sp.

Ianthella flabelliformis

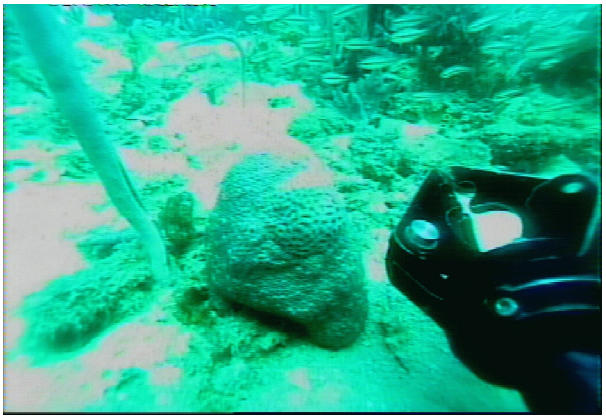

Scleractinia (hard coral)

Solenocaulon sp.

Nephtheidae

Dichotella divergens

Bebryce sp.

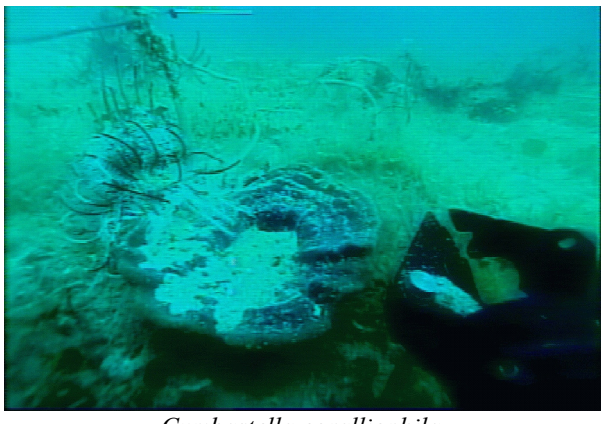

Cymbastella coralliophila

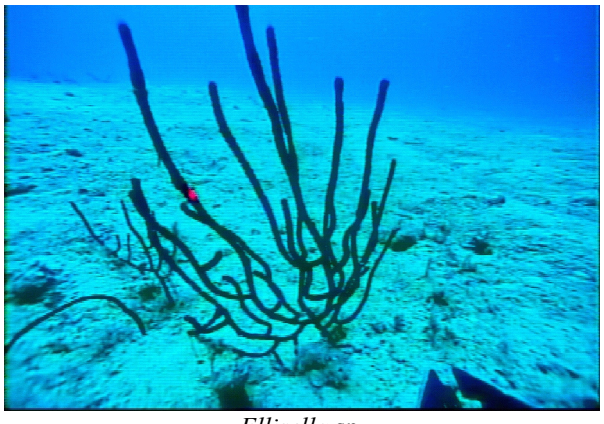

Ellisella sp.

Figure 3-3: ROV video images of selected megabenthos species analysed

3.3 Results by species

A few species were abundant or very abundant and dominated the physical structure of the sessile megabenthos assemblages in the area, ie. *Ctenocella pectinata*, *Junceella juncea*, *Ianthella flabelliformis* and *Dichotella divergens*. On the other hand, many of the species considered frequent enough to attempt analysis were rather patchy in occurrence among the factors analysed, which meant that it was challenging to identify a depletion-recovery signal among the natural variability — particularly when effect sizes were small, even though they may have been real. Further, the natural variability in these sessile faunal assemblages, even among the more numerous taxa, was substantial and dominated the data. In all cases the random effects and natural variability exceeded the signal that the analyses were intended to detect, often by as much as or more than, an order of magnitude.

In this section, results for attributes measured and analysed are described by species, grouped into approximate categories of high, medium and low rates of impact and recovery (acknowledging substantial uncertainty in these catgories and some conflicting indications from Sled and ROV data or different models fitted) — and then in order of abundance, as tabulated below (Table 3-6). Figures of the results are presented with the text for several of the more abundant species.

Table 3-6: Species grouped into approximate categories of high, medium and low rates of impact and recovery and ordered by abundance.

Impact \ Recovery	Slow	Medium	Fast
High		*Sarcophyton* sp.	*Turbinaria frondens* *Subergorgia* sp. *Annella reticulata* *Ianthella basta* *Semperina brunea* *Ellisella* sp. *Xestospongia testudinaria* *Bebryce* sp. Ascideacea
Medium	*Subergorgia suberosa* *Cymbastela coralliophila* *Echinogorgia* sp.	*Ctenocella pectinata* *Ianthella flabelliformis* Nephtheidae Scleractinia *Hypodistoma deeratum*	Porifera
Low	Alcyonacea *Junceella fragilis* *Solenocaulon* sp.	*Junceella juncea* *Dichotella divergens*	

As described in the methods, several submodels were analysed and the first consideration regarding analysis results was the model comparison tests. These helped decide the most appropriate model fit to the data. Typically five models were fitted and the sequence of tests was 5 vs 4, 4 vs 3, 3 vs 2, 2 vs 1 and testing ceased when the more complex model could not be rejected, ie. the test was significant. The differences between the fixed effects of the five models were:

Model 5: Topography + Intensity + Time*Intensity + Time²*Intensity + Time*Intensity²
Model 4: Topography + Intensity + Time*Intensity + Time²*Intensity
Model 3: Topography + Intensity + Time*Intensity
Model 2: Topography + Intensity
Model 1: Topography

Models 4 and 5 make some allowance for variable recovery rate changes with respect to Time and trawl Intensity. Model 3 was the constant rate impact-recovery model and was usually the minimum model presented because it included the recovery term (ie. Time*Intensity). In some cases, the model 2 vs 1 test could provide an indication of the significance of trawl Intensity.

In order to facilitate interpretation of the results, some schematic diagrams of various types of possible response models are presented below. An idealised scenario might be: tests of model comparisons 5 vs 4 and 4 vs 3 are rejected, allowing consideration of a simpler model 3, which may show moderate impact and recovery (eg. Figure 3-4) — greater and lesser rates of impact and recovery are possible, as are positive impact and/or negative recovery. If the model comparisons do not reject model 4 then the Time²*Intensity term needs to be considered, which may slow or hasten recovery with time (eg. Figure 3-5a). If the model comparisons do not reject model 5 then the Time*Intensity² term needs to be considered, which may lead to different recovery rates at diffent trawl intensities (eg. Figure 3-5b). Many potential alternate scenarios exist depending on the relative rates, signs and combinations of all terms.

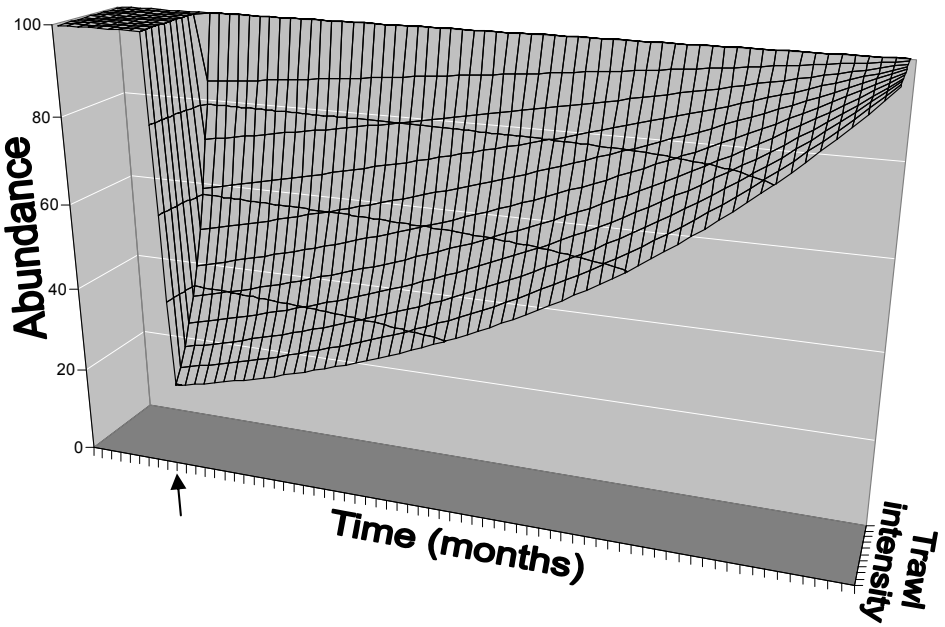

Figure 3-4: Schematic diagram of idealized impact and recovery model type 3 for a moderate negative impact of ~ -15% per trawl and moderate positive recovery of ~ +3.3% per year per trawl. Potential alternates include different rates of impact and recovery, or even positive impact and/or negative recovery.

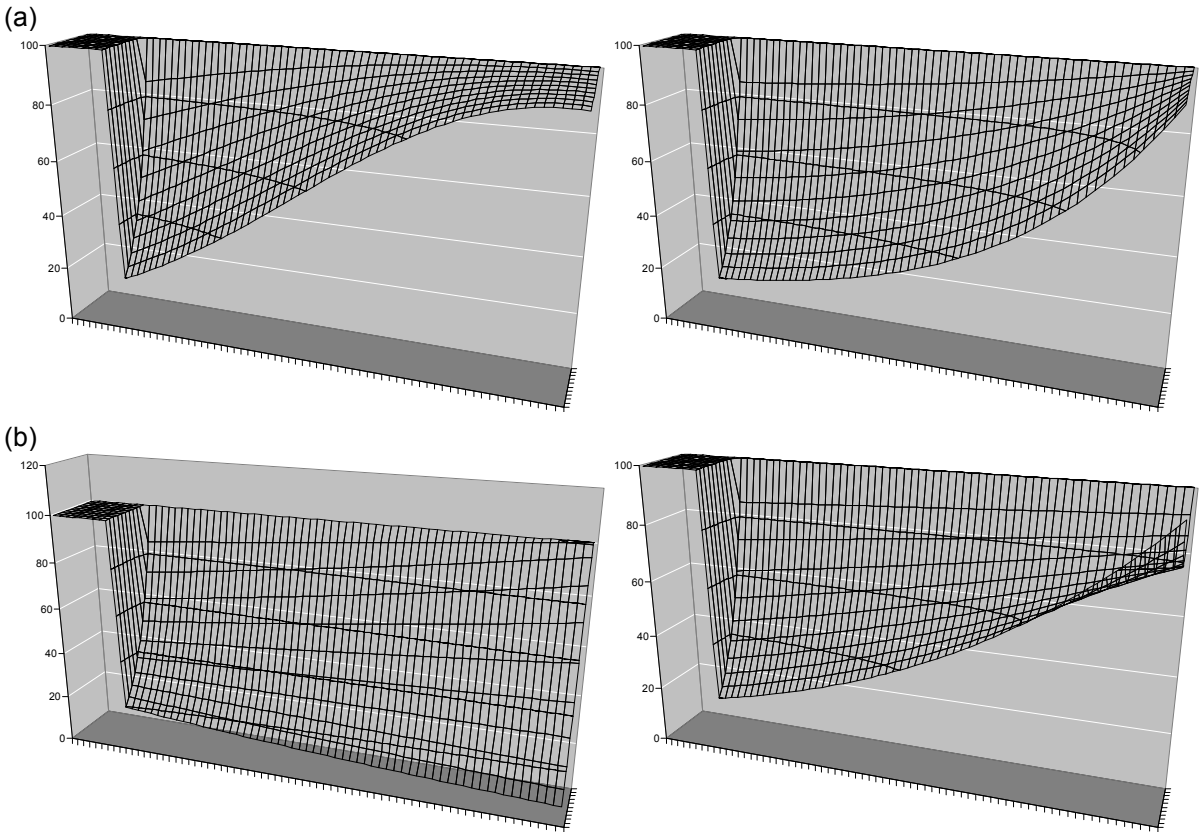

Figure 3-5: Schematic diagrams of alternative impact and recovery models: (a) type 4, (left) moderate impact with fast intial recovery due to large positive Time*Intensity term that slows due to negative Time²*Intensity term and (right) moderate impact with slow intial recovery due to small positive Time*Intensity term that becomes faster due to positive Time²*Intensity term; (b) type 5, (left) moderate impact with recovery at low intensity due to a positive Time*Intensity term but ongoing decline at high intensity due to negative Time*Intensity² term and (right) moderate impact with slow intial recovery due to small positive Time*Intensity term that is faster at high intensity due to a positive Time*Intensity² term. Many potential alternatives include different rates, signs and combinations of all terms.

3.3.1 Medium impact, medium recovery

3.3.1.1 Ctenocella pectinata

3.3.1.1.1 Abundance (numbers/density)

The gorgonian fan *Ctenocella pectinata* was abundant on Sled tracks, typically about 20 per Sled replicate. These gorgonians were visually and structurally the most dominant animals in seabed habitat gardens. On most Sled tracks, raw numbers appeared to increase from surveys before impact to 1 month after, then decrease at months 10 or 23 or both, and either increase (on low-intensity strata) or decrease (controls and high-intensity strata) by month 61. Models 5 and 4 were rejected and model 3 fit to these data followed each plot-track through time and indicated that deep tracks tended to have greater and more variable abundance than shallow tracks, and that deep control tracks in particular tended to decrease by month 61 (Figure 3-6a). The model 3 vs 2 test was significant (p = 0.0263) suggesting that the Time*Intensity recovery term was required. Test of coefficients of model 3 fixed effects, which included change after trawling on impacts relative to controls, suggested a depth effect (p < 0.0001), an impact effect (approximately -9.8% per trawl, p = 0.0339); and recovery after trawling (approximately +2.7% per year per trawl, p = 0.0115) (Figure 3-6b).

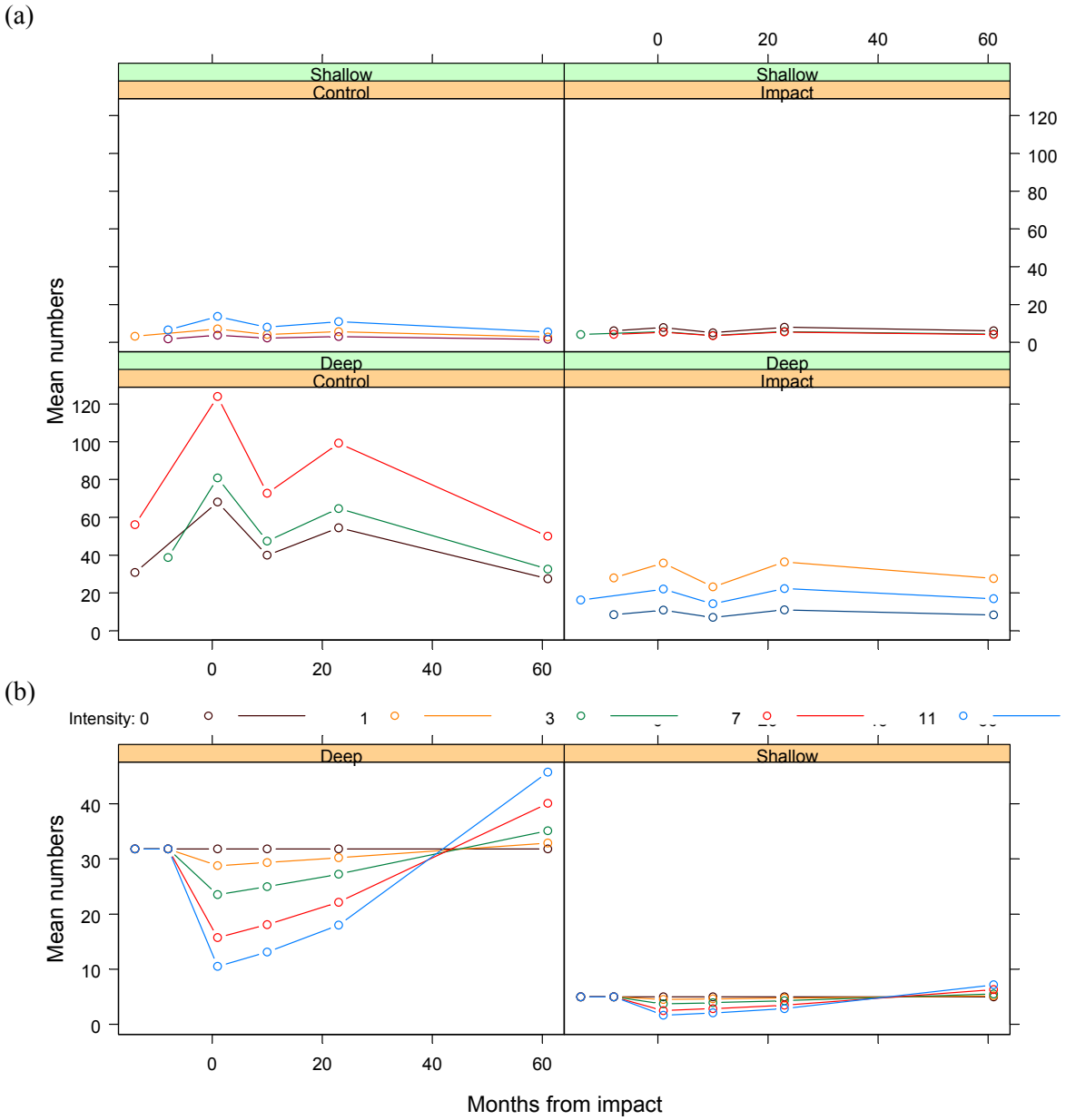

Figure 3-6: Plots of model 3 fit to numbers of *Ctenocella pectinata* per Sled track by month: (a) fixed and random effects less residual variation (coloured lines follow individual tracks), (b) fixed effects only (coloured lines show predictions for different trawl intensities). Note that plots (a) and (b) have different scales.

Ctenocella pectinata, like most structural benthos, were more numerous in habitat patches surveyed by the ROV than elsewhere on Sled tracks, with typical numbers in the order of 30 per patch. On several control patches, census numbers appeared to increase from month 10 to 20, then decrease slightly by month 61. On impact patches, there was little obvious evidence of recovery, but some decreases to months 23 or 61. The model comparisons for census numbers indicated that model 4 was significant (p = 0.0276) and suggested a decline from month 10 to 23 then a levelling off relative to changes on controls (Figure 3-7), but neither the intensity or recovery terms were significant. The model comparisons for ROV numbers standardised for patch footprint-area did not distinguish among models. Model 3 indicated continued decrease in density on trawled areas (Figure 3-8), but again neither the intensity nor recovery coefficients were significant. All models confirmed that deep patches had significantly higher numbers/densities of *Ctenocella pectinata*.

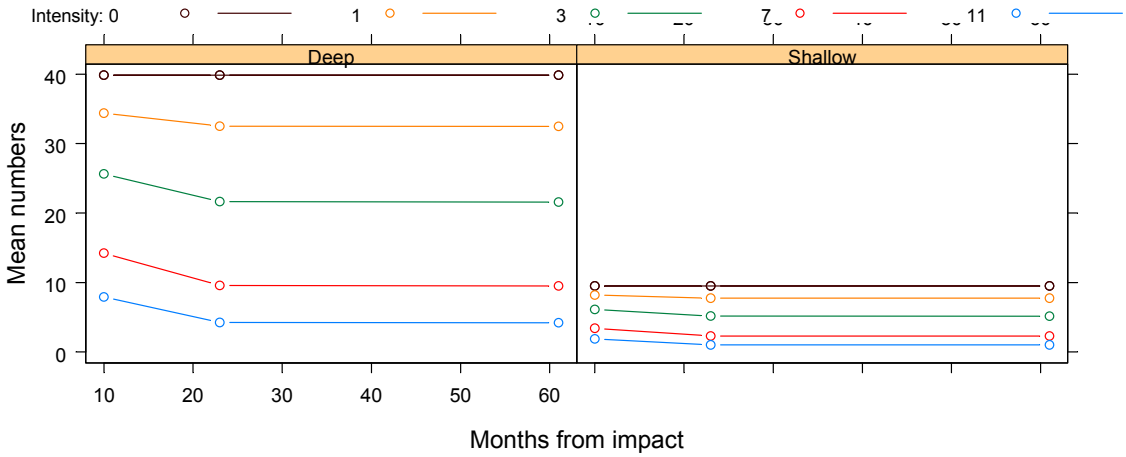

Figure 3-7: Plots of model 4 predictions for ROV patch census numbers for *Ctenocella pectinata* against month after impact, by depth. The predictions show only the fixed effects and attempt to isolate the recovery signal from other sources of variation. The coloured lines show predictions for different trawl intensities.

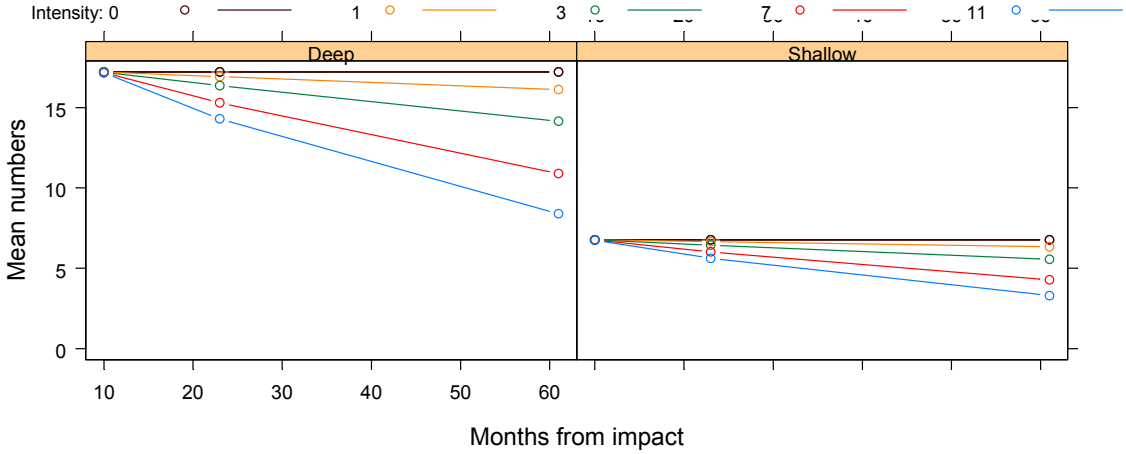

Figure 3-8: Plots of model 3 predictions for ROV patch density for *Ctenocella pectinata* against month after impact, by depth. These represent census counts standardised for patch footprint-area, and are scaled to average patch footprint area. The predictions show only the fixed effects and attempt to isolate the recovery signal from other sources of variation. The coloured lines show predictions for different trawl intensities.

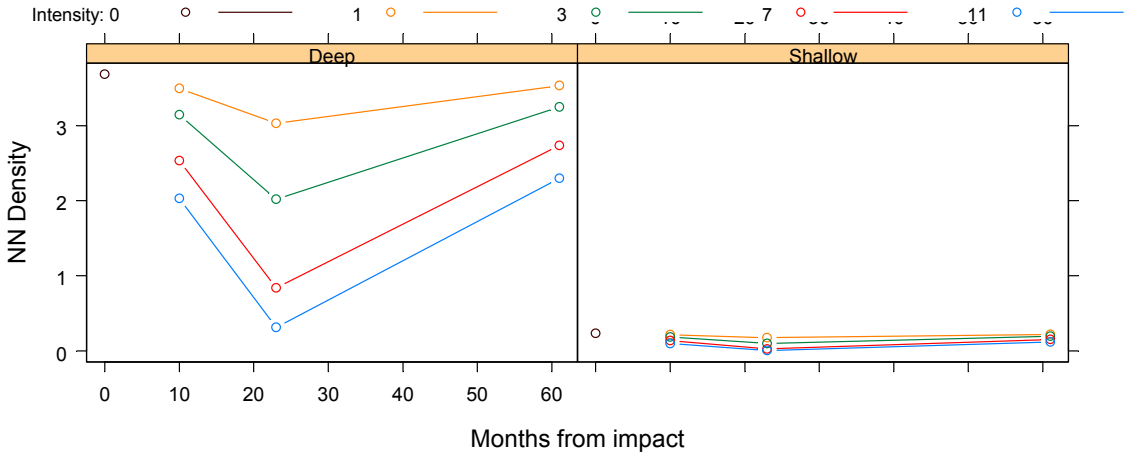

Figure 3-9: Plots of model 4 predictions for ROV nearest-neighbour densities (number per m²) for *Ctenocella pectinata* against month after impact, by depth. These represent transformed nearest-neighbour distances (see methods). The predictions show only the fixed effects and attempt to isolate the recovery signal from other sources of variation. The coloured lines show predictions for different trawl intensities.

The model comparisons for ROV individual nearest-neighbour densities indicated that model 4 was significant (p = 0.0253) and suggested no initial intensity effect (positive, but NS) followed by a significant decline to month 23 (p = 0.0279) and then recovery (p = 0.0219) (Figure 3-9). This is consistent with a scenario of delayed mortality and thinning out of individuals, and to some extent with the patterns in some of the census and patch-density data for this species.

3.3.1.1.2 Size attributes

The pattern of size-distributions for *Ctenocella pectinata* by trawl strata and months differed between deep and shallow Sled tracks. At month 1 on deep tracks, across trawl strata the larger size classes were progressively less frequent; but with time, the size structure of the trawled populations tended to progress to larger individuals while maintaining a high proportion in smaller classes, presumably due to recruitment (Figure 3-10). Over the same period, the controls appeared relatively stable. This pattern would be consistent with impact and recovery. At month 1 on shallow tracks, however, a notable decrease in numbers on higher intensity strata was accompanied by a reduction in the breadth of the size-structure but not to smaller classes. Then with time, the size-structures did not appear to progress as clearly as on the deep tracks, except perhaps for controls and stratum (1,5] at month 10 or 23.

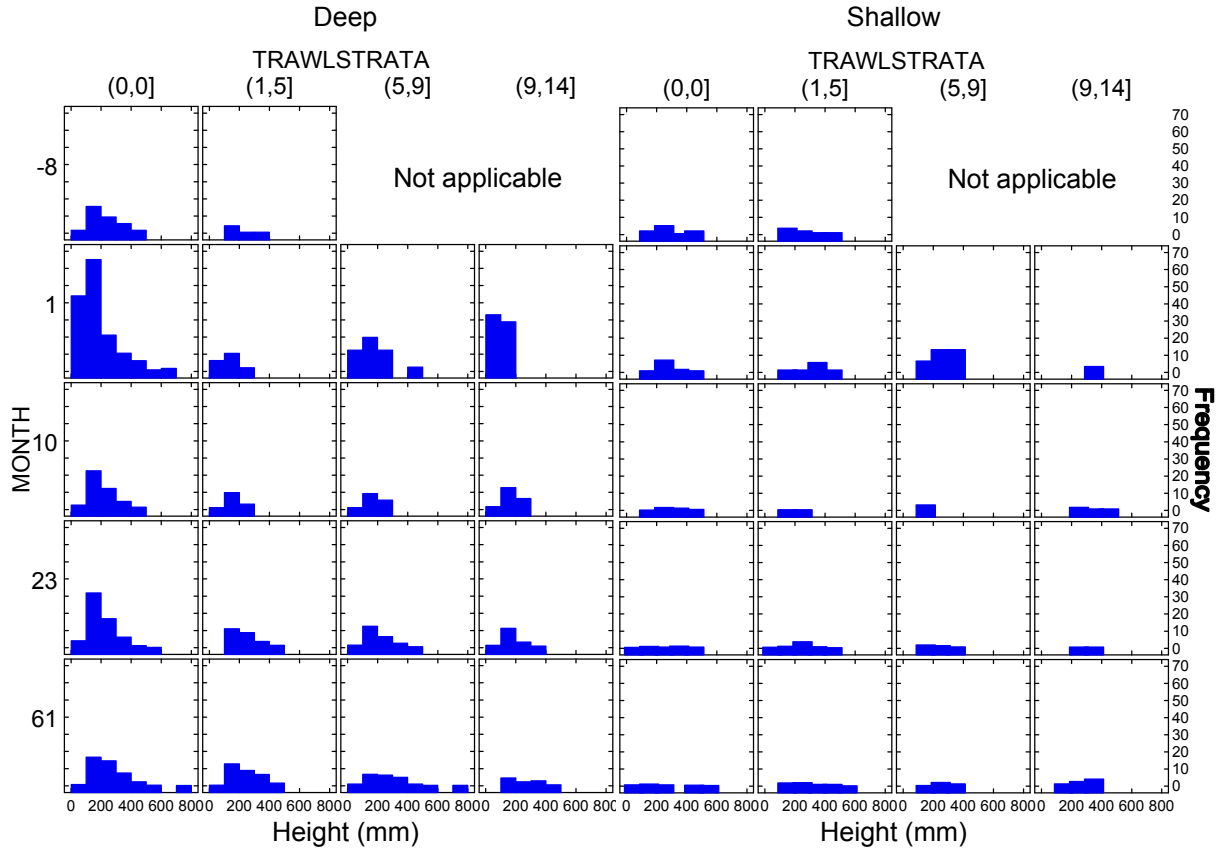

Figure 3-10: Size-frequency distributions of *Ctenocella pectinata* heights observed by the Sled, by depth, trawl intensity strata (columns) and month after impact (rows), standardized by Sled swept area. Size categories are 100 mm intervals. Note that the "before" status of impact tracks is indicated by month –8 and trawl strata (1,5], which includes the single coverage of the earlier BACI experimental plots; the higher intensity strata did not occur until the repeated-trawling experiment.

Analysis model comparisons of Sled heights indicated only model 1 (Topography) was significant ($p < 0.0001$). Model 3 predictions of heights of individual *Ctenocella pectinata* confirmed that animals on shallow tracks were taller and suggested a slight decrease with trawl intensity at month 0 that was consistent with an impact effect, followed by small increases with subsequent surveys (Figure 3-11); however, neither the impact nor recovery coefficients were significant.

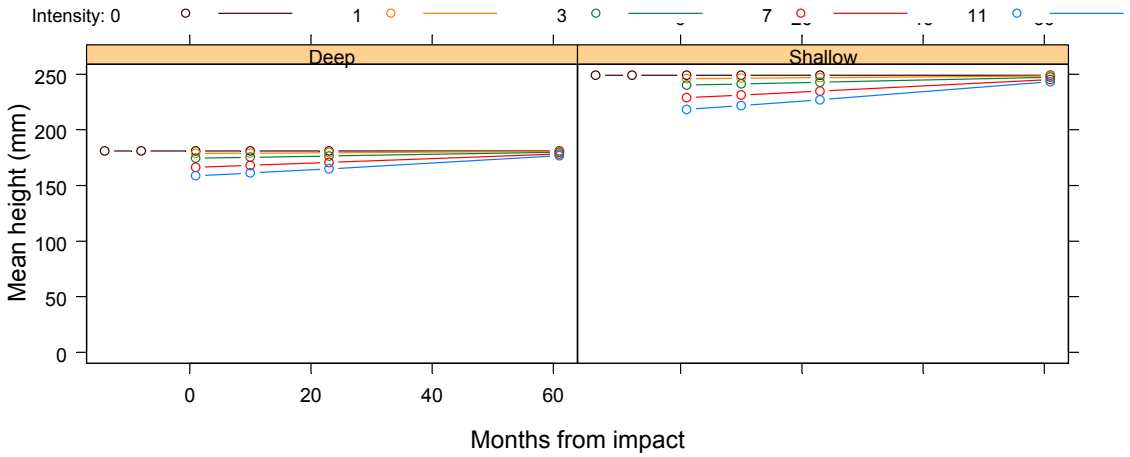

Figure 3-11: Plots of model 3 predictions for mean heights of individual *Ctenocella pectinata* observed by the Sled against month after impact, by depth. The predictions show only the fixed effects and attempt to isolate the recovery signal from other sources of variation. The coloured lines show predictions for different trawl intensities.

The size-structure of the *Ctenocella pectinata* populations observed by the ROV, at month 10, on more heavily trawled strata of deep patches tended to be of smaller individuals than on controls — a pattern consistent with a differential trawl effect on larger individuals. This pattern appeared to strengthen with time, with little if any indication of recovery (Figure 3-12). On shallow patches, however, such differences in size-structure across trawl strata were less clear.

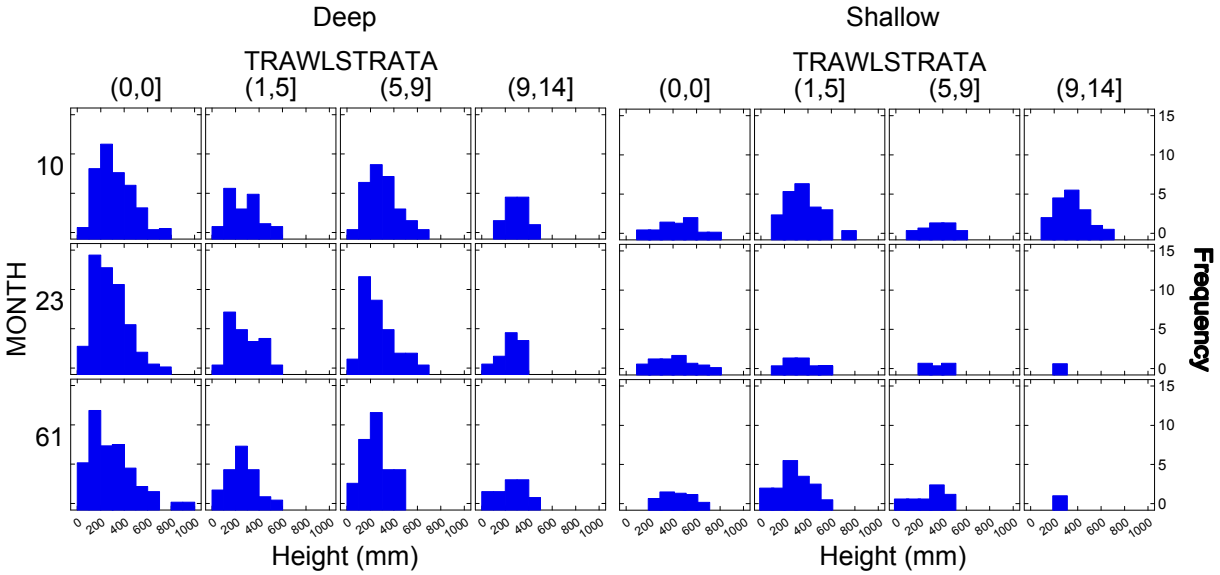

Figure 3-12: Size-frequency distributions of *Ctenocella pectinata* heights observed by the ROV, by depth, trawl intensity strata (columns) and month after impact (rows), standardized by number of replicate observations. Size categories are 100 mm intervals.

The model comparisons for individual *Ctenocella pectinata* heights measured by the ROV supported model 1 (a Topography effect $p = 0.0003$). Model 3 indicated a slight negative trawl intensity effect and continued decrease in height on trawled areas (Figure 3-13a), but neither the intensity nor recovery coefficients were significant. Results for width and area were similar, although the recovery trend was positive in both cases and the model comparisons for area give some support for model 2 (a trawl impact $p = 0.06$). Again, however, neither the intensity nor recovery coefficients were significant.

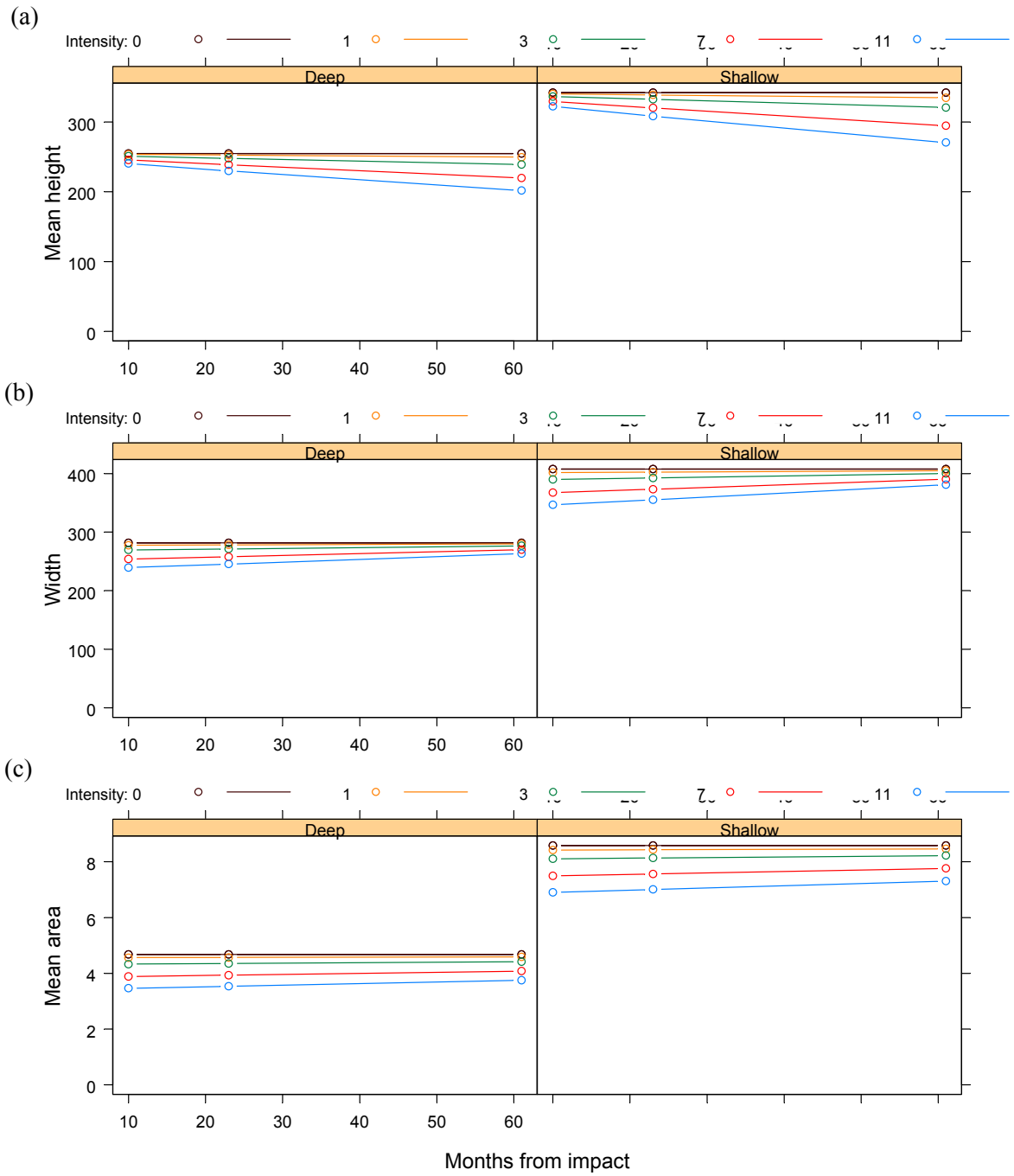

Figure 3-13: Plots of model 3 predictions for measured (a) height, (b) width and (c) area of *Ctenocella pectinata* observed by the ROV, against month after impact, by depth. The predictions show only the fixed effects and attempt to isolate the recovery signal from other sources of variation. The coloured lines show predictions for different trawl intensities.

3.3.1.1.3 Condition index

The raw indices of condition of *Ctenocella pectinata* varied among Sled track replicates and time. A small proportion of *Ctenocella pectinata* on both impact and control tracks were in poor condition initially, and there were indications of some individuals being in worse condition at month 10, and generally, improved condition at month 61. This was consistent with field observations of the occurrence of some *Ctenocella pectinata* on impact tracks with missing fingers and/or branches, and/or branches having had living polyps stripped from their skeletons at month 1, and these stripped areas being encrusted by other organisms at month 10. The model comparisons for *Ctenocella pectinata* condition on Sled tracks did not distinguish among models. Model 3 (Figure 3-14) hinted that relative to controls (i.e. fixed effects only), *Ctenocella pectinata* on impact tracks tended to become slightly poorer in condition after impact and then improve; however, the model coefficients were not significant.

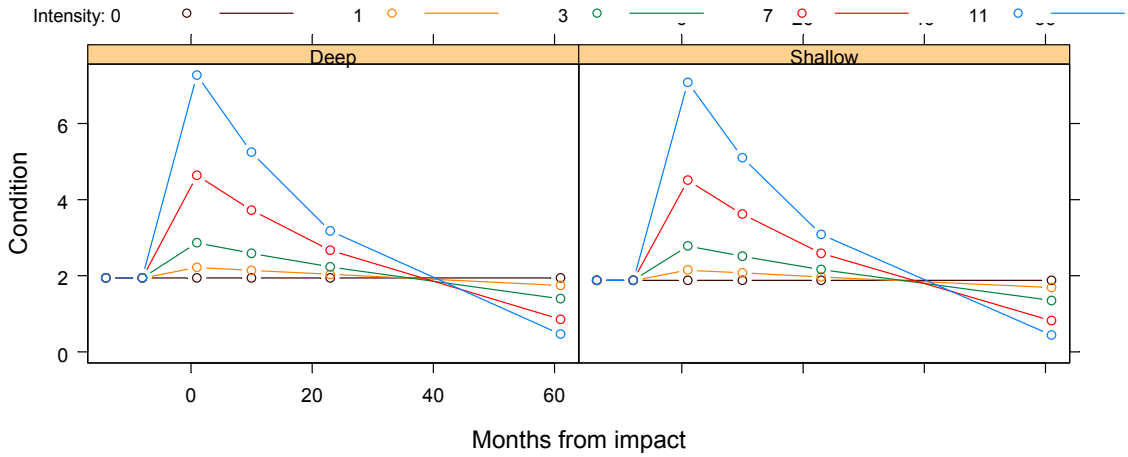

Figure 3-14: Plots of model 3 predictions for *Ctenocella pectinata* Condition Index (%) observed by the Sled. Poorer condition is indicated by values >0. The predictions show only the fixed effects and attempt to isolate the recovery signal from other sources of variation. The coloured lines show predictions for different trawl intensities.

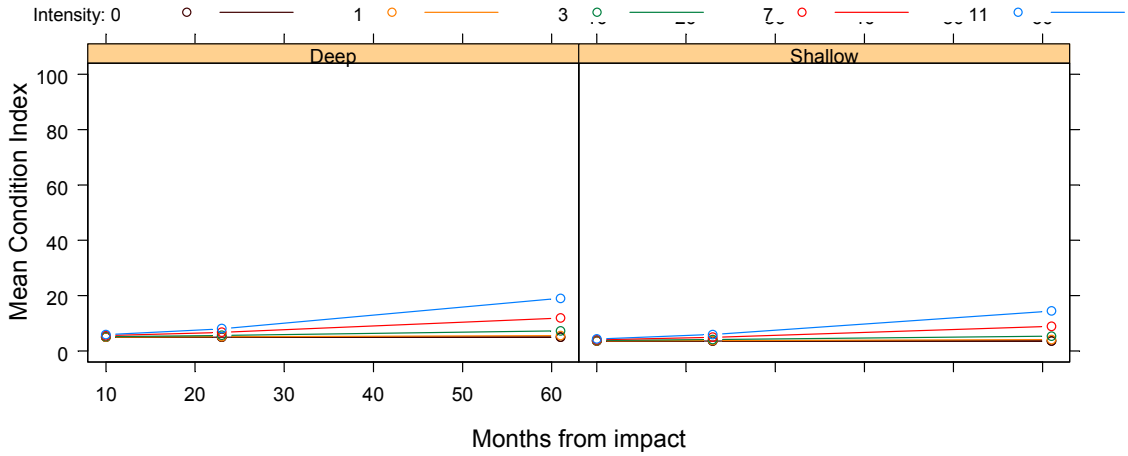

Figure 3-15: Plots of model 3 predictions for *Ctenocella pectinata* Condition Index (%) observed by the ROV. Poorer condition is indicated by values >0. The predictions show only the fixed effects and attempt to isolate the recovery signal from other sources of variation. The coloured lines show predictions for different trawl intensities.

The raw condition index for *Ctenocella pectinata* on ROV patches seemed to show a similar pattern to the Sled data, with condition on impact patches appearing to be worse at month 10 and/or 23, and then appearing to improve by month 61 on some patches. However, the model comparisons did not distinguish among models and Model 3 (Figure 3-15) showed no evidence of an impact and hinted at a worsening of condition with time ($p = 0.085$).

3.3.1.1.4 Summary

Ctenocella pectinata appeared to show a significant impact effect of around -10% per trawl, followed by significant recovery within the time frame of the Project (5 years) — at least for the Sled transects. The evidence for recovery on ROV patches was mixed; depending on the view of the data, abundance initially decreased then might have stayed about the same, declined further or increased.

There may also have been weak negative trawl effects on mean size of *Ctenocella pectinata*, hinting that larger individuals might be more vulnerable to removal, followed by some recovery. However, model coefficients were not significant.

In the field, there appeared to be clear indications of impact effects on condition of *Ctenocella pectinata*, followed by recovery — but analyses of the Sled data, though suggestive of this pattern, were not significant and analysis results for animals on ROV patches were similar.

While interpretation would be more straightforward if both Sled and ROV results were consistent, the animals observed by the two methods have limited overlap. The Sled passed quickly through ROV patches and would have observed only a small proportion of those patch animals observed by the ROV. Also, the Sled also passed over much larger areas between patches, which provided the opportunity to observe the recovery of other animals that may have been impacted in other patches or in the different inter-patch habitat.

3.3.1.2 Ianthella flabelliformis

3.3.1.2.1 Abundance (numbers/density)

The sponge *Ianthella flabelliformis* was moderately common on Sled tracks, with typical numbers of about 10 per Sled replicate. These large, flat, erect sponges were one of the main contributors to the structure of seabed habitat gardens. Abundance was notably higher on deep tracks, where the patterns of density on impact tracks suggested a decrease after trawling, with indications of a subsequent recovery — perhaps less so on high-intensity areas.

The model comparisons provided strong support for Model 2 ($p = 0.0009$), indicating that the Intensity term was likely to be important. Model 3 fit to these data indicated that deep control tracks tended to have more variable abundance than other tracks (Figure 3-16 a). The fixed effects indicated substantial depth differences ($p < 0.0001$) and that, relative to controls, impact tracks were substantially depleted (approximately -20.6% per trawl, $p < 0.0001$) and there was good evidence for a recovery after trawling (approximately +3.8% per year per trawl, $p = 0.004$) (Figure 3-16 b).

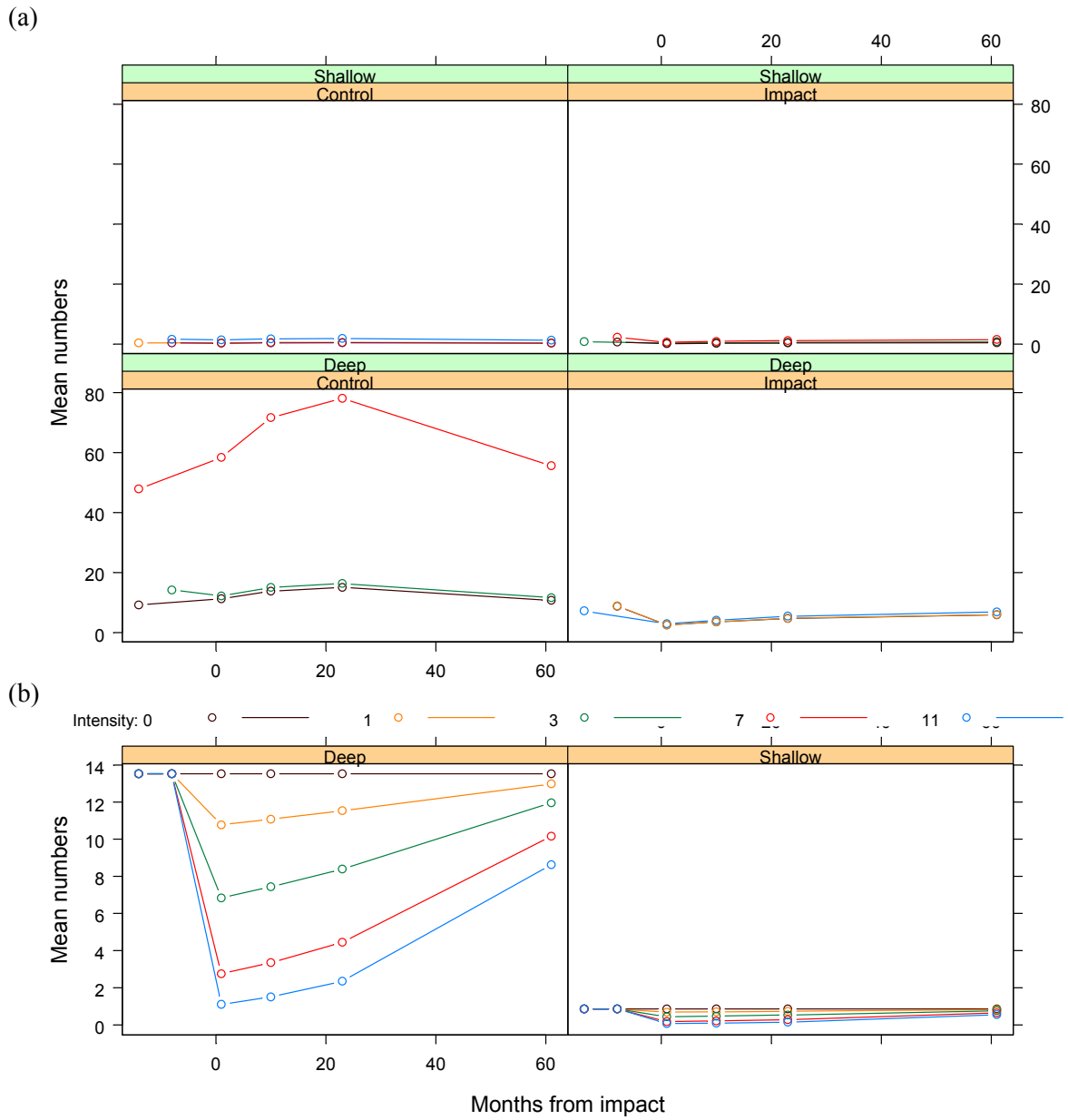

Figure 3-16: Plots of model 3 fit to numbers of *Ianthella flabelliformis* per Sled track by month: (a) fixed and random effects less residual variation (coloured lines follow individual tracks), (b) fixed effects only (coloured lines show predictions for different trawl intensities).

Ianthella flabelliformis was the second most important structural contributor to ROV patches after *Ctenocella*, and numbers typically were about 10 per patch. Abundance was notably higher on deep patches. On impact patches, census numbers tended to be lower in higher-intensity strata and there were trends indicative of some recovery over the period of observations.

The model comparisons provided strong support for Model 2 ($p = 0.0009$), indicating that the Intensity term was likely to be important. Model 3 fit to the *Ianthella flabelliformis* census data showed significant Intensity term ($p = 0.0005$) and hinted of a slight but non-significant ($p = 0.717$) recovery (Figure 3-17). The model comparisons for ROV numbers standardised for patch footprint-area also supported Model 2 ($p = 0.0077$), but the model 2 intensity coefficient was not significant and there was a slight but non-significant decline after impact ($p = 0.953$) (Figure 3-18).

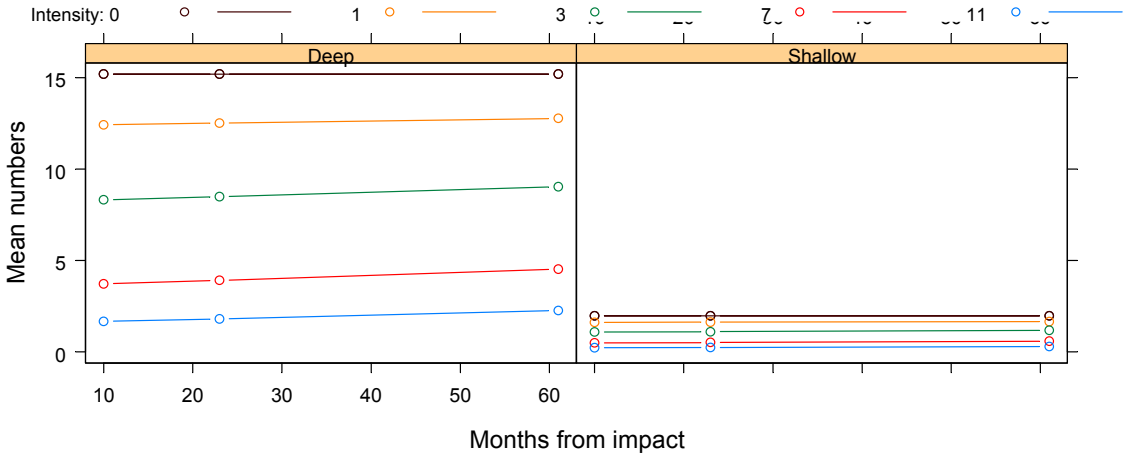

Figure 3-17: Plots of model 3 predictions for ROV patch census numbers for *Ianthella flabelliformis* against month after impact, by depth. The predictions show only the fixed effects and attempt to isolate the recovery signal from other sources of variation. The coloured lines show predictions for different trawl intensities

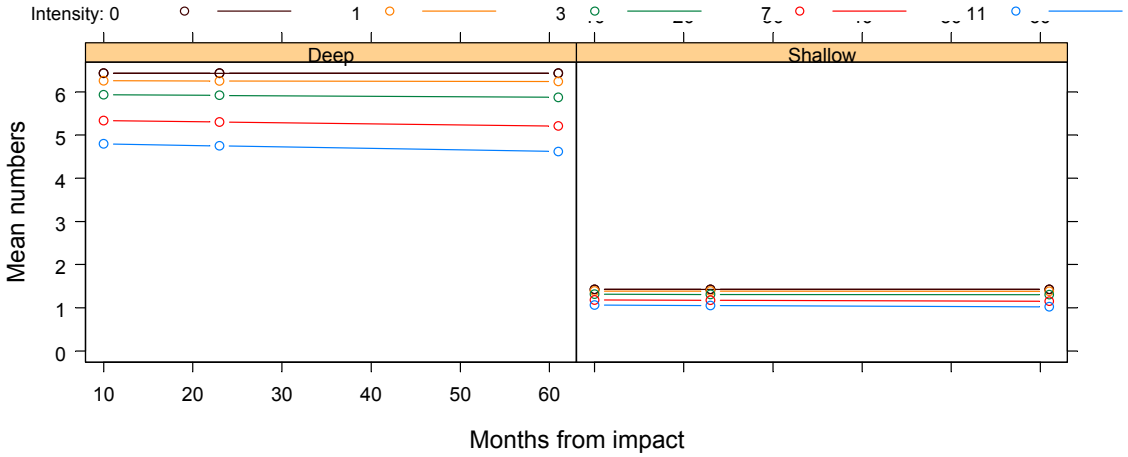

Figure 3-18: Plots of model 3 predictions for ROV patch density for *Ianthella flabelliformis* against month after impact, by depth. These represent census counts standardised for patch footprint-area, and are scaled to average patch footprint area. The predictions show only the fixed effects and attempt to isolate the recovery signal from other sources of variation. The coloured lines show predictions for different trawl intensities.

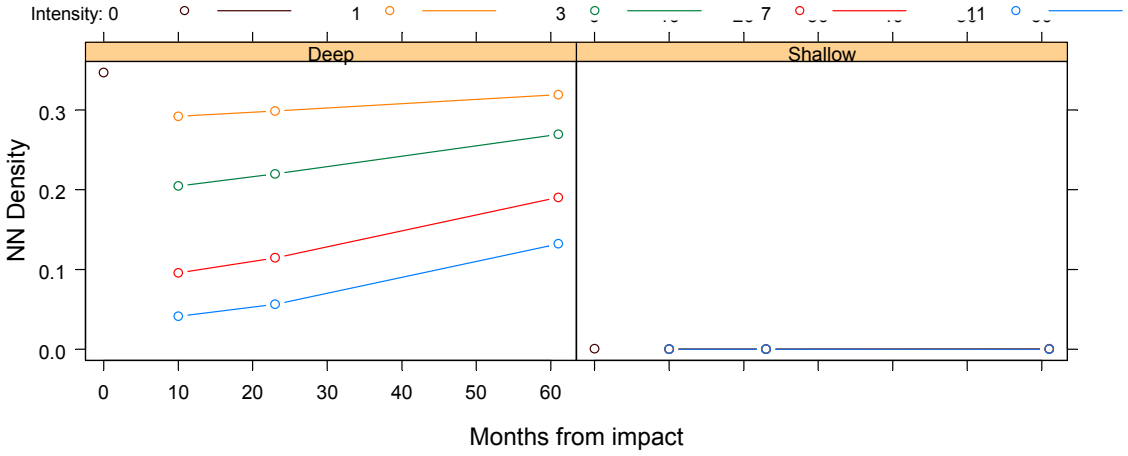

Figure 3-19: Plots of model 3 predictions for ROV nearest-neighbour densities (number per m²) for *Ianthella flabelliformis* against month after impact, by depth. These represent transformed nearest-neighbour distances (see methods). The predictions show only the fixed effects and attempt to isolate the recovery signal from other sources of variation. The coloured lines show predictions for different trawl intensities.

The model comparisons for ROV individual nearest-neighbour densities also indicated that Model 2 was significant (p = 0.0056). Model 3 showed evidence of an initial decrease with trawl-intensity consistent with impact (approximately -25.8% per trawl, p = 0.0141) followed by a slow recovery (but p = 0.401) (Figure 3-19).

All models confirmed that deep patches had significantly higher numbers/densities of *Ianthella flabelliformis*.

3.3.1.2.2 Size attributes

Ianthella flabelliformis was much more abundant on deep Sled tracks where the pattern of size-distributions by trawl strata and months was indicative of an impact on size structure, followed by some recovery (Figure 3-20). At month 1, across trawl strata, the size structures were narrower and the larger size classes were less frequent. With time, the size structures of the trawled populations progressed to larger classes while retaining smaller classes. Over the same period, controls were relatively stable. On shallow tracks these sponges were very sparse; nevertheless the patterns of size-distributions were similar, although they increased on the control, as well as the impact tracks.

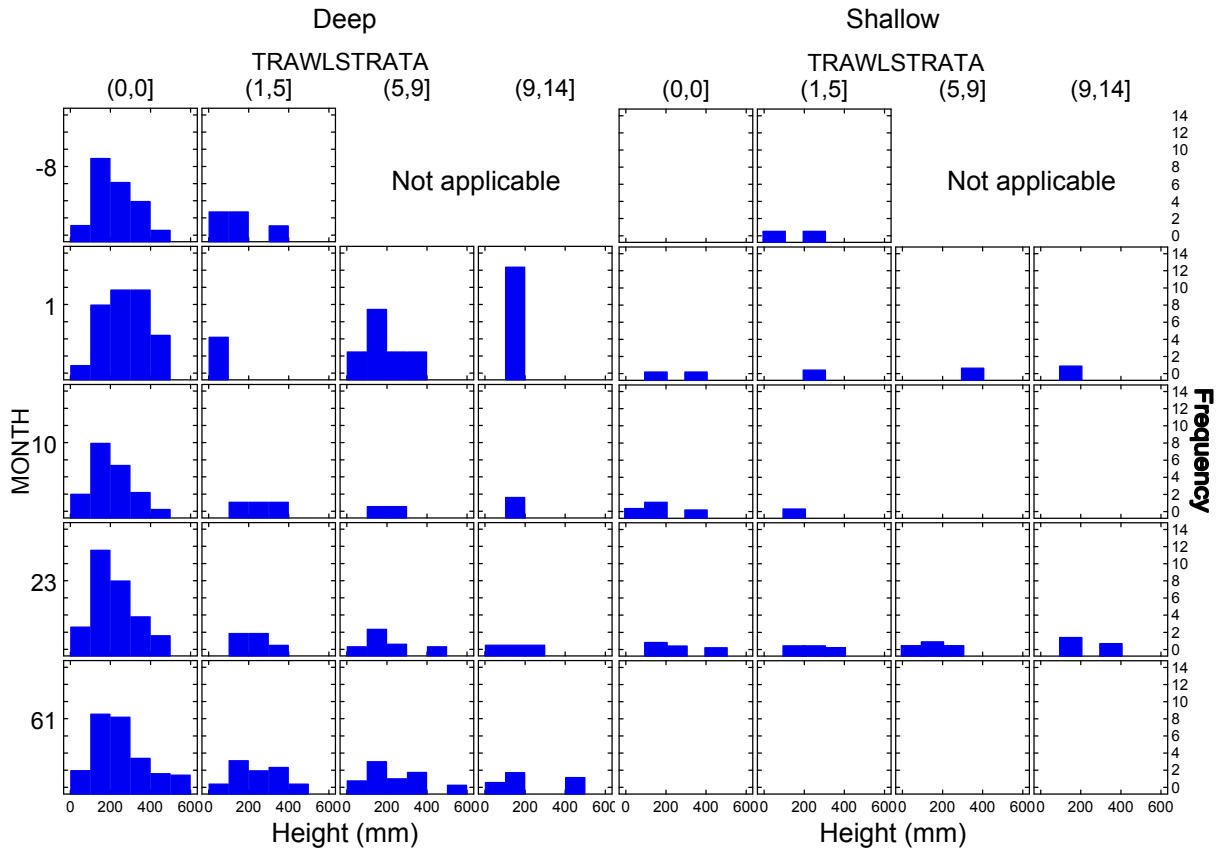

Figure 3-20: Size-frequency distributions of *Ianthella flabelliformis* heights observed by the Sled video, by depth, trawl-intensity strata (columns) and month after impact (rows), standardized by Sled swept area. Size categories are 100 mm intervals. Note that the "before" status of impact tracks is indicated by month –8 and trawl strata (1,5], which includes the single coverage of the earlier BACI experimental plots; the higher intensity strata did not occur until the repeated-trawling experiment.

Analysis model comparisons of Sled heights did not distinguish among models. Model 3 predictions of heights of individual *Ianthella flabelliformis* suggested a decrease with trawl intensity at month 0 that was consistent with an impact effect, followed by small increases with subsequent surveys (Figure 3-21); however, neither the impact nor recovery coefficients were significant.

The pattern of size-distributions for *Ianthella flabelliformis* by trawl strata and months on ROV patches was consistent with a trawl effect on size structure and limited recovery. That is, at month 10 on the higher-intensity trawl strata, the size structures were narrower and the larger size classes less frequent. With time, there was limited progression of modes or evidence of significant recruitment (Figure 3-22).

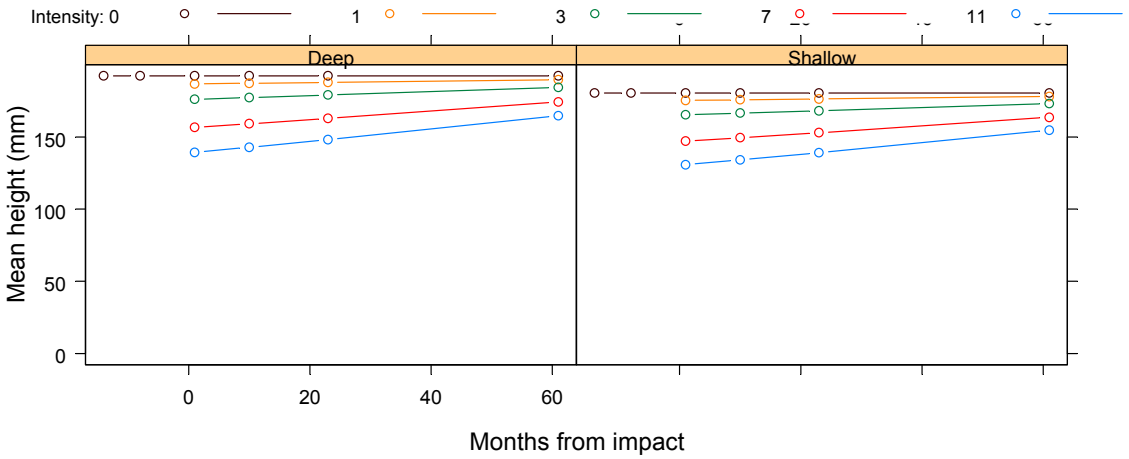

Figure 3-21: Plots of model 3 predictions for mean heights of individual *Ianthella flabelliformis* observed by the Sled against month after impact, by depth. The predictions show only the fixed effects and attempt to isolate the recovery signal from other sources of variation. The coloured lines show predictions for different trawl intensities.

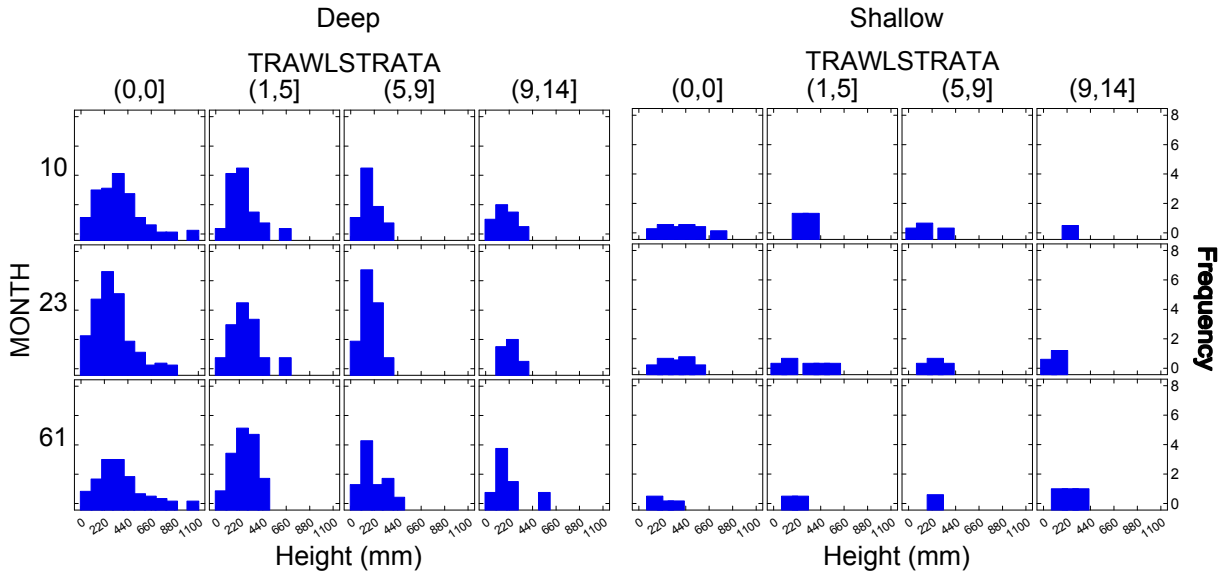

Figure 3-22: Size-frequency distributions of *Ianthella flabelliformis* heights observed by the ROV video, by depth, month after impact (columns) and trawl-intensity strata (rows), standardized by number of replicate observations. Size categories are 100 mm intervals.

The model comparisons for individual *Ianthella flabelliformis* heights measured by the ROV supported model 2 (an Intensity effect $p < 0.0001$). Model 3 confirmed a negative trawl intensity effect ($p < 0.0001$) followed by a recovery trend (but $p = 0.143$) (Figure 3-23a). Results for width and area were similar, with significant impact effects ($p < 0.0001$) and similar recovery trends (width $p = 0.122$) — ~significant in the case of area ($p = 0.059$) (Figure 3-23bc).

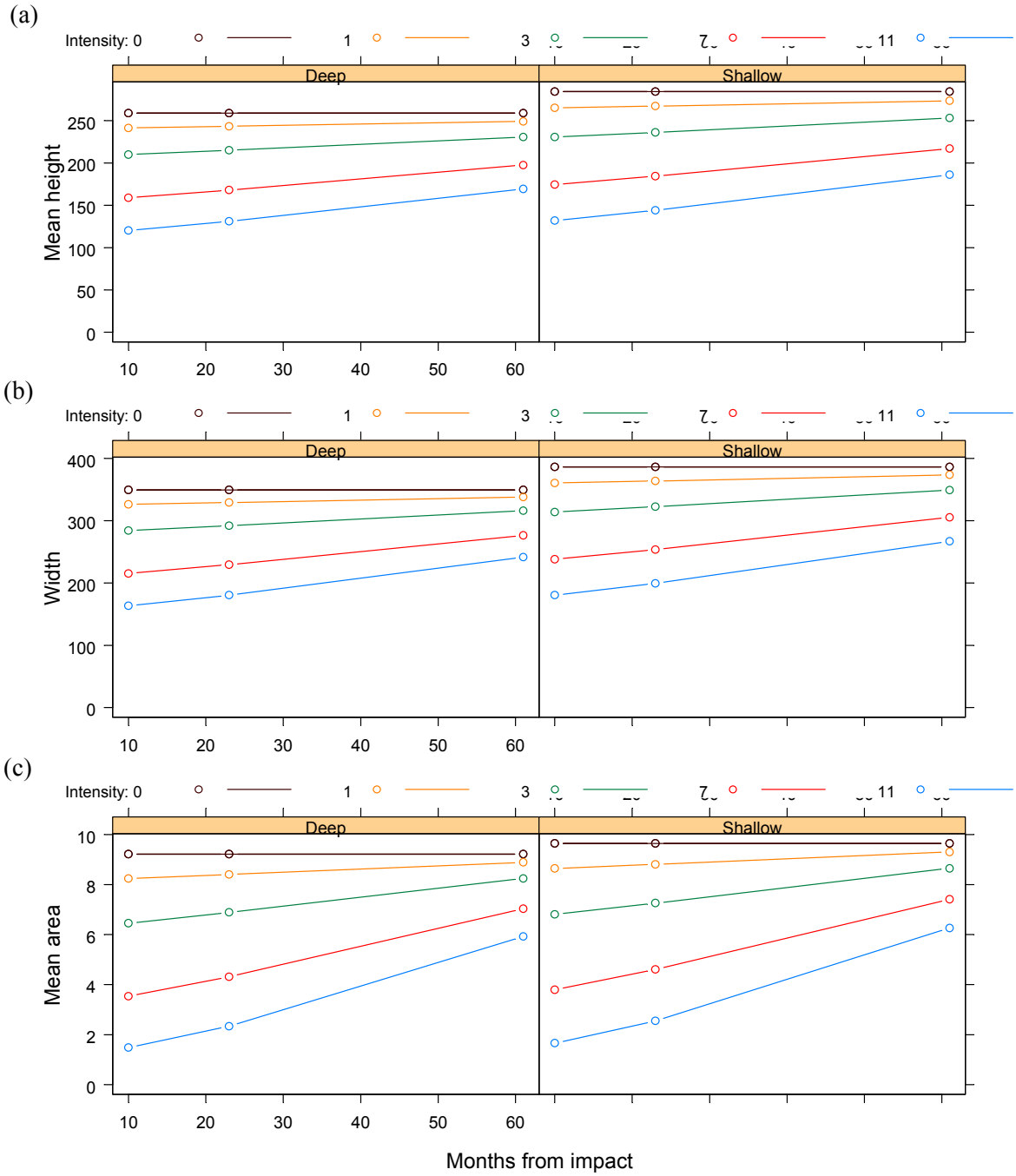

Figure 3-23: Plots of model 3 predictions for measured (a) height, (b) width and (c) area of *Ianthella flabelliformis* observed by the ROV, against month after impact, by depth. The predictions show only the fixed effects and attempt to isolate the recovery signal from other sources of variation. The coloured lines show predictions for different trawl intensities.

3.3.1.2.3 Condition index

The *Ianthella flabelliformis* sponges observed by both the Sled and ROV had essentially no deviation from good condition. Nevertheless, the analyses indicated that condition was fractionally worse initially on impact patches ($p = 0.003$) but recovered quickly ($p = 0.004$).

3.3.1.2.4 Summary

Ianthella flabelliformis appeared to show a significant impact effect of around -20% to -25% per trawl, followed by recovery (at least for the Sled transects) that extends somewhat beyond the time frame of the Project (>5 years). The evidence for recovery on ROV patches was not significant, and somewhat mixed.

There were also negative trawl effects on mean size of *Ianthella flabelliformis*, suggesting that larger individuals might be more vulnerable to removal, followed by some recovery. In this case, the significant evidence came from the ROV data, particularly area measurements.

In the field, there was little indication of impact effects on condition of *Ianthella flabelliformis* that remained on the seabed after repeat-trawling, and the significant analysis results from the ROV data were of negligible effect-size and in reality were inconsequential.

Both Sled and ROV results were largely consistent, at least in trend if not magnitude, which provides some confidence in the impact and recovery patterns presented.

3.3.1.3 Nephtheidae

3.3.1.3.1 Abundance (numbers/density)

The nephtheid soft corals were also very abundant on most Sled tracks, particularly at the time of the last survey, with average numbers in the order of 100 per Sled replicate though highly variable. The model comparison tests supported Model 3 ($p = 0.059$), suggesting an important Time*Intensity recovery term. The fit of this model indicated that deep tracks tended to have greater and more variable abundance than shallow tracks, and that impact tracks tended to increase relatively more than controls by month 61 after impact (Figure 3-24a). The fixed-effects (Figure 3-24b), indicated higher abundance on deep tracks ($p = 0.0019$), a negative impact effect (approximately -26.4% per trawl, $p = 0.0023$) and subsequent rapid recovery in numbers above the pre-impact state (approximately +7.2% per year per trawl, $p = 0.0006$).

The Nephtheid soft corals were less numerous on ROV patches than Sled tracks, with typical numbers in the order of 5-10 per patch. The overall observed trend of raw census numbers was to increase everwhere over the period of the surveys, except on deep controls which decreased after month 23.

The model comparisons for census numbers indicated that model 3 was significant ($p = 0.042$), suggesting that the Time*Intensity (recovery) term was important. The model 3 fit to the Nephtheid census data (Figure 3-25) showed a significant negative impact ($p = 0.0159$) and suggested a recovery trend (but $p = 0.191$, despite the model comparison result). The model comparisons for ROV numbers

standardised for patch footprint-area supported Model 2 (p = 0.0055), suggesting an important intensity term. However, the model 3 negative intensity coefficient was not significant and the positive recovery term was also not significant (p = 0.29) (Figure 3-26).

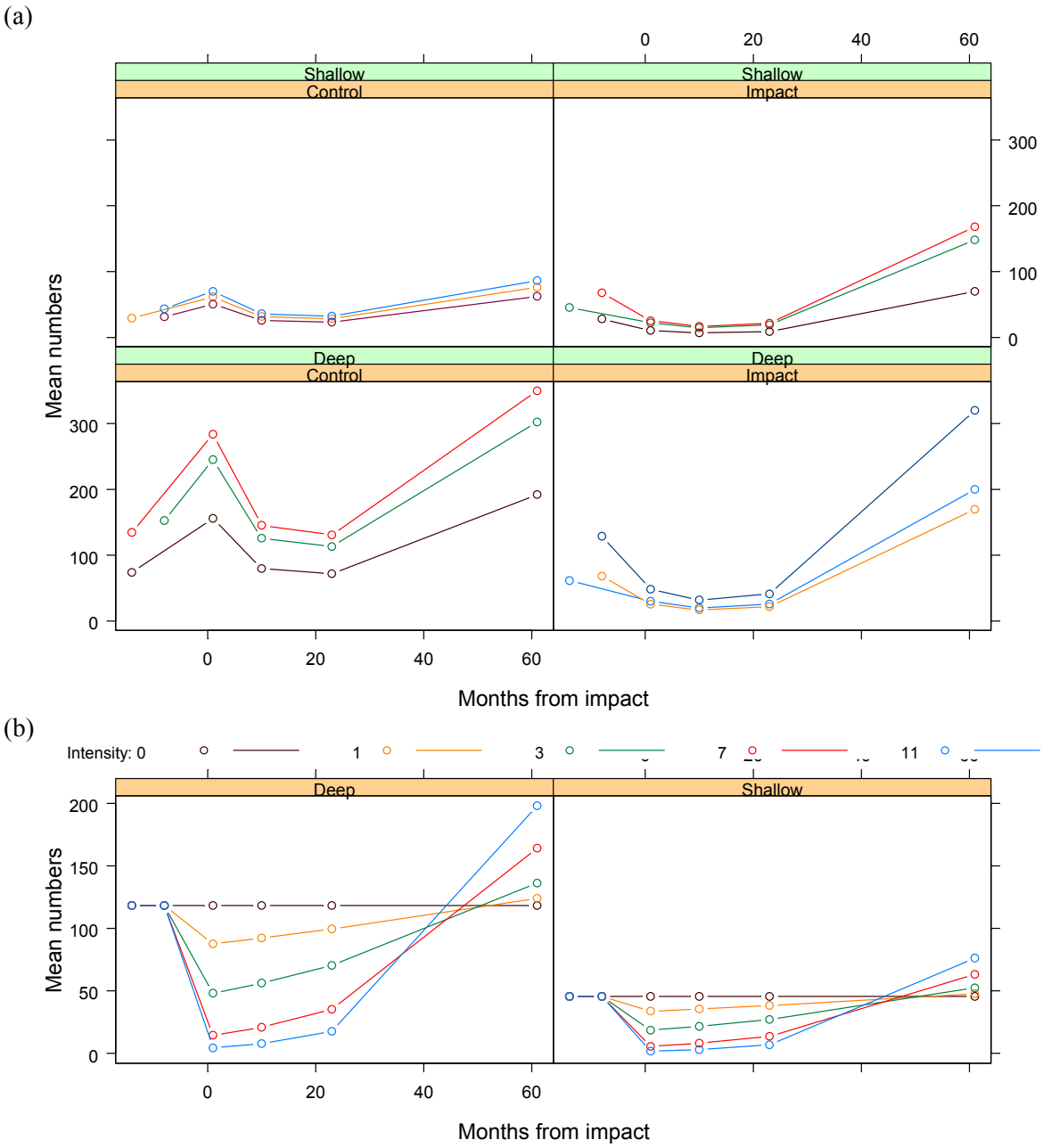

Figure 3-24: Plots of model 3 fit to numbers of *Nephtheidae* per Sled track by month: (a) fixed and random effects less residual variation (coloured lines follow individual tracks), (b) fixed effects only (coloured lines show predictions for different trawl intensities).

The model comparisons for ROV individual nearest-neighbour densities indicated that Model 1 was significant (p = 0.0091), suggesting an important topography (depth strata) term. The Model 3 predictions suggested a negative impact and positive recovery trend but neither coefficient was significant (Figure 3-27). The census and NND models confirmed that deep patches had significantly higher numbers/densities of Nephtheid soft corals.

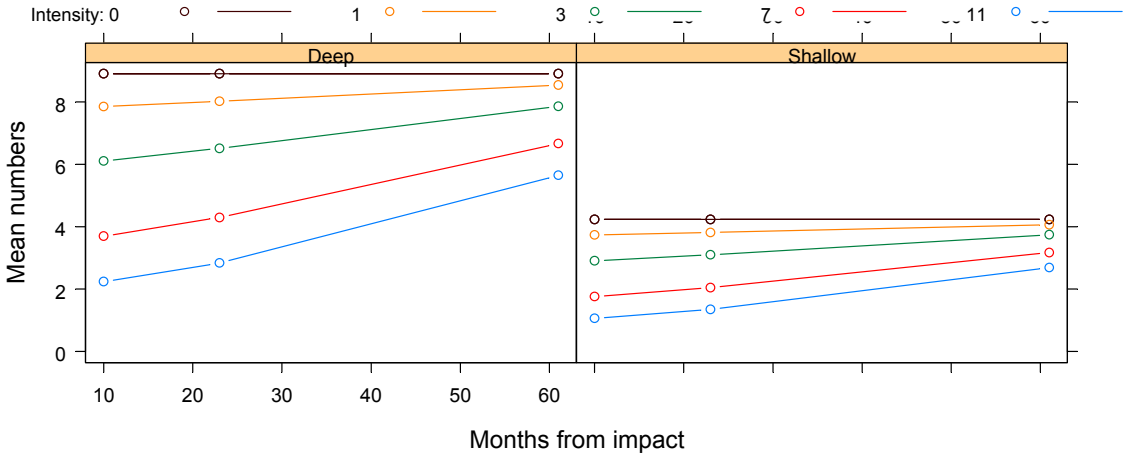

Figure 3-25: Plots of model 3 predictions for ROV patch census numbers for *Nephtheidae* against month after impact, by depth. The predictions show only the fixed effects and attempt to isolate the recovery signal from other sources of variation. The coloured lines show predictions for different trawl intensities

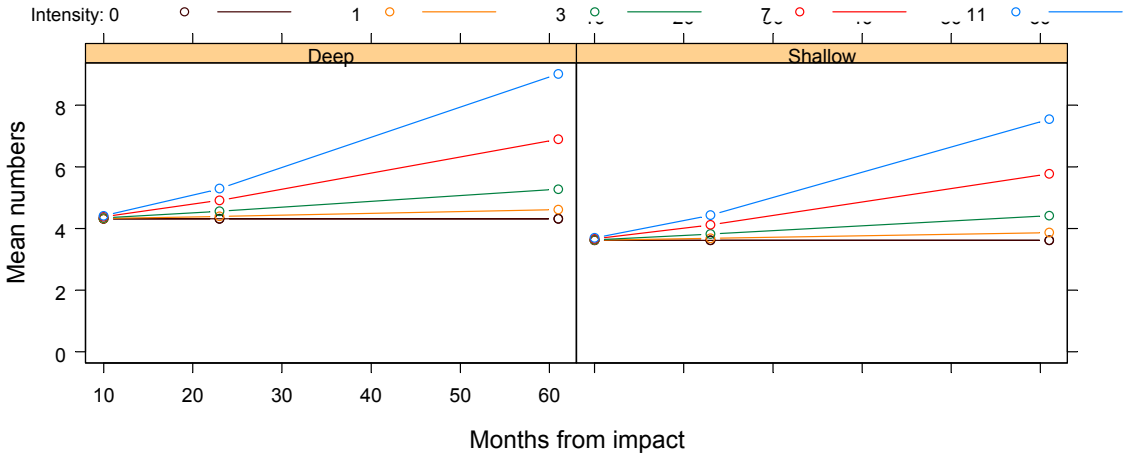

Figure 3-26: Plots of model 3 predictions for ROV patch density for *Nephtheidae* against month after impact, by depth. These represent census counts standardised for patch footprint-area, and are scaled to average patch footprint area. The predictions show only the fixed effects and attempt to isolate the recovery signal from other sources of variation. The coloured lines show predictions for different trawl intensities.

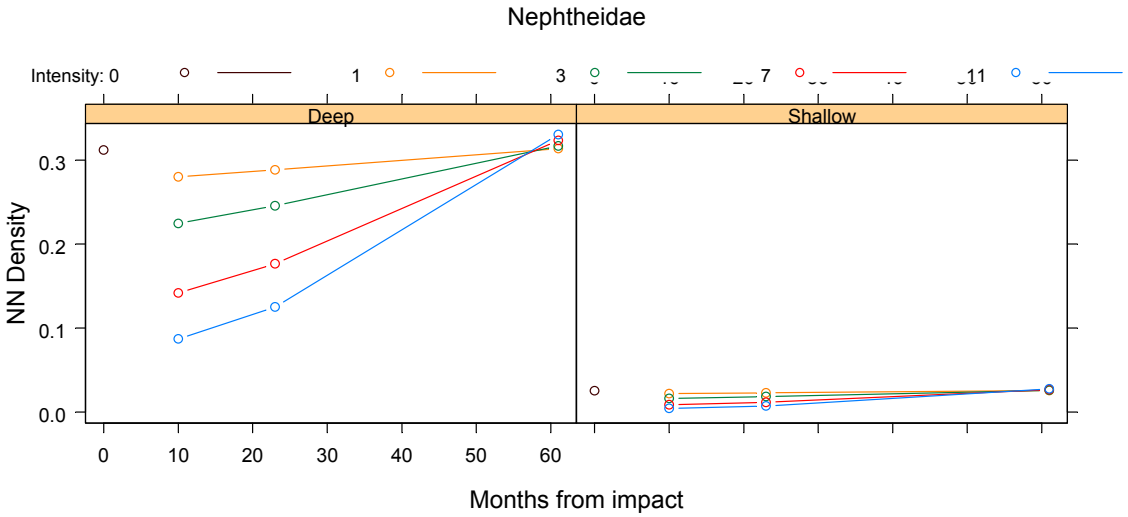

Figure 3-27: Plots of model 3 predictions for ROV nearest-neighbour densities (number per m²) for *Nephtheidae* against month after impact, by depth. These represent transformed nearest-neighbour distances (see methods). The predictions show only the fixed effects and attempt to isolate the recovery signal from other sources of variation. The coloured lines show predictions for different trawl intensities.

3.3.1.3.2 Size attributes

Most nephtheid soft corals observed by the Sled were in the 0-600 mm size class of the size-frequency distributions, generally with progressively fewer larger individuals (Figure 3-28). One month after impact, nephtheids on higher impact strata were almost exclusively small individuals. After month 10, the size distributions on impact strata were similar to the controls and to their state before impact. By month 61, there was evidence of substantial recruitment and growth across the experiment since month 23.

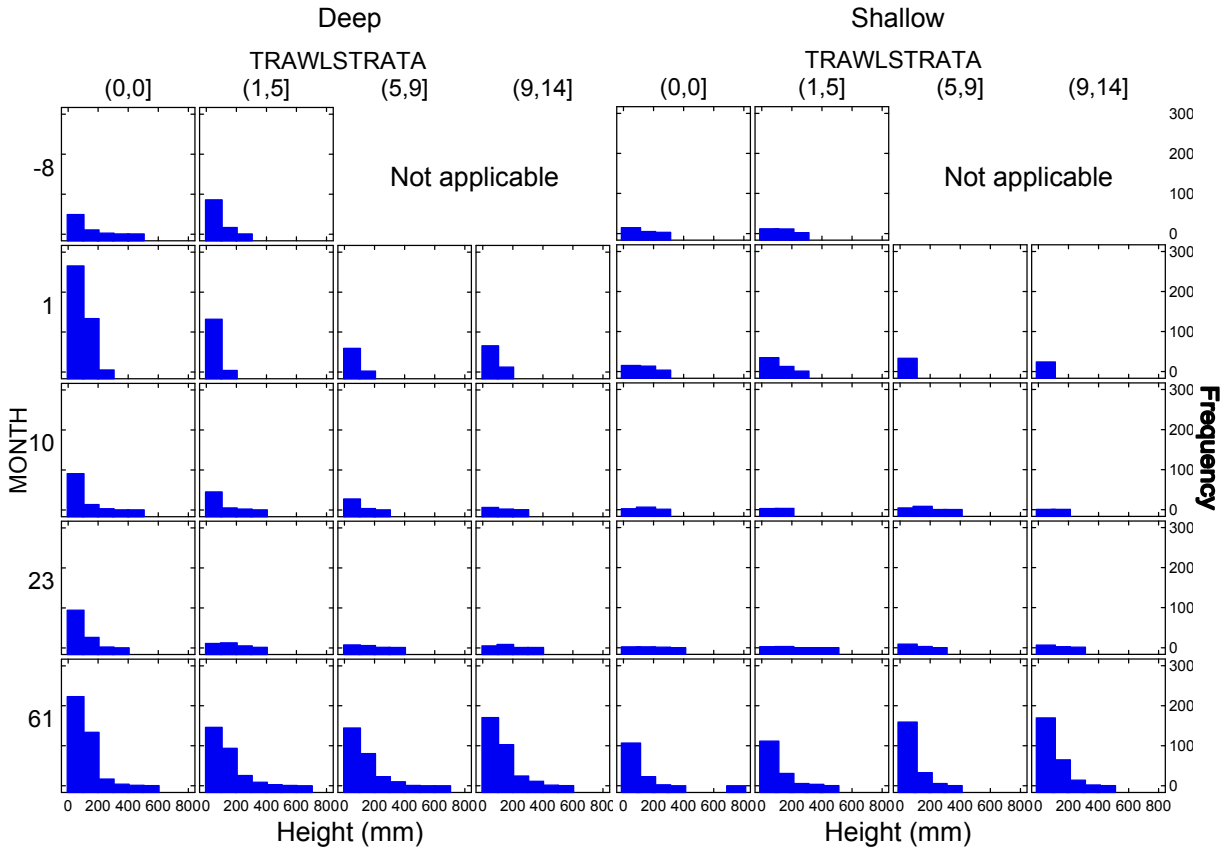

Figure 3-28: Size-frequency distributions of *Nephtheidae* heights observed by the Sled, by depth, trawl intensity strata (columns) and month after impact (rows), standardized by Sled swept area. Size categories are 100 mm intervals. Note that the "before" status of impact tracks is indicated by month -8 and trawl strata (1,5], which includes the single coverage of the earlier BACI experimental plots; the higher intensity strata did not occur until the repeated-trawl experiment.

Analysis model comparisons of Sled heights supported Model 2 (p = 0.013). However, Model 3 predictions of mean nephtheid height on impacts relative to controls showed no evidence of an impact effect, and subsequently there was a slight negative trend in mean height, consistent with the substantial recruitment observed (Figure 3-29); however, the coefficient was not significant. The dominant observation was substantial recruitment and growth on both impact and controls between month 23 and 61.

Full surveys of the patches were not made with the ROV until month 10 after impact; at the same time nephtheids on Sled videos of impacts tracks were of a similar size-structure as those on control tracks. At month 10, the sparse nephtheid population observed by the ROV on trawled strata may have comprised slightly smaller individuals than on controls (Figure 3-30). By months 23 and 61, there had

been substantial recruitment, with some growth, across the experiment, particularly on deep impact areas, possibly indicative of a "weed-like" response to disturbance.

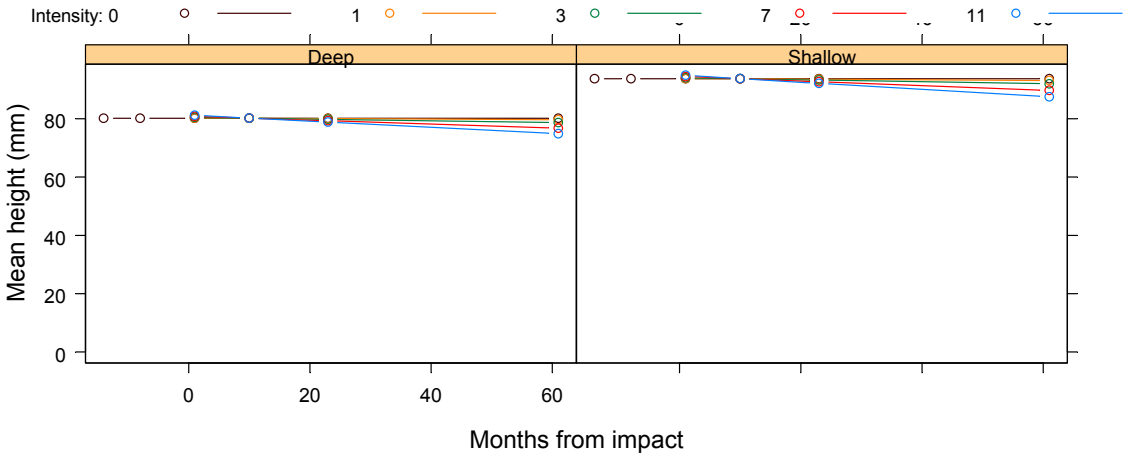

Figure 3-29: Plots of model 3 predictions for mean heights of individual *Nephtheidae* observed by the Sled against month after impact, by depth. The predictions show only the fixed effects and attempt to isolate the recovery signal from other sources of variation. The coloured lines show predictions for different trawl intensities.

The model comparisons for nephtheid heights measured by the ROV supported model 4 (a Time² effect $p < 0.0008$). The Model 4 predictions of changes in mean height on impacts relative to controls indicated a negative trawl intensity effect ($p < 0.0082$) followed by recovery ($p = 0.0002$) to greater mean height than controls, then return to similar mean height as controls ($p = 0.0001$) (Figure 3-31a). Model comparisons and predictions for width and area were almost identical, with significant impact effect ($p = 0.0101$, 0.0927), recovery above controls ($p = 0.0002$, 0.0112) and then return to control sizes ($p = 0.0001$, 0.0059) (Figure 3-31bc). The mean size of Nephtheids on shallow patches was significantly larger in each case, possibly due to apparently greater recruitment of small individual on deep patches.

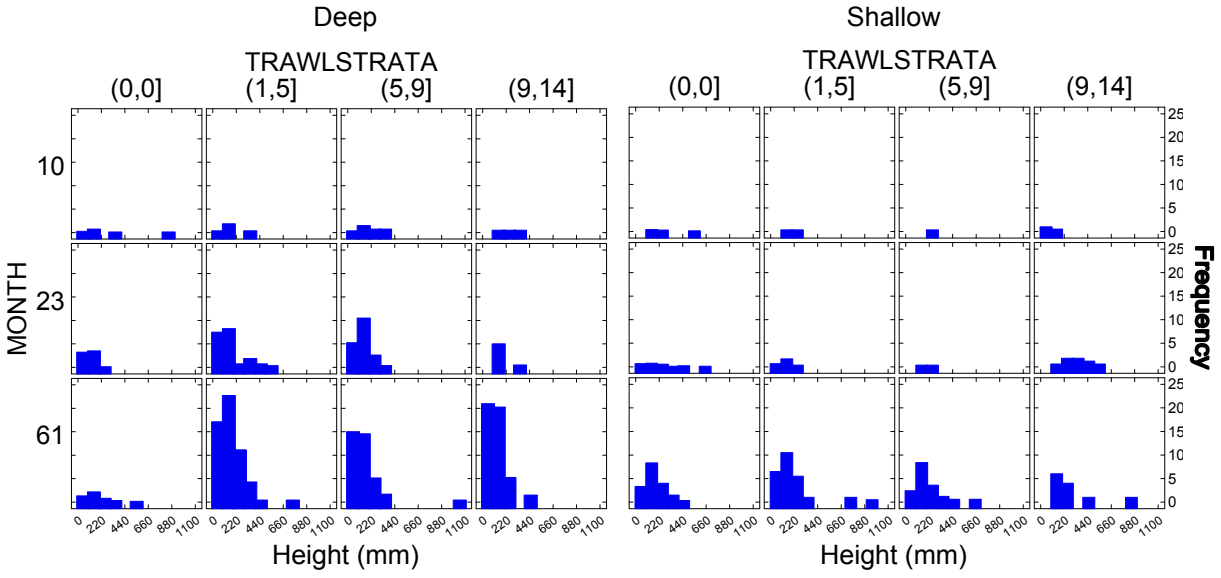

Figure 3-30: Size-frequency distributions of *Nephtheidae* heights observed by the ROV, by depth, month after impact (columns) and trawl-intensity strata (rows), standardized by number of replicate observations. Size categories are 100 mm intervals.

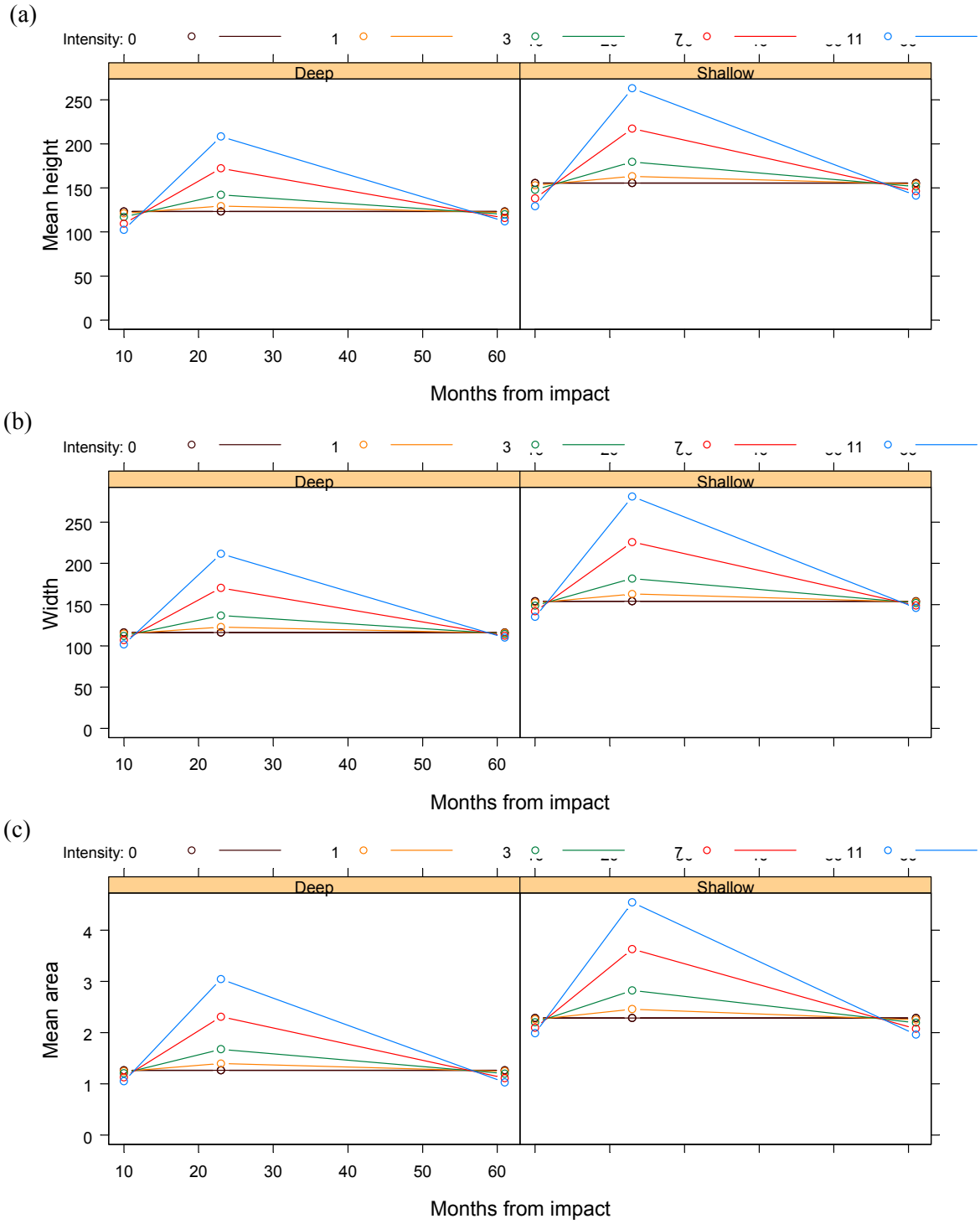

Figure 3-31: Plots of model 3 predictions for measured (a) height, (b) width and (c) area of *Nephtheidae* observed by the ROV, against month after impact, by depth. The predictions show only the fixed effects and attempt to isolate the recovery signal from other sources of variation. The coloured lines show predictions for different trawl intensities

3.3.1.3.3 Condition index

The nephtheid soft corals observed by the Sled had little observable deviation from good condition, and what little effect there was appeared to be consistent on shallow and deep impact tracks.

The model comparisons for nephtheid condition on Sled tracks did not distinguish among models. Model 3 predictions (Figure 3-32) hinted that relative to controls (i.e. fixed effects only), nephtheidae on impact tracks tended to improve a few fractions of a percent in condition after impact and then return to the reference state; however, the coefficients were negligible and not significant. The nephtheid soft corals observed by the ROV showed no variation from good condition.

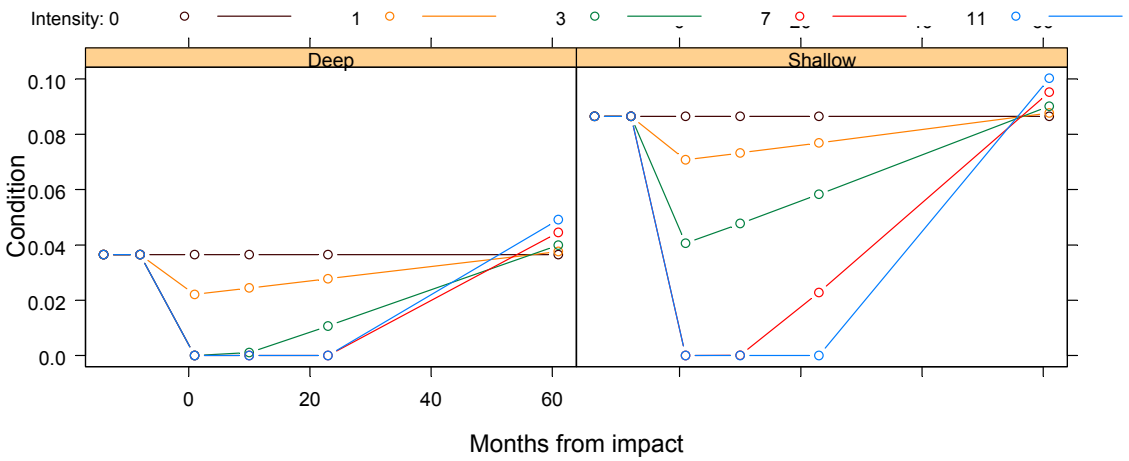

Figure 3-32: Plots of model 3 predictions for *Nephtheidae* Condition Index (%) observed by the Sled. Poorer condition is indicated by values >0. The predictions show only the fixed effects and attempt to isolate the recovery signal from other sources of variation. The coloured lines show predictions for different trawl intensities.

3.3.1.3.4 Summary

The nephtheid soft corals appeared to show a significant impact effect of around -15% to -25% per trawl, followed by recovery approximately within the time frame of the Project (5 years) — at least for the Sled transects. The trends for impact and recovery on ROV patches were similar, though somewhat mixed and in most cases not significant.

There was substantial and widespread recruitment and growth of nephtheidae recruits across the study area and for the Sled tracks, there appeared to be no significant difference in mean size between controls and impacts. On ROV patches, there appeared to be significant negative trawl effects on mean size initially, followed by relatively greater growth on impact patches and then convergence of size distributions, with possibly greater abundance on impacted areas.

In the field, there were no observations of dramatic impact effects on the condition of nephtheid soft corals, and the impact/recovery trend apparent from the Sled data was small and not significant.

The results for the Sled and ROV were more-or-less consistent, providing some confidence in the impact and recovery patterns presented. It is possible that the substantial recruitment of nephtheid soft corals at about the time of the depletion experiment represented a “weed-like” response to disturbance, although controls as well as impacts were involved, and there appeared to have been a second larger wave of recruitment later, between the month 23 and 61 surveys.

3.3.1.4 Scleractinia

3.3.1.4.1 Abundance (numbers/density)

The numbers of unidentified hard corals observed by the Sled were typically about 2-3 per replicate, but varied by at least two orders of magnitude among tracks — at the beginning of the surveys, one control replicate had over 200 individuals but at the end, there were close to zero. The model comparisons supported Model 4, indicating a significant Intensity*Time² term ($p = 0.0001$), and while the model predictions suggested a negative trawl impact, with a recovery above controls by month 23 followed by a return to reference levels or lower by month 61, none of the Model 4 coefficents were significant.

On ROV patches, *Scleractinia* numbered only about 2 per patch on controls and less on impacts; census numbers tended to decrease with higher trawl-intensity strata. Subsequently, numbers on most patches tended to decrease, including on controls. The model comparisons supported Model 4, indicating a significant Intensity*Time² term ($p = 0.0264$); however, the predictions showed little change with time (no coefficents in time were significant) after an initial negative trend with trawl intensity. ROV numbers standardised for patch footprint-area showed very similar patterns and analysis results.

The ROV nearest-neighbour densities for *Scleractinia* showed a steep decrease with trawl-intensity, which levelled off at higher intensities. The model comparisons supported Model 5, indicating a significant Time*Intensity² term ($p = 0.0172$), to accommodate this pattern. The Model 5 coefficents corroborated this (T*I², $p = 0.0130$) and suggested a negative impact effect ($p = 0.0721$) followed by a non-significant declining trend.

3.3.1.4.2 Size attributes

The overall size frequency for Scleractinia on Sled tracks, by trawl strata and months, showed broader size structures with larger size classes on control than on impact tracks, with some evidence of recovery apparent at month 23 but not month 61. Model comparison tests did not distinguish among models and despite the size frequency observations, Model 3 showed no evidence of either impact of recovery trends.

On ROV patches, size-frequency distributions of *Scleractinia* were, as with the Sled tracks, indicative of an impact effect, with narrowing of the size-class range to smaller classes at higher intensities, but showed little evidence of recovery. Model comparison tests did not distinguish among models. Model 3 showed initial trends of decreased height at higher intensities ($p = 0.065$), followed by a trend for recovery by month 61 (but $p = 0.247$). For both width and area, model comparison tests did not distinguish among models and the Model 3's suggested negative impact trends (but $p = 0.614$, 0.419 respectively), but no hint of recovery.

3.3.1.4.3 Condition index

The unidentified hard corals observed by both the Sled and ROV had essentially no deviation from zero (good) condition and could not be analysed.

3.3.1.4.4 Summary

Unidentified hard corals were rather low in abundance and very unevenly distributed making analysis and interpretation difficult. *Scleractinia* appeared to show negative impact effects of uncertain rate per trawl, followed by (in the case of Sled tracks) some evidence of recovery approximately within the time frame of the Project (5 years). There was little evidence of a recovery trend on ROV patches, and numbers may even have declined further.

On Sled tracks, there appeared to be no trends in size with trawl intensity or time, whereas on ROV patches, there appeared to be some evidence of initial negative trawl effects on mean size, and suggestion of recovery for height but none for width or area.

There was no evidence of trawl effects on the condition of unidentified hard corals.

The results for the Sled and ROV were weak for impact, and inconsistent for recovery; consequently there is wide uncertainty in the impact and recovery estimates and timeframes.

3.3.1.5 Hypodistoma deeratum

3.3.1.5.1 Abundance (numbers/density)

The numbers of the solitary ascidian *Hypodistoma deeratum* observed by the Sled were around 1-2 per replicate. By month 23 after impact, the numbers of these ascidians had increased noticeably (>40 on some shallow impact tracks), to levels above corresponding controls, then decreased everwhere by month 61. The model comparison tests supported Model 3 (p = 0.0168), suggesting an important recovery term. The Model 3 predictions suggested a small negative trawl impact (not significant), followed by a fast recovery rate (approximately +7% per year per trawl, p = 0.0227).

On ROV patches, *Hypodistoma deeratum* numbers were less than ~0.3 per patch overall. The ROV census began at month 10 when the Sled observations showed that numbers had already increased after impact, and at month 10, the ROV recorded that *H. deeratum* were more numerous on several shallow impact than control patches. Subsequently, numbers on most patches tended to decrease. For the ROV census data, no models converged. For ROV numbers standardised for patch footprint-area, model comparisons supported Model 4 ($p < 0.0001$), suggesting an important Intensity*Time² term; however, none of the Model 4 coefficients were significant.

The ROV nearest-neighbour densities for *H. deeratum* were very low and initially showed negative trends in individual density with higher trawl intensities, which reversed at month 23 on shallow impact patches, where there was an overall increase in individual density, and then decreased again at month 61. The model comparisons supported Model 4, indicating a significant Time²*Intensity term (p = 0.0035). The Model 4 coefficents corroborated this and suggested a negative impact effect (approximately -44.8% per trawl, p = 0.0014) followed by a recovery relative to controls (p = 0.0047) and then a declining trend (T²*I, p = 0.0041).

3.3.1.5.2 Size attributes

The size structures of *Hypodistoma deeratum* on Sled tracks showed evidence of post impact recruitment and growth on controls and more so on impacts. Model comparison tests provided some support for Model 5 (p = 0.065), which was corroborated by Model 5 coefficients ($T*I^2$, p = 0.054) and suggested that post impact trends differed with trawl intensity. There were suggestions of slight negative impact on mean height followed by some recovery, but none significant.

On ROV patches, size distributions were similar, but sample sizes decreased with time, with larger size classes disappearing. Model comparison tests provided some support for Model 4 (p = 0.065). Model 4 showed trends of negative impact on mean height, followed by a trend for recovery and then decline, but none were significant. For width, comparison tests supported Model 4 (p = 0.0159) and the Model 4 coefficients showed significant negative impact on mean width followed by recovery and then decline (p = 0.0420, 0.0318, 0.0267). The trends for area were the same: Model 4 (p = 0.053), negative impact, recovery and decline (p = 0.1013, 0.0829, 0.0744).

3.3.1.5.3 Condition index

Hypodistoma deeratum observed by both the Sled and ROV had no observable deviation from good condition.

3.3.1.5.4 Summary

The solitary ascidians *Hypodistoma deeratum* were initially low in abundance, but then there was noticeable recruitment and growth of these ascidians across the study area, particularly shallow Sled tracks and more so on impact tracks, after which numbers declined. Few *Hypodistoma deeratum* were observed in ROV patches, though the trends were similar. The ROV results were mixed making interpretation difficult. The ROV census results showed no significant trends whereas the nearest-neighbour density indicated a high impact rate followed by complete recovery and then decline — giving a low overall recovery apparent over the duration of the observations. However, the very low ROV numbers make the NND results questionable and in this case the more reliable Sled results showed a small non-significant impact effect of around -7.5% per trawl, followed by rapid recovery within 1–2 years.

The size distributions showed some support for the recruitment, growth and senescence of *Hypodistoma deeratum*. Analyses of size showed trends for a small impact effect, followed by recovery and then some decline, with mixed significance test results.

There were no indications of impact effects on the condition of these solitary ascidians.

While the results for the Sled and ROV both showed impact and recovery patterns, the magnitude and significance of the estimates differed markedly. More emphasis should be given to the Sled results due to the greater numbers observed. It is possible that the recruitment of these ascidians represented an opportunistic “weed-like” response to disturbance followed by senescence, although controls as well as impacts were involved to some extent.

3.3.2 Low impact, medium recovery

3.3.2.1 Junceella juncea

3.3.2.1.1 Abundance (numbers/density)

The red seawhip *Junceella juncea* was the most numerous of the sessile megabenthos, with typical numbers in the order of 125 per Sled replicate. Estimates of densities were variable, and on all tracks mean numbers appeared to increase from surveys before impact to 1 month after, then decrease by month 10 or 23, and either increase or decrease by month 61.

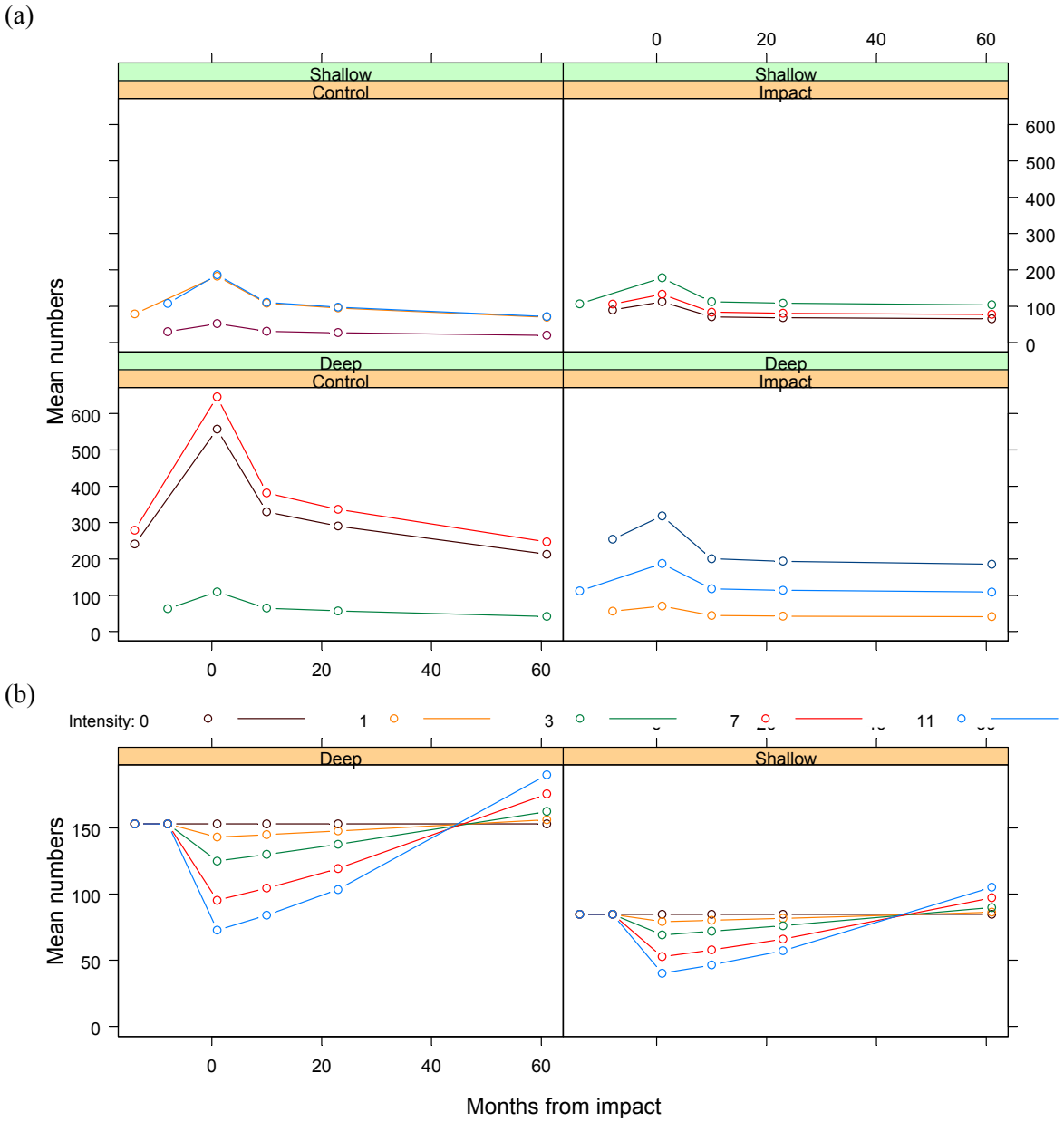

Figure 3-33: Plots of model 3 fit to numbers of *Junceella juncea* per Sled track by month: (a) fixed and random effects less residual variation (coloured lines follow individual tracks), (b) fixed effects only (coloured lines show predictions for different trawl intensities).

Models 4 and 5 were rejected and model 3 fit to these data followed each plot-track through time and indicated that deep tracks tended to have greater and more variable abundance than shallow tracks, and that some control tracks tended to decrease by month 61 after impact (Figure 3-33a). The model 3 vs 2 test was significant (p = 0.0153) suggesting that the Time*Intensity recovery term was required. Test of coefficients of model 3 fixed effects, which included change after trawling on impacts relative to controls, suggested an impact effect (approximately -6.7% per trawl, p = 0.0269); and recovery after trawling (approximately +1.8% per year per trawl, p = 0.0066) (Figure 3-33b).

ROV raw census numbers for *Junceella juncea* averaged about 65 per patch and were also variable. On deep patches, numbers tended to increase from month 10 to 23, then remain fairly steady. On shallow patches, numbers tended to decrease slightly from month 10 to 23, then either increase or decrease by month 61. The model comparisons for census numbers indicated that model 2 was significant (p < 0.001), suggesting a significant intensity term. Model 3 fit to these data indicated that higher intensity strata had fewer animals (p = 0.0002), and there was negligible recovery trend with time (<0.1%/yr/trawl, p = 0.95) relative to changes on controls (Figure 3-34). For ROV numbers standardised for patch footprint-area, model 3 indicated positive intensity trends (p = 0.0764) followed by non-significant decreasing trends in density on trawled areas (Figure 3-35).

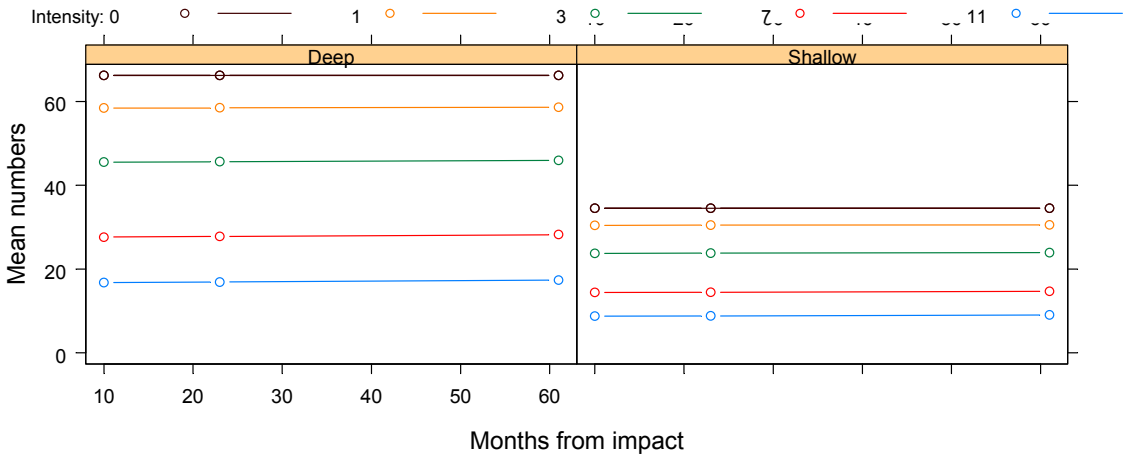

Figure 3-34: Plots of model 3 predictions for ROV patch census numbers for *Junceella juncea* against month after impact, by depth. The predictions show only the fixed effects and attempt to isolate the recovery signal from other sources of variation. The coloured lines show predictions for different trawl intensities.

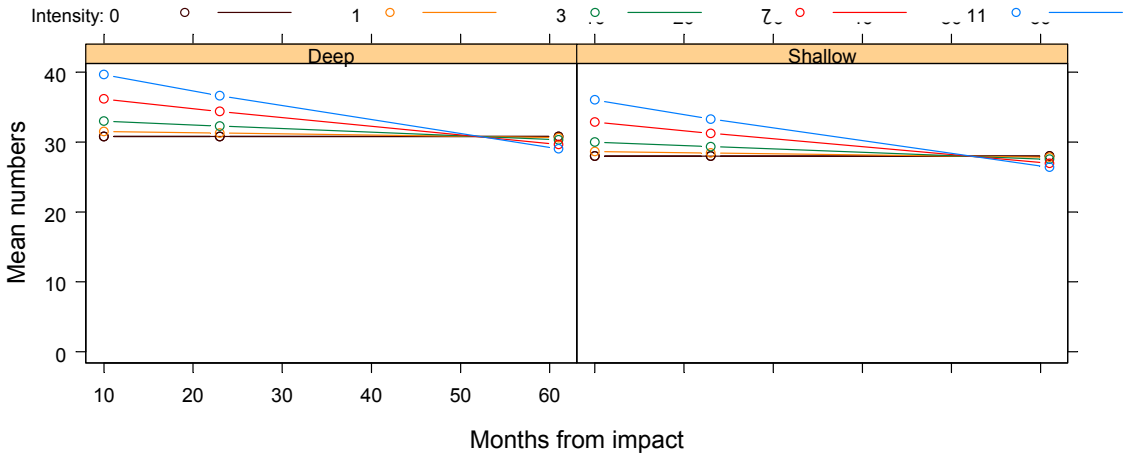

Figure 3-35: Plots of model 3 predictions for ROV patch density for *Junceella juncea* against month after impact, by depth. These represent census counts standardised for patch footprint-area, and are scaled to average patch footprint area. The predictions show only the fixed effects and attempt to isolate the recovery signal from other sources of variation. The coloured lines show predictions for different trawl intensities.

The model comparisons for ROV individual nearest-neighbour densities indicated that model 1 was significant (p = 0.018), suggesting higher densities in deep patches. Model 3 confirmed this (p = 0.019) and while there were trends for an initial intensity effect (approx. -3.82%/trawl) followed by a slight recovery (~0.5%/yr/trawl) neither were significant (p = 0.229 and p = 0.674) (Figure 3-36).

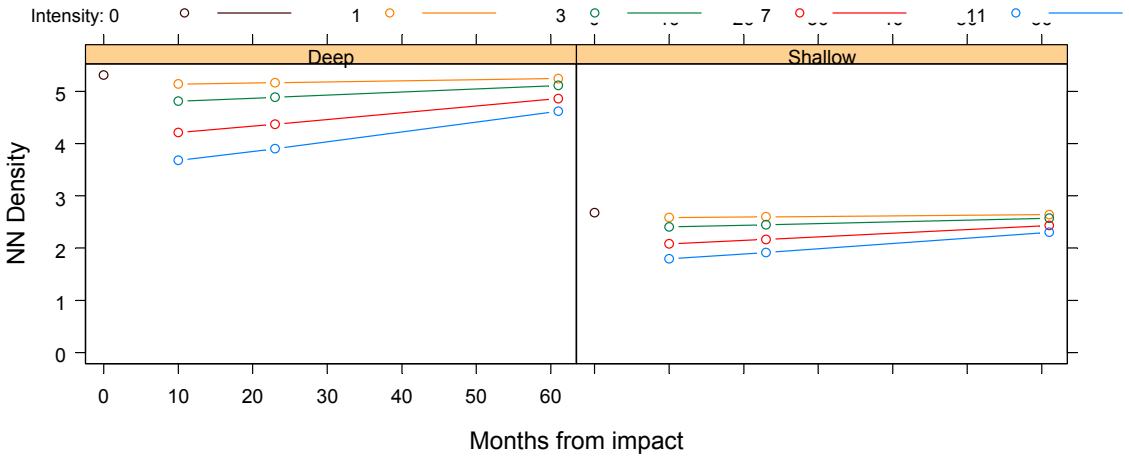

Figure 3-36: Plots of model 3 predictions for ROV nearest-neighbour densities (number per m²) for *Junceella juncea* against month after impact, by depth. These represent transformed nearest-neighbour distances (see methods). The predictions show only the fixed effects and attempt to isolate the recovery signal from other sources of variation. The coloured lines show predictions for different trawl intensities.

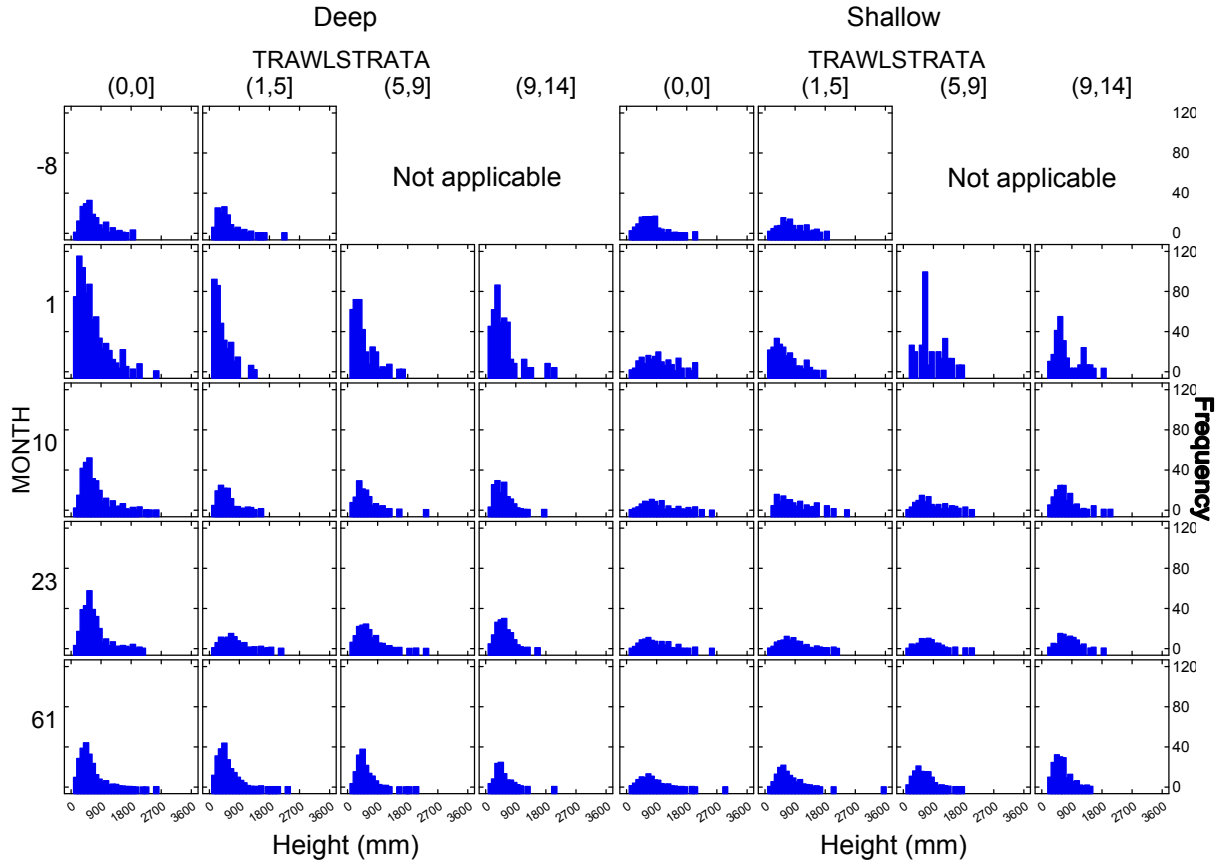

Figure 3-37: Size-frequency distributions of *Junceella juncea* heights observed by the Sled, by depth, trawl intensity strata (columns) and month after impact (rows), standardized by Sled swept area. Size categories are 100 mm intervals. Note that the "before" status of impact tracks is indicated by month –8 and trawl strata (1,5], which includes the single coverage of the earlier BACI experimental plots; the higher intensity strata did not occur until the repeated-trawling experiment.

3.3.2.1.2 Size attributes

The size-frequency distributions for *Junceella juncea* suggest that there were fewer longer whips on deep Sled tracks than on shallow tracks (Figure 3-37). There were also slight indications of fewer longer whips with both time and intensity, with a some skewing to shorter individuals. Analysis model comparisons of Sled heights supported model 4 ($p = 0.0018$). The model 4 predictions of mean heights of individual *Junceella juncea* suggested a slight initial increase with trawl intensity ($p = 0.0093$) possibly indicative of selective removal of smaller whips, followed by small decreases in two subsequent surveys ($p = 0.0007$) and finally an increase to about reference levels by month 61 ($p = 0.0016$) (Figure 3-38). The mean height of whips on deep plots was significantly shorter ($p < 0.0001$). The length of seawhips could not be measured properly by the ROV, so there were no data for height changes on ROV patches.

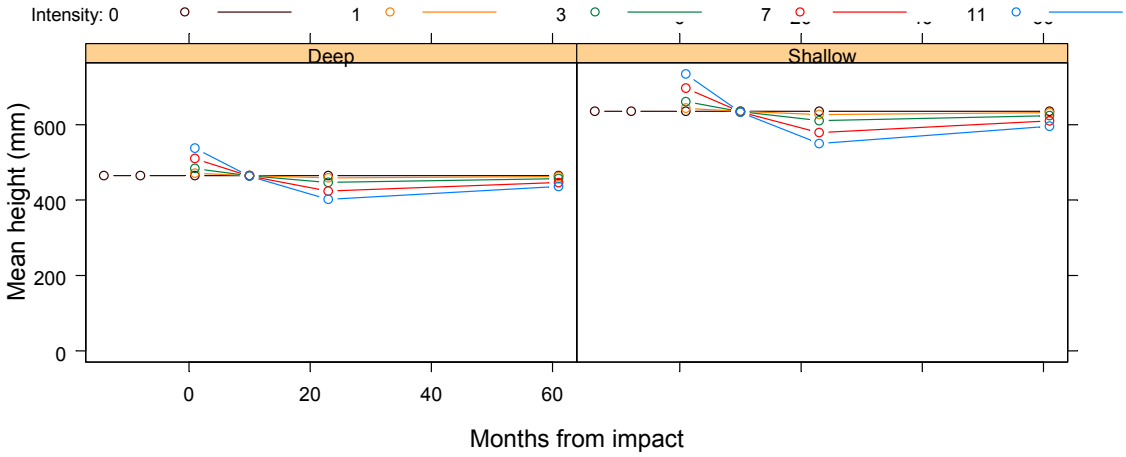

Figure 3-38: Plots of model 4 predictions for mean heights of individual *Junceella juncea* observed by the Sled against month after impact, by depth. The predictions show only the fixed effects and attempt to isolate the recovery signal from other sources of variation. The coloured lines show predictions for different trawl intensities.

3.3.2.1.3 Condition index

The raw indices of condition of *Junceella juncea* varied among track replicates and time. *Junceella juncea* on both impact and control tracks were in good condition initially, but tended to be in worse condition later. Red whips on impact tracks appeared to be in worse condition at months 10 or 23 or both, and generally improved condition slightly at month 61. This was consistent with observations that some seawhips on impact tracks had living polyps stripped from part of their skeletons at month 1, but that these stripped areas became encrusted by month 10.

The model comparisons for *Junceella juncea* condition on Sled tracks distinguished model 2 ($p = 0.03$), suggesting impact was important. The model 3 predictions (Figure 3-39) showed that relative to controls (i.e. fixed effects only), *Junceella juncea* on impact tracks tended to become slightly poorer in condition after impact ($p = 0.0294$) and then improve though not significantly ($p = 0.355$). *Junceella juncea* on shallow tracks appeared to be in slightly worse condition than those on deep tracks ($p = 0.024$).

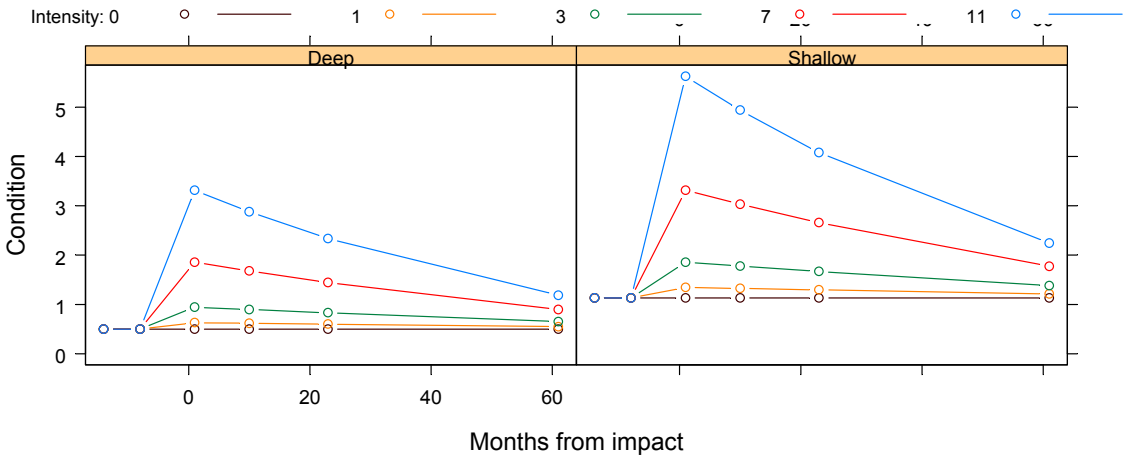

Figure 3-39: Plots of model 3 predictions for *Junceella juncea* Condition Index (%) observed by the Sled. Poorer condition is indicated by values >0. The predictions show only the fixed effects and attempt to isolate the recovery signal from other sources of variation. The coloured lines show predictions for different trawl intensities.

The raw indices of condition of *Junceella juncea* on ROV patches showed a similar pattern to the Sled data, with condition on impact patches appearing to be worse at month 10 or 23 or both, and then possibly improving by month 61. There was also a tendency for condition to become worse on high-intensity strata than on low-intensity strata. The model comparisons supported Model 4 (p = 0.012) and the model 4 predictions showed no significant immediate impact but a slight worsening of condition by month 23 (p = 0.053) and recovery by month 61 (p = 0.036) (Figure 3-40).

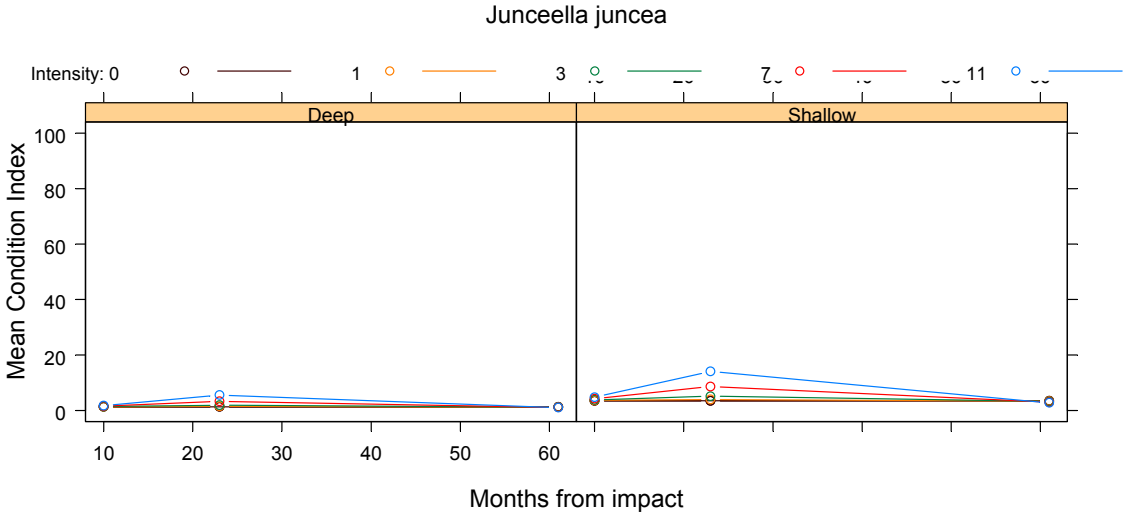

Figure 3-40: Plots of model 4 predictions for *Junceella juncea* Condition Index (%) observed by the ROV. Poorer condition is indicated by values >0. The predictions show only the fixed effects and attempt to isolate the recovery signal from other sources of variation. The coloured lines show predictions for different trawl intensities

3.3.2.1.4 Summary

The red seawhip *Junceella juncea* was the most numerous of the sessile megabenthos. These whips appeared to show a significant impact effect of around -7% per trawl, followed by significant recovery before the end of the Project (5 years) — at least for the Sled transects. The evidence for impact and recovery on ROV patches was mixed — in the case of nearest neighbour density, the estimates were similar to the Sled though not significant.

There may also have been small significant effects on mean size of *Junceella juncea* measured by the Sled, possibly consistent with selective removal of smaller individuals, followed by some recruitment and then growth. Length of whips could not be measured from the ROV.

There were indications of impact effects worsening the condition of *Junceella juncea*, followed by almost complete recovery — though the significance of these patterns varied between the Sled and ROV.

The Sled and ROV results were relatively consistent in pattern and magnitude, even if significance tests were mixed. *Junceella juncea* appeared to show relatively low impact and then approximately recovered in numbers, size and condition roughly within the timeframe of the project.

3.3.2.2 Dichotella divergens

3.3.2.2.1 Abundance (numbers/density)

The branched gorgonian *Dichotella divergens* was common on Sled tracks, with typical numbers of almost 20 per Sled replicate. These gorgonians were a medium-sized structural component of seabed habitat gardens. The patterns for density were very similar to the red seawhips: variable, and on most tracks mean numbers appeared to increase from surveys before impact to 1 month after, then decrease at months 10 or 23, and trend to increase by month 61 — perhaps less so on high-intensity strata. The model comparisons did not reject model 5 (p = 0.035), indicative of a Time*Intensity² term. The model 5 fit to these data indicated low negative impact (~ -9%/trawl) and positive recovery terms (both ns) and a significant Time*Intensity² term (p = 0.0205) suggesting that low and medium intensity strata recovered above controls while highest intensity strata continued to decline (Figure 3-41 a,b).

Dichotella divergens was more numerous on ROV patches than Sled tracks, with typical numbers of almost 25 per patch. On impact patches, census numbers tended to be lower in higher-intensity strata and there were trends indicative of recovery, particularly on low-impact strata. The model comparisons provided some support for model 3 (p = 0.093), suggestive of recovery. The model 3 fit to these data provided some evidence of a recovery trend with time (at about 1.8%/yr/trawl, p = 0.062) relative to changes on controls (Figure 3-42), as well as lower numbers with intensity (p < 0.0001). ROV numbers standardised for patch footprint-area did not distinguish models and while model 3 showed similar but less marked patterns to census numbers, no terms were significant (Figure 3-43).

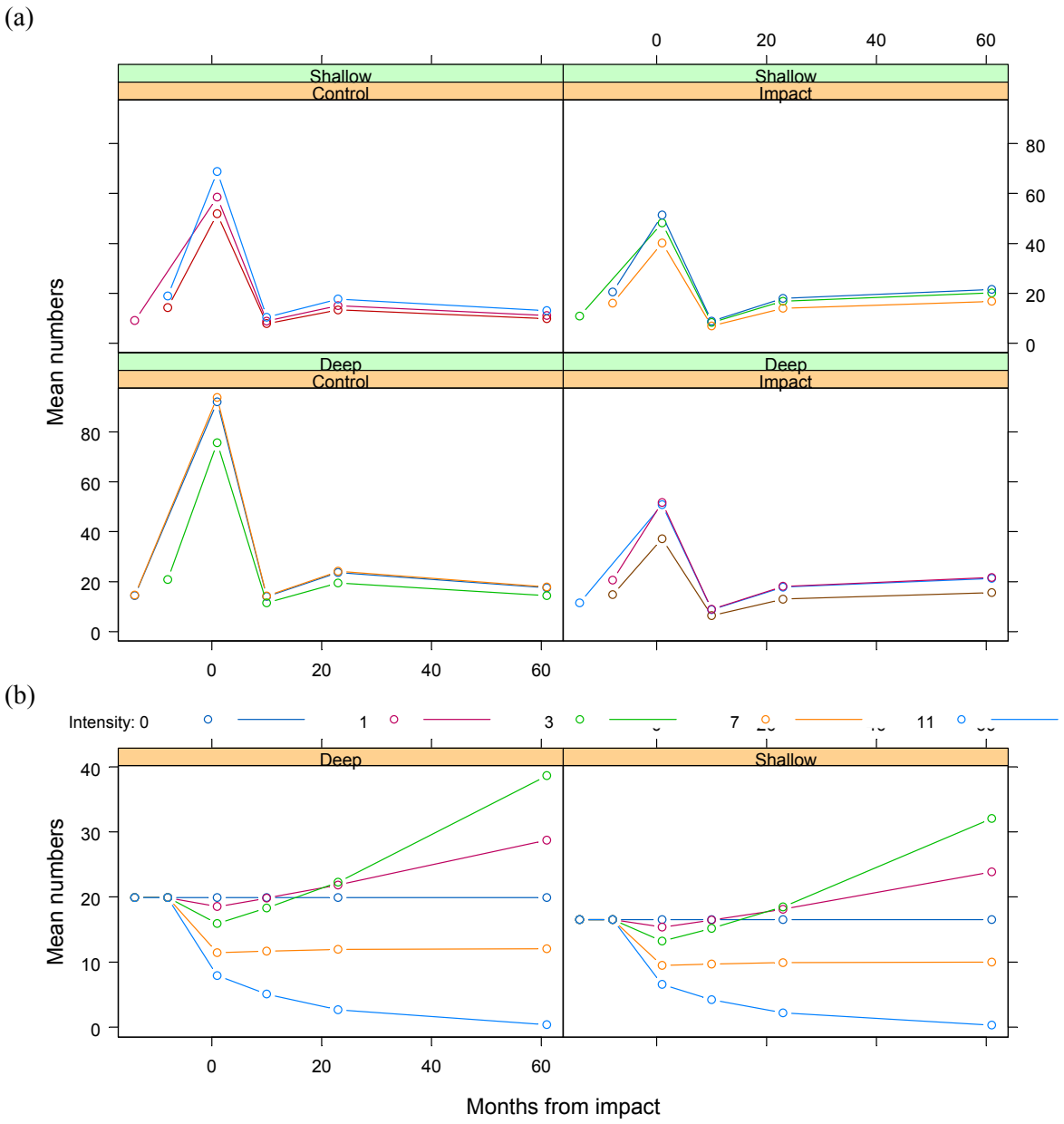

Figure 3-41: Plots of model 5 fit to numbers of *Dichotella divergens* per Sled track by month: (a) fixed and random effects less residual variation (coloured lines follow individual tracks), (b) fixed effects only (coloured lines show predictions for different trawl intensities).

The model comparisons for ROV individual nearest-neighbour densities supported model 2 (p = 0.013), suggesting an impact effect. The model 3 fit to these data showed trends of decreasing density with trawl-intensity, and in constrast to the census data then showed trends for subsequent declines in density; however, the coefficients were not significant (Figure 3-44).

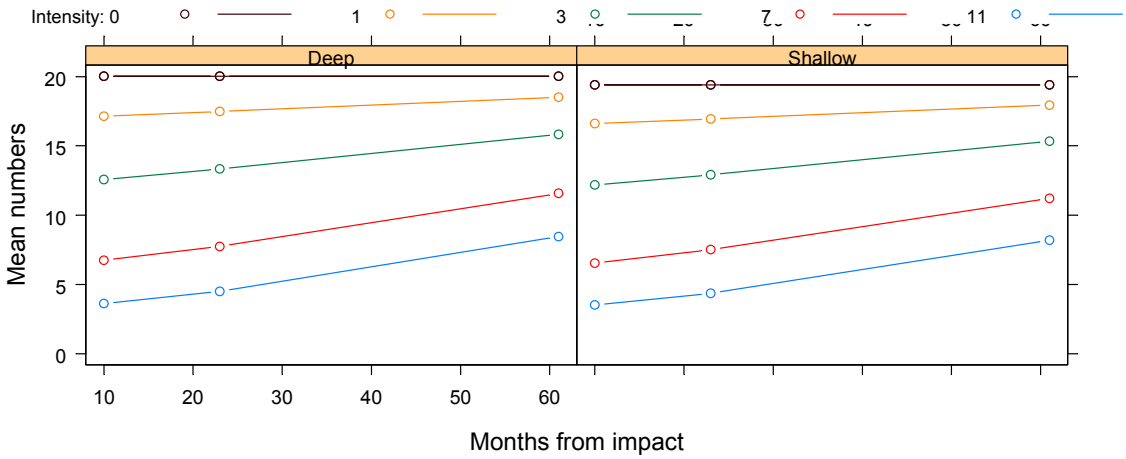

Figure 3-42: Plots of model 3 predictions for ROV patch census numbers for *Dichotella divergens* against month after impact, by depth. The predictions show only the fixed effects and attempt to isolate the recovery signal from other sources of variation. The coloured lines show predictions for different trawl intensities.

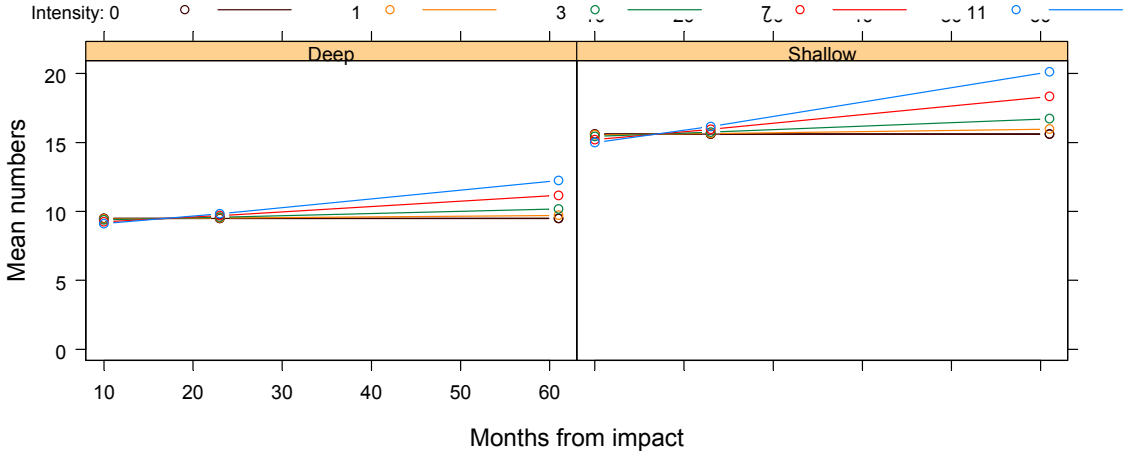

Figure 3-43: Plots of model 3 predictions for ROV patch density for *Dichotella divergens* against month after impact, by depth. These represent census counts standardised for patch footprint-area, and are scaled to average patch footprint area. The predictions show only the fixed effects and attempt to isolate the recovery signal from other sources of variation. The coloured lines show predictions for different trawl intensities

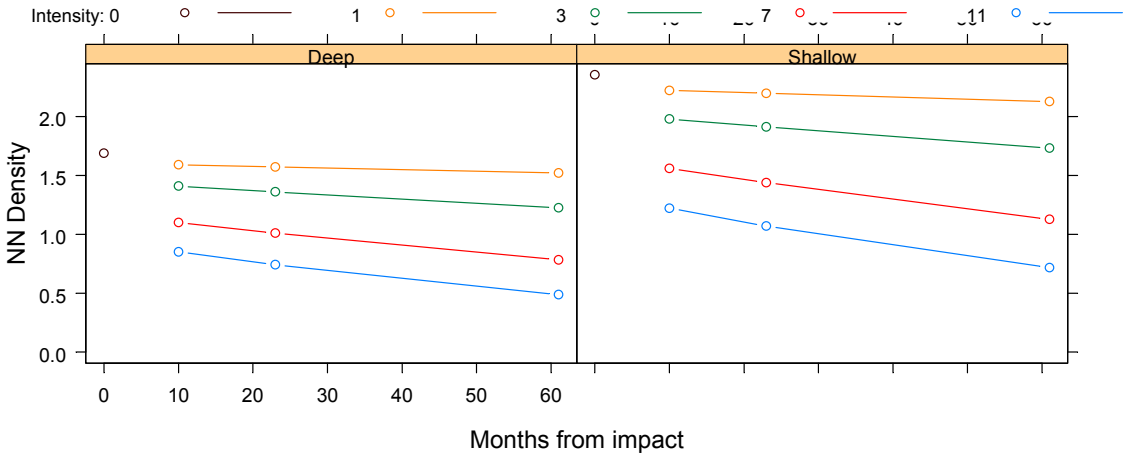

Figure 3-44: Plots of model 3 predictions for ROV nearest-neighbour densities (number per m²) for *Dichotella divergens* against month after impact, by depth. These represent transformed nearest-neighbour distances (see methods). The predictions show only the fixed effects and attempt to isolate the recovery signal from other sources of variation. The coloured lines show predictions for different trawl intensities.

3.3.2.2.2 Size attributes

The pattern of size-distributions for *Dichotella divergens* by trawl strata and months was similar for deep and shallow tracks. At month 1, across trawl strata the size structures were slightly narrower and the larger size classes were slightly less frequent. With time, the size structures of the trawled populations and controls tended to progress to larger individuals, while maintaining smaller classes presumably due to recruitment (Figure 3-45). This pattern would be consistent with impact and recovery, but the changes need to be appraised relative to changes on controls.

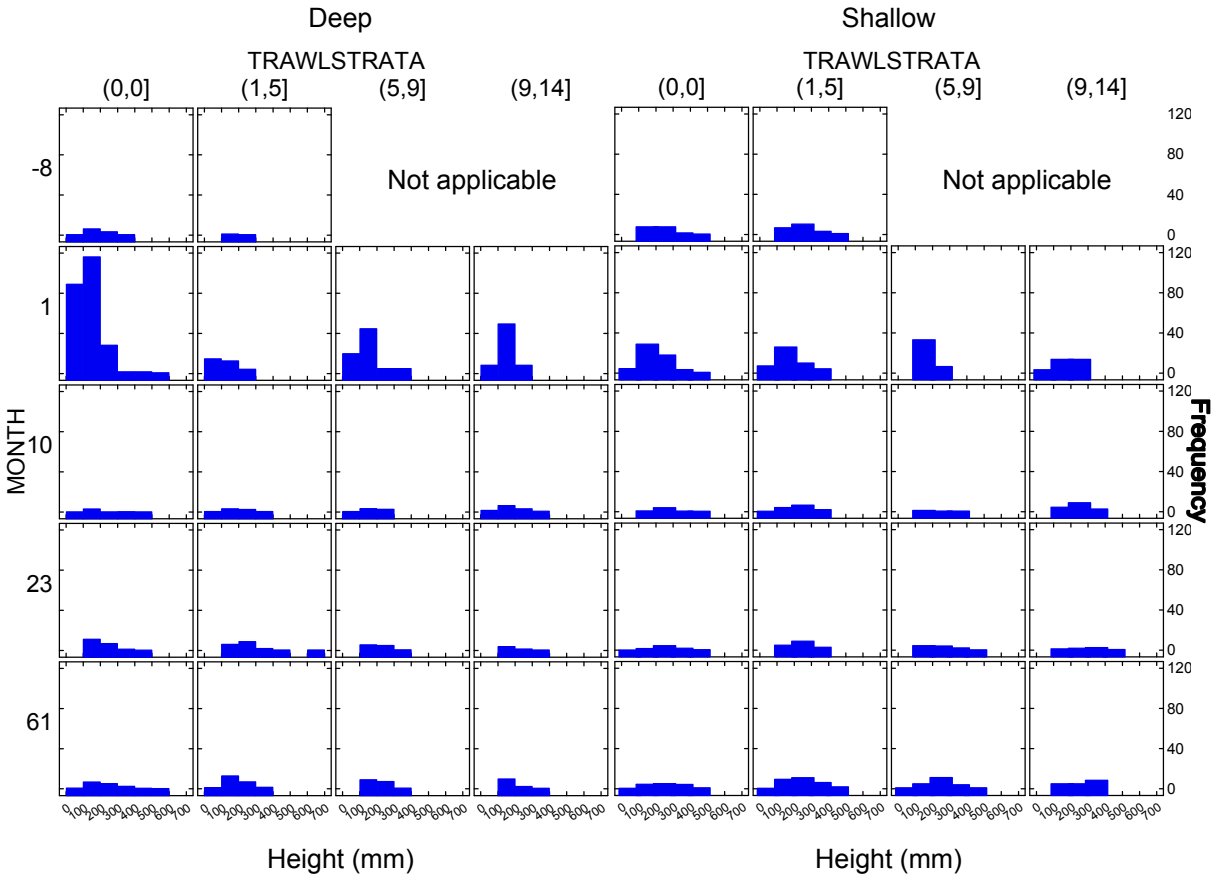

Figure 3-45: Size-frequency distributions of *Dichotella divergens* heights observed by the Sled video, by depth, trawl-intensity strata (columns) and month after impact (rows), standardized by Sled swept area. Size categories are 100 mm intervals. Note that the "before" status of impact tracks is indicated by month –8 and trawl strata (1,5], which includes the single coverage of the earlier BACI experimental plots; the higher intensity strata did not occur until the repeated-trawl experiment.

The model comparisons of Sled heights indicated only model 1 (Topography) was significant ($p < 0.0001$). Model 3 predictions of mean heights of individual *Dichotella divergens* confirmed that animals on shallow tracks were taller and suggested a very slight decrease with trawl intensity at month 0 that was consistent with a small impact effect, followed by small increases with subsequent surveys (Figure 3-46); however, neither the impact nor recovery coefficients were significant.

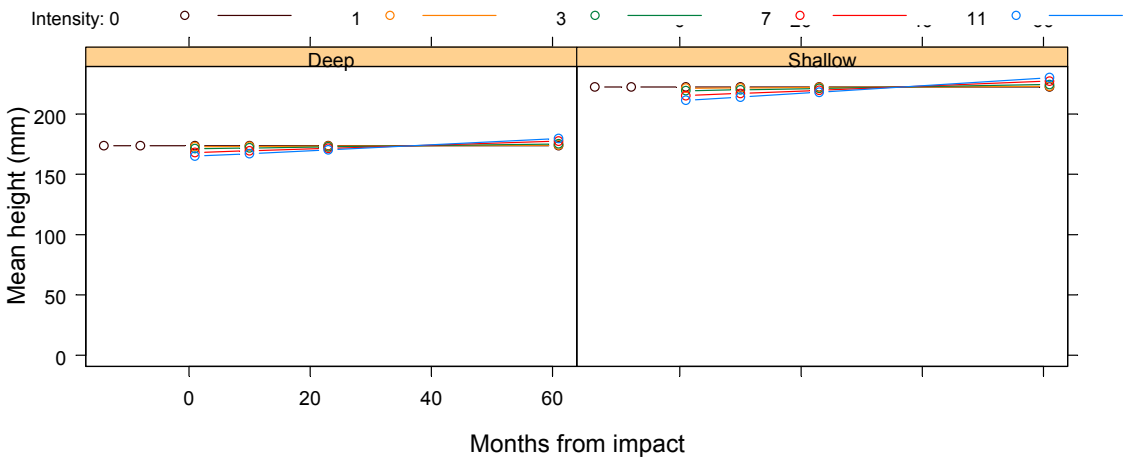

Figure 3-46: Plots of model 3 predictions for mean heights of individual *Dichotella divergens* observed by the Sled against month after impact, by depth. The predictions show only the fixed effects and attempt to isolate the recovery signal from other sources of variation. The coloured lines show predictions for different trawl intensities.

The pattern of size-distributions for *Dichotella divergens* on ROV patches, by trawl strata and months, was similar to that recorded by the Sled video. That is, patterns for deep and shallow patches were similar and, at month 10 across trawl strata, the size structures were slightly narrower, with the larger size classes slightly less frequent. With time, the proportion of the small class size increased, presumably due to recruitment, while maintaining a similar proportion of larger classes (Figure 3-47).

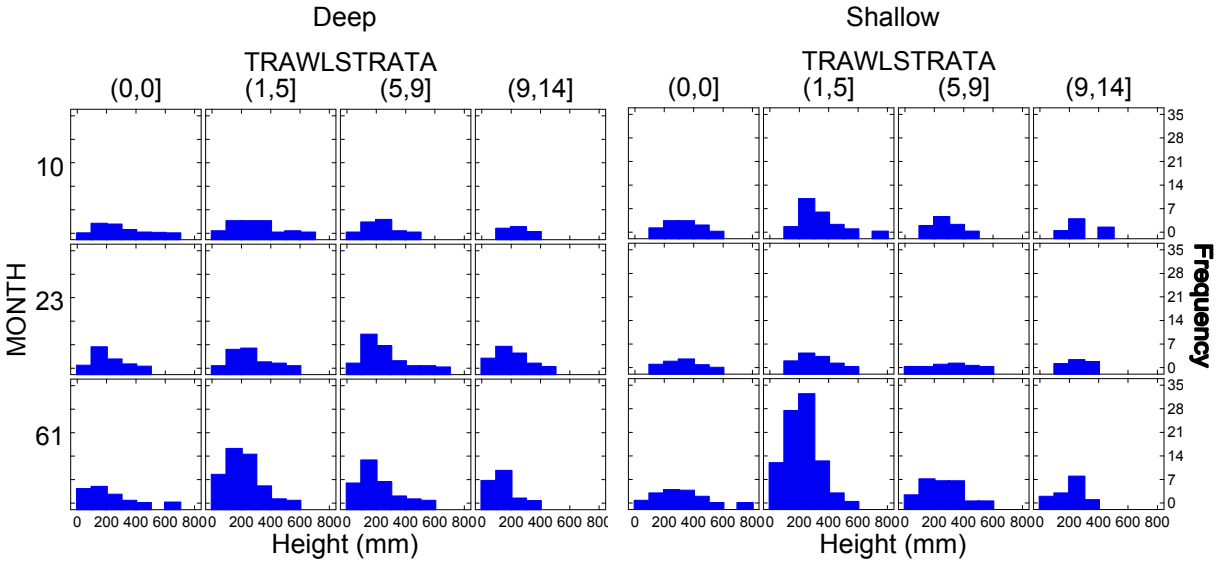

Figure 3-47: Size-frequency distributions of *Dichotella divergens* heights observed by the ROV, by depth, month after impact (columns) and trawl-intensity strata (rows), standardized by number of replicate observations. Size categories are 100 mm intervals.

Overall, on ROV control and impact patches, there was a decrease in mean height with time, possibly due to the recruitment of smaller individuals. The model comparisons for individual *Dichotella divergens* heights measured by the ROV supported model 2 (Intensity, $p = 0.0045$). Model 3 confirmed that shallow animals were larger than those deeper ($p < 0.0001$) and indicated a slight negative trawl intensity effect and continued decrease in height on trawled areas (Figure 3-48), but

neither the intensity nor recovery coefficients were significant. The patterns of ROV individual width and individual area data for *Dichotella divergens* were consistent with those for height.

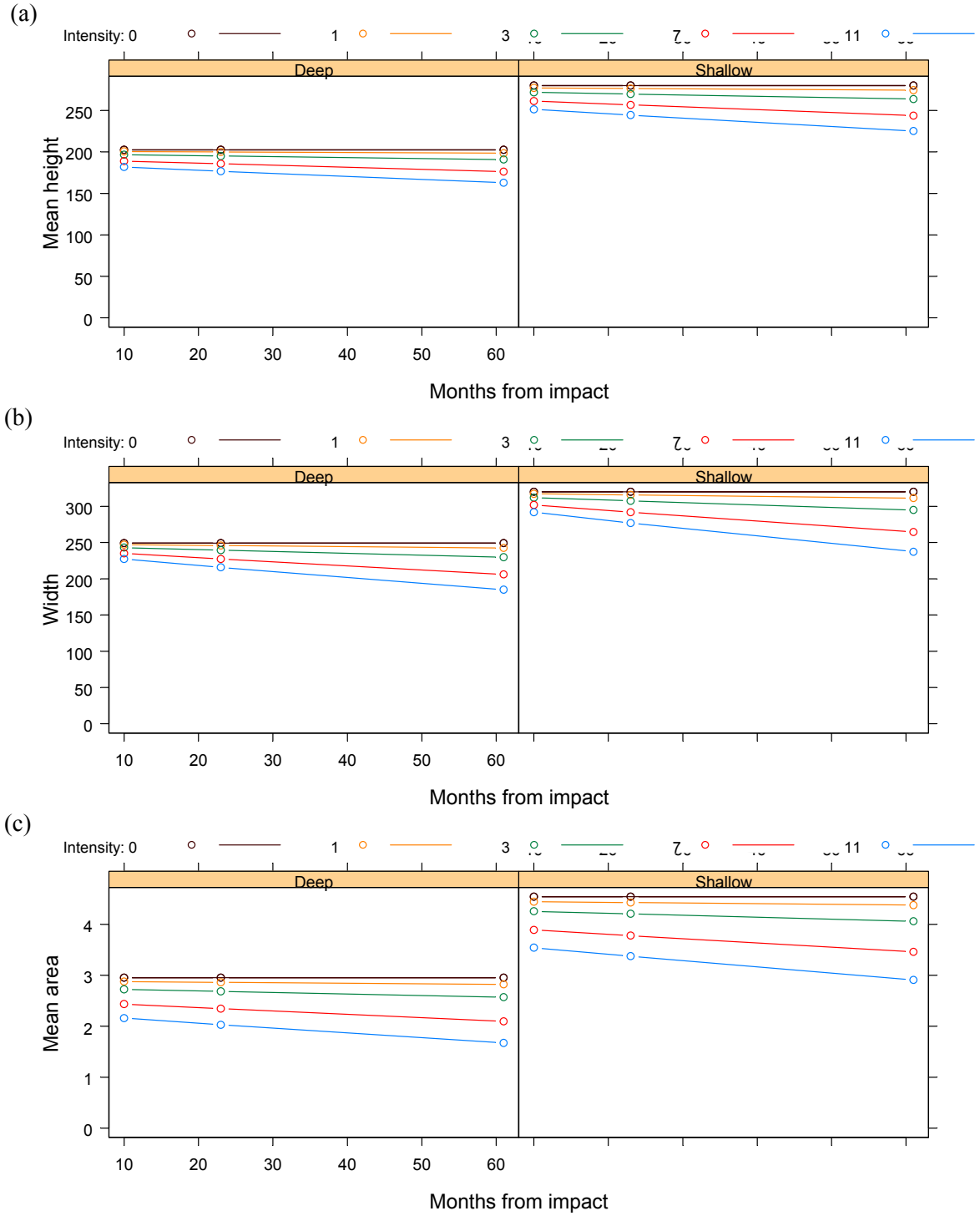

Figure 3-48: Plots of model 3 predictions for measured (a) height, (b) width and (c) area of *Dichotella divergens* observed by the ROV, against month after impact, by depth. The predictions show only the fixed effects and attempt to isolate the recovery signal from other sources of variation. The coloured lines show predictions for different trawl intensities.

3.3.2.2.3 Condition index

The raw indices of condition of *Dichotella divergens* varied among track replicates and time, with many impact tracks showing a higher proportion of animals in poor condition at months 1 or 10 or both; then generally, improved condition at month 61. The model comparisons for *Dichotella divergens* condition on Sled tracks supported model 1 (Topography, $p = 0.036$). The model 3 fixed effects indicated that, relative to controls, *Dichotella divergens* on impact tracks tended to in poorer condition at month 1 and then to improve(Figure 3-49); however, the impact and recovery terms were not significant ($p = 0.136$, $p = 0.203$).

The raw indices of condition of *Dichotella divergens* observed by the ROV showed that at months 10 or 23, condition on a number of patches — controls as well as impacts — tended to be poorer; and by month 61, condition on most patches had improved. The model 3 fit to these data showed no significant trawl or recovery effects on impacts relative to controls (Figure 3-50).

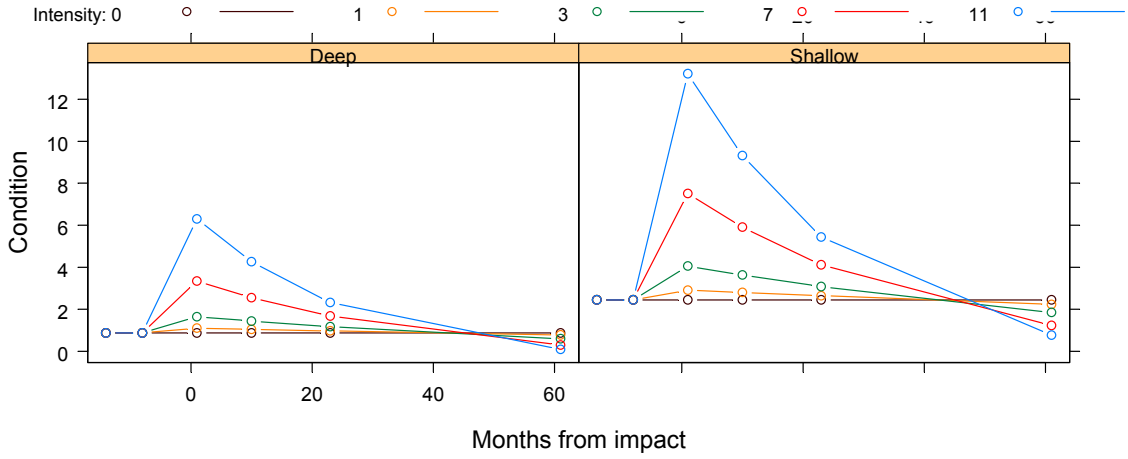

Figure 3-49: Plots of model 3 predictions for *Dichotella divergens* Condition Index (%) observed by the Sled. Poorer condition is indicated by values >0. The predictions show only the fixed effects and attempt to isolate the recovery signal from other sources of variation. The coloured lines show predictions for different trawl intensities.

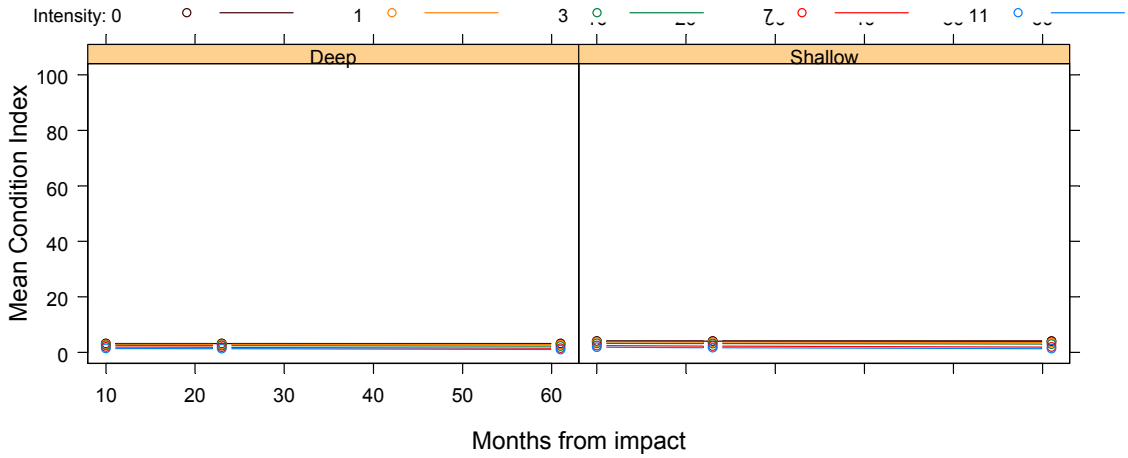

Figure 3-50: Plots of model 3 predictions for *Dichotella divergens* Condition Index (%) observed by the ROV. Poorer condition is indicated by values >0. The predictions show only the fixed effects and attempt to isolate the recovery signal from other sources of variation. The coloured lines show predictions for different trawl intensities.

3.3.2.2.4 Summary

The branched gorgonian *Dichotella divergens* was a common structural sessile megabenthos. In Sled transects, these gorgonians showed a non-significant impact trend of around -9% per trawl, followed by non-significant overall recovery trend. However, a significant Time*Intensity² term (p = 0.0205) suggested that low and medium intensity strata recovered above controls while high intensity strata continued to decline. The evidence for impact and recovery on ROV patches was mixed — the nearest neighbour density estimates indicated impact trends and the census data indicated recovery trends.

There were trends for negative effects on mean size of *Dichotella divergens* but none were significant. Evidence of recovery in mean size was mixed, possibly due to the recruitment of new small individuals interacting with growth of existing individuals.

On Sled transects, there were indications of impact effects worsening the condition of *Dichotella divergens*, followed by recovery — though neither were significant. The ROV data showed no clear trends.

The Sled and ROV overall numbers results were relatively consistent in pattern and magnitude, even if significance tests were mixed. *Dichotella divergens* appeared to show relatively low impact and then approximately recovered in numbers, and condition, roughly within the timeframe of the project.

3.3.3 Low impact, slow recovery

3.3.3.1 Alcyonacea

3.3.3.1.1 Abundance (numbers/density)

The soft corals *Alcyonacea* were reasonably common on Sled tracks, with typical numbers of almost 20 per Sled replicate. Estimates of densities tended to be higher— much higher on some tracks both impacts and controls — in earlier (months 1-23) in the Sled time series, then decrease by month 61. The model comparisons did not clearly reject model 5 (p = 0.059), indicative of a Time*Intensity² term. The model 5 fit to these data indicated low non-significant negative impact (~ -9%/trawl) with positive recovery (p = 0.056) and a borderline Time*Intensity² term (p = 0.088) suggesting that low and medium intensity strata recovered above controls while highest intensity strata continued to decline (Figure 3-51, a,b).

The Alcyonacea had similar occurrence on ROV patches on Sled tracks, with typical numbers in the order of 15-20 per patch. The general trend of raw census numbers on all patches was to decrease over the period of surveys, although on deep controls, numbers were notably higher at month 23. The model comparisons supported model 4 (p = 0.029), indicative of a significant Intensity*Time² term representing changing recovery with time. The model 4 fit to these data suggested non-signficant positive treatment response then decline followed by a levelling off, relative to changes on controls (Figure 3-52). ROV numbers standardised for patch footprint-area also supported model 4 (p = 0.0202), with a positive treatment response (p = 0.038), with subsequent trends for decline and levelling off (Figure 3-53).

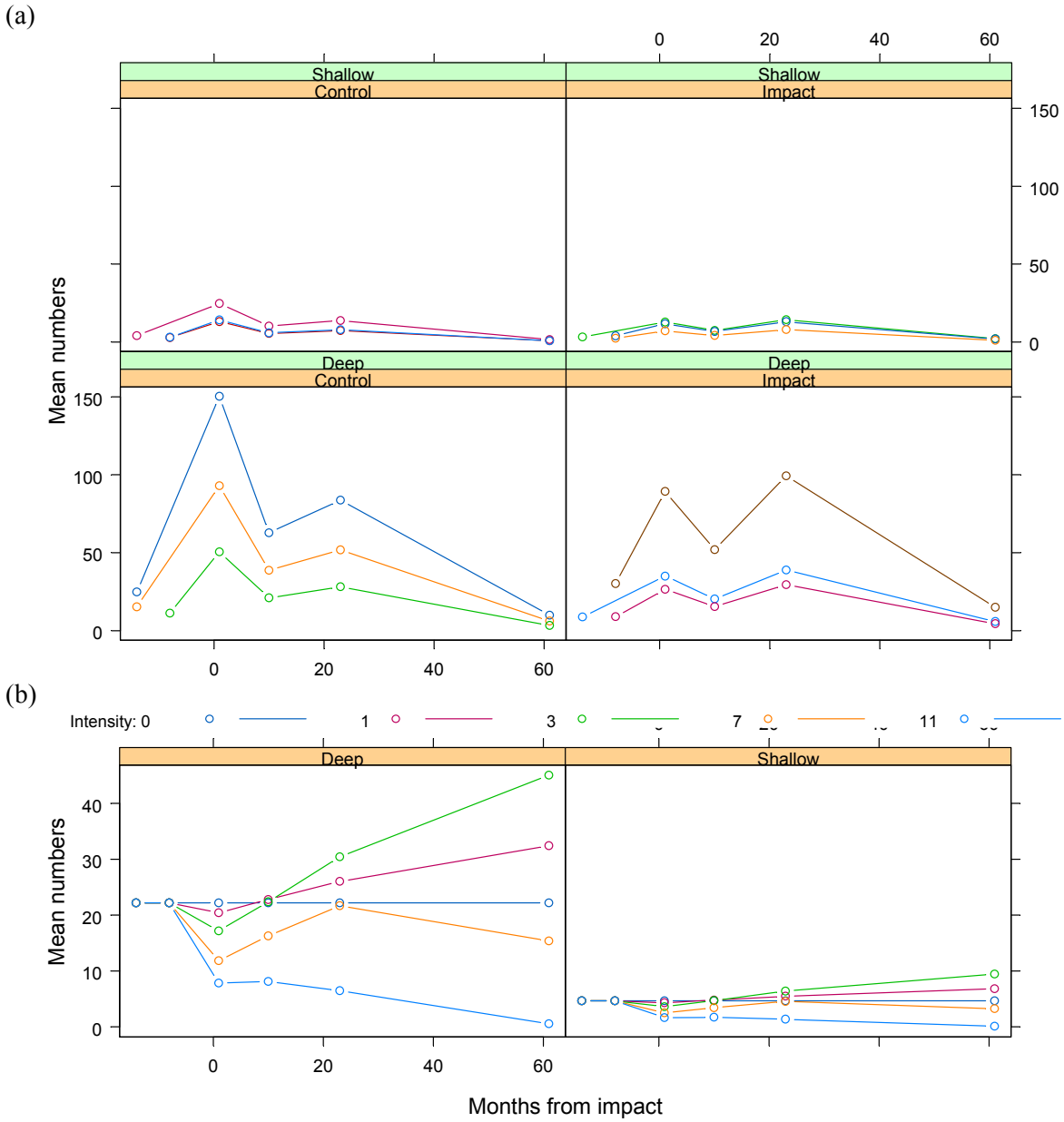

Figure 3-51: Plots of model 3 fit to numbers of Alcyonacea per Sled track by month: (a) fixed and random effects less residual variation (coloured lines follow individual tracks), (b) fixed effects only (coloured lines show predictions for different trawl intensities).

The model comparisons for ROV individual nearest-neighbour densities supported model 5 (p = 0.013), indicative of a Time*Intensity² term. The model 5 fit to these data suggested non-signficant positive treatment response then decline, which was more marked for intermediate trawl intensities than low or high intensity (p = 0.002) (Figure 3-54).

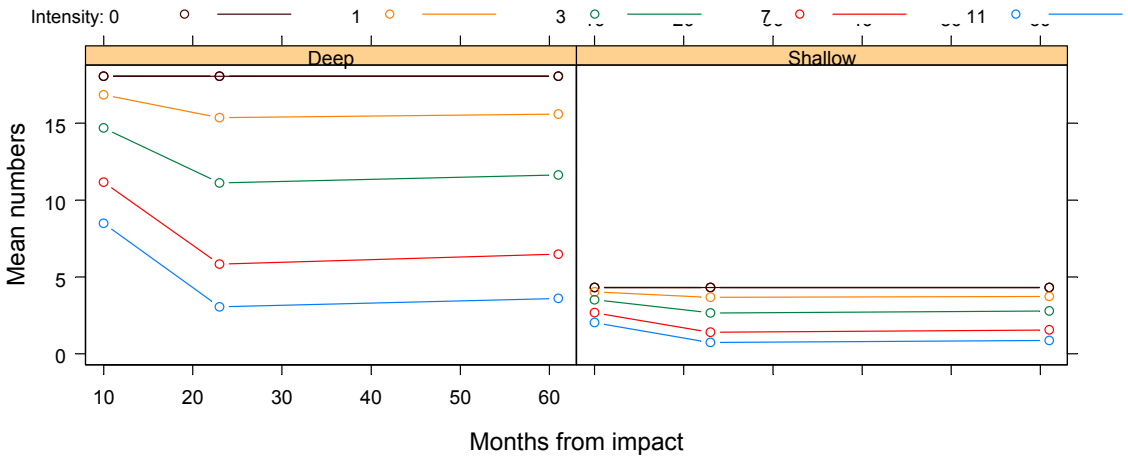

Figure 3-52: Plots of model 4 predictions for ROV patch census numbers for Alcyonacea against month after impact, by depth. The predictions show only the fixed effects and attempt to isolate the recovery signal from other sources of variation. The coloured lines show predictions for different trawl intensities.

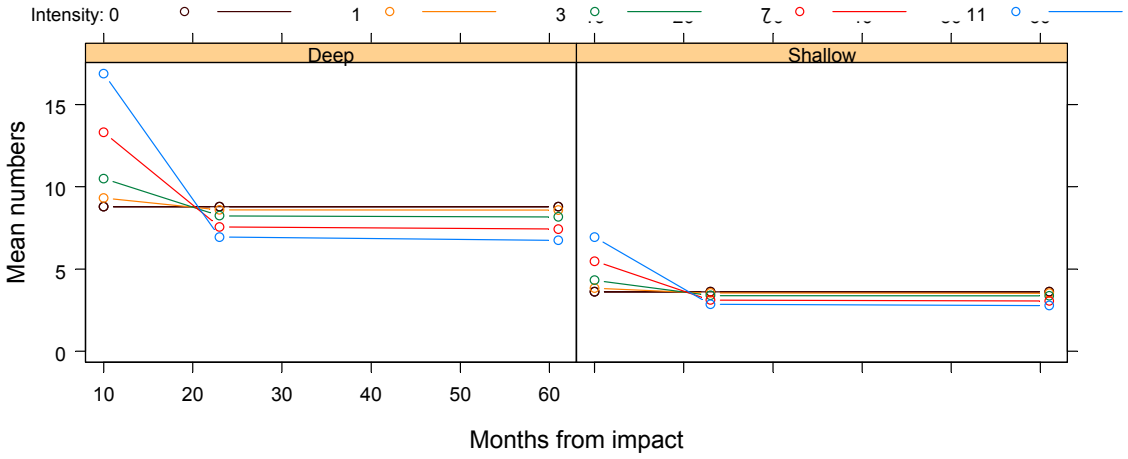

Figure 3-53: Plots of model 4 predictions for ROV patch density for Alcyonacea against month after impact, by depth. These represent census counts standardised for patch footprint-area, and are scaled to average patch footprint area. The predictions show only the fixed effects and attempt to isolate the recovery signal from other sources of variation. The coloured lines show predictions for different trawl intensities

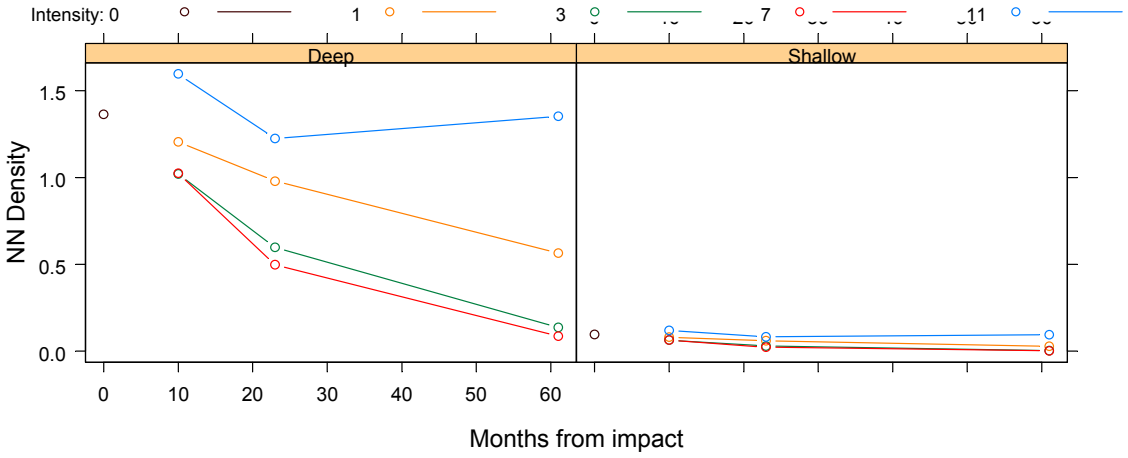

Figure 3-54: Plots of model 5 predictions for ROV nearest-neighbour densities (number per m²) for Alcyonacea against month after impact, by depth. These represent transformed nearest-neighbour distances (see methods). The predictions show only the fixed effects and attempt to isolate the recovery signal from other sources of variation. The coloured lines show predictions for different trawl intensities.

3.3.3.1.2 Size attributes

The overall pattern of *Alcyonacea* on both deep and shallow Sled videoed tracks was progression of size structures over time, on both controls and impacts, with notably higher proportions of the smallest class at month 1 (which could be interpreted as recruits), which were absent at month 61. On shallow tracks at month 1, there were fewer larger individuals on higher-intensity strata consistent with a trawl effect (Figure 3-55). By month 23 the size structures were similar across all strata.

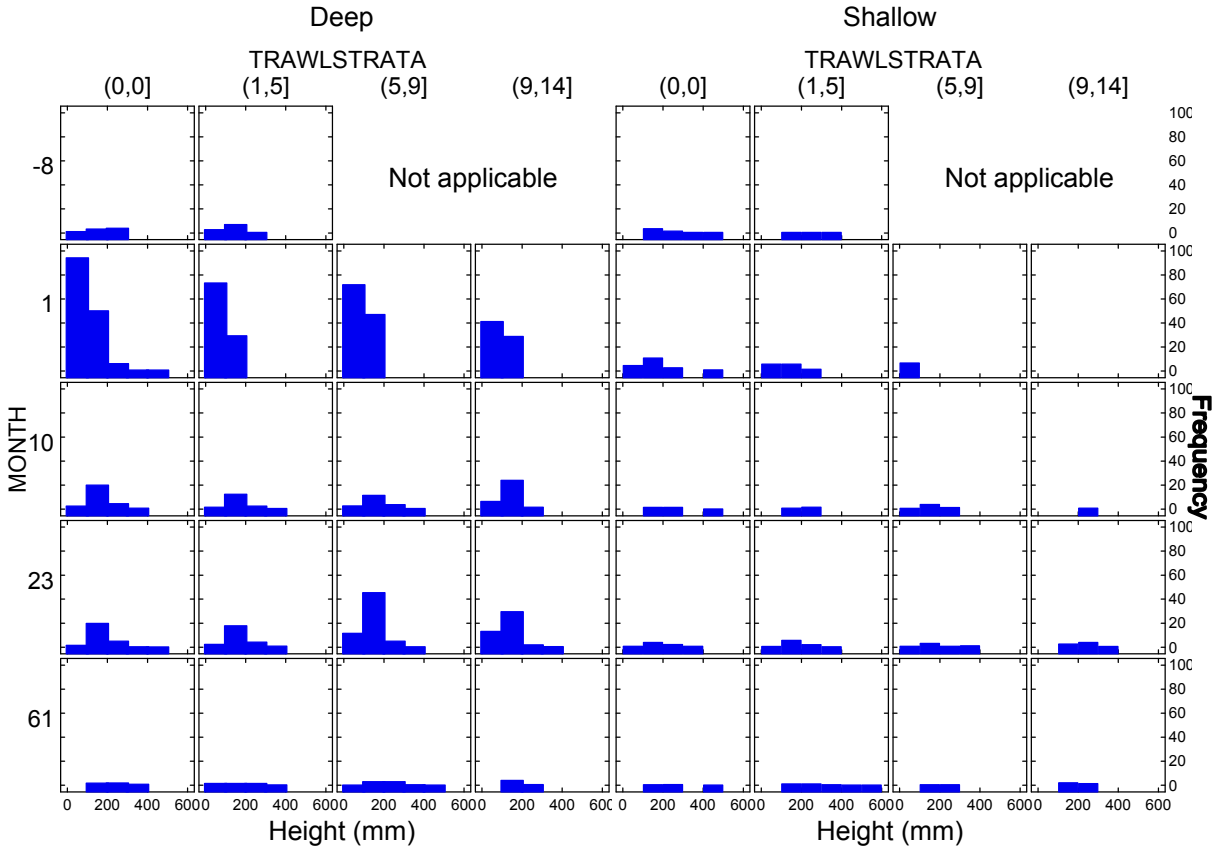

Figure 3-55: Size-frequency distributions of Alcyonacea heights observed by the Sled, by depth, trawl-intensity strata (columns) and month after impact (rows), standardized by Sled swept area. Size categories are 100 mm intervals. Note that the before status of impact tracks is indicated by month –8 and trawl strata (1,5], which includes the single coverage of the earlier BACI experimental plots; the higher intensity strata did not occur until the repeated-trawling experiment.

The model comparisons of Sled heights provided limited support for model 4 ($p = 0.094$), suggesting a variable response in time post-impact. Model 4 predictions of mean height of individual Alcyonacea showed that animals on shallow tracks were taller ($p = 0.0012$), no change with trawl intensity, and suggested ($p = 0.089$) a decrease after impact consistent with new recruitment followed by an increase consistent with subsequent growth — after accounting for changes on control tracks (Figure 3-56). Sample numbers were notably less at month 61 than month 23, despite equivalent sampling effort, and is possibly indicative of senescence of the population.

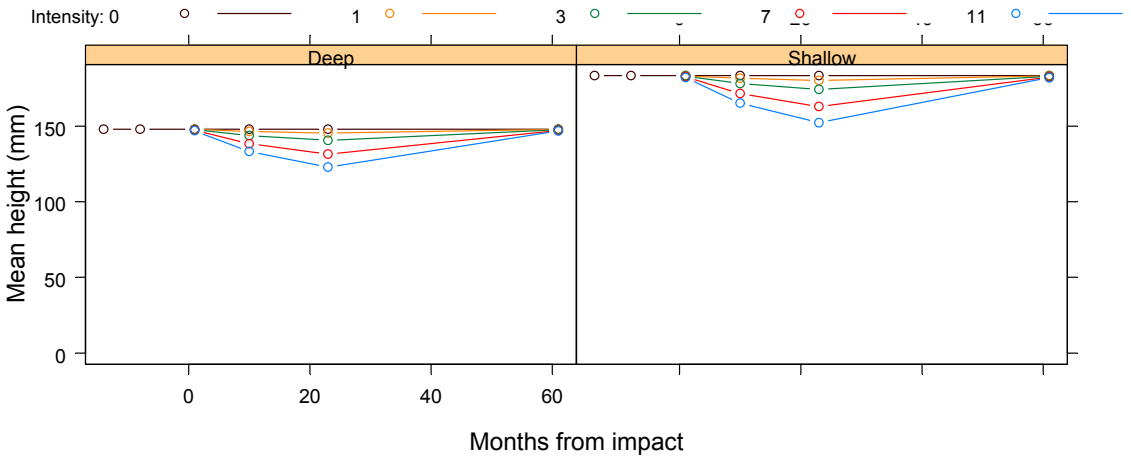

Figure 3-56: Plots of model 3 predictions for mean heights of individual Alcyonacea observed by the Sled against month after impact, by depth. The predictions show only the fixed effects and attempt to isolate the recovery signal from other sources of variation. The coloured lines show predictions for different trawl intensities.

The pattern of size-distributions for Alcyonacea by trawl strata and months on ROV patches shared some similarities to that for the Sled, considering that in month 1 there were limited ROV observations when the Sled had observed substantial recruitment. For example, there were some indications of progression of size structures over time, on both controls and impacts. There were slightly fewer larger individuals on higher intensity strata at month 10, consistent with a trawl effect, more so on shallow tracks (Figure 3-57). On deep patches at month 61 the proportion of the small size class increased and is possibly evidence of recruitment.

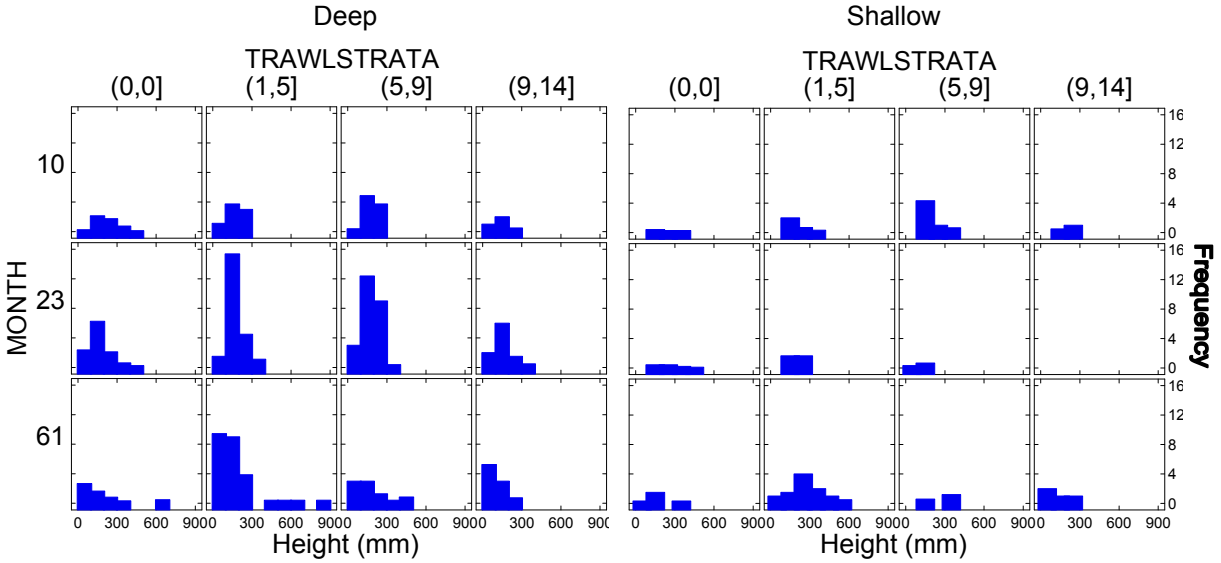

Figure 3-57: Size-frequency distributions of Alcyonacea heights observed by the ROV, by depth, month after impact (columns) and trawl-intensity strata (rows), standardized by number of replicate observations. Size categories are 100 mm intervals.

The model comparisons for individual Alcyonacea heights measured by the ROV supported model 2 (suggesting a trawl effect $p = 0.011$). Model 3 indicated a slight negative trawl intensity effect and continued decrease in mean height (consistent with recruitment) on trawled areas relative to controls

(Figure 3-58), but neither coefficients were significant. The patterns of ROV individual width and individual area data for Alcyonacea were consistent with those for height. All models hinted that animals on shallow patches were larger than those on deep (p = 0.136, 0.074, 0.066) (Figure 3-58).

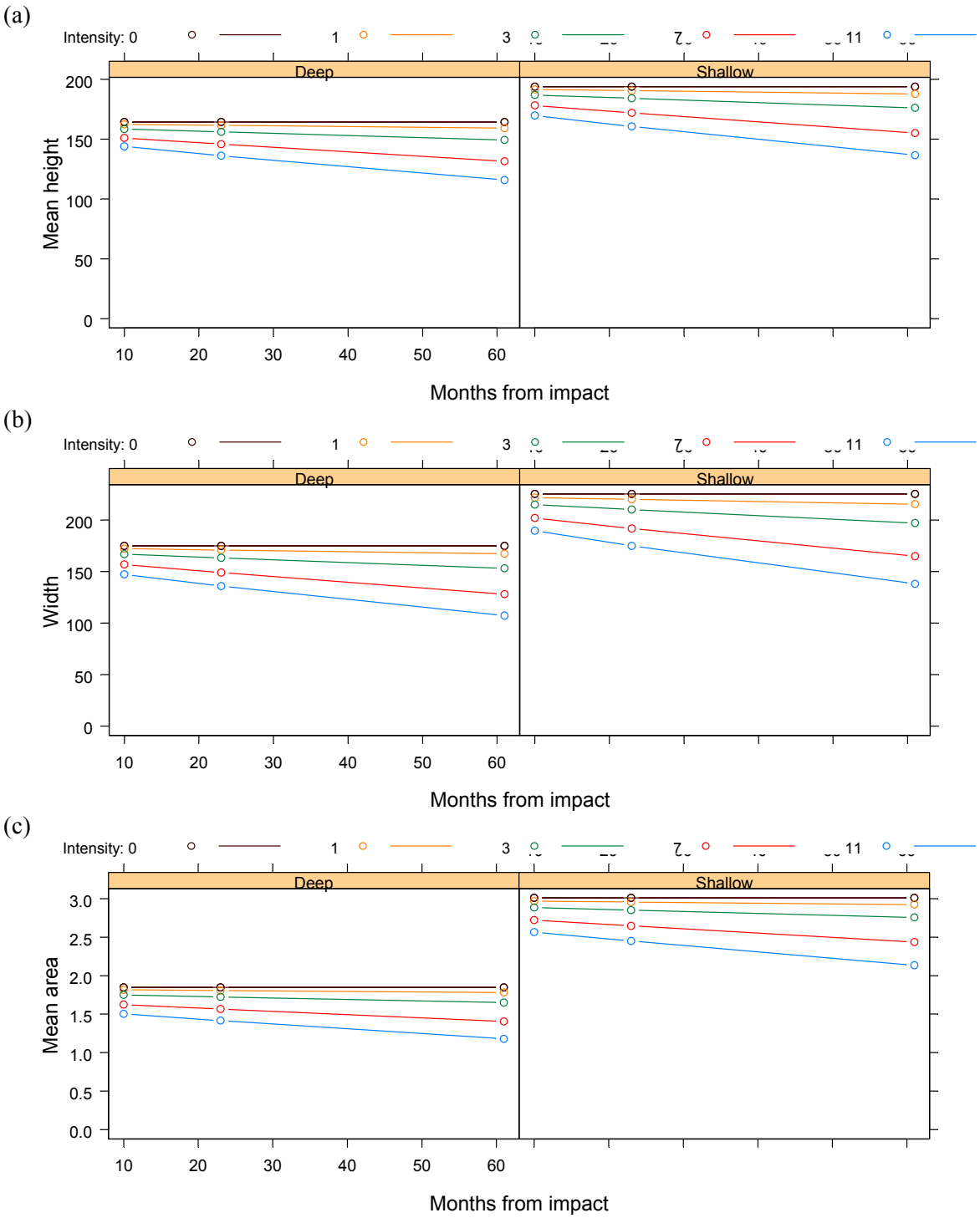

Figure 3-58: Plots of model 3 predictions for measured (a) height, (b) width and (c) area of Alcyonacea observed by the ROV, against month after impact, by depth. The predictions show only the fixed effects and attempt to isolate the recovery signal from other sources of variation. The coloured lines show predictions for different trawl intensities.

3.3.3.1.3 Condition index

The raw indices of condition of Alcyonacea varied among Sled replicates and time, with many transects showing a higher proportion of animals in poor condition at months 10 or 23 or both, on control as well as impact tracks, generally with improved condition at month 61. The model comparisons for Alcyonacea condition on Sled tracks supported model 5 (p = 0.0425), indicative of an important time*intensity² term. The model 5 fixed effects corroborated this (p = 0.0542) and, relative to controls, indicated that condition of Alcyonacea on impact tracks showed no immediate trawl effect but those in very high intensity strata tended to be in poorer condition after more than about a year and then to improve (note that Figure 3-59 shows straight-line predictions between observation times, not the actually curvilinear model, which peaks at about month 40).

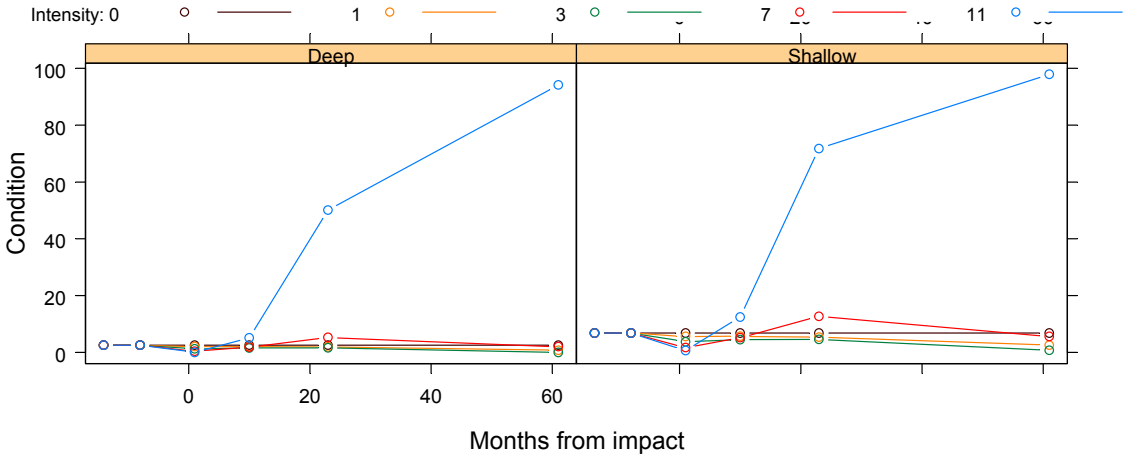

Figure 3-59: Plots of model 3 predictions for Alcyonacea Condition Index (%) observed by the Sled. Poorer condition is indicated by values >0. The predictions show only the fixed effects and attempt to isolate the recovery signal from other sources of variation. The coloured lines show predictions for different trawl intensities.

The raw indices of condition of Alcyonacea observed by the ROV showed that at months 10 or 23 or both, condition on a number of patches — controls as well as impacts — was poor. By month 61, condition on most patches had improved. No models converged to fit the ROV data for condition of Alcyonacea.

3.3.3.1.4 Summary

The soft corals Alcyonacea were relatively common, though smaller contributors to benthic structure. Like Nephtheidae, there was noticeable widespread recruitment, growth and senescence of these benthos across the study area with little differential in this pattern between controls and impacts. In Sled transects, these soft corals showed a non-significant impact trend of around -9% per trawl, followed by an overall recovery trend of about 1.9% per year per trawl, though low and medium intensity strata may have recovered above controls while high intensity strata continued to decline. The ROV surveys, which began at month 10, appeared to coincide with the end of a similar broad recruitment of Alcyonacea onto ROV patches and with the senescence phase of the bloom. There was no clear pattern of impact and recovery on on impacts relative to controls.

Size frequencies were consistent with recruitment and growth. There was limited evidence of any trawl effect on mean size, though some evidence of a reduction in mean size due to recruitment and — on Sled tracks — followed by an increase due to growth.

Field observations showed that a higher proportion of Alcyonacea soft corals were in poorer condition everwhere at month 10 and/or 23 followed by improvement. Analyses of impacts relative to controls suggested this pattern was emphasized at high intensities.

Like Nephtheidae, it is possible that the substantial recruitment of Alcyonacea soft corals at about the time of the depletion experiment represented a “weed-like” response to disturbance, although controls as well as impacts were involved. Possibly because of this response, the impact-relative-to-control results for Sled and ROV abundance were not consistent and of variable significance: the Sled showed a small negative impact with slow recovery while the ROV showed a small positive 'impact' followed by decline. The extensive bloom of soft corals may actually be indicative of a rapid recovery potential for these benthos, which was not clearly apparent from the contrasts of impacts relative to controls.

3.3.3.2 Junceella fragilis

3.3.3.2.1 Abundance (numbers/density)

The white seawhip *Junceella fragilis* was almost an order of magnitude less abundant than the red seawhip, with typical numbers in the order of 15 per Sled replicate. Estimates of densities were variable and raw numbers showed some indication of an impact effect at month 1 and/or 10, and low-intensity strata showed some evidence of recovery, whereas high-intensity strata appeared to decline further. The model comparisons provided support for Model 2 ($p = 0.05$), indicating that the Intensity term was likely to be important. Model 3 fit to these data indicated that deep control tracks tended to have greater and more variable abundance, and that some impact tracks showed slight declines (Figure 3-60a). The coefficients of model 3 fixed effects, indicated low non-significant negative impact (-5.8% per trawl) with ongoing non-significant decline (Figure 3-60b).

ROV raw census numbers for *Junceella fragilis* averaged about 30 per patch and were also highly variable. On deep controls, numbers appeared to increase from month 10 to 20, then remain approximately steady; shallow controls changed little overall. Numbers on low-intensity strata on shallow patches appeared to increase from month 10 through 61, whereas numbers on high-intensity strata on deep patches appeared to decrease; others were variable.

The model comparisons for census numbers indicated that model 2 was significant ($p = 0.0009$), suggesting an important trawl intensity term. The model 3 fit to these data confirmed that higher intensity strata had fewer animals ($p = 0.0002$), and there was no recovery trend with time ($p = 0.92$) relative to changes on controls (Figure 3-61). For ROV numbers standardised for patch footprint-area, the model 3 indicated significantly higher densities in shallow patches ($p = 0.0001$), and that higher intensity strata had lower densities (but $p = 0.25$) and there was no recovery trend with time ($p = 0.95$) (Figure 3-62).

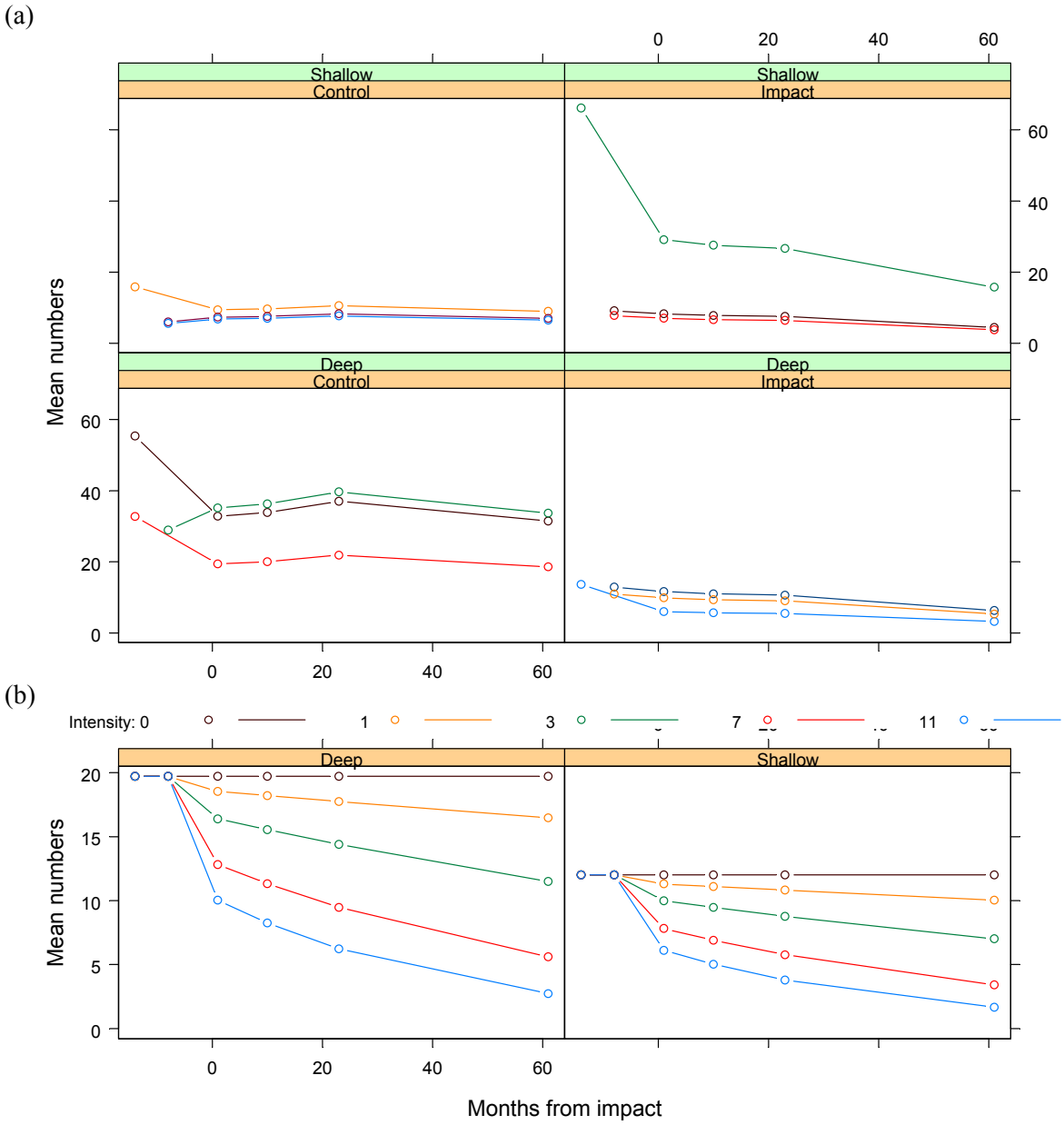

Figure 3-60: Plots of model 3 fit to numbers of *Junceella fragilis* per Sled track by month: (a) fixed and random effects less residual variation (coloured lines follow individual tracks), (b) fixed effects only (coloured lines show predictions for different trawl intensities).

The model comparisons for ROV individual nearest-neighbour densities provided some support for model 3 (p = 0.08), possibly suggesting an important time*intensity term. Model 3 indicated that shallow patches had higher densities (p = 0.0019), a trend for an initial intensity effect (approx. -5.8%/trawl, but p = 0.329) followed by ongoing decline (-3.6%/yr/trawl, p = 0.0714) (Figure 3-63).

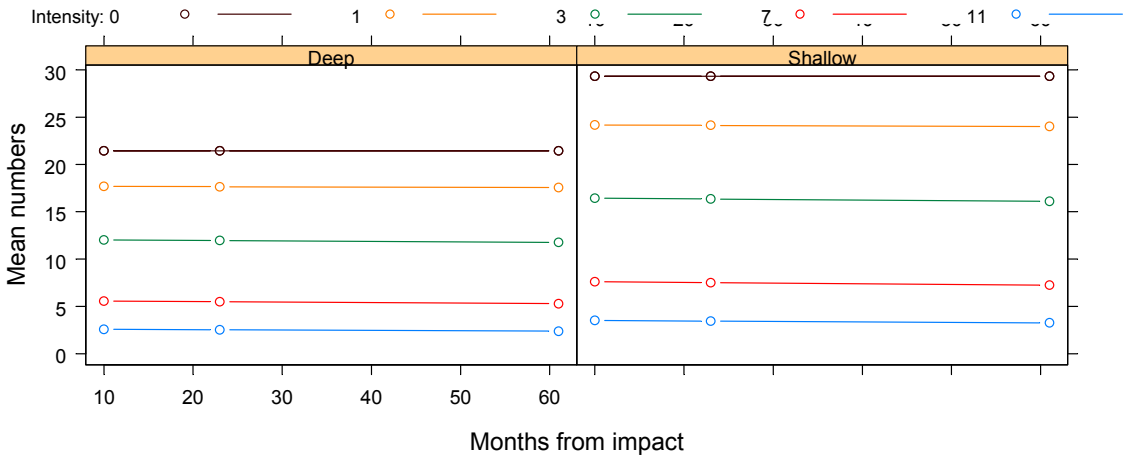

Figure 3-61: Plots of model 3 predictions for ROV patch census numbers for *Junceella fragilis* against month after impact, by depth. The predictions show only the fixed effects and attempt to isolate the recovery signal from other sources of variation. The coloured lines show predictions for different trawl intensities.

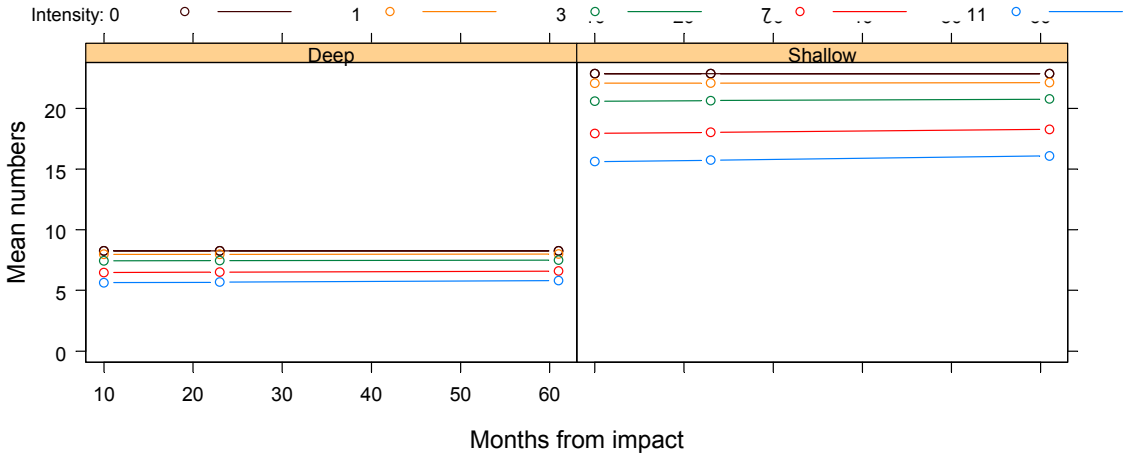

Figure 3-62: Plots of model 3 predictions for ROV patch density for *Junceella fragilis* against month after impact, by depth. These represent census counts standardised for patch footprint-area, and are scaled to average patch footprint area. The predictions show only the fixed effects and attempt to isolate the recovery signal from other sources of variation. The coloured lines show predictions for different trawl intensities.

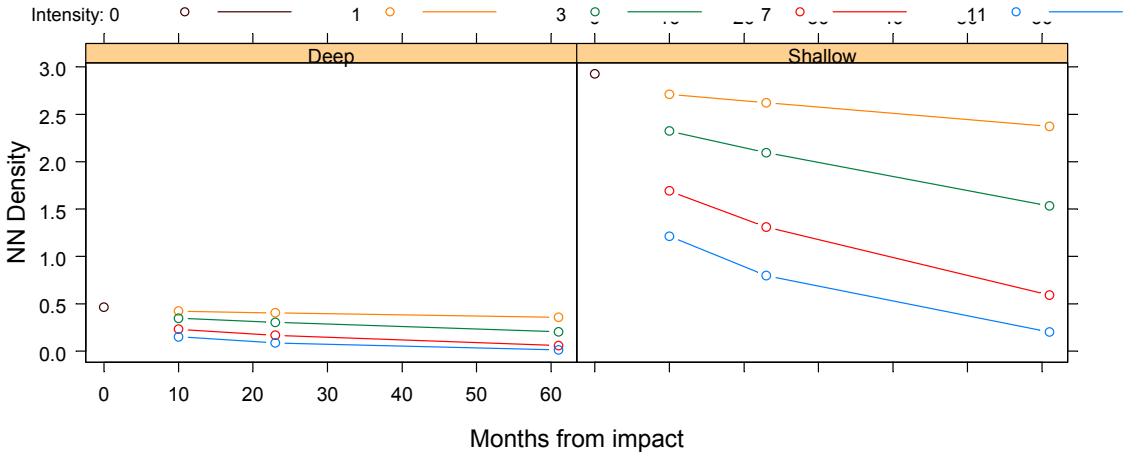

Figure 3-63: Plots of model 3 predictions for ROV nearest-neighbour densities (number per m²) for *Junceella fragilis* against month after impact, by depth. These represent transformed nearest-neighbour distances (see methods). The predictions show only the fixed effects and attempt to isolate the recovery signal from other sources of variation. The coloured lines show predictions for different trawl intensities.

3.3.3.2.2 Size attributes

The size-frequency distributions for *Junceella fragilis* (Figure 3-64) have few individuals in impact strata at month 1, and on deep tracks, these size structures were shorter than controls. With time, the sample numbers increased, partly because of additional replicates and presumably recruitment as well, and size structures broadened, though without obvious progression from shorter modes. On shallow tracks, the sample numbers increased greatly after month 1, although the height trend with intensity changed little.

The model comparisons of Sled mean heights supported model 1 (p = 0.0067), suggesting a deep–shallow difference in height. The model 3 predictions of mean heights of individual *Junceella fragilis* confirmed that shallow whips were longer (p < 0.0067) and showed a slight non-significant trend for initial decrease with trawl intensity (p = 0.501), followed by slight non-significant trend for ongoing decreases (p = 0.707) (Figure 3-65) that could have been due to recruitment of new, shorter, animals. The length of seawhips could not be measured properly by the ROV, so there were no data for height changes on ROV patches.

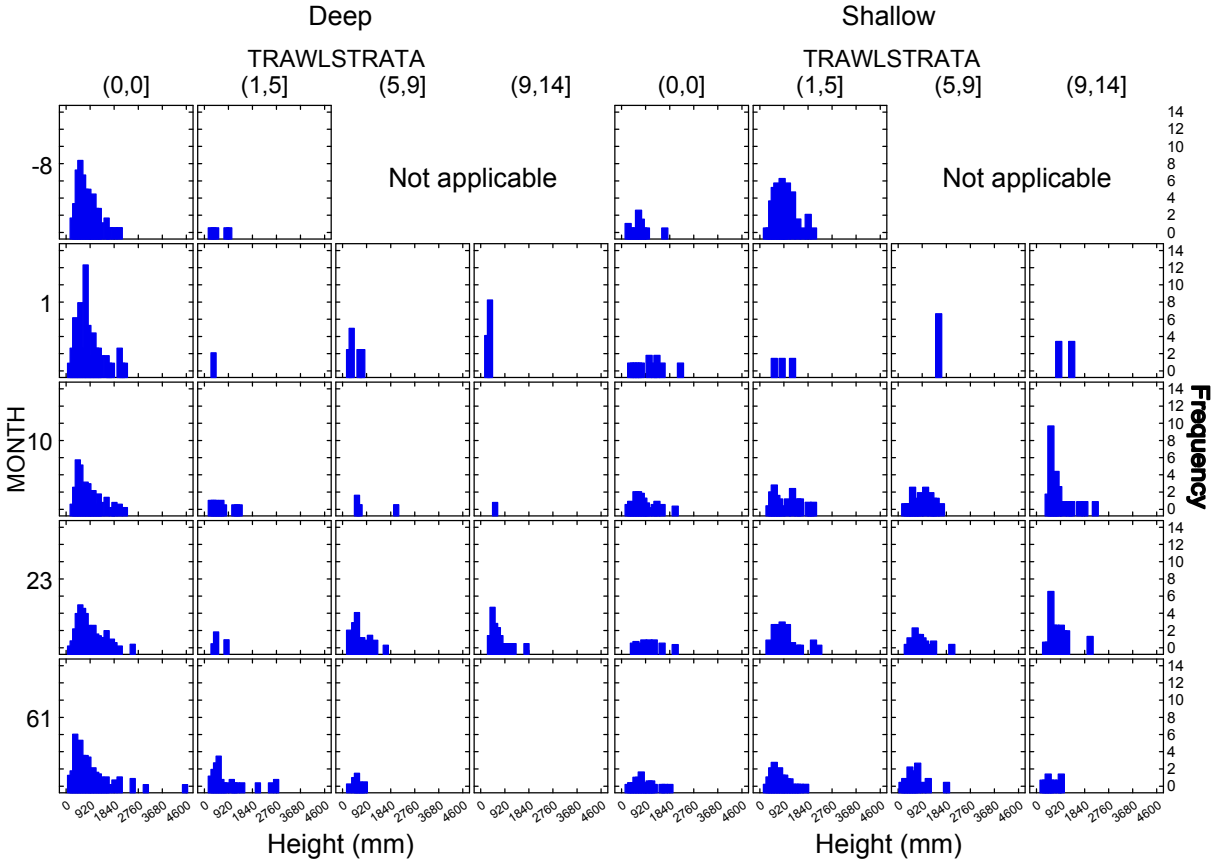

Figure 3-64: Size-frequency distributions of *Junceella fragilis* heights observed by the Sled, by depth, trawl-intensity strata (columns) and month after impact (rows), standardized by Sled swept area. Size categories are 100 mm intervals. Note that the "before" status of impact tracks is indicated by month –8 and trawl strata (1,5], which includes the single coverage of the earlier BACI experimental plots; the higher intensity strata did not occur until the repeated-trawling experiment.

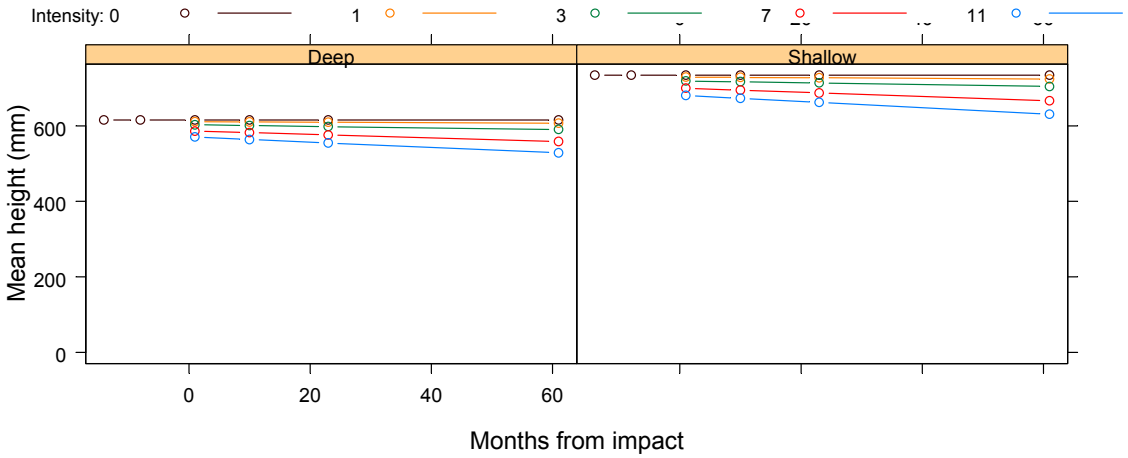

Figure 3-65: Plots of model 4 predictions for mean heights of individual *Junceella fragilis* observed by the Sled against month after impact, by depth. The predictions show only the fixed effects and attempt to isolate the recovery signal from other sources of variation. The coloured lines show predictions for different trawl intensities.

3.3.3.2.3 Condition index

The raw indices of condition of *Junceella fragilis* was variable among track replicates and time. *Junceella fragilis* on both impacts and controls were in good condition initially, but tended to be in worse condition at month 10 on shallow impacts, with some improvement subsequently. As with red whips, this was consistent with observations of some seawhips on impact tracks having had living polyps stripped from their skeletons at month 1, and these stripped areas becoming more obvious and encrusted at month 10. The model comparisons for *Junceella fragilis* condition on Sled tracks did not distinguish among models. The model 3 predictions (Figure 3-66) showed that relative to controls *Junceella fragilis* on impact tracks tended to be very slightly and non-significantly poorer in condition after impact (p = 0.85) and then become very slightly worse with time though not significantly (p = 0.68).

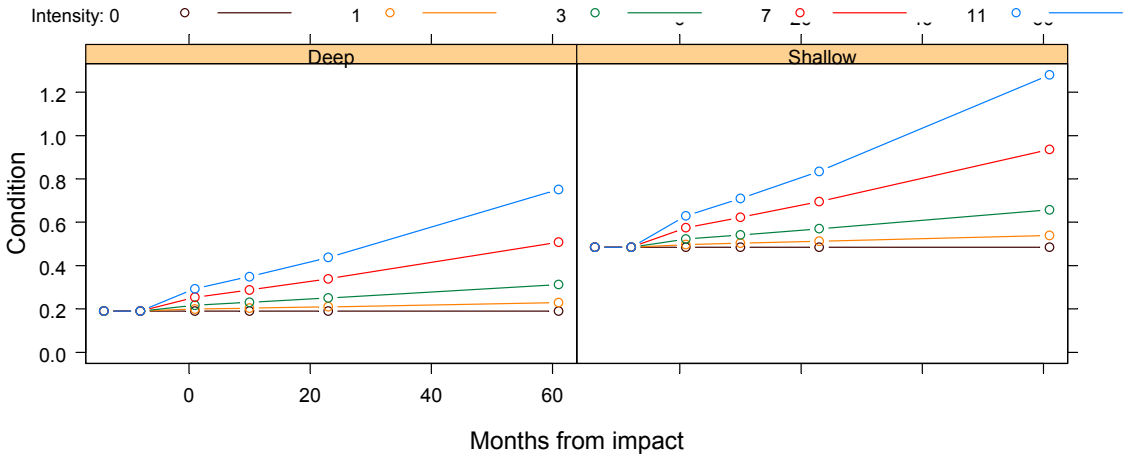

Figure 3-66: Plots of model 3 predictions for *Junceella fragilis* Condition Index (%) observed by the Sled. Poorer condition is indicated by values >0. The predictions show only the fixed effects and attempt to isolate the recovery signal from other sources of variation. The coloured lines show predictions for different trawl intensities.

The raw indices of condition of *Junceella fragilis* on ROV patches showed a somewhat similar pattern to the Sled data, with condition on some impact patches appearing to be worse at month 10, then possibly improving by month 61. There was also a tendency for condition to become worse on higher-intensity strata than on low-intensity strata. The model comparisons provided some support for Model 2 (p = 0.087), hinting at a possible impact effect. The model 3 predictions confirm a small impact effect of a few percent (p = 0.038) followed by a slight non-significant recovery trend (p = 0.58) (Figure 3-67).

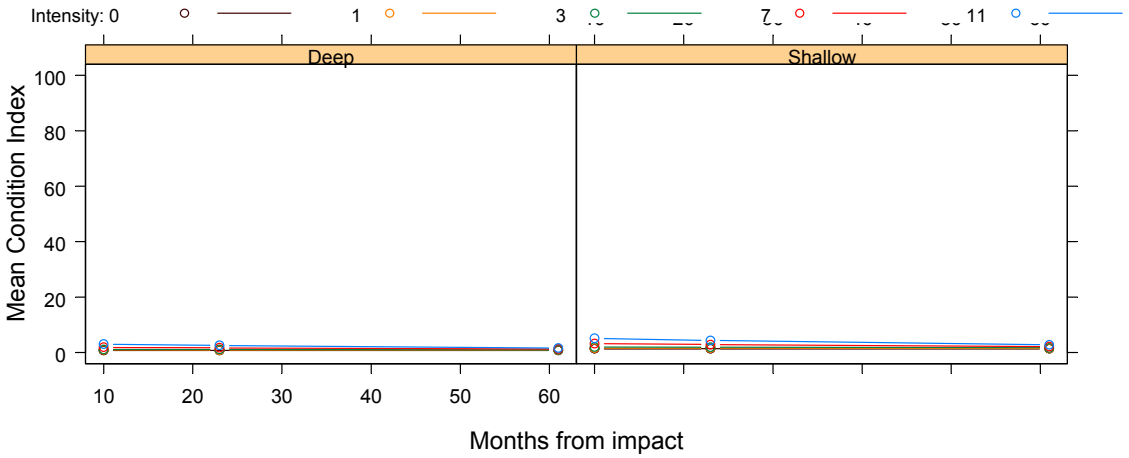

Figure 3-67: Plots of model 4 predictions for *Junceella fragilis* Condition Index (%) observed by the ROV. Poorer condition is indicated by values >0. The predictions show only the fixed effects and attempt to isolate the recovery signal from other sources of variation. The coloured lines show predictions for different trawl intensities

3.3.3.2.4 Summary

The white seawhip *Junceella fragilis* was common but much less numerous than the red whip. The white whips appeared to show a low non-significant impact effect of around -5.8% per trawl, followed by an ongoing non-significant decline. The evidence from the ROV patches and Sled transects was consistent.

While the mean size of *Junceella fragilis*, as measured from the Sled, was shorter on deep tracks, there were no significant impact/recovery effects. The slight trends observed may have been consistent with somewhat selective removal of larger individuals, followed by some recruitment and then growth. Length of whips could not be measured from the ROV.

There were indications of impact effects worsening the condition of *Junceella fragilis* slightly (significant for ROV), but the Sled and ROV provided conflicting post-impact trends (neither significant).

The Sled and ROV results for abundance trends were quite consistent in pattern and magnitude, even if non-significant. *Junceella fragilis* showed a relatively low impact and then appeared to continue declining in numbers, during the timeframe of the project.

3.3.3.3 Solenocaulon sp.

3.3.3.3.1 Abundance (numbers/density)

The often encrusted *Solenocaulon* gorgonian stalks were moderately common on Sled tracks, typically about 10 per Sled replicate, and made a small contribution to habitat structure. As with all other species, estimates of densities were variable. Numbers tended to be higher at months 1 and 23 and lower at months 10 and 61. The model comparisons did not distinguish among models. The model 3 predictions showed a small positive trend with intensity initially followed by a slight decline with time, but none of the coefficents were significant.

ROV raw census numbers for *Solenocaulon* sp. averaged about five per patch and were highly variable, with no obvious consistent patterns with intensity strata or time. No models converged with the raw census data. After standardising ROV numbers for patch footprint-area, model comparisons supported model 1, indicating a significant topography (depth strata) term ($p < 0.0001$). The model 3 predictions confirmed this and indicated a positive intensity term ($p = 0.0108$) then followed by a non significant declining trend ($p = 0.332$).

The model comparisons for ROV nearest-neighbour densities for *Solenocaulon* provided some support for model 5 ($p = 0.069$) indicating an important Time*Intensity² term. The model 5 coefficents corroborated this (T*I², $p = 0.071$) and also suggested a non significant ($p = 0.642$) negative impact trend of ~1% per trawl followed by a declining trend at intermediate intensities and recovery at high intensities.

3.3.3.3.2 Size attributes

The pattern of size-frequency distributions for *Solenocaulon* sp. on Sled tracks, by trawl strata and months, was consistent with an effect on size structure, followed by recovery with progression of size structures with time — over the same period, size distributions on controls remained relatively stable — particularly on shallow tracks.

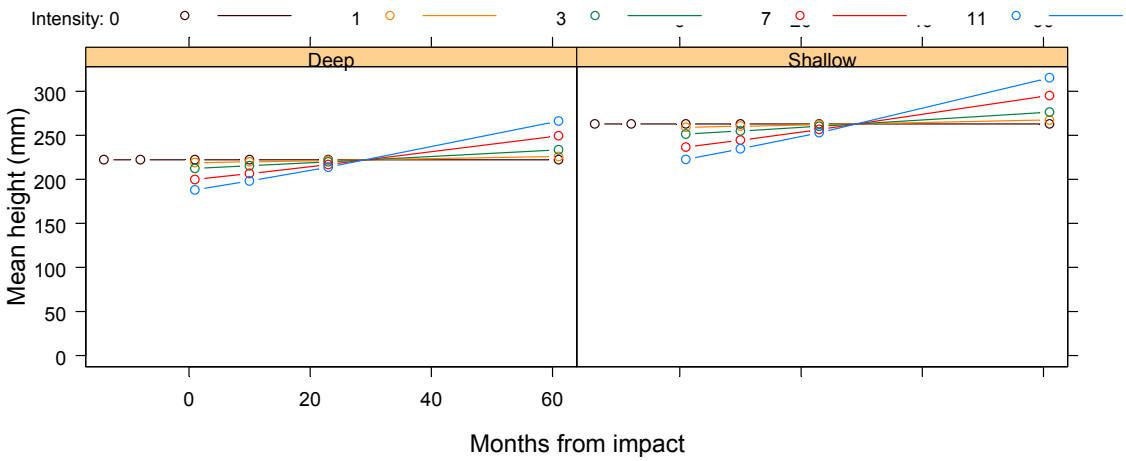

Figure 3-68: Plots of model 3 predictions for mean heights of individual *Solenocaulon sp.* observed by the Sled against month after impact, by depth. The predictions show only the fixed effects and attempt to isolate the recovery signal from other sources of variation. The coloured lines show predictions for different trawl intensities.

Model comparison tests supported Model 3 (p = 0.023). The model 3 predictions of mean heights of individual *Solenocaulon* sp. (Figure 3-68) confirmed that shallow animals were taller (p < 0.0063) and showed a slight trend for initial decrease in height with trawl intensity (p = 0.056), followed by recovery in mean height (p = 0.022), presumably due to growth of recruited animals.

On ROV patches, the size of *Solenocaulon* sp. could not be measured properly or consistently, as was the case for whips. The ROV size data for this species were not modelled.

3.3.3.3.3 Condition index

The raw indices of condition of *Solenocaulon* sp. varied among track replicates and time on shallow tracks, tending to be worse at month 23 on some replicates. The model comparisons for *Solenocaulon* sp. condition on Sled tracks distinguished model 1, suggesting a shallow vs deep difference. The model 3 predictions confirmed the slight depth diffference, and indicated that relative to controls *Solenocaulon* sp. on impact tracks tended to be very slightly and non-significantly poorer in condition after impact (p = 0.69) and then become very slightly worse with time though not significantly (p = 0.73). The raw indices of condition of *Solenocaulon* sp. on ROV patches had virtually no observable variation.

3.3.3.3.4 Summary

The *Solenocaulon* gorgonians appeared to show little impact and/or recovery response. The non-significant slight trends hinted at small increases on impacts relative to controls, followed by small relative decline. The ROV census results were similar, while the nearest-neighbour density trends were opposite though also small and non-significant.

The size distributions of *Solenocaulon* on Sled tracks showed some support for a small negative effect on mean height followed by some growth.

There were no significant impact effects on the condition of these gorgonians.

While the results for the Sled and ROV were somewhat mixed, any observed effects were very small and clearly non-significant.

3.3.4 High impact, fast recovery

3.3.4.1 Turbinaria frondens

3.3.4.1.1 Abundance (numbers/density)

The hard coral *Turbinaria frondens* was the most common hard coral species: typically about five per Sled replicate, though one deep control track had about 10-fold higher numbers. The highest numbers occurred on deep controls, but *Turbinaria frondens* was almost absent from deep impact tracks. On shallow tracks, numbers were also higher on controls and progressively less abundant with trawl

intensity on impact tracks. With time, numbers tended to be lower at month 10 and then generally increase at months 23 and 61.

The model comparisons supported model 5 (p = 0.022), indicative of a Time*Intensity² term. The model 5 fit to these data suggested a very high negative impact (~ -50%/trawl, p = 0.072) and complex post impact terms (Time*Intensity, Time²*Intensity, Time*Intensity² terms — all individually ns: p = 0.17, 0.33, 0.21) suggesting that low and medium intensity strata recovered quickly while highest intensity strata recovered little (Figure 3-69), and hinting at recovery due to self-recruitment. Overall recovery was approximately +7% per year per trawl (p = 0.021).

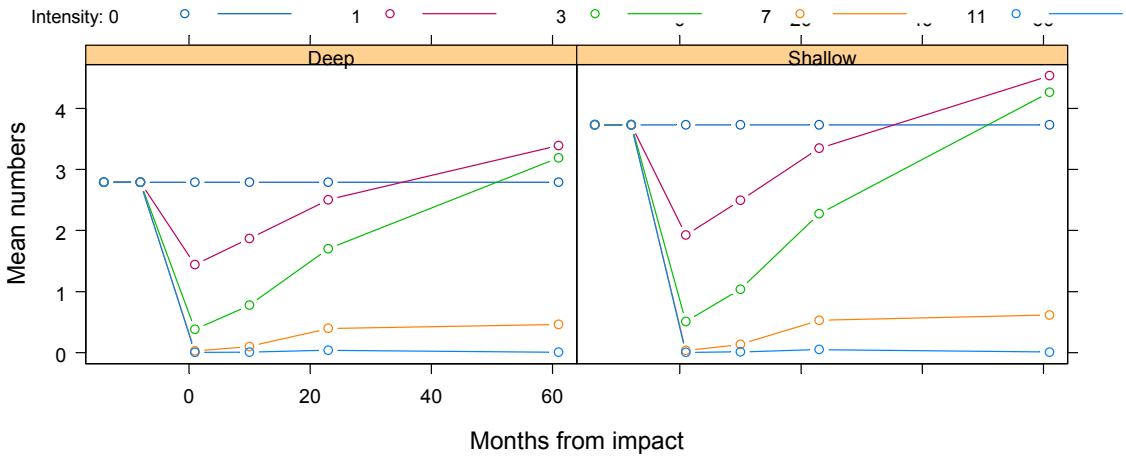

Figure 3-69: Plots of model 3 fit to numbers of *Turbinaria frondens* per Sled track by month: fixed effects only (coloured lines show predictions for different trawl intensities).

ROV raw census numbers for *Turbinaria frondens* averaged about six per patch, and showed similar patterns to the Sled by depth, treatment, trawl intensity and time. The model comparisons for census numbers indicated that model 4 was significant (p < 0.0001), suggesting an important time²*intensity term. The model 4 fit to these data confirmed that higher intensity strata had fewer animals (p = 0.0102), and indicated a slowing recovery trend with time (+time*intensity, -time²*intensity, both ns) relative to changes on controls. The overall recovery trend was +4.8%/yr/trawl (but p = 0.25). For ROV numbers standardised for patch footprint-area, no models converged.

The model comparisons for ROV individual nearest-neighbour densities supported model 5 (p = 0.003), suggesting an important time*intensity² term. Model 5 showed a strong trawl impact effect (approx. -60%/trawl, p = 0.0078) followed by complex post impact terms (-Time*Intensity, +Time²*Intensity, +Time*Intensity² terms; p = 0.32, 0.98, 0.003) suggesting that low intensity strata continued to decline while high intensity strata showed signs of recovery. Overall recovery rate was moderate (+5.3%/yr/trawl), but not significant (p = 0.37).

3.3.4.1.2 Size attributes

The pattern of size-frequency distributions for *Turbinaria frondens* on Sled tracks, by trawl strata and months (Figure 3-70), was indicative of some impact on size structure, followed by some recruitment and growth with time. Over the same period, the size-distributions of controls were relatively stable.

The model comparisons did not distinguish among models and the model 3 showed no significant trends (except perhaps that shallow individuals tended to be slightly larger than deep individuals, p = 0.091).

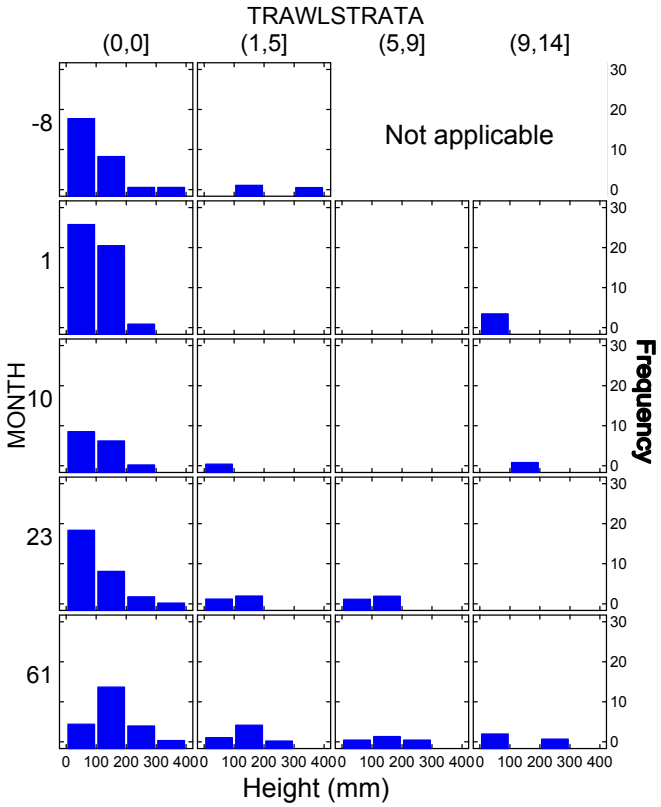

Figure 3-70: Size-frequency distributions of *Turbinaria frondens* heights observed by the Sled, by trawl intensity strata (columns) and month after impact (rows), standardized by Sled swept area (depths combined). Size categories are 100 mm intervals. Note that the "before" status of impact tracks is indicated by month –8 and trawl strata (1,5], which includes the single coverage of the earlier BACI experimental plots; the higher intensity strata did not occur until the repeated-trawling experiment.

On ROV patches, size-frequency distributions of *Turbinaria frondens* were similarly indicative of an impact effect, followed by some observed recruitment with no clear progression of modes. The model comparisons supported model 2 (p = 0.021), suggesting an intensity effect. However, model 3 showed no significant trends with depth, intensity or time. The patterns of ROV individual width and individual area data for *Turbinaria frondens* were consistent with those for height, with perhaps a clearer (though ns) trend of declining mean height with time, possibly due to recruitment of small individuals.

3.3.4.1.3 Condition index

Turbinaria frondens on both impact and control tracks were in good condition initially, but after trawling, many of these corals on impact tracks were badly broken. Subsequently, observations of broken corals were fewer. The model comparisons for *Turbinaria frondens* condition on Sled tracks distinguished model 4 ($p < 0.0001$), suggesting the Time²*Intensity term was important. The model 4 predictions (Figure 3-71) showed that relative to controls *Turbinaria frondens*, on impact tracks were

in much worse condition after impact ($p < 0.0001$) and then improved rapidly ($p < 0.0001$). The models for the ROV data failed to converge.

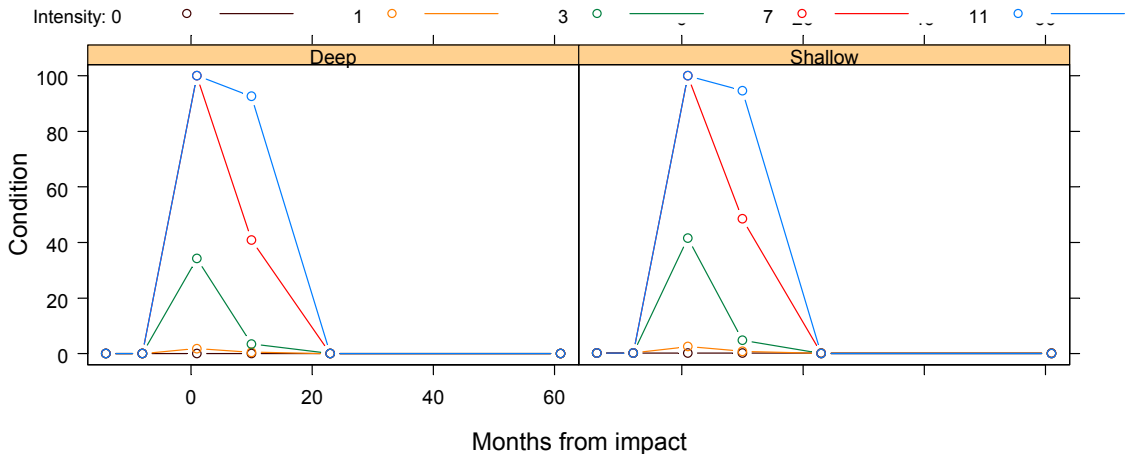

Figure 3-71: Plots of model 4 predictions for *Turbinaria frondens* Condition Index (%) observed by the Sled. Poorer condition is indicated by values >0. The predictions show only the fixed effects and attempt to isolate the recovery signal from other sources of variation. The coloured lines show predictions for different trawl intensities.

3.3.4.1.4 Summary

While the significance tests were somewhat mixed, indicating substantial uncertainty, *Turbinaria frondens* appeared to show a large impact effect and a fast relative recovery response for low and medium intensity strata, though from a highly impacted state recovery may have been slow in an absolute sense — in a timeframe beyond the 5 years of the project. The Sled and ROV data provided relatively consistent estimates of the impact and recovery rates.

Examination of size distributions of *Turbinaria frondens* indicated evidence of some recruitment and growth, but analyses did not support any significant effects on mean size.

These corals appeared to be easily broken by the trawl and there was evidence of substantial significant impact effects on their condition, followed by rapid recovery.

3.3.4.2 Subergorgia sp.

3.3.4.2.1 Abundance (numbers/density)

The numbers of the gorgonian *Subergorgia* sp. observed by the Sled were very low at less than 0.5 per replicate, so analyses was not attempted. On ROV patches, *Subergorgia* sp. were slightly more numerous at about two per patch overall. On impact patches, numbers tended to be lower, particularly at month 10, and to decrease with trawl intensity. Numbers tended to be higher at months 23 or 61. The model comparisons for the ROV census data did not converge and that for ROV nearest-neighbour densities showed some support for model 4 ($p = 0.0527$), suggesting the Time²*Intensity term was important. Model 4 fit to these data suggested a very high negative impact (~ -42%/trawl, *p*

= 0.0071) and complex post impact terms (+Time*Intensity, -Time²*Intensity terms; p = 0.046, 0.054) suggesting that impacted strata recovered quickly between months 10 and 23 but declined again by month 61. Overall recovery was approximately +5.4% per year per trawl (but p = 0.55).

3.3.4.2.2 Size attributes

On ROV patches, at month 10, *Subergorgia* sp. size structures were indicative of a trawl effect at higher intensities (fewer and smaller animals at higher intensities); with time, some additional and larger animals were present at higher intensities. The model comparisons for the ROV mean height did not distinguish among models. Model 3 fit to these data showed trends consistent with the size-frequency observations, but no terms were significant. Width and area models were also not significant.

3.3.4.2.3 Condition index

The *Subergorgia* sp. observed on deep patches by the ROV tended to have some instances of poorer condition initially that recovered quickly, but the models could not fit the data.

3.3.4.2.4 Summary

The gorgonian *Subergorgia* sp. appeared to show a significant strong impact effect with a non-significant recovery trend, beyond the timeframe of the project, at least for the ROV nearest-neighbour density data. There were hints of negative size and condition effects followed by recovery, but none significant.

3.3.4.3 Annella reticulata

3.3.4.3.1 Abundance (numbers/density)

The numbers of the gorgonian *Annella reticulata* observed by the Sled were low at about 1–2 per replicate and heterogeneous; most individuals were on deep tracks. The model comparisons supported model 4 (p = 0.008), indicative of a Time²*Intensity term. The model 4 fit to these data suggested a negative impact (~ -12%/trawl, but p = 0.402) and complex post impact terms (-Time*Intensity, +Time²*Intensity; p = 0.288, 0.0682) suggesting that numbers were static for about two years before recovering quickly. Overall recovery was approximately +10% per year per trawl (p < 0.0001).

On ROV patches, *Annella reticulata* were slightly more numerous: about two per patch overall. Again, highest raw numbers were on deep control patches, where they tended to decrease with time. On impact patches, raw numbers tended to decrease with trawl intensity and with time. The model comparisons for the ROV census data did not converge and for ROV numbers standardised for patch footprint-area, some support was observed for model 4 (p = 0.0527). However, no model 4 terms were significant (p > 0.7).

The model comparisons for ROV nearest-neighbour densities showed support for model 2 (p = 0.050), suggesting the Intensity term was important. Model 3 fit to these data confirmed this with a very high

negative impact (~ -46%/trawl, p = 0.045) term, followed by fast (but p = 0.31) recovery trend of approximately +12% per year per trawl relative to changes on controls.

3.3.4.3.2 Size attributes

The size structures of *Annella reticulata* were indicative of a trawl effect (fewer and smaller animals in trawled strata); with time, some additional and larger animals were present in trawled strata. The model comparisons for the Sled-recorded mean heights provided limited support for model 5 (p = 0.074), suggesting the Time*Intensity² term may be important. The model 5 fit to these data showed trends for negative impact on mean height followed by recovery (no terms significant) more so at higher intensities (ie. +Time*Intensity², p = 0.084).

On ROV patches, *Annella reticulata* size structures tended to fewer and smaller animals on higher trawl-intensity strata. The models fit to these data tended to show negative impact on mean size followed by recovery but were not significant for height and area. For width, model comparisons supported model 3 (p = 0.041), suggesting recovery, and the model 3 showed a significant negative effect on width (p = 0.018) followed by significant recovery (p = 0.045) in size within about two years.

3.3.4.3.3 Condition index

The condition data for *Annella reticulata* observed by the Sled were also very sparse with negligible observed effects. *Annella reticulata* observed by the ROV showed some instances of poor condition at month 10; by month 61, there were no instances of poor condition. However, none of the statistical models showed any significant effests.

3.3.4.3.4 Summary

The gorgonian *Annella reticulata* appeared to show a strong impact effect with a fast recovery over a timeframe similar to that of the project; a result that was relatively consistent between the Sled and ROV observations. However, the significance of these effects was mixed between the two data sources. There were hints of negative size and condition effects followed by recovery, but non significant — except for ROV width measurements.

3.3.4.4 Ianthella basta

3.3.4.4.1 Abundance (numbers/density)

The numbers of the erect flat sponge *Ianthella basta* observed by the Sled were low, at about 0.5 per replicate and most individuals were on deep control tracks. The models could not be fit to this sparse data and no analysis results were available.

On ROV patches, *Ianthella basta* were uncommon: about 1.5 per patch overall. Again, these sponges were observed almost exclusively on deep control patches. The model comparisons were also incomplete but nevertheless showed support for model 4 ($p < 0.0001$), indicating a Time²*Intensity term. The model 4 fit to these data indicated that the higher-intensity trawl strata had lower numbers, and showed a non-significant recovery trend that slowed with time on impact patches relative to controls. ROV numbers standardised for patch footprint-area showed almost identical patterns. The overall census recovery rate was ~8.5% per year per trawl (but $p = 0.21$).

The model comparisons for ROV nearest-neighbour densities for *Ianthella basta* showed support for model 2 ($p = 0.0553$) indicating an impact effect. The model 3 fit to these data showed a high negative impact trend (~ -48%/trawl, but $p = 0.151$) in individual density, followed by a non-significant recovery trend ($p = 0.81$).

3.3.4.4.2 Size attributes

The size structures of *Ianthella basta* by treatment and time were very sparse. Very low numbers of individuals on impacts tracks limited examination of Sled-recorded mean heights against trawl intensity, but suggested an initial negative trend followed by recovery in height on these tracks. The model comparisons provided some support for model 3 ($p = 0.076$) suggesting a possible recovery effect. The model 3 predictions indicated a negative trawl-intensity trend (but $p = 0.52$) and corrobated the positive recovery trend relative to controls ($p = 0.088$).

On ROV patches, the *Ianthella basta* size structures were also very sparse. Patterns of individual heights against trawl intensity were very heterogeneous, due to the low numbers and none of the model fixed effects on ROV size were significant.

3.3.4.4.3 Condition index

The *Ianthella basta* sponges observed by both the Sled and ROV had no apparent deviation from good condition.

3.3.4.4.4 Summary

The numbers of *Ianthella basta* observed were low and heterogeneously distributed, making analyses difficult. While impact and recovery effect sizes may have been large, the variability in the data was even larger and the results were uncertain and non-significant.

Average size of *Ianthella basta* may also have been negatively impacted, with some evidence of subsequent recovery. No apparent variation in condition was observed.

3.3.4.5 Semperina brunea

3.3.4.5.1 Abundance (numbers/density)

The numbers of the gorgonian *Semperina brunea* observed by the Sled were too low for analysis. On ROV patches, *Semperina brunea* were also uncommon — about 0.5 per patch overall — and tended to be even less common on the higher-intensity trawl strata. None were observed on the highest-intensity strata. Models could not be fit to the ROV census data and no analysis results were available.

The model comparisons for ROV nearest-neighbour densities for *Semperina brunea* showed support for model 5 ($p = 0.045$), indicating a Time*Intensity² term. The model 5 fit to these data confirmed this ($p = 0.048$) showing that while intermediate trawl intensity strata recovered from the impact trend, high intensity strata did not. Overall, *Semperina brunea* showed a high negative impact on individual density (~ -61%/trawl, $p = 0.010$), followed by a non-significant overall recovery trend of ~8.2% per year per trawl ($p = 0.53$).

3.3.4.5.2 Size attributes

The size structures of *Semperina brunea* on ROV patches showed trends with trawl intensity and time that were consistent with impact and recovery, except no individuals were recorded on the highest-intensity strata. On deep patches, individual heights showed negative trends with trawl intensity initially, which tended to level by month 61; on shallow patches, samples were very sparse. Trends for width and area were the same. The model results were similar for all size measurements, as exemplified by those for area: model comparisons supported model 2 ($p = 0.038$), suggesting an impact effect that was corroborated by the model 3 fit, which showed a large negative effect ($p = 0.016$) followed by a non-significant recovery ($p = 0.172$) in size of about 50%.

3.3.4.5.3 Condition index

The condition index of some *Semperina brunea* observed by the ROV was worse at month 23 on low-impact strata, but the data were too sparse to complete a model test.

3.3.4.5.4 Summary

The numbers of *Semperina brunea* observed were low and heterogeneously distributed, making analyses difficult. For ROV nearest-neighbour density data, the impact effect was large and significant but while the recovery trend was fast this result was uncertain and non-significant, and extended beyond the timeframe of the project.

Average size of *Semperina brunea* was also negatively impacted, with a non-significant recovery trend. Some variation in condition was observed, but the data were inadequate for analyses.

3.3.4.6 Ellisella sp.

3.3.4.6.1 Abundance (numbers/density)

The numbers of the gorgonian *Ellisella* sp. observed by the Sled were too low for analysis. On ROV patches, *Ellisella* sp. were also uncommon, with numbers of about 1 per patch overall, and tending to be lower on higher-intensity trawl strata of impact tracks. Analyses were also not possible with the ROV census data. For the ROV nearest-neighbour densities, the model comparisons supported model 2 (p=0.044) suggesting an impact effect. The model 3 fit to these data showed some support for a large impact effect (~ -47%/trawl, p = 0.061), followed by a non-significant recovery trend of ~9.2% per year per trawl (p = 0.445).

3.3.4.6.2 Size attributes

The sample sizes for the size structures of *Ellisella* sp. on ROV patches were small, and showed only vague trends with trawl intensity and time that were somewhat consistent with impact and recovery. Trends for height, width and area were variable and the model results did not confirm any trends, except that shallow individuals tended to be larger that deep.

3.3.4.6.3 Condition index

The condition index of *Ellisella* sp. observed by the ROV had no significant trends.

3.3.4.6.4 Summary

The numbers of *Ellisella* observed were low and heterogeneously distributed, making analyses difficult. For ROV nearest-neighbour density data, the impact effect was large and significant but while the recovery trend was fast it extended beyond the timeframe of the project and this result was uncertain and non-significant.

Average size of *Ellisella* showed no consistent trends, as was the case for condition.

3.3.4.7 Xestospongia testudinaria

3.3.4.7.1 Abundance (numbers/density)

The numbers of the barrel sponge *Xestospongia testudinaria* observed by the Sled were low, at about 0.7 per replicate, though tended to be more frequent on shallow tracks. On impact tracks, there were some indications of decreased numbers after impact and of a subsequent recovery trend. The model comparisons supported model 4 (p = 0.003) indicating a Time²*Intensity term. The model 4

predictions suggested a negative impact trend (but $p = 0.62$), followed by non-significant trends for further decline and subsequently recovering by month 61 ($p = 0.34$, 0.19). Overall impact was about -25% per trawl ($p = 0.036$) and overall recovery was approx +5.7% per year per trawl ($p = 0.062$).

On ROV patches, *Xestospongia testudinaria* were also uncommon; about 0.5 per patch overall. These sponges were observed more often on shallow patches, and fewer were seen in the higher-intensity trawl strata on patches. Models could not be fit to these census data. The model comparisons for the ROV nearest-neighbour densities for *Xestospongia testudinaria* supported model 4 ($p = 0.042$) indicating a Time²*Intensity term. The model 4 predictions suggested a large negative impact rate of ~ -71% per trawl ($p = 0.0005$), followed by complex post impact terms (Time*Intensity, Time²*Intensity terms; $p = 0.028$, 0.035) suggesting initial rapid recovery but then further decline. Overall recovery was approximately +8.2% per year per trawl (but $p = 0.465$).

3.3.4.7.2 Size attributes

The size structures of *Xestospongia testudinaria* by treatment and time were very sparse. Lack of individuals on impacts tracks limited examination of Sled-observed mean heights against trawl-intensity. The model predictions indicated a slight impact and recovery trend but no terms were significant. On ROV patches, the *Xestospongia testudinaria* size structures were also very sparse, and the patterns were suggestive of an initial impact with limited recovery. The model predictions for ROV size show similar trends as the Sled, and again but no terms were significant.

3.3.4.7.3 Condition index

The *Xestospongia testudinaria* sponges observed by both the Sled and ROV had little observable deviation from good condition.

3.3.4.7.4 Summary

The numbers of *Xestospongia testudinaria* observed were low and heterogeneously distributed, making analyses difficult. The predicted impact effects were large and significant, but while the recovery trends were fast — with timeframes within the 5 years of the project for the Sled and beyond for the ROV — the significance of this result was mixed between the Sled and ROV, hence uncertain.

Average size of *Xestospongia testudinaria* showed slight impact and recovery trends but none were significant.

No trends were observed for condition.

3.3.4.8 Bebryce sp.

3.3.4.8.1 Abundance (numbers/density)

On ROV patches, *Bebryce* sp. numbered about two per patch overall. Numbers were higher on deep patches and tended to be lower with trawl intensity but increased with time. The model comparisons for raw census numbers indicated that model 3 was significant ($p < 0.0001$), suggesting an important time*intensity recovery term. The model 3 fit to these data confirmed a recovery trend ($p = 0.0013$) relative to changes on controls and that shallow patches had fewer animals ($p = 0.019$). The overall recovery trend was +6.8%/yr/trawl. For ROV numbers standardised for patch footprint-area, the model comparisons indicated that model 4 was significant ($p < 0.0047$), suggesting an important time²*intensity term. However, while the model 4 fit to these data showed similar trends as the raw census numbers, no coefficients were significant.

The model comparisons for ROV individual nearest-neighbour densities supported model 2 ($p = 0.024$), suggesting an important trawl intensity term. The model 3 fit to these data showed some support for a large impact effect (approx. -50%/trawl, $p = 0.072$) followed by a non-significant recovery trend of +7.7%/yr/trawl ($p = 0.534$).

3.3.4.8.2 Size attributes

The size structures of *Bebryce* sp. on ROV patches increased with time, with both growth and recruitment, but showed little trend with trawl-intensity strata. On deep patches, individual heights tended to decrease with time; on shallow patches, samples were very sparse. Trends for width and area were similar. The fitted model 3 had no significant terms and indicated a trend for decreasing mean height with time ($p = 0.35$), which may have been due to recruitment.

3.3.4.8.3 Condition index

The *Bebryce* sp. observed on deep patches by the ROV appeared to show little variation in condition and the models did not converge properly.

3.3.4.8.4 Summary

The numbers of *Bebryce* sp. observed were low, making analyses difficult. The predicted impact and recovery effects were large and significant in some tests, with recovery timeframes extending beyond the 5 year project. However, significance was mixed between the different ROV datatypes, making these results somewhat uncertain.

Average size of *Bebryce* sp. showed a declining but non-significant trend with time.

No trends were observed for condition.

3.3.4.9 Ascideacea

3.3.4.9.1 Abundance (numbers/density)

The numbers of unidentified ascidians observed by the Sled were too low for analysis. On ROV patches, Ascideacea were also rare, with less than one per patch overall, and tending to be fewer on the higher-intensity trawl strata. Numbers tended to be higher at month 23, then to disappear from almost all patches at month 61. The models fit to the raw census numbers did not converge properly, but nevertheless followed the observed trends.

The model comparisons for ROV individual nearest-neighbour densities for Ascideacea supported model 2 (p = 0.011), suggesting an important trawl intensity term. The model 3 fit to these data confirmed a large impact effect (approx. -55%/trawl, p = 0.039) followed by a fast but non-significant recovery trend of +8.4%/yr/trawl (p = 0.567).

3.3.4.9.2 Size attributes

The frequency of Ascideacea individuals in size distributions increased from month 10 to 23, but then all but disappeared, as noted above. The month 23 distributions on trawl strata had more and larger animals than the month 10 distributions, whereas the controls changed little. However, the sample sizes were too small for complete model comparisons of size of Ascideacea, and the trends were mixed with no significant fixed effects.

3.3.4.9.3 Condition index

The condition index of Ascideacea observed by the ROV had no variation.

3.3.4.9.4 Summary

The numbers of Ascideacea sp.s observed were low, making analyses difficult. The predicted impact and recovery effects were large and significant in some tests, with recovery from the low base extending beyond the timeframe of the project. However, significance was mixed between the different ROV datatypes, making these results somewhat uncertain.

Size frequency distributions of Ascideacea sp.s showed some signs of recruitment and growth on impacted strata, but no trends were significant. No trends were observed for condition.

The numbers of these ascidians were very low initially, and while there may have been some trawl impact, it is possible that the recruitment and growth of these ascidians represented an opportunistic "weed-like" response to disturbance followed by senescence, similar to that for *Hypodistoma deeratum*.

3.3.5 Medium impact, fast recovery

3.3.5.1 Porifera

3.3.5.1.1 Abundance (numbers/density)

Various other sponges that could not be identified to species were pooled. They tended to be more numerous on deep controls and overall, averaged about 2-3 per Sled track. The model comparisons did not distinguish among models. Nevertheless, the model 3 fit to these data provided some support for depth differences ($p < 0.069$) and that, relative to controls, trawled tracks had a medium impact effect of -13.7% per trawl ($p = 0.0527$), and there was some evidence of a recovery after trawling (approximately +3.3% per year per trawl, $p = 0.085$) (Figure 3-72).

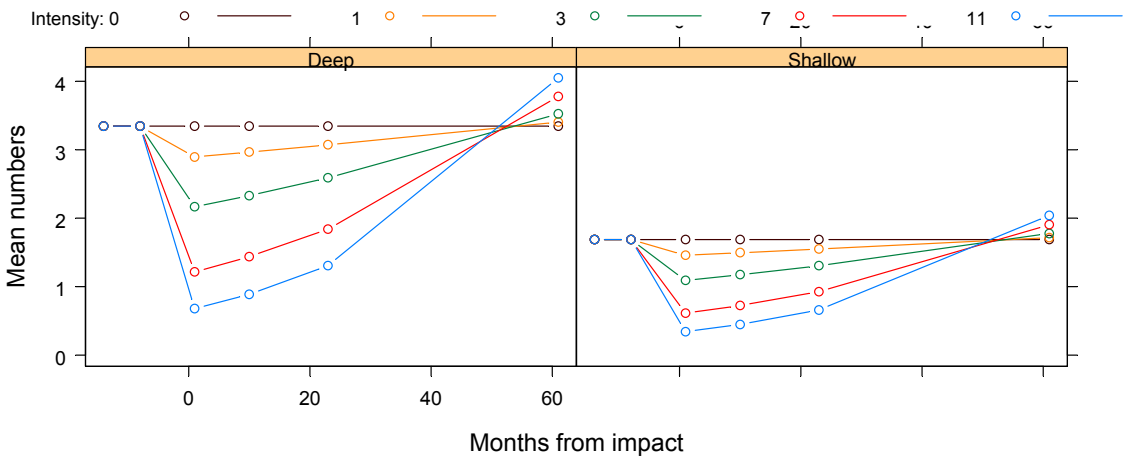

Figure 3-72: Plots of model 3 fit to numbers of Porifera sp.s per Sled track by month, fixed effects only (coloured lines show predictions for different trawl intensities).

On ROV patches, unidentified sponges were more numerous on controls; overall average numbers were about 4-8 per patch. On impact patches, at month 10, census numbers tended to be lower on higher trawl-intensity strata. Subsequently, numbers on impact patches tended to increase, consistent with recovery.

The model comparisons for raw census data provided support for Model 3 ($p = 0.025$), indicating that the trawl Intensity term was likely to be important. The Model 3 fit to the Porifera census data indicated fewer animals in trawled strata ($p = 0.0001$) and suggested a non-significant recovery trend of +1.9% per year per trawl ($p = 0.16$). The model comparisons for ROV numbers standardised for patch footprint-area did not distinguish among models. Model 3 showed impact and recovery trends but no coefficients were significant.

The model comparisons for ROV individual nearest-neighbour densities indicated that Model 3 was significant ($p = 0.037$) indicating an important recovery term. Model 3 showed evidence of an initial impact effect (~ -31% per trawl, $p = 0.0005$) followed by a fast recovery of 7.6% per year per trawl ($p = 0.0246$).

3.3.5.1.2 Size attributes

The pattern of size frequency for sponges on Sled tracks, by trawl strata and months, was indicative of some impact on size structure, followed by some recruitment and growth. Model comparisons of Sled heights distinguished model 2 (p = 0.035), suggesting an important trawl intensity term. Model 3 predictions of mean heights of individual sponges showed trends consistent with an impact effect followed by recovery; however, neither coefficients were significant (p = 0.12, p = 0.77).

On ROV patches, size-frequency distributions of sponges were indicative of an impact effect, with size-class range narrowing towards smaller classes at higher intensity, and some evidence of recovery over time, along with an increase in the frequency of small classes, possibly recruits. This pattern was more evident for deep patches than shallow. The model comparisons for individual mean heights of sponges measured by the ROV did not distinguish among models. Contrarily, model 3 indicated positive trawl intensity and negative recovery terms but neither were significant. Results for width were similar, and those for area showed some support for decreasing mean size (p = 0.065), possibly consistent with the observed recruitment of small individuals offsetting the growth of earlier recruits.

3.3.5.1.3 Condition index

The pooled unidentified sponges observed by both the Sled and ROV had little observable deviation from good condition.

3.3.5.1.4 Summary

The various unidentified sponges tended to be more numerous on deep controls. The Sled data provided support for a medium impact effect and recovery within the timeframe of the project. The ROV data indicated a medium-large impact effect followed by a medium or fast recovery rate at or beyond the timeframe of the project, depending on the datatype.

Size frequency distributions of the unidentified sponges showed some signs of recruitment and growth on impacted strata, but most trends were not significant — though there was some evidence of decreasing mean size possibly due to recruitment. No trends were observed for condition.

3.3.6 Medium impact, slow recovery

3.3.6.1 Subergorgia suberosa

3.3.6.1.1 Abundance (numbers/density)

The numbers of the gorgonian *Subergorgia suberosa* observed by the Sled were low overall at less than 1 per replicate and extremely heterogeneous. The model comparisons could not be completed for the Sled data and no analysis results were available.

On ROV patches, *Subergorgia suberosa* were more numerous, at about four per patch overall. The highest numbers were on deep controls, where they increased with time. On impact patches, numbers tended to decrease with trawl intensity and with time. The model comparisons for raw census data provided some support for Model 4 ($p = 0.086$), possibly indicating that the Time²*Intensity term may be important. The Model 4 fit to the census data tended to indicate fewer animals in trawled strata and suggested a slight increase then a decline but no terms were significant (other than depth). The model comparisons for ROV numbers standardised for patch footprint-area supported Model 3 ($p = 0.0346$). Model 3 hinted at higher densities in trawled strata ($p = 0.146$) followed by decline ($p = 0.060$).

The model comparisons for ROV individual nearest-neighbour densities indicated that Model 5 was significant ($p = 0.033$) indicating an important Time*Intensity² term. Model 5 showed trends for an initial impact effect (~ -27% per trawl, but $p = 0.38$) followed by non-significant decline of -3.4% per year per trawl. The Time*Intensity² term was positive and signiciant ($p = 0.0327$) indicating that the negative trends were less at higher intensity and with time.

3.3.6.1.2 Size attributes

The size data for *Subergorgia suberosa* were very sparse among combinations of topography, time, and trawl intensity. The Model comparisons of Sled mean heights did not distinguished any models. Model 3 predictions of mean heights of individuals showed trends consistent with a small impact effect followed by slight recovery; however, neither coefficients were significant ($p = 0.27$, $p = 0.88$).

On ROV patches, size distributions tended to smaller size classes and fewer individuals on higher trawl-intensity strata, a trend that appeared to become more evident with time. The model comparisons for individual mean heights measured by the ROV supported model 3 ($p < 0.0001$). The model 3 predictions indicated larger mean size with trawl intensity ($p = 0.003$) followed by decline ($p < 0.0001$). Results for width and area were the same.

3.3.6.1.3 Condition index

The condition data for *Subergorgia suberosa* observed by the Sled were also very sparse. The model comparisons supported model 4 ($p = 0.016$), which hinted that Sled animals were in worse condition by month 23 after trawling (up to ~20%, $p = 0.094$), but then recovered by month 61 ($p = 0.082$).

Subergorgia suberosa observed by the ROV showed similar patterns, particularly on deep patches. The model 3 fit to these data suggested that condition was initially worse on the trawled strata (again up to ~20%, $p = 0.078$), then showed a non significant recovery trend ($p = 0.156$).

3.3.6.1.4 Summary

Subergorgia suberosa were very patchily distributed, though tended to be more numerous on deep controls. The Sled data could not be analysed successfully and while the ROV data results were mixed and uncertain, the nearest-neighbour densities showed a non-signficant medium impact trend. There was no evidence of recovery in numbers during the project.

Size frequency distributions of *Subergorgia suberosa* were sparse though consistent with an impact on larger animals that become more evident with time. The analyses contradicted any initial impact but confirmed decreasing mean size with time.

Condition appeared to be moderately worse after trawling but recovered by the end of the surveys.

3.3.6.2 Cymbastela coralliophila

3.3.6.2.1 Abundance (numbers/density)

The numbers of the prostrate sponge *Cymbastela coralliophila* observed by the Sled were low, at just over one per replicate; most individuals were on control tracks. The model comparisons supported model 5 ($p = 0.0002$) indicating a Time*Intensity² term. The model 5 fit to these data provided some support for a medium-large impact effect of about -33% per trawl ($p = 0.0955$), followed by complex recovery trends where low intensity trawl strata recovered quickly but high intensity strata did not (however, no post impact terms were significant). The overall rate of recovery was very slow and non-signficant (approximately +0.6% per year per trawl, $p = 0.86$).

On ROV patches, *Cymbastela coralliophila* were uncommon, with numbers of about 0.5 per patch overall. Again, highest numbers were on control patches, and on shallow impact patches where they tended to decrease with trawl-intensity. The model comparisons for raw census data supported Model 4 ($p = 0.018$), indicating that the Time²*Intensity term may be important. The Model 4 fit to the census data tended to indicate fewer animals in trawled strata and, with time, suggested a very slight increase then a decline but no terms were significant; the overall decline was about -7% per year per trawl. The analyses of ROV data standardised for patch footprint-area did not converge.

The model comparisons for ROV individual nearest-neighbour densities distinguished Model 2 ($p = 0.0026$), possibly indicating an important Intensity term. Model 3 showed trends for a medium initial impact effect (~ -22% per trawl, but $p = 0.52$) followed by ongoing decline of -20% per year per trawl.

3.3.6.2.2 Size attributes

The size structures of *Cymbastela coralliophila* on Sled control tracks changed little with time, while those on Sled impact tracks showed little evidence of recovery. Lack of individuals on impact tracks limited analysis of Sled-recorded mean heights against trawl intensity. The model comparisons did not distinguish any models and the model 3 predictions hinted a slight negative impact effect on mean height followed by recovery but no terms were significant.

On ROV patches, the pattern of *Cymbastela coralliophila* size structures was similar to and sparse like those of the Sled. The pattern of individual heights against trawl-intensity was very heterogeneous due to the low numbers. The model comparisons did not distinguish any models and the model 3 predictions hinted a slight positive impact effect on mean height followed by decline but again no terms were significant.

3.3.6.2.3 Condition index

The condition data for *Cymbastela coralliophila* showed no significant trends.

3.3.6.2.4 Summary

Cymbastela coralliophila were patchily distributed, and tended to be more numerous on controls. The Sled data suggested a medium-large impact effect, followed by variable though overall very slow recovery beyond the timeframe of the project. The ROV data tended to suggest a medium impact effect with no evidence of recovery but rather an ongoing deceline. The significance of effects was mixed and results are thus uncertain.

Size frequency distributions of *Cymbastela coralliophila* were sparse and the analyses did not show any consistent effects.

No trends in condition were observed.

3.3.6.3 Echinogorgia sp.

3.3.6.3.1 Abundance (numbers/density)

The numbers of the gorgonian *Echinogorgia* sp. observed by the Sled were low, at about 0.5 per replicate, and most individuals were on deep control tracks. At month 1, no individuals were observed on impact tracks; a few individuals were observed later. The model comparisons did not complete and the model 3 analysis showed no significant impact effects or recovery.

On ROV patches, *Echinogorgia* sp. was similarly rare: about 0.5 per patch overall. These gorgonians were observed almost exclusively on deep patches; highest numbers were observed on intermediate trawl strata. The model comparisons for raw census data supported Model 3 (p = 0.012), indicating that the Time*Intensity recovery term may be important. The Model 3 fit to the census data tended to indicate fewer animals in trawled strata and a trend for an overall recovery rate of about +3.4% per year per trawl (but p = 0.14). The analyses of ROV data standardised for patch footprint-area supported Model 2 (p = 0.009), indicating that the Intensity term may be important. The Model 3 fit to the these data also tended to indicate fewer animals in trawled strata and a significant overall recovery rate of about +5% per year per trawl (p = 0.0034).

The model comparisons for ROV individual nearest-neighbour densities provided some support for Model 3 (p = 0.081), suggesting the recovery term may be important. Model 3 showed trends for a large initial impact effect (~ -45% per trawl, but p = 0.29), with weak support for an apparently rapid recovery of 40% per year per trawl (but p = 0.082).

3.3.6.3.2 Size attributes

The size structures of *Echinogorgia* sp. by treatment and time were very sparse. Lack of individuals on impacts tracks limited examination of Sled-observed mean heights against trawl intensity. The model comparisons provided some support for model 5 ($p = 0.053$) and the model 5 terms were largely non-significant, except perhaps for a Time*Intensity² term ($p = 0.055$) hinting that with time after impact mean size on high intensity strata was greater than low and intermediate strata.

On ROV patches, the *Echinogorgia* sp. size structures were also very sparse and the patterns of individual heights against trawl intensity were very heterogeneous, due to the low numbers. None of the model comparisons were significant and no models had any significant terms.

3.3.6.3.3 Condition index

The *Echinogorgia* observed by both the Sled and ROV had no apparent deviation from good condition.

3.3.6.3.4 Summary

Echinogorgia were sparse and heterogensously distributed. The Sled data suggested no impact or recovery effects. The ROV datatypes provided results with mixed significance of effects and are thus uncertain. The census data provided reasonable evidence of a moderate recovery rate whereas the nearest-neighbour densities hinted at large impact followed by extraordinary recovery — the recovery timeframes of both were within about 2 years.

Size frequency distributions of *Echinogorgia* were sparse and the analyses showed no consistent effects. No trends in condition were observed.

3.3.7 High impact, medium recovery

3.3.7.1 Sarcophyton sp.

3.3.7.1.1 Abundance (numbers/density)

The numbers of the soft coral *Sarcophyton* sp. observed by the Sled were generally low — around three per replicate — and tended to be lower on impact tracks. The model comparisons supported model 4 ($p = 0.0004$) indicating a Time²*Intensity term. The model 4 fit to these data indicated a large impact effect of about -45% per trawl ($p = 0.027$), followed by complex recovery trends where all trawl strata appeared to recover quickly and completely by month 23 but decline slightly by month 61 ($p = 0.015$, 0.018). The overall average rate of recovery over the period of the surveys was more moderate (approximately +4.3% per year per trawl, $p = 0.118$).

On ROV patches, *Sarcophyton* sp. numbers were low, about two per patch, but more numerous on control patches. On impact patches, censused numbers tended to be lower on higher trawl-intensity strata; none were recorded on the highest intensity stratum. Subsequently, numbers on many patches, including shallow controls, tended to decrease. The model comparisons for raw census data were incompleted but appeared to support Model 4 (p = 0.0001), indicating that the Time²*Intensity term may be important. The Model 4 fit to the census data indicated fewer animals in trawled strata (p = 0.028) and a trend for some initial recovery followed by a decline (but p = 0.12, 0.078). The analyses of ROV data standardised for patch footprint-area showed approximately the same patterns.

The model comparisons for ROV individual nearest-neighbour densities supported Model 2 (p = 0.0001), suggesting the trawl intensity term may be important. Model 3 showed trends for a large initial impact effect (~ -55% per trawl, p = 0.007), with a hint of a very slow recovery of 0.5% per year per trawl (but p = 0.96).

3.3.7.1.2 Size attributes

Sarcophyton sp. initially were low in number or absent from higher-intensity areas of Sled tracks. By month 23 and 61, there had been some recruitment and growth of size distributions. The model comparisons supported model 3 (p = 0.024) and the model 3 predictions indicated a possible negative impact on mean height (p = 0.074) followed by an increase in mean height (p = 0.025).

The results were similar on ROV patches for size-frequency distributions. Model comparisons did not distinguish models and the model 3 for height, width and area all showed negative impact and positive recovery trends but no terms were significant.

3.3.7.1.3 Condition index

Sarcophyton sp. observed by both the Sled and ROV had no observable deviation from good condition that could be analysed.

3.3.7.1.4 Summary

Sarcophyton numbers were low but not uncommon. The Sled data suggested with some certainty a substantial impact followed by rapid recovery and then slight decline, with overall moderate recovery rate within about 2 years. The ROV data supported a large impact but provided little evidence of any recovery.

Size frequency distributions of *Sarcophyton* were sparse on impact strata and the analyses showed negative impact and positive recovery trends on mean height, significant in the case of Sled data.

No trends in condition were observed.

3.4 Physical habitat structure

The contribution of individual species to overall habitat structure of the study sites is indicated in Table 3-7.

Table 3-7: Contribution to habitat structure by taxon, as indexed by cross-sectional area (m²), of megabenthos fauna recorded by the Sled and ROV.

Rank	Species	Type	ROV (m²)	Sled (m²)	Total (m²)	Proportion
1	*Ctenocella pectinata*	Gorgonian	159.89	71.26	231.15	20.65
2	*Junceella juncea*	Red whips	46.66	121.14	167.80	14.99
3	*Ianthella flabelliformis*	Fan sponge	91.92	51.91	143.84	12.85
4	*Dichotella divergens*	Gorgonian	83.14	54.10	137.24	12.26
5	Nephtheidae	Soft coral	23.06	89.71	112.77	10.07
6	Alcyonacea	Soft coral	37.14	33.53	70.67	6.31
7	*Junceella fragilis*	White whips	25.29	13.99	39.28	3.51
8	*Solenocaulon* sp.	Gorgonian	9.81	21.56	31.37	2.80
9	*Turbinaria frondens*	Hard coral	17.38	10.19	27.57	2.46
10	Scleractinia	Hard coral	7.16	14.78	21.94	1.96
11	*Subergorgia* sp.	Gorgonian	16.91	3.54	20.45	1.83
12	Porifera	Sponge	14.06	6.36	20.42	1.82
13	*Annella reticulata*	Gorgonian	10.91	4.86	15.77	1.41
14	*Subergorgia suberosa*	Gorgonian	12.16	2.15	14.31	1.28
15	*Sarcophyton* sp.	Soft coral	4.63	6.58	11.21	1.00
16	*Ianthella basta*	Fan sponge	7.88	2.87	10.75	0.96
17	*Semperina brunea*	Gorgonian	4.57	3.07	7.63	0.68
18	*Cymbastela coralliophila*	Flat Sponge	2.24	3.72	5.97	0.53
19	*Hypodistoma deeratum*	Solitary ascidian	0.96	4.73	5.70	0.51
20	*Ellisella* sp.	Gorgonian	5.27	0.10	5.37	0.48
21	*Echinogorgia* sp.	Gorgonian	2.59	2.64	5.22	0.47
22	*Xestospongia testudinaria*	Barrel sponge	1.67	2.32	3.99	0.36
23	*Bebryce* sp.	Gorgonian	2.18	0.04	2.22	0.20
24	*Plumigorgia* sp.	Gorgonian	1.85	0.05	1.90	0.17
25	Hydroid	Hydroid	1.01	0.46	1.46	0.13
26	Ascideacea	Colonial ascidian	0.92	0.22	1.14	0.10
27	Alcyoniidae	Soft coral	0.03	0.75	0.78	0.07
28	Unknown		0.11	0.63	0.73	0.07
29	*Lobophytum* sp.	Soft coral	0.13	0.23	0.36	0.03
30	*Acabaria* sp.	Gorgonian	0.25		0.25	0.02
31	*Pteroeides* sp.	Sea pen	0.01	0.09	0.10	0.01
32	*Mopsella* sp.	Gorgonian		0.04	0.04	0.00
33	*Hippospongia elastica*	Sponge		0.02	0.02	0.00
34	*Virgularia* sp.	Sea pen		0.02	0.02	0.00
35	*Amphimedon* sp.	Sponge		0.02	0.02	0.00
36	Pennatulacea	Sea pen		0.01	0.01	0.00
	Totals	**Totals**	**591.78**	**527.69**	**1119.47**	**100.00**

Five species account for most of the structural contribution: *Ctenocella pectinata, Junceella juncea, Ianthella flabelliformis, Dichotella divergens,* and Nephtheidae. Of these, the sometimes very numerous soft corals Nephtheidae tend to be relatively small and short-lived. The sea whips *Junceella*

juncea are individually very slender and have little cross-sectional area; however, they are extremely numerous and often occur in clumps. *Dichotella divergens* are a medium-sized open-branched gorgonian. The dominant contributors to habitat structure are *Ctenocella pectinata,* followed by *Ianthella flabelliformis*. Both can grow to over 1 m in height and width, and their large cross-sectional areas provide habitat for other fauna. The other less common megabenthos that can be large as individuals and make similar individual contributions are species of *Turbinaria, Subergorgia, Annella, Semperina,* and *Xestospongia.*While the structural contribution of these few species dominated, the cross-sectional areas of all species were totalled as an index of living habitat structure. On the Sled control tracks, raw structure appeared to peak at month 1, then either increase (shallow tracks) or decrease (deep tracks) slightly. On the Sled impact tracks, structure generally appeared to dip at month 10 then recover — perhaps less so in high-intensity strata.

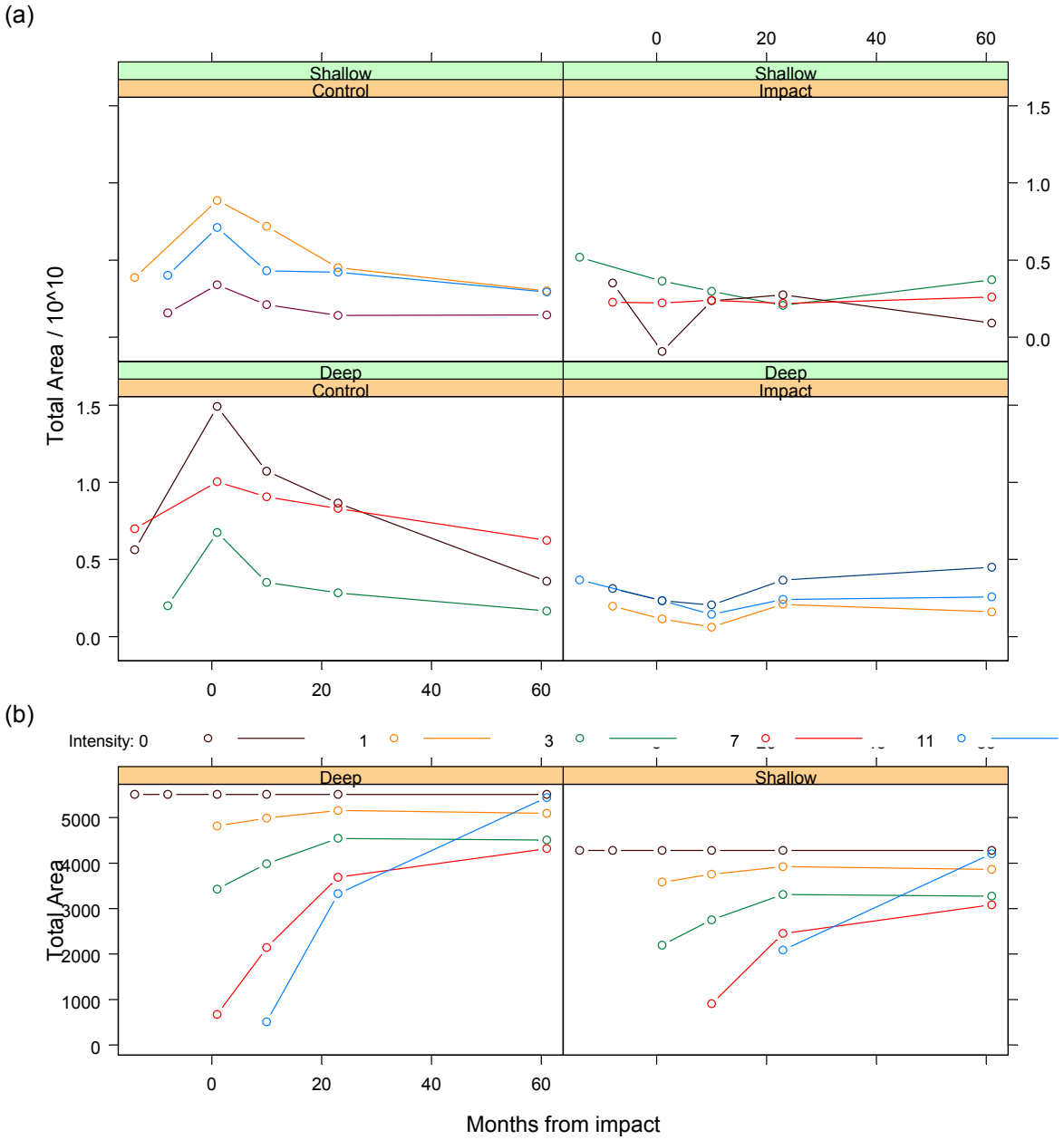

Figure 3-73: Plots of model 5 fit to Sled track total Structure Index (swept area standardised) against months after impact: (a) fixed and random effects less residual variation (coloured lines follow individual tracks), (b) fixed effects only (coloured lines show predictions for different trawl intensities).

Model comparisons analogous to those for Sled species data supported model 5 (p = 0.046), potentially indicating an important Time*Intensity² term in the recovery of total structure. The model 5 fit to these data followed each plot-track through time and indicated that deep and control tracks tended to have greater and more variable structure than shallow and impact tracks, and that structure on control tracks tended to decrease by month 61 (Figure 3-73a). The model fixed effects, which assessed change after trawling on impacts relative to controls, indicated a substantial impact on total structure of approximately -15% per trawl, p = 0.027); followed by complex recovery terms (Figure 3-73b, though non significant, p = 0.43, 0.39, 0.62). Overall recovery after trawling was approximately +1.5% of intial structure per year per trawl (but p = 0.28). Deep tracks may have had more structure than shallow tracks (p = 0.096).

However, while total structure appeared to recover at a moderate rate to within about 80% of intial/controls after 5 years, it is possible that the composition of the recovering structure was different. As noted in the individual species section above, some of the smaller quick growing species recovered faster than most of the larger megabenthos, so it is possible that the recovering structure was made up of smaller benthos and provided less structural complexity — hence, size-frequency distributions of structure were examined. On trawled strata, at months 1 and 10, size-frequency distributions of cross-sectional areas of all species had no individuals larger than about 300 mm linear dimensions (approx. 45 on transformed scale in Figure 3-74), whereas by months 23 and 61, the frequency of larger structure was recovering and approaching that of controls. The mean cross-sectional area of benthos structure also appeared to show recovery following impact, relative to controls (Figure 3-75). These observations indicate that the compostion of the structure was recovering along with the total structure.

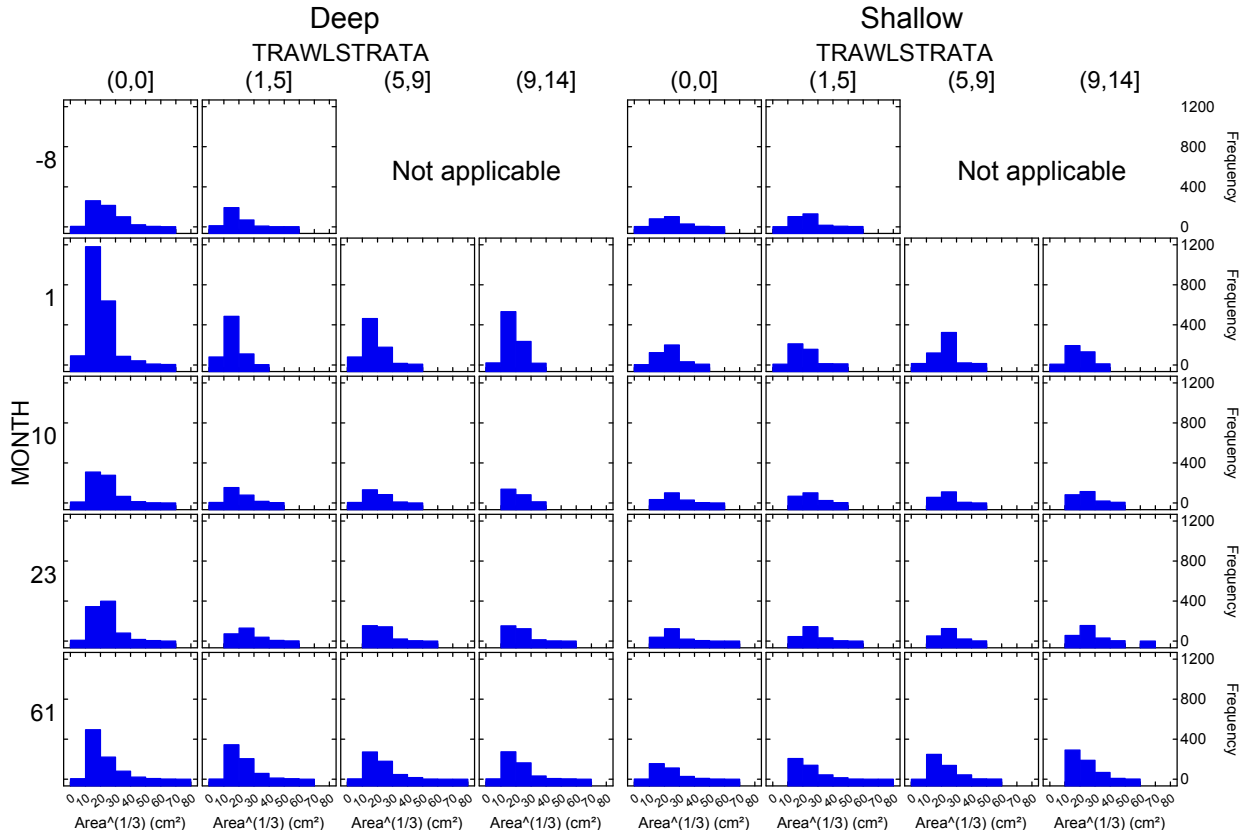

Figure 3-74: Size-frequency distributions of cross-sectional areas of all benthos observed by the Sled video, by depth, trawl-intensity strata (columns) and month after impact (rows). Note that the "before" status of impact tracks is indicated by month –8 and trawl strata (1,5], which includes the single coverage of the earlier BACI experimental plots; the higher intensity strata did not occur until the repeated-trawl experiment.

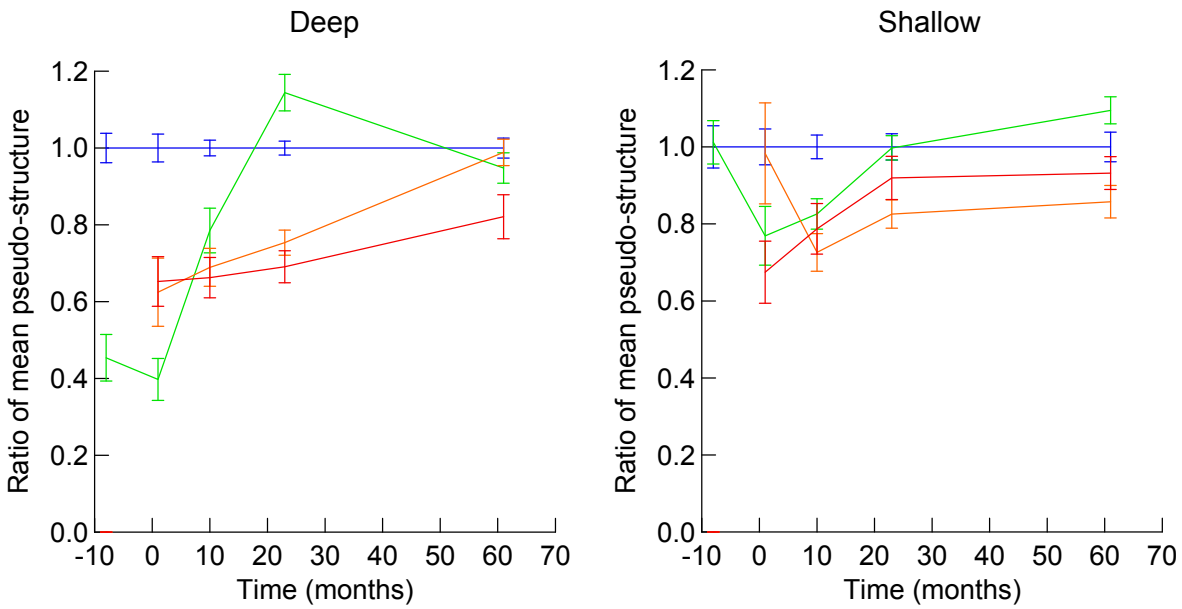

Figure 3-75: Ratio of mean benthos cross-sectional areas (as a pseudo measure of structure) on trawled strata relative to controls. Trawl intensity strata (0,0], (1,5], (5,9], (9,14]. Error bars are relative standard error.

The habitat structure index on deep ROV control patches was slightly greater at month 23; on shallow controls, the index decreased. On impact patches, the index decreased with trawl intensity and responded variably in time. The model comparisons supported model 5 (p = 0.0040), potentially indicating an important Time*Intensity^2 term in the recovery of total structure. The model 5 suggested a substantial impact on total structure followed by complex recovery terms (Figure 3-76) showing slight trends for ongoing decline (but, p = 0.56, 0.77) on all but the highest intensity stratum (p = 0.0043). There was no overall recovery trend after trawling (p = 0.91).

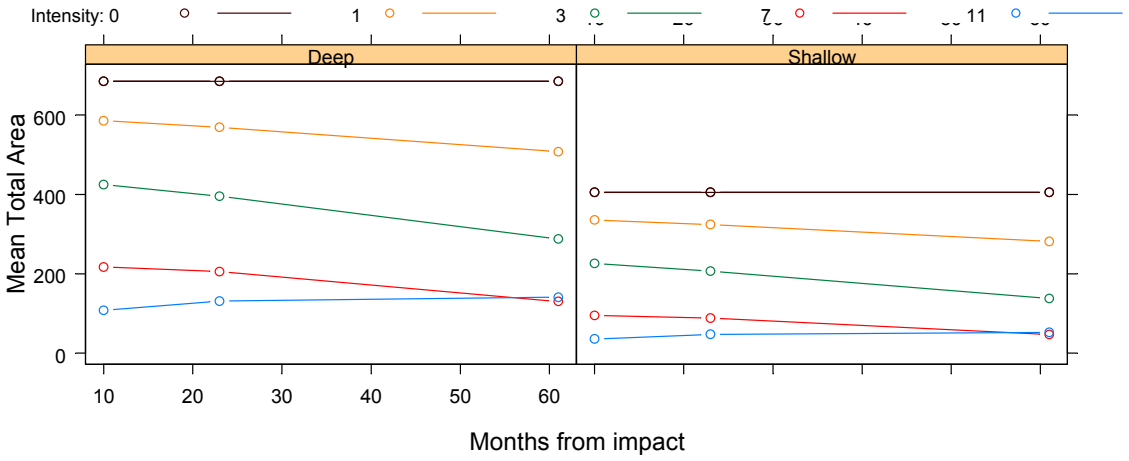

Figure 3-76: Plots of model 5 fit to ROV patch total Structure Index (replicate standardised) against months after impact: fixed effects only (coloured lines show predictions for different trawl intensities).

The size-frequency distributions of ROV structure and mean cross-sectional area relative to controls were also examined. On trawled strata, at months 10 and 23, few benthos were larger than about 300 mm linear dimensions (approx. 45 on transformed scale in Figure 3-77), whereas by month 61, the frequency of larger structure had increased slightly on most strata. The mean cross-sectional area of

benthos structure relative to controls (Figure 3-78) showed variable patterns. On deep patches, there appeared to be intial recovery followed by decline, whereas on shallow patches there appeared to be intial decline followed by recovery. So, while some signs of recovery of the compostion of the structure were observed, the patterns were inconsistent with no overall recovery, like that seen with total structure.

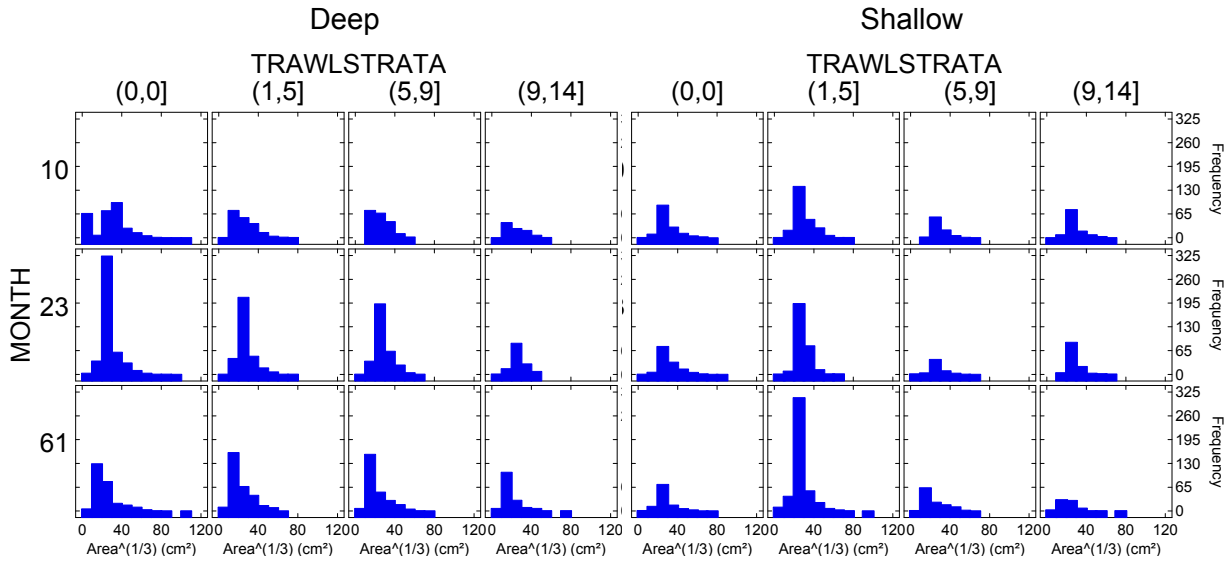

Figure 3-77: Size-frequency distributions of cross-sectional areas of all benthos observed by the Sled video, by depth, trawl-intensity strata (columns) and month after impact (rows). Note that the "before" status of impact tracks is indicated by month –8 and trawl strata (1,5], which includes the single coverage of the earlier BACI experimental plots; the higher intensity strata did not occur until the repeated-trawl experiment.

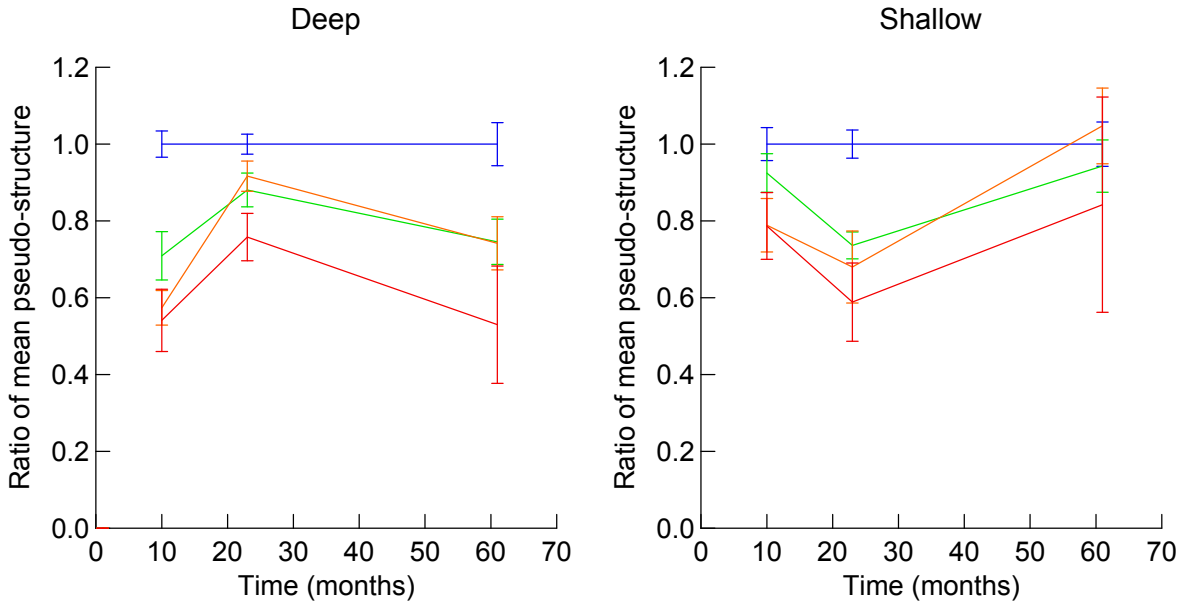

Figure 3-78: Ratio of mean benthos cross-sectional areas (as a pseudo measure of structure) on trawled strata relative to controls. Trawl intensity strata (0,0], (1,5], (5,9], (9,14]. Error bars are relative standard error.

3.5 Assemblage analyses

The two-dimensional ordinations of plots from the multi-dimensional scaling (MDS) of the ROV data for (a) relative abundance, (b) density and (c) volume are shown in Figure 3-79. All three MDS ordinations clearly showed overall differences between the epibenthic assemblages of deep and shallow plots (Figure 3-79), although they were not completely distinct. The depth differences were expressed more strongly for the numbers-based ordinations than that of volume. The ordinations had goodness-of-fit stress values that ranged between 0.15 and 0.22 and could be considered representative of the general assemblage patterns, as measured by the Bray-Curtis dissimilarity matrices (Clarke and Warwick. 2001). However, the volume ordination (with stress of 0.22) could not represent the fine details well in as few as 2-dimensions.

The ordinations of plots from MDS of the Sled data for (a) density and (b) volume were also considered representative of the assemblage patterns, and showed similar, though weaker, trends with respect to depth (Figure 3-80), compared with ROV plots.

Given the strong effect of depth, the multivariate analyses of both ROV and Sled data sets — for relative abundance, density and volume — were conducted separately for deep and shallow plots, so that any changes in assemblages due to trawl-intensity and time may be expressed more clearly.

3.5.1 Species assemblage patterns

3.5.1.1 ROV assemblage similarities

The MDS ordinations of assemblage similarity based on relative abundance of ROV taxa in deep and shallow plots are show in Figure 3-81. The control plots tended to cluster more closely and clearly separated from impact plots, particularly in deep water, but less so in shallow water (Figure 3-81). This indicated that assemblage similarity among control plots was closer than among the impact strata, which were more variable and dissimilar to each other (Figure 3-81). These patterns were quantified by the results of analysis of similarities (ANOSIM), which showed larger *R*-values and separation between controls and higher trawl-intensity strata, but no consistent trend among trawl strata (Table 3-8) — again, the patterns of *R*-values were weaker and less consistent on shallow plots. The pair-wise significance levels were of limited assistance because there were only 10 permutations in these tests and it was not possible to obtain a probability of less than 10%; consequently, reference should be made to the *R*-values (Clarke and Gorley. 2001).

There was also no consistent progression of the plot-level assemblages with time (Figure 3-81). Nevertheless, on deep plots, several of the trawled strata did move somewhat in the direction of controls at month 23, with a larger shift away from controls by month 61 (though one control also moved in the same direction, Figure 3-81a). The *R*-values between controls and trawl strata also increased at month 61 (Table 3-8a), also suggesting that assemblages on impact strata became more different from controls and did not converge as might be expected if recovery had occurred. The trend in global significance levels (Table 3-8a) was consistent with this pattern.

Very similar patterns were found in the MDS ordinations of assemblage similarity based on patch density of ROV taxa (Figure 3-82). Again, the control plots clustered more closely compared with the different trawl intensities. On the deep plots, higher trawl intensity strata tended to be more distance from the controls and, with time, tended to diverge further from the controls (Figure 3-82a). These trends were corroborated by the pair-wise *R*-values and the global significance levels (Table 3-9a). The patterns on shallow plots were less marked, the trawl strata almost surrounded the controls and were not very dissimilar from them (Figure 3-82b and Table 3-9b).

The MDS ordinations of assemblage similarity based on volume density of ROV taxa showed similar patterns, though slightly more interspersed, as those based on numbers (Figure 3-83). On both deep and shallow plots, the control plots clustered more closely than the trawl strata and higher-intensity strata tended to be more separated from the controls (Figure 3-83), as confirmed by the *R*-values (Table 3-10). With time, the deep plots did not diverge at month 61 as obviously as in the numbers ordinations, but nevertheless did not converge with controls (Figure 3-83a, Table 3-10a). The ordination of shallow volumes showed more variability than the number ordinations, and with time, the separation of trawled strata from controls tended to increase from months 10 to 23 and then to decrease a little at month 61 (Figure 3-83b, Table 3-10b), this slight convergence was consistent with a limited level of recovery in the surrogate for assemblage biomass.

3.5.1.2 Sled assemblage similarities

The MDS ordinations of assemblage similarity based on track density of Sled taxa in deep and shallow plots are show in Figure 3-84. As with the ROV ordinations (above), the control plots, particularly in deep water, tended to cluster more closely and were separated from impact plots (Figure 3-84a). These patterns were quantified by the ANOSIM results, which tended to show larger *R*-values and separation between controls and higher trawl-intensity strata, but no trend among trawled strata (Table 3-11a). Again, the ordination patterns and *R*-values were weaker and less consistent on shallow plots, though the high impact strata of one plot was highly divergent (Figure 3-84b, Table 3-11b). Again, the pair-wise significance levels were of limited assistance due to the limited number of permutations (only 10) and reference was made to the *R*-values.

As with the ROV ordinations, there was also no stand-out or coordinated progression of the plot-level Sled density assemblages with time, in either deep or shallow plots (Figure 3-84). Nevertheless, for the deep plots (Figure 3-84a), it can be seen that the before (–8 months) assemblages of the impact tracks (smallest green triangles) were well separated from the controls (smallest blue triangles), whereas at the last survey (month 61), the low and medium trawl strata (largest green and yellow triangles) were closer to the controls (largest blue triangles) than they were initially — a slight convergence suggestive of limited assemblage recovery. In contrast, the high impact strata were more distant from controls at month 61. The trends in *R*-values were broadly consistent with the ordination patterns (Table 3-11a). On the shallow tracks (Figure 3-84b), the before assemblages of controls and impact tracks were not separated and the *R*-value was small (Table 3-11b), though the tracks themselves were heterogenous. At months 1 and 10, many of the trawled strata on impact plots were positioned further away from the controls and several of the *R*-values were larger. By months 23 and 61, all the trawled strata, except one, were positioned among the controls and the *R*-values indicated they were essentially not separable. Again, this can be interpreted as evidence for recovery of assemblages on shallow plots.

The MDS ordinations of assemblage similarity based on track volume densities of Sled taxa in deep and shallow plots (Figure 3-85) were broadly similar to the Sled numbers ordinations. Again, the control plots in deep water tended to cluster more closely and were generally separated from impact plots (Figure 3-85a), with larger *R*-values for separation between controls and trawled strata, but no trend among trawled strata (Table 3-12). The higher trawl-intensity strata, on some occasions, tended to be located further from controls (Figure 3-85a). The shallow control plots were more dispersed, and while some impact strata at some times were separated from the region of the controls, there was no evidence of a trend for higher-intensity strata to be more distant and the *R*-values were weaker (Figure 3-85, Table 3-12).

The Sled volume based ordinations, like those for numbers, did not show obvious progression of assemblages through time; however, close examination does reveal some trends. For the deep plots (Figure 3-85a, Table 3-12a), like numbers, the volume assemblages at –8 months on impact tracks (smallest green triangles) were separated from the controls (smallest blue triangles) with a medium *R*-value; at months 1 and 10 most trawl strata were further from controls and *R*-values increased; whereas at the last survey (month 61), many of the trawl strata were located closer to the controls, with smaller *R*-values, than before impact. This convergence was suggestive of some assemblage recovery. On the other hand, the high impact stratum on at least one plot was further from controls at month 61. On the shallow tracks (Figure 3-85b, Table 3-12b), the Sled volume assemblages at –8 months on control and impact plots, though scattered, were not separated (*R*-value = 0.11). At months 1 and 10, a number of the trawled strata on impact plots were positioned further away from the controls and several of the *R*-values indicated small to medium separation. By months 23 and 61, all the trawled strata were positioned among the controls and the *R*-values indicated they were not separable. This was also interpreted as evidence for recovery of assemblages on shallow plots.

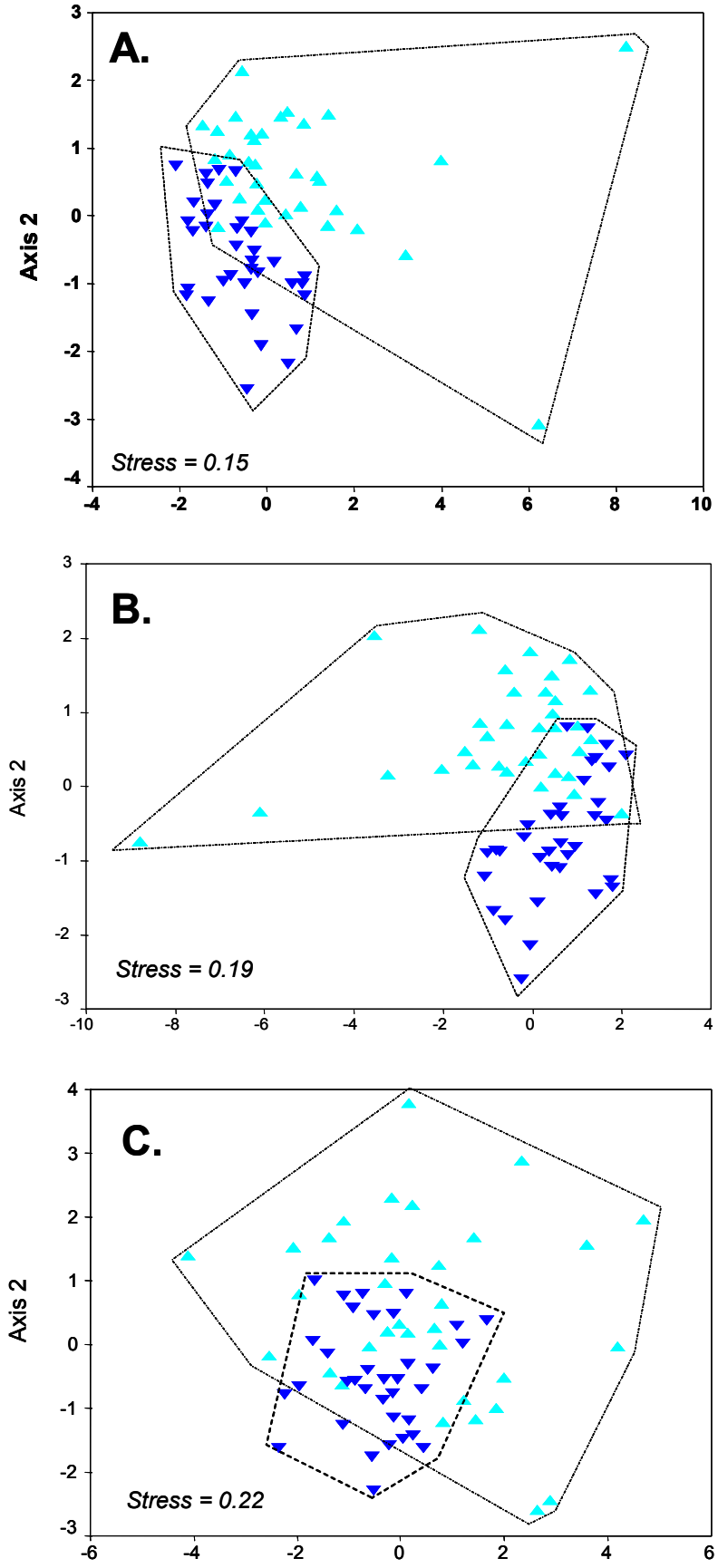

Figure 3-79: ROV. MDS plots for (a) the overall relative abundance, (b) density and (c) volume for all treatment and control plots according to depth. Light blue is shallow while dark blue is deep.

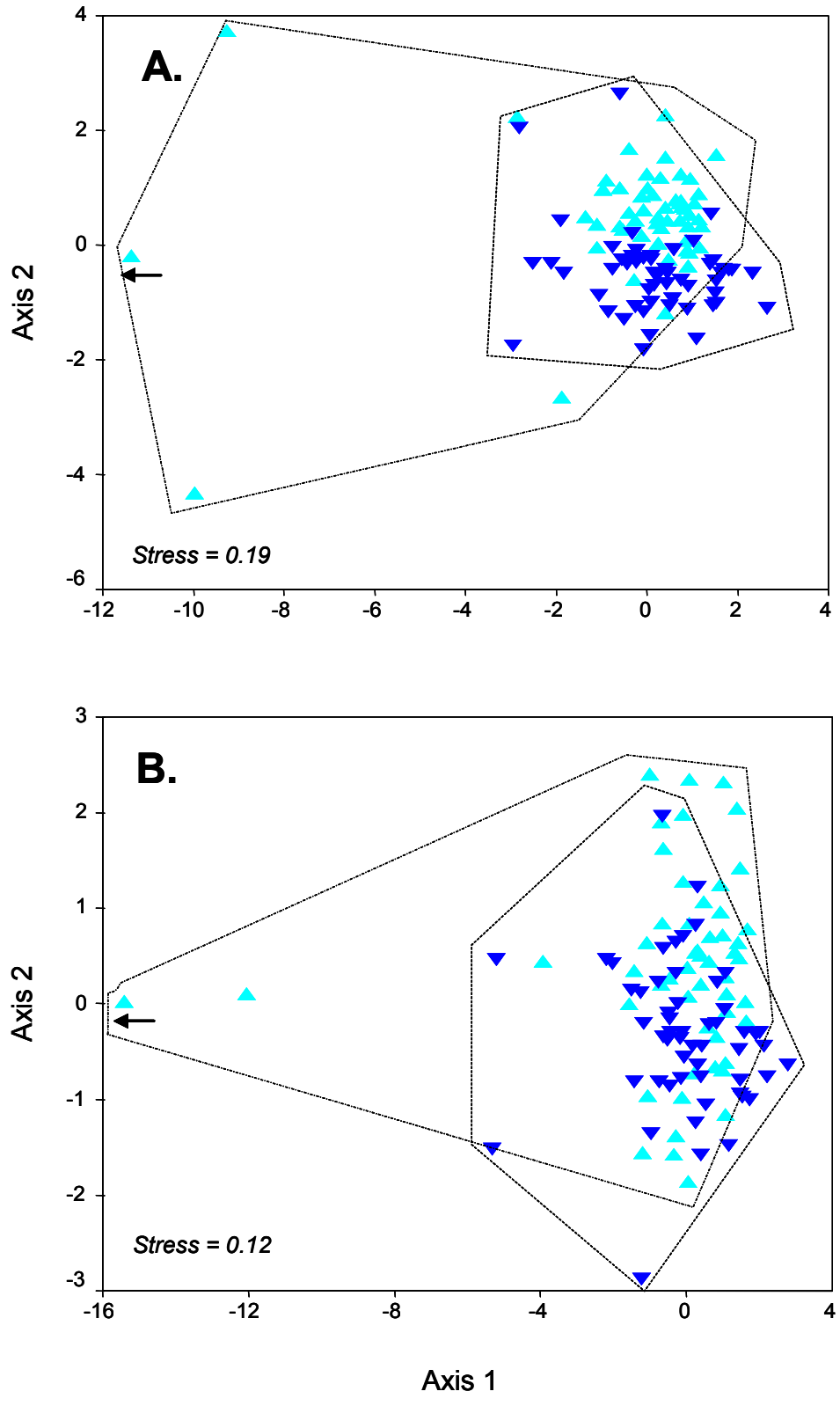

Figure 3-80: Sled. MDS ordination plots for (a) the density and (b) volume for all treatment and control plots according to depth. Light blue is shallow while dark blue is deep. The arrow at the left indicates that points are outside of the plotted scale.

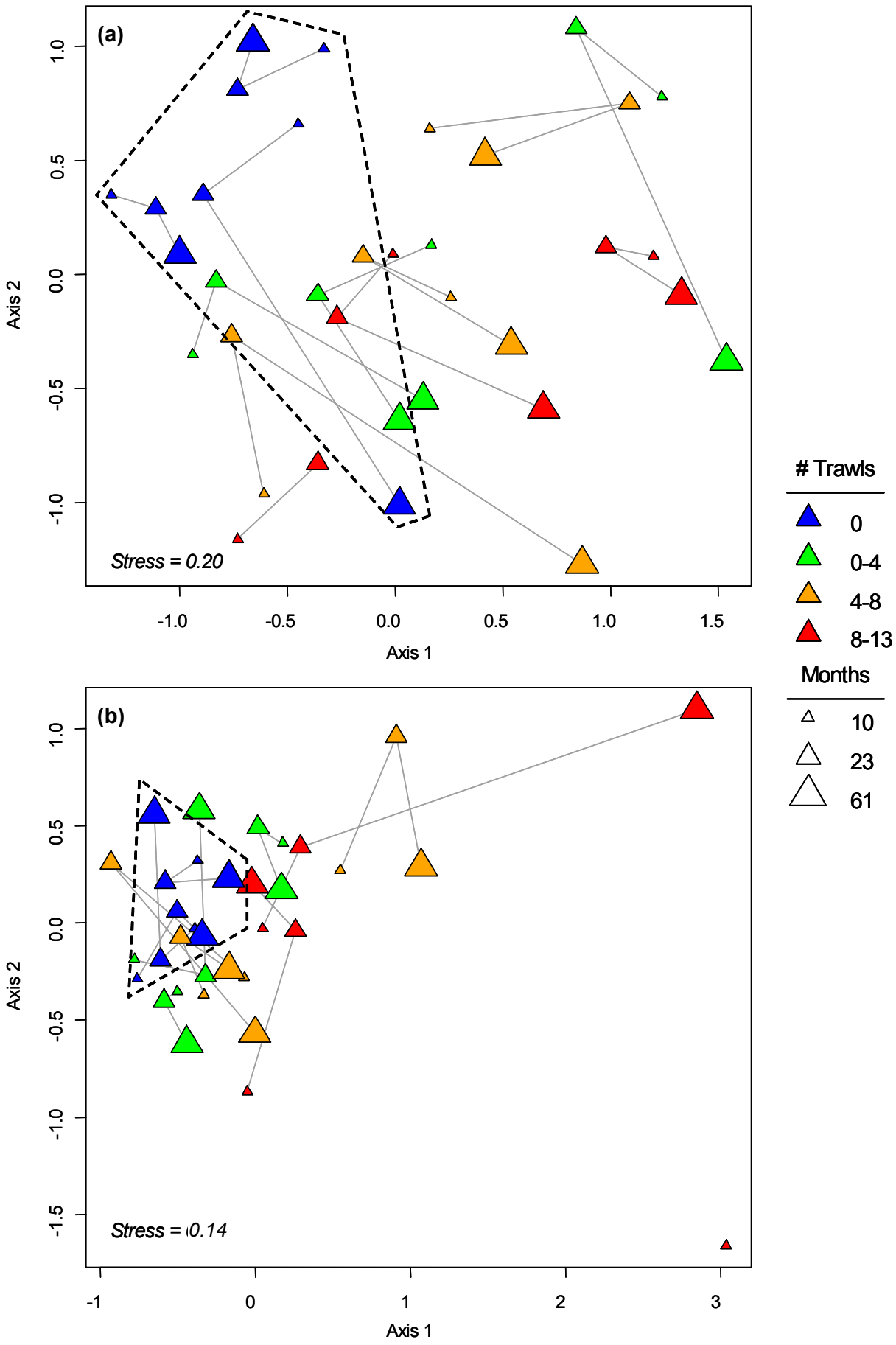

Figure 3-81: ROV. MDS plots for the relative abundance for all treatment and control plots in (a) deep and (b) shallow water. Colored symbols indicate trawl-intensity and symbol size indicates time. Connecting lines join plots through time and dotted lines indicate the boundary of control plots.

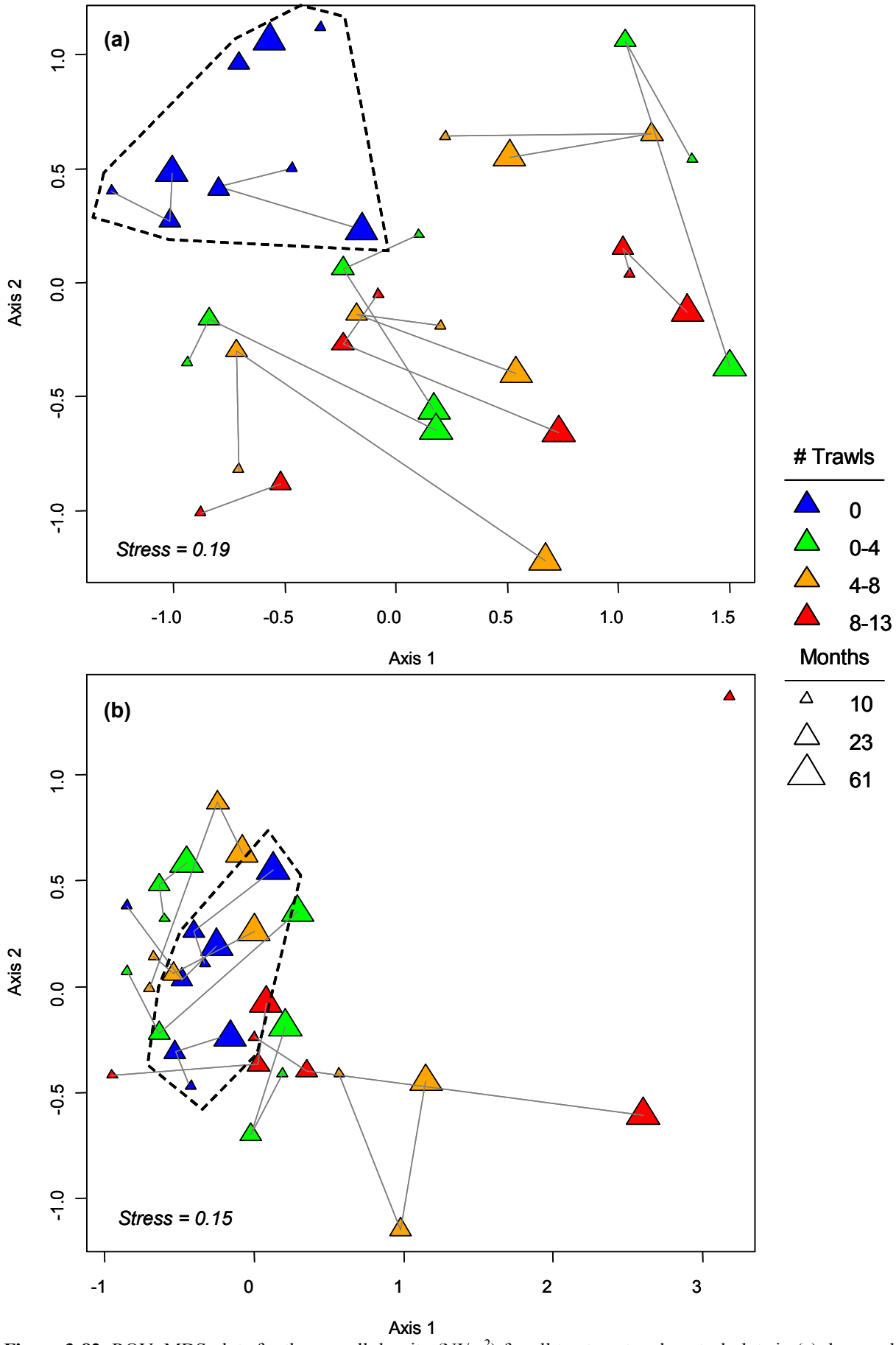

Figure 3-82: ROV. MDS plots for the overall density (NI/m^2) for all treatment and control plots in (a) deep and (b) shallow waters. Colored symbols indicate trawl-intensity and symbol size indicates time. Connecting lines join of plots through time and dotted lines indicate the boundary of control plots.

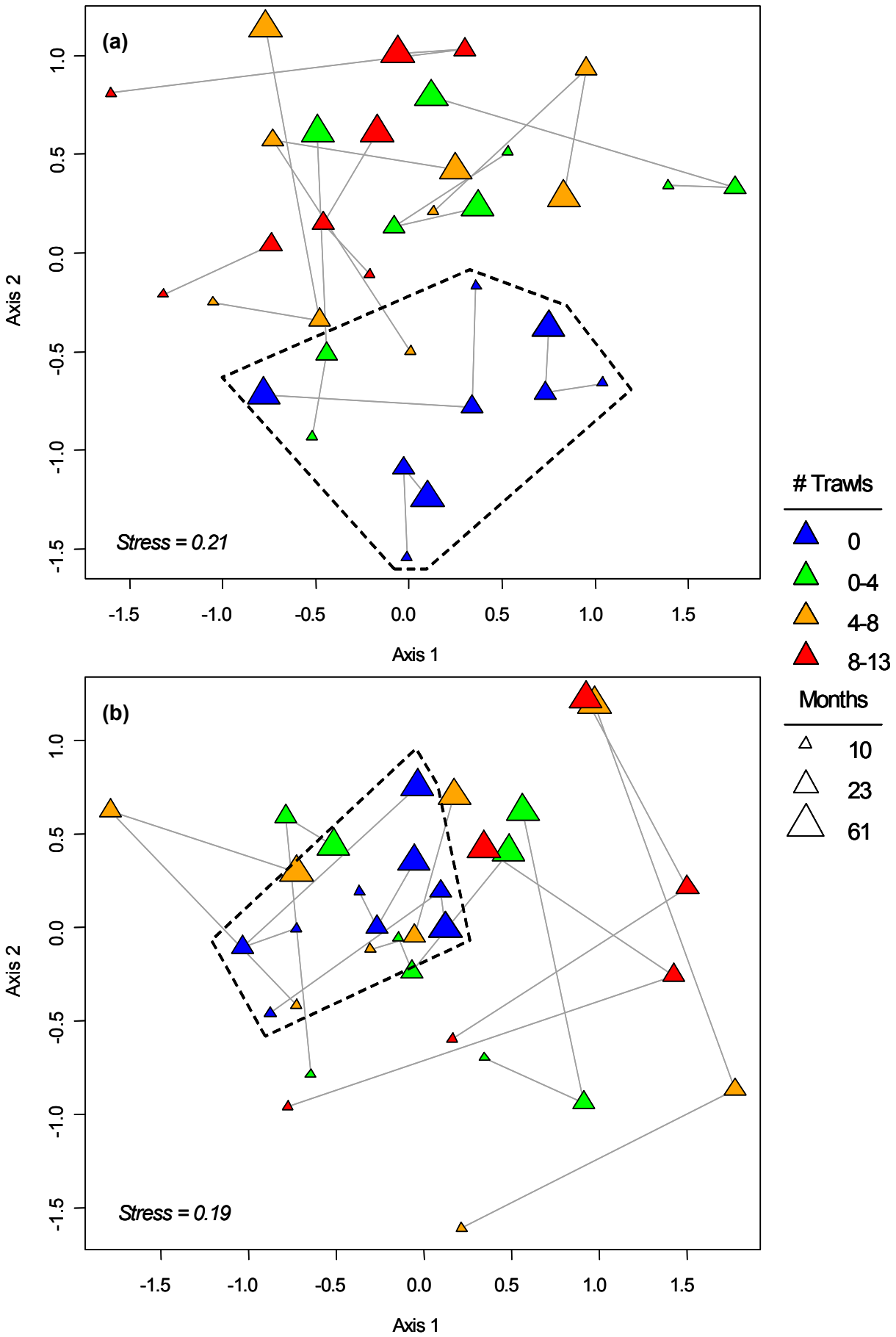

Figure 3-83: ROV. MDS plots for the overall volume (cm^3/m^2) for all treatment and control plots in (a) deep and (b) shallow waters. Colored symbols indicate trawl-intensity and symbol size indicates time. Connecting lines join plots through time and dotted lines indicate the boundary of control plots.

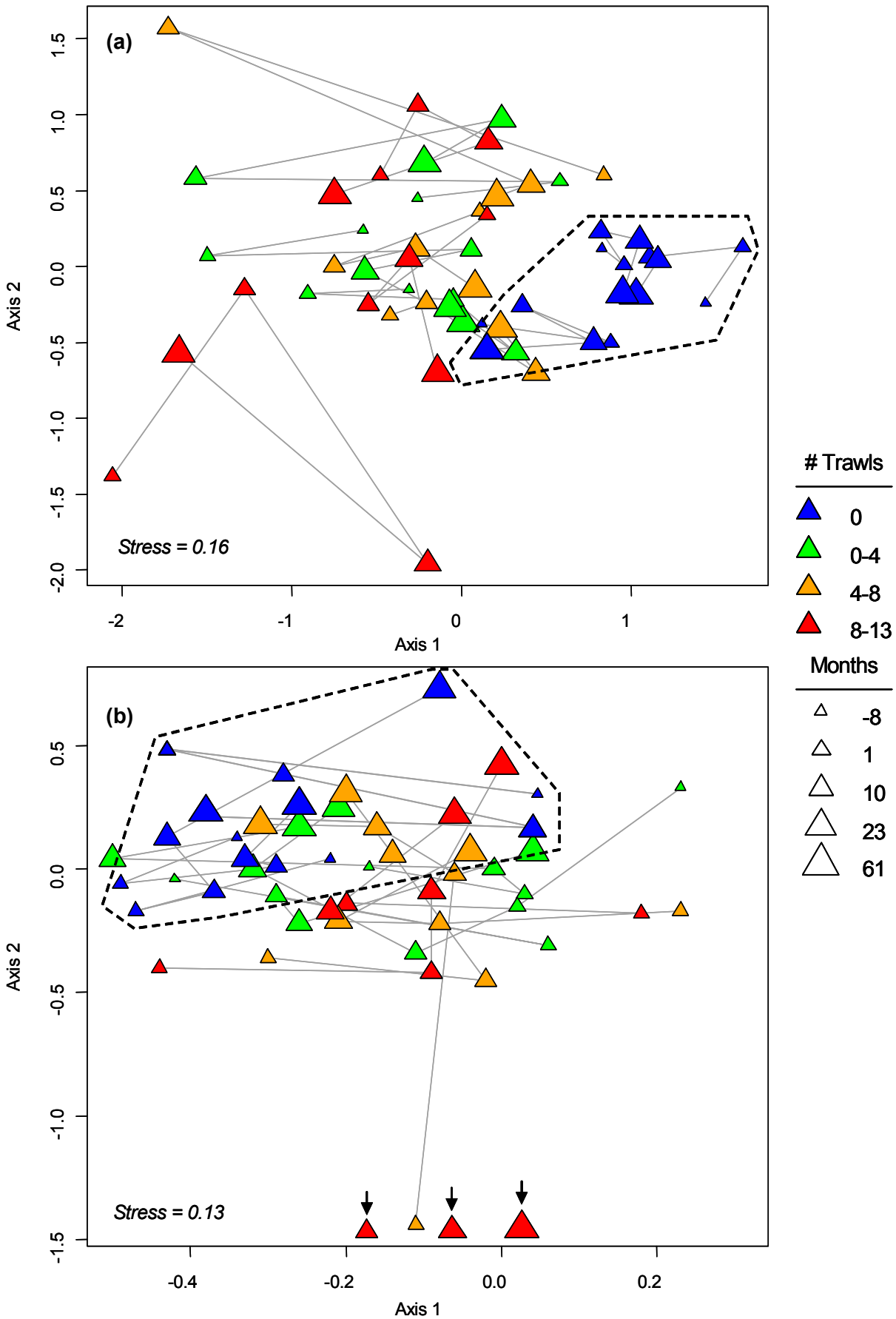

Figure 3-84: Sled. MDS plots for the overall density (N/m^2) for all treatment and control plots in (a) deep and (b) shallow waters. Colored symbols indicate trawl-intensity and symbol size indicates time. Connecting lines join plots through time and dotted lines indicate the boundary of control plots. Arrows indicate points outside of the plotted scale.

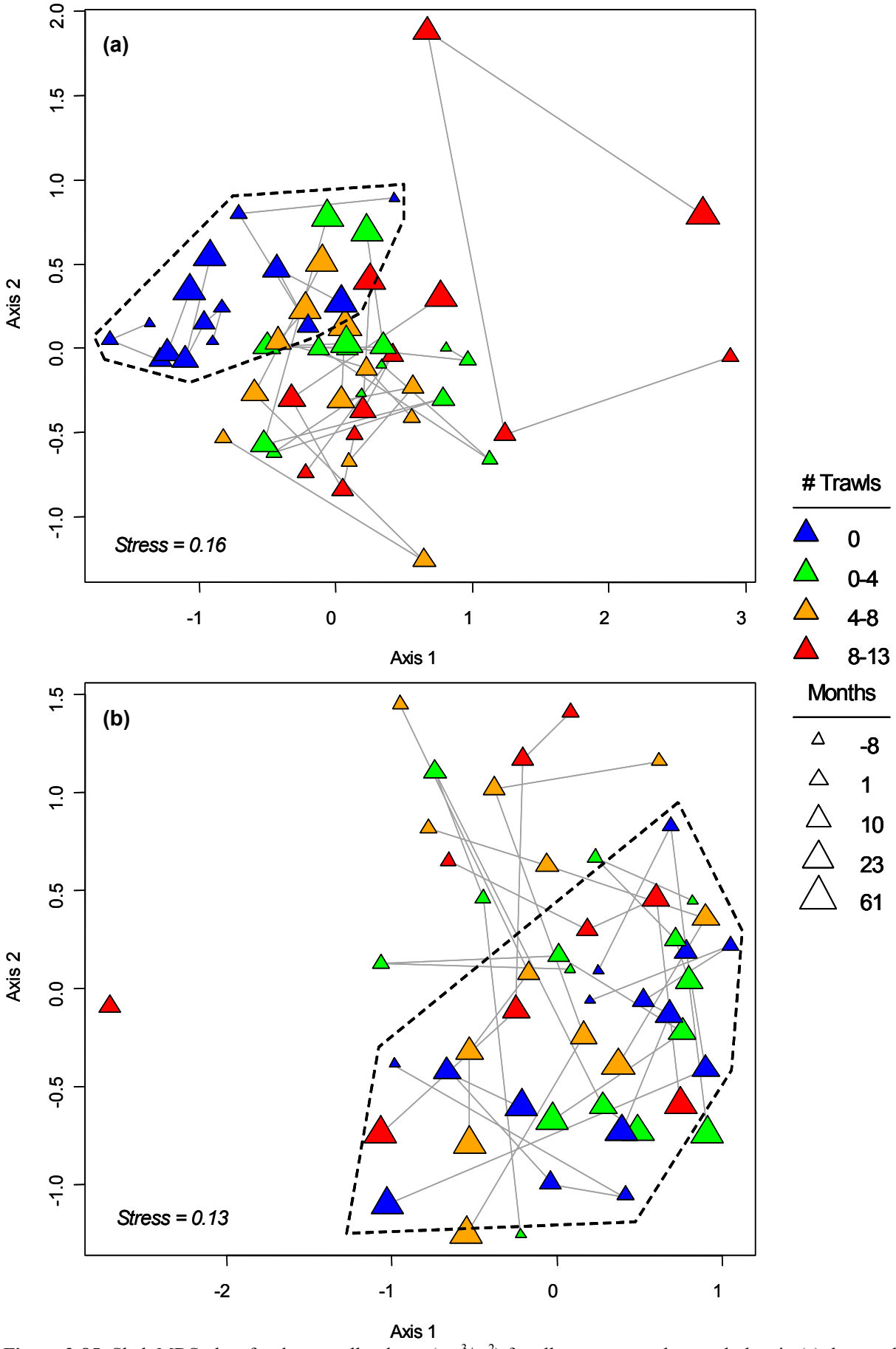

Figure 3-85: Sled. MDS plots for the overall volume (cm^3/m^2) for all treatment and control plots in (a) deep and (b) shallow waters. Colored symbols indicate trawl-intensity and symbol size indicates time. Connecting lines join plots through time and dotted lines indicate the boundary of control plots.

Table 3-8: ROV relative abundance, results of ANOSIM comparisons among trawl-intensity strata by survey month, for (a) deep plots and (b) shallow plots. Global sig. level is the percent probablity of the overall *R* across all trawl strata, *R*-value is the similarity statistic for each comparison, sig. level is the test probablity expressed as a percetage, #perm>obs is the number of random permutations having *R* greater than *R*-value, group separation is a categorization of the amount of separation of the treatment groups (ns: essentially not separable, +: small separation, ++: medium separation, +++: large separation).

(a) Deep plots

Time	Statistic	Trawl-Intensity Groups Contrasted						Global Sig. Level
		0 vs. 0-4	0 vs. 4-8	0 vs. 8-13	0-4 vs. 4-8	0-4 vs. 8-13	4-8 vs. 8-13	
10 months	*R*-value	0.259	0.407	0.667	-0.407	-0.111	-0.37	37.2%
	Sig. Level %	30	10	10	100	60	100	
	#perm>obs	3	1	1	10	6	10	
	Group separation	+	+	++	ns	ns	ns	
23 months	*R*-value	0.185	0.333	0.889	-0.296	0	-0.074	13.1%
	Sig. Level %	20	20	10	80	60	60	
	#perm>obs	2	2	1	8	6	6	
	Group separation	ns	+	+++	ns	ns	ns	
61 months	*R*-value	0.444	0.519	0.917	-0.111	0.083	0.417	3.6%
	Sig. Level %	20	10	10	80	40	10	
	#perm>obs	2	1	1	8	4	1	
	Group separation	+	++	+++	ns	ns	+	

(b) Shallow plots

Time	Statistic	Trawl-Intensity Groups Contrasted						Global Sig. Level
		0 vs. 0-4	0 vs. 4-8	0 vs. 8-13	0-4 vs. 4-8	0-4 vs. 8-13	4-8 vs. 8-13	
10 months	*R*-value	-0.185	0.148	0.407	-0.222	0.037	-0.111	47.6%
	Sig. Level %	80	20	10	70	60	80	
	#perm>obs	8	2	1	7	6	8	
	Group separation	ns	ns	+	ns	ns	ns	
23 months	*R*-value	0.111	0.074	1	-0.296	0.083	-0.167	27.3%
	Sig. Level %	30	30	10	90	50	80	
	#perm>obs	3	3	1	9	5	8	
	Group separation	ns	ns	+++	ns	ns	ns	
61 months	*R*-value	0	0.444	0.167	-0.111	0.167	0	29.7%
	Sig. Level %	50	10	40	60	40	50	
	#perm>obs	5	1	4	6	4	5	
	Group separation	ns	+	ns	ns	ns	ns	

Table 3-9: ROV patch density, results of ANOSIM comparisons among trawl-intensity strata by survey month, for (a) deep plots and (b) shallow plots. Global sig. level is the percent probablity of the overall *R* across all trawl strata, *R*-value is the similarity statistic for each pairwise comparison, sig. level is the test probablity expressed as a percetage, #perm>obs is the number of random permutations having *R* greater than *R*-value, group separation is a categorization of the amount of separation of the treatment groups (ns: essentially not separable, +: small separation, ++: medium separation, +++: large separation).

(a) Deep plots

Time	Statistic	Trawl-Intensity Groups Contrasted						Global Sig. Level
		0 vs. 0-4	0 vs. 4-8	0 vs. 8-13	0-4 vs. 4-8	0-4 vs. 8-13	4-8 vs. 8-13	
10 months	*R*-value	0.296	0.519	0.741	-0.444	-0.259	-0.333	34.8%
	Sig. Level %	30	10	10	100	90	90	
	#perm>obs	3	1	1	10	9	9	
	Group separation	+	++	++	ns	ns	ns	
23 months	*R*-value	0.259	0.37	0.815	-0.333	0	-0.148	17.8%
	Sig. Level %	20	10	10	80	60	70	
	#perm>obs	2	1	1	8	6	7	
	Group separation	+	+	+++	ns	ns	ns	
61 months	*R*-value	0.519	0.481	0.917	-0.074	0	0.5	4.8%
	Sig. Level %	10	20	10	70	40	10	
	#perm>obs	1	2	1	7	4	1	
	Group separation	++	+	+++	ns	ns	++	

(b) Shallow plots

Time	Statistic	Trawl-Intensity Groups Contrasted						Global Sig. Level
		0 vs. 0-4	0 vs. 4-8	0 vs. 8-13	0-4 vs. 4-8	0-4 vs. 8-13	4-8 vs. 8-13	
10 months	*R*-value	-0.259	0.148	0.37	-0.222	-0.074	-0.074	61.0%
	Sig. Level %	90	30	10	70	70	60	
	#perm>obs	9	3	1	7	7	6	
	Group separation	ns	ns	+	ns	ns	ns	
23 months	*R*-value	0.185	-0.037	1	-0.222	0	-0.167	27.5%
	Sig. Level %	20	70	10	80	50	70	
	#perm>obs	2	7	1	8	5	7	
	Group separation	ns	ns	+++	ns	ns	ns	
61 months	*R*-value	-0.148	0.222	0.167	-0.148	0.083	0.083	55.3%
	Sig. Level %	80	20	30	70	50	50	
	#perm>obs	8	2	3	7	5	5	
	Group separation	ns	ns	ns	ns	ns	ns	

Table 3-10: ROV volume density, results of ANOSIM comparisons among trawl-intensity strata by survey month, for (a) deep plots and (b) shallow plots. Global sig. level is the percent probablity of the overall *R* across all trawl strata, *R*-value is the similarity statistic for each comparison, sig. level is the test probablity expressed as a percetage, #perm>obs is the number of random permutations having *R* greater than *R*-value, group separation is a categorization of the amount of separation of the treatment groups (ns: essentially not separable, +: small separation, ++: medium separation, +++: large separation).

(a) Deep plots

Time	Statistic	Trawl-Intensity Groups Contrasted						Global Sig. Level
		0 vs. 0-4	0 vs. 4-8	0 vs. 8-13	0-4 vs. 4-8	0-4 vs. 8-13	4-8 vs. 8-13	
10 months	*R*-value	0.11	0.3	0.48	-0.11	0.04	-0.15	27.9%
	Sig. Level %	20	20	10	70	40	90	
	#perm>obs	5	2	1	7	4	9	
	Group separation	ns	+	+	ns	ns	ns	
23 months	*R*-value	0.26	0.26	0.93	-0.22	0.11	0	9.8%
	Sig. Level %	30	30	10	90	50	50	
	#perm>obs	3	3	1	9	5	5	
	Group separation	+	+	+++	ns	ns	ns	
61 months	*R*-value	0.44	0.33	0.75	0.48	0.25	-0.08	4.0%
	Sig. Level %	10	20	20	10	30	80	
	#perm>obs	1	2	2	1	3	8	
	Group separation	+	+	+++	+	+	ns	

(b) Shallow plots

Time	Statistic	Trawl-Intensity Groups Contrasted						Global Sig. Level
		0 vs. 0-4	0 vs. 4-8	0 vs. 8-13	0-4 vs. 4-8	0-4 vs. 8-13	4-8 vs. 8-13	
10 months	*R*-value	0.19	0.26	0.41	-0.22	-0.22	-0.11	39.7%
	Sig. Level %	20	30	10	80	100	80	
	#perm>obs	2	3	1	8	10	8	
	Group separation	ns	+	+	ns	ns	ns	
23 months	*R*-value	0.37	0.04	1	-0.04	0.67	0	10.3%
	Sig. Level %	10	50	10	60	20	40	
	#perm>obs	1	5	1	6	2	4	
	Group separation	+	ns	+++	ns	++	ns	
61 months	*R*-value	-0.3	0.3	0.25	-0.33	-0.17	-0.42	76.2%
	Sig. Level %	100	10	20	90	70	90	
	#perm>obs	10	1	2	9	7	9	
	Group separation	ns	+	+	ns	ns	ns	

Table 3-11: Sled track density, results of ANOSIM comparisons among trawl-intensity strata by survey month, for (a) deep plots and (b) shallow plots. Global sig. level is the percent probablity of the overall *R* across all trawl strata, *R*-value is the similarity statistic for each comparison, sig. level is the test probablity expressed as a percetage, #perm>obs is the number of random permutations having *R* greater than *R*-value, group separation is a categorization of the amount of separation of the treatment groups (ns: essentially not separable, +: small separation, ++: medium separation, +++: large separation).

(a) Deep plots

Time		Trawl-Intensity Groups Contrasted						Global
months	Statistic	0 vs. 0-4	0 vs. 4-8	0 vs. 8-13	0-4 vs. 4-8	0-4 vs. 8-13	4-8 vs. 8-13	Sig. Level
	R-value	0.704	-	-	-	-	-	
-8	Sig. Level %	10	-	-	-	-	-	10.0%
	#perm>obs	2	-	-	-	-	-	
	Group separation	++	-	-	-	-	-	
	R-value	0.63	0.704	0.481	0.074	-0.222	-0.185	
1	Sig. Level %	10	10	10	40	90	90	11.1%
	#perm>obs	1	1	1	4	9	9	
	Group separation	++	++	+	ns	ns	ns	
	R-value	0.333	0.481	0.815	-0.185	-0.259	-0.185	
10	Sig. Level %	10	10	10	90	100	100	10.3%
	#perm>obs	1	1	1	9	10	10	
	Group separation	+	+	+++	ns	ns	ns	
	R-value	0.593	0.481	0.519	-0.259	-0.296	-0.148	
23	Sig. Level %	10	10	10	70	100	80	11.9%
	#perm>obs	1	1	1	7	10	8	
	Group separation	++	+	++	ns	ns	ns	
	R-value	0.333	0.556	0.667	0.037	0.148	0.074	
61	Sig. Level %	20	20	10	50	30	40	6.1%
	#perm>obs	2	2	1	5	3	4	
	Group separation	+	++	++	ns	ns	ns	

(b) Shallow plots

Time		Trawl-Intensity Groups Contrasted						Global
months	Statistic	0 vs. 0-4	0 vs. 4-8	0 vs. 8-13	0-4 vs. 4-8	0-4 vs. 8-13	4-8 vs. 8-13	Sig. Level
	R-value	0.037	-	-	-	-	-	
-8	Sig. Level %	50	-	-	-	-	-	50.0%
	#perm>obs	2	-	-	-	-	-	
	Group separation	ns	0	0	0	0	0	
	R-value	0.481	0.185	0.583	0	0.417	-0.25	
1	Sig. Level %	10	20	10	60	10	70	20.5%
	#perm>obs	1	3	1	6	1	7	
	Group separation	+	ns	++	ns	+	ns	
	R-value	0.148	0.926	0.111	-0.333	-0.37	-0.074	
10	Sig. Level %	20	10	30	90	100	90	24.7%
	#perm>obs	2	1	3	9	10	9	
	Group separation	ns	+++	ns	ns	ns	ns	
	R-value	-0.185	-0.148	0.148	0	-0.074	-0.074	
23	Sig. Level %	90	90	30	50	80	80	71.8%
	#perm>obs	9	9	3	5	8	8	
	Group separation	ns	ns	ns	ns	ns	ns	
	R-value	0	-0.333	-0.148	-0.37	0	-0.074	
61	Sig. Level %	60	100	90	100	70	70	80.6%
	#perm>obs	6	10	8	10	7	7	
	Group separation	ns	ns	ns	ns	ns	ns	

Table 3-12: Sled track volume density, results of ANOSIM comparisons among trawl intensity strata by survey month, for (a) deep plots and (b) shallow plots. Global sig. level is the percent probablity of the overall *R* across all trawl strata, *R*-value is the similarity statistic for each comparison, sig. level is the test probablity expressed as a percetage, #perm>obs is the number of random permutations having *R* greater than *R*-value, group separation is a categorization of the amount of separation of the treatment groups (ns: essentially not separable, +: small separation, ++: medium separation, +++: large separation).

(a) Deep plots

Time		Trawl-Intensity Groups Contrasted						Global
months	Statistic	0 vs. 0-4	0 vs. 4-8	0 vs. 8-13	0-4 vs. 4-8	0-4 vs. 8-13	4-8 vs. 8-13	Sig. Level
	R-value	0.556	-	-	-	-	-	
-8	Sig. Level %	10	-	-	-	-	-	10.0%
	#perm>obs	1	-	-	-	-	-	
	Group separation	++	-	-	-	-	-	
	R-value	0.741	0.815	0.481	0.037	-0.111	-0.037	
1	Sig. Level %	10	10	10	50	60	80	5.8%
	#perm>obs	1	1	1	5	6	8	
	Group separation	++	++	+	ns	ns	ns	
	R-value	0.519	0.778	0.704	0.074	0.037	-0.333	
10	Sig. Level %	10	10	10	50	40	100	2.9%
	#perm>obs	1	1	1	5	4	10	
	Group separation	++	++	++	ns	ns	ns	
	R-value	0.111	0.296	0.444	-0.148	-0.407	0.074	
23	Sig. Level %	30	20	10	70	100	50	31.4%
	#perm>obs	3	2	1	7	10	5	
	Group separation	ns	+	+	ns	ns	ns	
	R-value	0.481	0.222	0.37	-0.074	-0.111	0.074	
61	Sig. Level %	20	30	10	60	70	50	18.7%
	#perm>obs	2	3	1	6	7	5	
	Group separation	+	ns	+	ns	ns	ns	

(b) Shallow plots

Time		Trawl-Intensity Groups Contrasted						Global
months	Statistic	0 vs. 0-4	0 vs. 4-8	0 vs. 8-13	0-4 vs. 4-8	0-4 vs. 8-13	4-8 vs. 8-13	Sig. Level
	R-value	0.111	-	-	-	-	-	
-8	Sig. Level %	40	-	-	-	-	-	40.0%
	#perm>obs	2	-	-	-	-	-	
	Group separation	ns	-	-	-	-	-	
	R-value	0.259	0.222	0.25	0.074	0.583	-0.5	
1	Sig. Level %	20	30	30	50	10	100	21.6%
	#perm>obs	2	3	3	5	1	10	
	Group separation	+	ns	+	ns	++	ns	
	R-value	0.037	0.556	0.074	0	-0.37	0	
10	Sig. Level %	50	10	40	40	100	60	43.3%
	#perm>obs	5	1	4	4	10	6	
	Group separation	ns	++	ns	ns	ns	ns	
	R-value	-0.222	-0.296	-0.111	0.037	0	-0.148	
23	Sig. Level %	100	100	80	40	50	90	79.5%
	#perm>obs	10	10	8	4	5	9	
	Group separation	ns	ns	ns	ns	ns	ns	
	R-value	-0.148	-0.444	-0.222	-0.259	0.037	-0.148	
61	Sig. Level %	80	100	100	90	40	80	91.3%
	#perm>obs	8	10	10	9	4	8	
	Group separation	ns	ns	ns	ns	ns	ns	

3.5.2 Species dominance patterns

3.5.2.1 ROV species k–dominance

The cumulative, or *k*–, dominance distribution curves for epibenthos abundance on ROV patches in deep and shallow water, by survey month and by trawl-intensity strata, are shown in Figure 3-86. At the time of earlier ROV surveys after the depletion experiment, the *k*-dominance curves for the control plots were consistently below those for each of the three trawl-intensity strata, and the curves of the higher-intensity strata tended to be higher on the graph (Figure 3-86). These patterns indicated that the assemblages of the control plots were less dominated — ie. abundances of taxa were more evenly distributed — than those of the impacted plots, and that the higher-intensity strata tended to be more dominated by a few taxa. With time, the abundance *k*-dominance curves for controls and the trawl-intensity strata tended to merge and overlap more by month 61. On shallow plots, the patterns of *k*-dominance among the controls and the intensity strata were more different initially and some differences remained at month 61, relative to the curves for deep assemblages (Figure 3-86). Numerically, the top ranking (dominant) species for the ROV assemblages were *Junceella juncea, Junceella fragilis, Ctenocella pectinata, Dichotella divergens,* Alcyonacea, Nephtheidae and *Ianthella flabelliformis*.

The *k*–dominance curves for epibenthos volume on ROV patches are shown in Figure 3-87. The patterns for volume were similar to those for abundance, however, the differences between controls and impacts and among trawled strata were much more marked. With respect to volume, as a surrogate for biomass, trawled assemblages were more dominated and hence less diverse than controls. With time, the differences between the trawled strata and controls diminished, but still remained at month 61. Volumetrically, the dominant species for the ROV assemblages were Nephtheidae, Alcyonacea, Porifera and Scleractinia.

3.5.2.2 Sled species k–dominance.

The *k*–dominance curves for epibenthos abundance on Sled tracks are shown in Figure 3-88. The patterns for Sled abundance were similar to those for the ROV, although the general pattern of the Sled curves were indicative of more highly dominated assemblages. Again, the lower curves of the control plots after impact indicated that the abundances of taxa were more evenly distributed than on impacts. At the same time, the assemblages of higher-intensity strata tended to be more dominate and less diverse. With time, the differences between the trawled strata and controls decreased, but were still apparent at month 61. Numerically, the dominant species for the Sled assemblages were *Junceella juncea,* Nephtheidae, *Ctenocella pectinata,* Alcyonacea*, Dichotella divergens* and *Junceella fragilis*.

The *k*–dominance curves for epibenthos volume on Sled tracks are shown in Figure 3-89. The patterns for volume were very highly dominated by only one or two taxa and there was little difference between the curves for controls and impacts or among trawled strata. There was also little observable difference between the curves for deep and shallow plots. With time, there was some change in the relative dominance of the top one or two species. Volumetrically, the dominant species for the Sled assemblages were *Junceella juncea,* Nephtheidae and Alcyonacea.

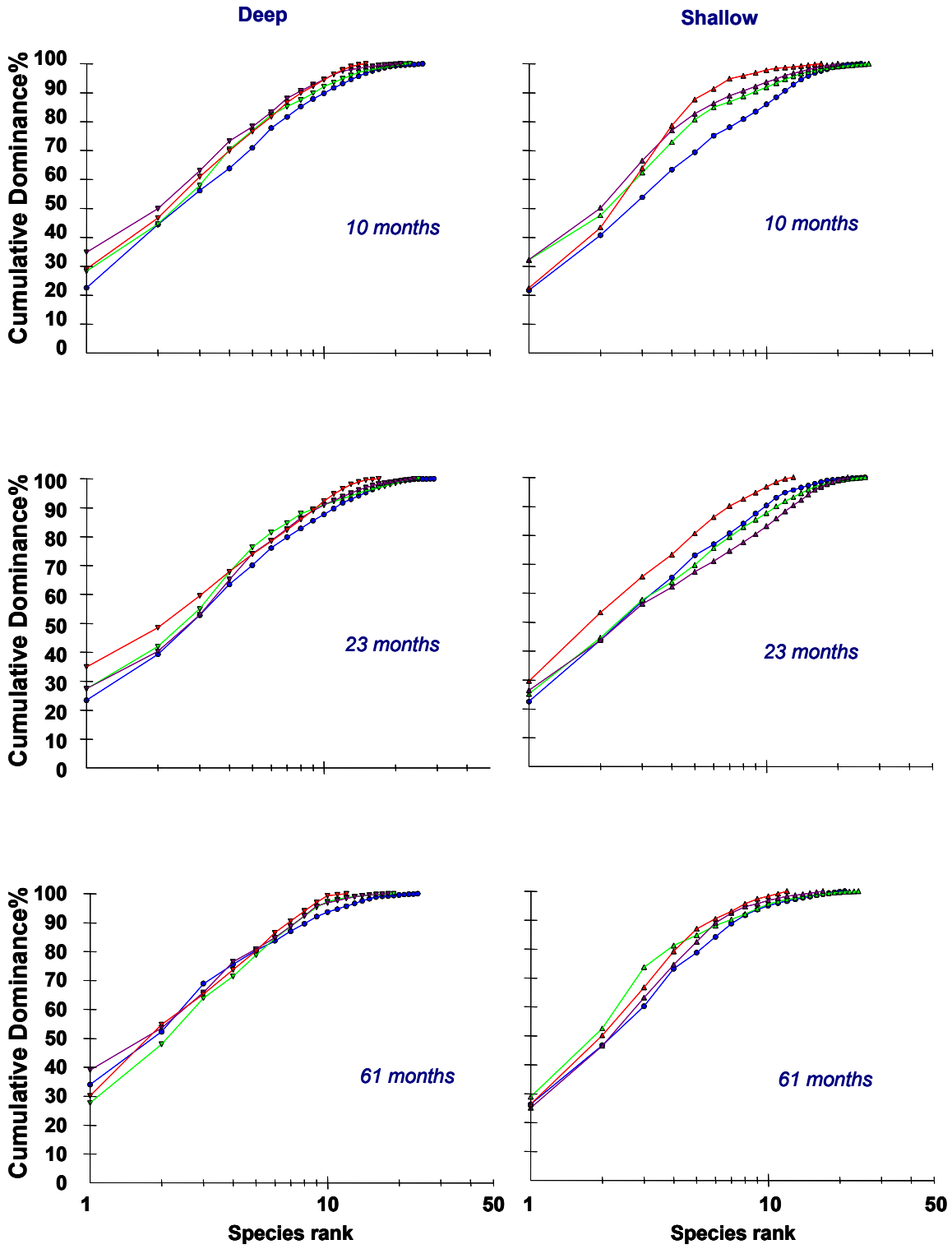

Figure 3-86: ROV. Dominance curves for abundance on both deep and shallow plots, by survey month and by trawl-intensity. Blue = controls, green = 0-4 trawls, maroon = 4-8 trawls, and red = 8-13 trawls.

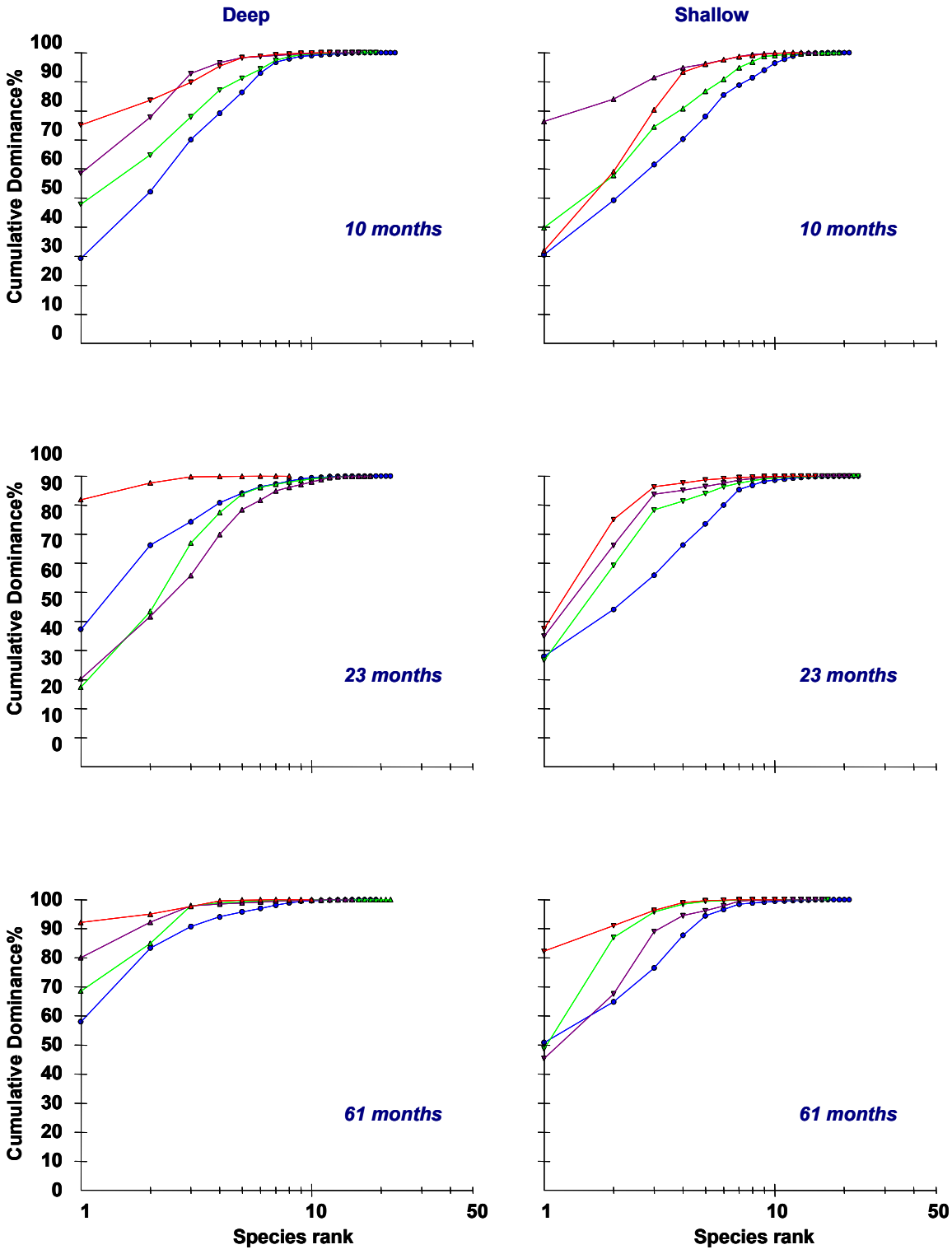

Figure 3-87: ROV. Dominance curves for volume on both deep and shallow plots, by survey month and by trawl-intensity. Blue = controls, green = 0-4 trawls, maroon = 4-8 trawls, and red = 8-13 trawls.

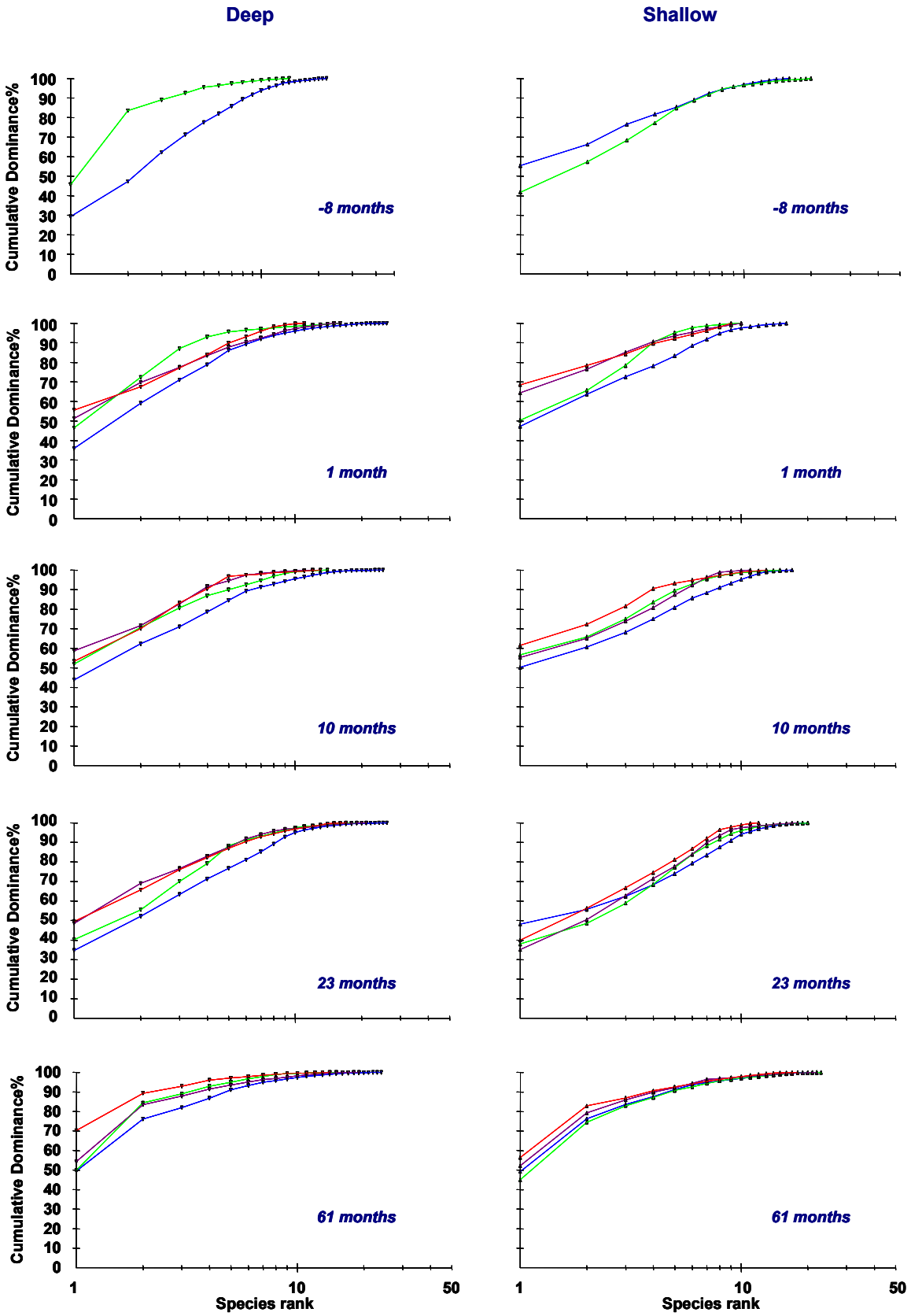

Figure 3-88: Sled. Dominance curves for abundance on both deep and shallow plots, by survey month and by trawl-intensity. Blue = controls, green = 0-4 trawls, maroon = 4-8 trawls, and red = 8-13 trawls.

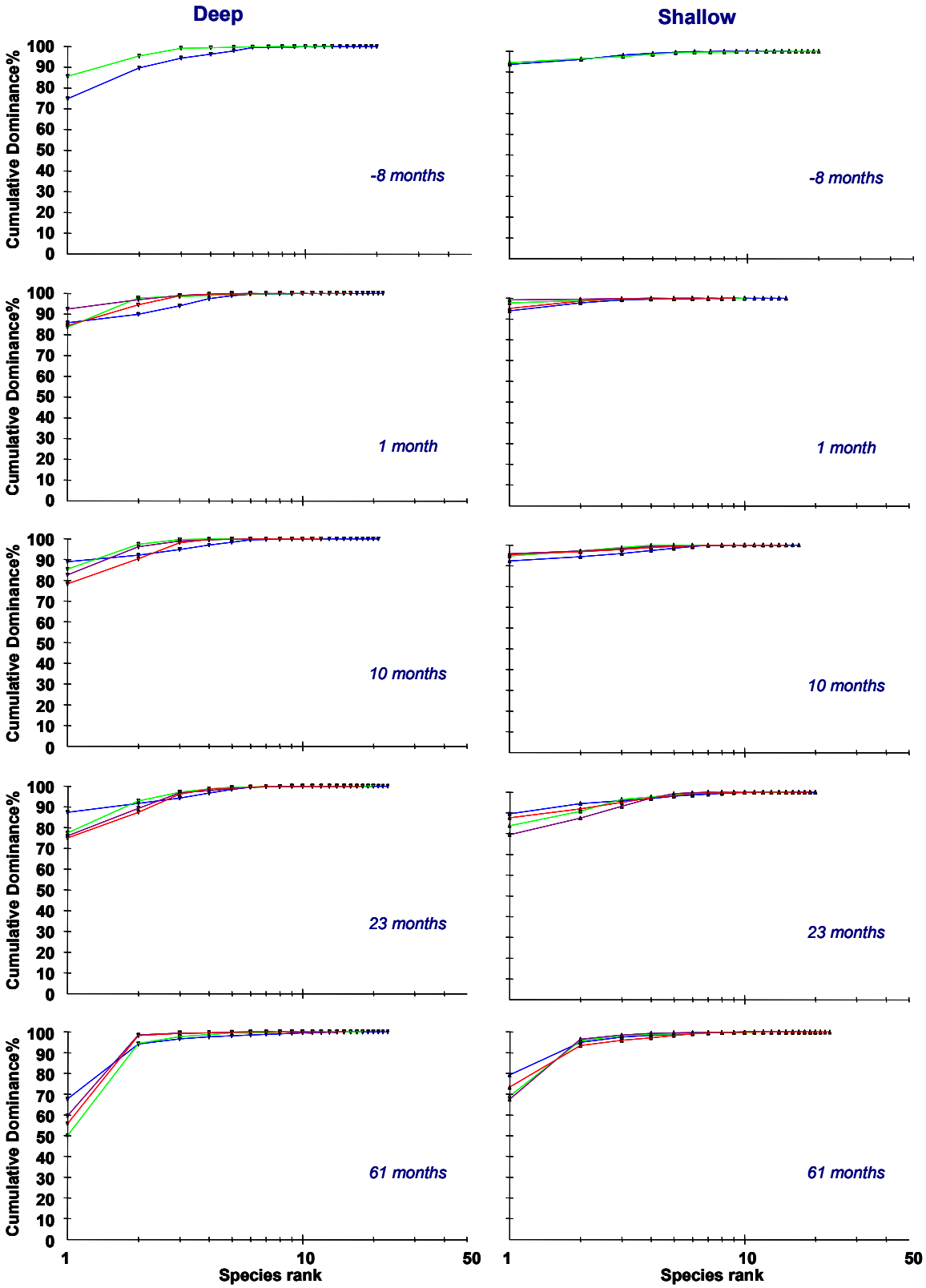

Figure 3-89: Sled. Dominance curves for volume on both deep and shallow plots, by survey month and by trawl-intensity. Blue = controls, green = 0-4 trawls, maroon = 4-8 trawls, and red = 8-13 trawls.

3.6 Recovery time frame projections

The depletion and recovery rates estimated from back-transformation of the trawl intensity and time*intensity coefficients in the Sled numbers models are shown in Table 3-13. Those for the ROV, (usually) estimated from back-transformation of the nearest neighbour density model trawl intensity coefficient, and the census-numbers time*intensity coefficient, are shown in Table 3-14. The means of the estimated depletion rates ranged from ~0% to ~70% per trawl, excluding possibly misleading positive estimates of immediate impact. The means of the estimated recovery rates ranged from ~0% to about 12% per year per trawl, excluding possibly misleading negative estimates of recovery.

The precision of the depletion and recovery estimates varied greatly, and the 90% confidence interval for most species was very broad. In many cases, this was due to low numbers of animals resulting in statistical imprecision, but it also highlights the large uncertainty arising from the naturally variable spatial and temporal dynamics of these megabenthos species. A number of upper-range depletion estimates were positive, and many lower-range recovery estimates were negative. However, in most (but not necessarily all) cases, immediate positive impact is unlikely, as is a negative capacity for recovery. In these cases, estimates derived from the alternative platform were generally considered more reliable. Species that had higher rates of depletion or lower rates of recovery or both are potentially vulnerable if trawled.

The estimates of time frames for recovery of megabenthos species affected by the repeated-trawl experiment of December 1995 were independent of the intensity of trawling due to the use of model 3 results for this purpose, where recovery was described by a single model term, ie. time*intensity; thus the relative rate of recovery increased with trawl intensity. Due to the uncertainty in depletion rates and particularly recovery rates, the recovery time frames were also estimated with considerable uncertainty (Table 3-15; Table 3-16). Two ranges of uncertainty are presented in the tables. The best and worst case scenarios were derived respectively from the upper depletion with upper recovery rates, and lower depletion with lower recovery rates (Table 3-13, Table 3-14). However, these scenarios are likely to be overly pessimistic due to the correlation between the errors for depletion and recovery, ie. an overestimate of the depletion rate would correspond with an overestimate of the recovery rate and lead to little change in the total recovery time, and vice-versa. A more realistic approximation was provided by the fast and slow extremes of the recovery uncertainty range, ie. mean depletion with upper recovery rate, and mean depletion with lower recovery rate, respectively.

At the time of the last survey in January 2001, after just over 5 years, 13 of 18 Sled species were estimated to have recovered, at the mean rate. *Cymbastela coralliophila* was estimated to need an average of 66 years to recover, whereas the recovery time for *Junceella fragilis* could not be estimated due to a negative time*intensity coefficient. However, the uncertainty was considerable, with seven species having a worst case confidence range of 0–∞. Mean recovery times for the ROV species tended to be slower. Of 24 species, at the mean rate, only 5 were estimated to have recovered by the last survey. Several species had multi-decadal recovery time estimes and for 3 species the recovery time could not be estimated due to negative time*intensity coefficients. Again, the uncertainties were considerable, with most ROV species having a worst case confidence range of 0–∞.

In a few cases, the mean recovery time was estimated to be zero due to positive trawl intensity terms, including: *Solenocaulon* sp. and *Echinogorgia* (Sled, Table 3-15) and *Alcyonacea* (ROV, Table 3-16). Very short recovery times may be reasonable for *Solenocaulon* sp. and *Alcyonacea*, although the initial impact of trawling was unlikely to have been positive (see Discussion 4.1.1). *Echinogorgia* more likely had similar responses as other gorgonians.

Table 3-13: Sled species depletion and recovery rate estimates, with 90% confidence range.

Sled		Depletion rate: % per trawl			Recovery rate: % per year per trawl		
Species	**Type**	**Lower**	**Mean**	**Upper**	**Lower**	**Mean**	**Upper**
Ctenocella pectinata	Gorgonian	-16.6	-9.8	-2.4	0.9	2.7	4.5
Junceella juncea	Red whips	-11.3	-6.7	-1.8	0.8	1.8	2.8
Ianthella flabelliformis	Fan sponge	-27.3	-20.6	-13.3	2.2	3.8	5.4
Dichotella divergens	Gorgonian	-17.2	-9.2	-0.5	-0.3	2.3	5.0
Nephtheidae	Soft coral	-37.4	-26.4	-13.4	3.9	7.2	10.7
Alcyonacea	Soft coral	-15.2	-6.5	3.0	-1.4	1.9	5.4
Junceella fragilis	White whips	-15.8	-5.8	5.4	-5.2	-2.4	0.6
Solenocaulon sp	Gorgonian	-5.1	1.3	8.1	-2.4	-0.8	0.7
Turbinaria frondens	Hard coral	-49.6	-36.8	-20.8	2.0	7.0	12.2
Scleractinia	Hard coral	-21.1	-0.4	25.9	-6.0	2.6	11.9
Porifera	Sponge	-23.8	-13.7	-2.3	0.1	3.3	6.6
Annella reticulata	Gorgonian	-42.1	-30.9	-17.6	6.3	10.3	14.6
Sarcophyton sp	Soft coral	-21.9	-7.5	9.4	-0.2	4.3	8.9
Cymbastela coralliophila	Sponge	-47.0	-32.6	-14.3	-4.8	0.6	6.3
Hypodistoma deeratum	Solitary ascidian	-20.2	-7.5	7.3	2.0	7.0	12.2
Echinogorgia sp	Gorgonian	-16.2	4.7	30.9	-6.2	-1.8	2.8
Xestospongia testudinaria	Barrel sponge	-39.3	-24.5	-6.1	0.8	5.7	10.8

Table 3-14: ROV species depletion and recovery rate estimates, with 90% confidence range.

ROV		Depletion rate: % per trawl			Recovery rate: % per year per trawl		
Species	**Type**	**Lower**	**Mean**	**Upper**	**Lower**	**Mean**	**Upper**
Ctenocella pectinata	Gorgonian	-22.1	-13.1	-3.1	-3.0	0.9	5.0
Junceella.juncea	Red whips	-8.8	-3.8	1.5	-1.5	0.5	2.5
Ianthella flabelliformis	Fan sponge	-39.3	-25.8	-9.4	-3.1	3.3	10.2
Dichotella divergens	Gorgonian	-13.4	-5.1	4.1	0.2	1.8	3.5
Nephtheidae	Soft coral	-29.6	-14.6	3.7	-0.5	2.0	4.6
Alcyonacea	Soft coral	-6.2	5.2	18.0	-8.3	-4.2	0.1
Junceella.fragilis	White whips	-14.8	-5.8	4.2	-6.8	-3.6	-0.3
*Solenocaulon.*sp.	Gorgonian	-20.6	-3.5	17.3	-5.0	2.7	10.9
Turbinaria frondens	Hard coral	-69.3	-59.6	-46.7	-2.0	4.8	12.0
Scleractinia	Hard coral	-60.9	-45.2	-23.3	-3.7	1.0	6.0
Subergorgia sp.	Gorgonian	-61.8	-42.4	-13.0	-8.8	5.4	21.7
Porifera	Sponge	-42.5	-31.4	-18.0	1.8	7.6	13.6
Annella reticulata	Gorgonian	-67.4	-46.0	-10.7	-6.9	12.3	35.5
Subergorgia suberosa	Gorgonian	-46.6	-26.6	0.9	-7.4	-3.4	0.8
Sarcophyton sp.	Soft coral	-72.2	-54.9	-26.7	-15.4	0.5	19.4
Ianthella basta	Fan sponge	-75.1	-47.7	9.9	-2.4	8.5	20.7
Semperina brunea	Gorgonian	-78.7	-61.3	-29.7	-11.8	8.2	32.6
Cymbastela coralliophila	Sponge	-57.9	-21.5	46.5	-14.9	-6.9	1.9
Hypodistoma deeratum	Solitary ascidian	-73.0	-44.8	12.8	-24.7	0.2	33.4
Ellisella sp.	Gorgonian	-69.4	-46.8	-7.6	-9.7	9.2	32.1
Echinogorgia sp.	Gorgonian	-78.1	-44.5	40.3	-0.3	3.4	7.2
Xestospongia testudinaria	Barrel sponge	-82.9	-71.0	-51.0	-9.4	8.2	29.2
Bebryce sp.	Gorgonian	-73.4	-49.9	-5.9	3.3	6.8	10.3
Ascideacea	Colonial ascidian	-76.1	-55.1	-15.6	-14.0	8.4	36.5

Table 3-15: Sled species estimates of possible recovery times following the depletion experiment, with 90% confidence range around the recovery rate. Species with recovery times of ≤5 years were expected to have recovered within the period of the project. "State" indicates the estimated initial post-impact population status relative to an un-impacted state for three trawl intensities. Mean = mean depletion and mean recovery rate; Fast = mean depletion and upper recovery rate; Slow = mean depletion and lower recovery rate; Best = upper depletion and upper recovery rate; Worst = lower depletion and lower recovery rate.

Sled	Post-impact state %			Experiment recovery time, Years				
Species	2 trawls	7 trawls	11 trawls	Best	Fast	Mean	Slow	Worst
Ctenocella pectinata	81%	49%	32%	1	2	4	12	21
Junceella juncea	87%	62%	47%	1	2	4	9	15
Ianthella flabelliformis	63%	20%	8%	3	4	6	11	15
Dichotella divergens	82%	51%	34%	0	2	4	∞	∞
Nephtheidae	54%	12%	3%	1	3	4	8	12
Alcyonacea	87%	62%	47%	0	1	4	∞	∞
Junceella fragilis	89%	66%	52%	0	10	∞	∞	∞
Solenocaulon sp	103%	109%	115%	0	0	0	0	∞
Turbinaria frondens	40%	4%	1%	2	4	7	23	35
Scleractinia	99%	97%	96%	0	0	0	∞	∞
Porifera	74%	36%	20%	0	2	5	205	378
Annella reticulata	48%	8%	2%	1	3	4	6	9
Sarcophyton sp	85%	58%	42%	0	1	2	∞	∞
Cymbastela coralliophila	45%	6%	1%	3	6	66	∞	∞
Hypodistoma deeratum	86%	58%	43%	0	1	1	4	11
Echinogorgia sp	110%	138%	166%	0	0	0	0	∞
Xestospongia testudinaria	57%	14%	5%	1	3	5	37	65

Table 3-16: ROV species estimates of possible recovery times following the depletion experiment, with 90% confidence range around the recovery rate. Details as for Table 3-15 above.

ROV	Post-impact state %			Experiment recovery time, Years				
Species	2 trawls	7 trawls	11 trawls	Best	Fast	Mean	Slow	Worst
Ctenocella pectinata	76%	37%	21%	1	3	15	∞	∞
Junceella.juncea	93%	76%	65%	0	2	8	∞	∞
Ianthella flabelliformis	55%	12%	4%	1	3	9	∞	∞
Dichotella divergens	90%	70%	57%	0	2	3	23	64
Nephtheidae	73%	33%	18%	0	4	8	∞	∞
Alcyonacea	111%	143%	175%	0	0	0	0	∞
Junceella.fragilis	89%	66%	52%	0	∞	∞	∞	∞
Solenocaulon.sp.	93%	78%	67%	0	0	1	∞	∞
Turbinaria frondens	16%	0%	0%	6	8	19	∞	∞
Scleractinia	30%	1%	0%	5	10	59	∞	∞
Subergorgia sp.	33%	2%	0%	1	3	11	∞	∞
Porifera	47%	7%	2%	2	3	5	21	31
Annella reticulata	29%	1%	0%	0	2	5	∞	∞
Subergorgia suberosa	54%	12%	3%	0	37	∞	∞	∞
Sarcophyton sp.	20%	0%	0%	2	4	158	∞	∞
Ianthella basta	27%	1%	0%	0	3	8	∞	∞
Semperina brunea	15%	0%	0%	1	3	12	∞	∞
Cymbastela coralliophila	62%	18%	7%	0	13	∞	∞	∞
Hypodistoma deeratum	30%	2%	0%	0	2	255	∞	∞
Ellisella sp.	28%	1%	0%	0	2	7	∞	∞
Echinogorgia sp.	31%	2%	0%	0	9	18	∞	∞
Xestospongia testudinaria	8%	0%	0%	3	5	16	∞	∞
Bebryce sp.	25%	1%	0%	1	7	11	21	40
Ascideacea	20%	0%	0%	1	3	10	∞	∞

4 DISCUSSION

This project has provided significant *in situ* information on the impact and recovery of sessile megabenthos following a previous project that conducted an intensive repeat trawl depletion experiment. With respect to the objectives, this project has successfully documented the extent of recovery of living seabed habitat 1, 2 and 5 years after the depletion experiment by measuring a range of attributes of the sessile megafaunal community; estimated recovery rates with quantification of uncertainty; identified those taxa that appeared to have recovered within the 5-year period of the project, and estimated the possible time frames for others with estimates of confidence intervals; and identified taxa that are vulnerable with respect to trawling. The outcomes against each objective are discussed below, but first some relevant information from the literature is discussed to provide comparative background to these outcomes.

Recent reviews (eg. Committee on Ecosystem Effects of Fishing, 2002) and meta-analyses (eg. Collie *et al.* 2000) of research on the effects of trawling have consistently concluded that the extent of impacts, from negligible to severe, are very dependent on the type of gear, the location and intensity of its use, the nature of the habitat and the type of fauna that the gear interacts with. Whether or not effects are found to be statistically significant may be largely dependent on the magnitude and frequency of natural disturbances and the dynamic rates of the populations adapted to live in the habitat in relation to the size of the trawl effect, which may be small or large in comparison. Many studies of the effects of benthic trawling in other systems, in Australia and elsewhere, have observed very large levels of natural variability and offered these as an explanation for not discerning significant trawl impact effects (eg. Gibbs *et al.* 1980; Currie & Parry 1999). Such mixed results, with anthropogenic effects such as benthic effects of trawling occurring within a myriad of natural effects has been common, in particular where different habitats, biota, depths, and natural levels of disturbance occur (Kaiser and De Groot 2000; Jennings *et al.* 2001; Duplisea *et al.* 2002; Kaiser *et al.* 2003). Further, such mixed effects have been observed in both temperate and tropical benthic ecosystems (Van Dolah *et al.* 1987; Freese, 2001; Thrush and Dayton 2002).

Differing levels of trawl impact and recovery in different habitats have been discussed in another recent review of the effects of trawling on benthic ecosystems (Thrush and Dayton 2002). For example, depth dependent differences could be due to the fact that shallower seafloor communities exhibit greater species turnover and dynamics due to stronger natural disturbances such as tidal and sediment exchanges or cyclones (Thrush and Dayton 2002). Consequently, a specified level of anthropogenic disturbance would be relatively smaller than the same disturbance on a deeper seabed. Depth, as with elevation in terrestrial ecosystems, is among the strongest environmental factors — or more likely is correlated with other factors — that influence the abundance, composition and variability of marine biodiversity (Mann and Lazier 1992, Mann 2000).

Most studies of the effects of trawling have examined impacts on smaller mobile macro-invertebrates and/or infauna and relatively few of them have examined recovery following trawl impact. The available information indicates that such macro/in-fauna typically recover in the range 100–500 days (see Collie *et al.* 2000 for a meta-analysis). There are very few studies that consider sessile megafauna of the types observed in this project, and even less have examined recovery. Those that do include Van Dolah *et al.* (1987), who observed ~30% damage to sponges and corals after a single experimental trawl off the southeastern USA and one year later could not distinguish the community from the pre-trawl state; Sainsbury *et al.* (1997 and 1993), who examined the effects of fish trawling on the northwest shelf of Australia, and Pitcher *et al.* (2004), who conducted an individual-based study of the

dynamics of several megabenthos species in the Great Barrier Reef Region, as a basis for modeling impacts of trawling (as reported in Poiner *et al.* 1998) and of cyclones, as well as subsequent recovery.

Sainsbury categorized biogenic structural habitat as either small epibenthos (<25 cm high) or large epibenthos (>25 cm high) and initially indicated that growth to ~25 cm would take about 6–10 years (Sainsbury 1991), but later revised that to >15 years (Sainsbury *et al.* 1997). They reported that recovery observed in an area closed to trawling was faster for small epibenthos than large epibenthos (Sainsbury *et al.* 1993). A simple analysis of their published data indicated that the proportion of seabed with presence of small benthos recovered by about 15% per year (± ~14%, p≈0.09 approx.) and for large benthos by about 11% per year (± ~40%, p≈0.54 approx.). Because small benthos initially had a presence of about 40%, their recovery was greater and faster in absolute terms than large benthos, which had an initial presence of about 10%.

The modeling by Pitcher *et al.* (2004), of a very similar suite of nine species as in this study, indicated that of the estimated 15%–75% (across all species) of recruits that survived to reach the largest size-class (typically ~45 cm high, range 30–75 cm), the average time taken to grow to this size ranged from about 3–9 years with an overall 90-percentile range of ~1–23 years. They also showed that the potential recovery rates after a cyclone or trawling were very dependent on the source and rate of recruitment (as well as the extent of initial impact). Where all recruitment came from an external source, recovery was faster than with 50:50 external:self-recruitment, which in turn was faster than with 100% self-recruitment. Time to half-recover was presented because their models included asymptotic density-dependent effects. The potential impact of and recovery from a single trawl was, in most cases, similar to that of a cyclone and half-recovery time ranged from about 2–20 years depending on the species and recruitment. The recovery after a multiple-trawl (14x) impact again was dependent on the recruitment scenario. The half-recovery time with 100% external recruitment was similar to that for a single trawl or cyclone at about 2.5–8 years over the suite of species. With 50:50 external:self-recruitment, the half-recovery time was longer at about 4–15 years. With 100% self-recruitment, half-recovery was ~14–58 years — notably longer than for a single trawl or cyclone due to the larger trawl impact reducing the populations to lower abundance and consequently reducing the absolute number of recruits in the self-recruiting scenario.

Despite the importance of the recruitment source, the reproductive and larvae ecology of few species of sessile epibenthic fauna has been well studied, other than scleractinian corals (see review Harrison & Wallace 1990) and to some extent soft corals (see Alino & Coll 1989). Sponges generally release relatively few larvae that may crawl or swim for a period of time before settlement — the duration of swimming larvae may be several hours, days or a few weeks (reviewed in Maldonado 2006). Sponges also reproduce asexually by fragmentation or gemmules. Some sponges may also broadcast spawn large numbers eggs and sperm (including *Xestospongia* sp.s) (Fromont & Bergquist 1994). Soft corals and most hard corals typically broadcast spawn numerous eggs and sperm; after fertilisation and development, larvae may remain planktonic for days to weeks and be dispersed by currents — direct asexual propagation is also common in soft and hard corals (Fabricius & Alderslade 2001). Most gorgonians (Brazeau & Lasker 1989) and a few hard corals brood low numbers of larvae, which may be negatively buoyant and have limited dispersal. Gorgonians also propagate asexually: the sea whip *Junceella fragilis* is known (Walker & Bull 1983) to bud off the branch tip leading to local clumps (as observed herein also); *Ctenocella* may also bud miniature independent colonies (*pers obs*). Colonial ascidians brood low numbers of well developed larvae that may swim for a few minutes to a few days; they can also propagate by budding; solitary ascidians broadcast spawn numerous gametes, which may drift during fertilisation, development and larval life (Lambert 2005ab).

Broadcasting is regarded as advantageous for dispersal and recolonising disturbed areas, whereas brooding and particularly asexual propagation have low dispersal and colonisation, and often lead to highly aggregated distributions. Given these generalisations, soft-corals and solitary ascidians may recruit in large numbers from external sources and rapidly colonise broad areas, as was observed here. Conversely, sponges and gorgonians may recruit in small numbers from an unknown mix of local and external sources, leading to an expectation of slower re-colonisation times.

4.1 Recovery dynamics

Like studies cited above, the variability in the natural dynamics of the patchy sessile faunal assemblages observed in this study was substantial and dominated the data. Nevertheless, within that background of spatial and temporal changes due to other processes, there were overall patterns of impact and recovery that are summarised in Table 4-1. Most species showed a negative impact and recovery on one or more attributes, though the extent of impact and recovery, and the uncertainty of the measurements, varied considerably.

4.1.1 Abundance of sessile megafauna species

The typical pattern of numbers/density displayed by the majority of species was some level of impact followed by some level of recovery (e.g. ↓↗ or similar, Table 4-1). For the Sled, ~14 of 18 taxa showed this pattern, though the effect size varied from minor (~1 taxon), intermediate (~4 taxa) to major (~9 taxa) — with the level of significance varying greatly. For the ROV, ~16 of 24 taxa showed this pattern, again with the effect size varying from minor (~3 taxa), intermediate (~6 taxa) to major (~7 taxa) — and again the level of significance varied similarly. Most of the tests were not significant; nevertheless, given that so many species had similar trends, some confidence may be placed in the overall general pattern that a fairly widespread impact and some recovery had been observed.

There were a number of exceptions to the general pattern. A few of these species showed strong dynamics that may have been at least partly unrelated to the experiment, and may have diminished estimates of their depletion and/or recovery rates. For example, soft corals *Alcyonacea* showed evidence of a large widespread recruitment pulse, on controls as well as impacts, followed by cohort growth and then senescence. The trawl experiment coincided roughly with the beginning of this sequence. While there was some evidence from the Sled that trawling had an initial impact, the period over which recovery was surveyed appeared to coincide with the generalised decline, particularly for the ROV observations, which were made only from month 10 onwards — after the recruitment pulse, and the analyses hinted a positive impact followed by mixed non-significant trends. Thus, the recovery dynamics that were interpreted relative to changes on controls (as is formally correct), do not indicate the substantial broad recruitment capacity that was observed and may be expected given the reproductive ecology of these fast-turnover species. Indeed, spawning and recruitment of soft-corals has been stimulated by experimental disturbance of adults, which subsequently also recovered well from their injuries (Henry *et al.* 2003). In this project, the disturbance by the experimental trawling potentially *caused* the widespread recruitment onto controls as well as impact tracks.

The numbers of soft corals *Nephtheidae* were lower at months 10–23 then increased substantially almost everywhere, on controls as well as impacts, possibly indicating a generalised recruitment event.

Again, because the analyses estimated recovery on impacts relative to events on controls, the trawl recovery estimates for this species do not reflect the apparent substantial broad recruitment capacity, as for *Alcyonacea*.

The numbers of the solitary ascidian *Hypodistoma deeratum* were generally low before the experiment and did not appear to be greatly impacted. Subsequently, their numbers increased broadly on most trawled shallow areas, then declined quickly everywhere. It is likely that this could have been an opportunistic response to disturbance, indicative of strong recovery potential and short lived fast turnover — as expected from the generalised life history of solitary ascidians. However, given the Sled observed both the increase and decrease on trawled tracks, the overall recovery rate for the duration of the project would underestimate the initial response. The ROV observed the same increase and decline, with similar issues; though the much lower numbers mean the ROV estimates may be less reliable than the Sled.

The soft corals *Sarcophyton* appeared to be maximally abundant at about month 1 then tended to decline in numbers over the duration of the surveys on both controls and impacts — again, the ROV observed only the declining phase from month 10 and may have compromised recovery estimates relative to the Sled.

The gorgonian *Solencaulon* appeared to have been affected little by the trawl experiment (slight positive trend). While it is highly unlikely that this species gained an instantaneous benefit, it is known from other observations to be highly resilient to benthic sampling devices. Its numbers on impacts increased a little relative to controls, before tending to decline slightly on most tracks regardless of treatment — possibly for reasons unrelated to impact. Again the ROV observations were made only during the declining phase, and may have compromised recovery estimates.

The estimated recovery rates for some species were negative. *Echinogorgia* appeared to recruit to Sled control tracks in greater numbers than to trawled tracks, which lead to positive estimates of impact and negative estimates of recovery (both non-significant) — the pattern in ROV patches was more typical albeit with much lower numbers. The sponge *Cymbastela coralliophila* appeared to recruit to ROV control patches in slightly greater numbers than to trawled patches, which lead to (non-significant) negative estimates of recovery— the recovery trend on Sled tracks was positive though very slow (and non-significant). On ROV patches, the gorgonian *Subergorgia suberosa* appeared to recruit to control patches but continued to decline in impact patches leading to (non-significant) negative estimates of recovery. The whip *Junceella fragilis* appeared to recruit to some low impact areas but continued to decline in high impact areas, again leading to (non-significant) overall negative estimates of recovery for both Sled tracks and ROV patches. While it is conceivable that trawl effects may continue to have negative consequences for some time, none of these negative recovery estimates were significant.

A few species (eg Sled: *Annella reticulata* and *Xestospongia testudinaria*) appeared to continue declining for the first part of the recovery monitoring period, but then appeared to recover subsequently. A few other species (eg. Sled: *Dichotella divergens*) appeared to remain static for the first part of the recovery period, but then appeared to recover.

The unidentified hard corals *Scleractinia* also showed discrepancies in estimates of recovery rates among data sources and types. The counts of these corals were highly heterogeneous among tracks and patches and all estimates were highly uncertain and non-significant. The different areas surveyed by the Sled and ROV and the difficulty of identifying coral species from video may have contributed.

Table 4-1: Summary of impact and recovery trends for attributes of species observed by the Sled and ROV. Arrows indicate trends in effect size and direction (eg. impact ↓↓↓↓↓↓, recovery ↗↗↗↗↗, corresponding to magnitude intervals of ~6%, ~12%, ~25%, ~50%, ~100%). For the Sled, the three symbols indicate initial impact, and subsequent recovery early and later in the survey period. For ROV NND, the symbols indicate initial impact and subsequent recovery in the survey period. ROV census numbers were used to indicate recovery in the survey period only. Arrow direction indicates trend against time, ie. initial impact (↓) then recovery (↗), no change (→) or decline (↘). The approximate probability of effect is indicated by: ***p*<0.05, <0.10, <0.25, >0.25.** In cases indicated by ∞ data were too sparse in some main factors for model fitting. Cases of suspected poor model fit are indicated by ?.

Species	Type	Sled numbers	ROV NN density	ROV census recovery	Sled height	ROV height	ROV width	ROV area	Sled condition	ROV condition
Ctenocella pectinata	Gorgonian	↓↗↗	↑↘↗	↘→	↓↗↗	↓↘↘	↓↗↗	↓↗↗	↓↗↗	↑↘↘
Junceella juncea	Red whips	↓↗↗	↓↗↗	→↗	↑↘↗				↓↗↗	~↘↗
Ianthella flabelliformis	Fan sponge	↓↗↗	↓↗↗	↗↗	↓↗↗	↓↗↗	↓↗↗	↓↗↗	~→→	?~→→
Dichotella divergens	Gorgonian	↓→↗	↓↘↘	↗↗	↓↗↗	↓↘↘	↓↘↘	↓↘↘	↓↗↗	~→→
Nephtheidae	Soft coral	↓↗↗	↓↗↗	↗↗	~→↘	↓↗↘	↓↗↘	↓↗↘	↓↗↗	~→→
Alcyonacea	Soft coral	↓↗↗	↑↘→	↘↗	↓→↗	↓↘↘	↓↘↘	↓↘↘	↑↘↗	∞
Junceella fragilis	White whips	↓↘↘	?↓↘↘	→↘	↓↘↘				~→→	↓↗↗
Solenocaulon.sp.	Gorgonian	↑↘↘	↓→→	∞	↓↗↗	∞	∞	∞	~→→	??
Turbinaria frondens	Hard coral	↓↗↗	↓↘↗	↗↗	↑↘↘	↓↘↘	~↘↘	↓↘↘	↓↗→	~→→
Scleractinia	Hard coral	↓↗↘	↓↘↘	↘↗	↑↗↗	↓↗↗	↓→→	↓↘↘	~→→	~→→
Subergorgia sp.	Gorgonian		↓↗↘	∞		↓↗↗	~→→	↓↘↘	~→→	?↓↗→
Porifera	Sponge	↓↗↗	↓↗↗	↗↗	↓↗↗	↑↘↘	↑↘↘	↑↘↘	~→→	∞
Annella reticulata	Gorgonian	↓↘↗	↓↗↗	→→	↓↗↗	↓↗↗	↓↗↗	↓↗↗	~→→	↓↗↗
Subergorgia suberosa	Gorgonian	?↑↘↘?	↓↘↘	↗↘	↓↗↗	↑↘↘	↑↘↘	↑↘↘	~↘↗	↓↗↗
Sarcophyton sp.	Soft coral	↓↗↘	↓→↗	↗↘	↓↗↗	↓↗↗	↓↗↗	↓↗↗	~→→	~→→
Ianthella basta	Fan sponge		?↓↗↗	↗↗	↓↗↗	↑↘↘	↓↗↗	↓↗↗	~→→	~→→
Semperina brunea	Gorgonian		↓↗↗	∞		↓↗↗	↓↗↗	↓↗↗		∞
Cymbastela coralliophila	Sponge	↓↗→	↓↘↘	↗↘	↓↗↗	↑↘↘	∞	∞	~→→	~→→
Hypodistoma deeratum	Solitary ascidian	↓↗↗	↓↗↘	∞	↓↗↗	↓↗↘	↓↗↘	↓↗↘	~→→	~→→
Ellisella sp.	Gorgonian		↓↗↗	∞		↓→↘	↑↘↘	↓↘↘		↓↗↗
Echinogorgia sp.	Gorgonian	↑↘↘	↓→↗	↗↗	~→→	↑↗↗	↓↗↗	↓↗↗	~→→	↓↗↗
Xestospongia testudinaria	Barrel sponge	↓↘↗	↓↗↘	∞	↓↗↗	↓↗↗	↑↗↗	↓↗↗	↓↗↗	?↓↗↗
Bebryce sp.	Gorgonian		↓↗↗	↗↗		~↘↘	↑↘↘	↑↘↘		~→→
Ascideacea	Colonial ascidian		?↓↗↗	??		~↘↘	↓↗↗	↓↘↘		~→→

In general, the tough and flexible gorgonians tended to be relatively resistant to impact, sponges tended to be intermediate, and the brittle plate hard coral *Turbinaria* was among the least resilient. There were no clear differences between these groups in recovery rates, other than the broad recruitment observations for soft corals and solitary ascidians noted above.

4.1.2 Size of sessile megafauna

Most species appeared to show some degree of size dependent impacts, where larger individuals were more likely than smaller individuals to be removed by trawling, that would be manifest by an initial negative trend in mean size against trawl intensity (e.g. ↓, Table 4-1) — typically however, these trends were not significant. Of species showing an impact trend, most showed some degree of trend for subsequent recovery (e.g. ↓↗↗, Table 4-1) — again most trends were small and not significant. For the Sled, ~14 of 19 taxa showed weak impact trends, and ~13 of these showed recovery trends. For the ROV, ~13–17 of ~20 taxa showed impact trends, and only ~9–11 of these indicated recovery. *Ianthella flabelliformis* was one species that showed consistent size effects. Nevertheless, a possible influence in identifying recovery in size is that recovery in numbers, through recruitment of small individuals, may create, maintain or exacerbate a negative trend in mean height against trawl intensity until the recruited individuals have grown, even if the original survivors had 'recovered' in size (e.g. *Junceella fragilis*; *Turbinaria frondens*).

4.1.3 Condition of sessile megafauna

Condition could be expected to be an indicator of trawl impact in cases where individuals may not be removed in great proportion, but the remaining individuals on the seabed may be damaged and show persistent physical signs of injury, which may or may not recover (e.g. ↓↗↗ or similar, Table 4-1). About a third of the species appeared to show negative trends on condition that were related to the trawl impact, although the effect size was generally small and not significant — either few individuals were effected even if badly, or individuals were affected only slightly even if many of them. Of the species that showed impact trends, most indicated a recovery trend to some extent within the time-frame of the recovery monitoring surveys. Gorgonians were the type of benthos most frequently showing some evidence of a negative condition effect — ~9 of the taxa showing any trend were gorgonians — because these animals are resilient to removal, so remain on the seabed, but the outer layer of living polyps can be stripped or damaged and subsequently becomes encrusted. Nevertheless, the overall effect size for gorgonians was small and the hard coral *Turbinaria frondens* (Sled) was the only species that showed marked condition effects — it was easily broken by trawl gear.

4.1.4 Physical habitat structure

The physical structure of living seabed habitat, due to the sessile animals therein, was reduced substantially and significantly by trawling. On Sled tracks, the total living physical structure and its size composition appeared to recover almost completely within the time frame of the study, though the mix of species contributing to the structure may have differed somewhat. Several of the common structurally dominant species were relatively resistant to trawling (e.g. *Ctenocella pectinata, Junceella juncea, Dichotella divergens* — with *Ianthella flabelliformis* moderately resistant) and recovered relatively rapidly. Hence it can be expected that much of the living physical habitat structure would be

relatively resilient to trawling and survive in most areas. However, some of the less common and less resilient structural species may be reduced in abundance and take somewhat longer to recover (eg, *Turbinaria frondens*) leading to qualitative changes in the value of the habitat that may persist longer before recovery.

Among ROV patches, there appeared to be negligible recovery trend in total living physical habitat structure. The size composition of the structure varied but there was no consistent recovery trend. However, for the ROV physical structure, there was no benchmark for the pre-impact state.

4.1.5 Assemblage composition

The patterns of epibenthic assemblage composition showed natural effects (e.g. depth), spatial variability and temporal dynamics that were large in relation to any changes observed in response to the experimental trawling intensities and to any indications of recovery. This pattern was consistent for each attribute examined of the benthic assemblages, i.e. similarity or dominance, whether based on relative abundance, density, or volume. Despite the background variability due to natural sources, of which depth was treated separately, there were significant observable effects of trawl-intensity and time that were consistent with impact and recovery. The impact effects were clearer in the early months after trawling. Higher levels of trawl-intensity tended to cause greater differentiation of epibenthic assemblages, which tended to persist and could cause longer recovery times.

The extent of trawl impact and subsequent recovery appeared to differ between deep and shallow assemblages. In deep areas, the trawl effect tended to be larger and more consistent, whereas in shallow areas it was less clear and inconsistent. Conversely, in deep areas some trawled assemblages continued to diverge from controls and others showed only limited recovery convergence that was dependent on trawl-intensity — higher-intensity areas tended to converge less than lower-intensity areas. On the other hand, trawled assemblages on shallow areas tended to converge more towards controls, consistent with recovery, sometimes completely although the recovered state was relatively heterogeneous. This suggests a differential, habitat dependent effect of trawling and subsequent recovery response of these epibenthic assemblages.

The control plots clearly demonstrated the substantial natural variability and natural dynamics of these epibenthic assemblages. Nevertheless, the control assemblages tended to be less heterogeneous than the trawled assemblages, which exhibited higher levels of variability not all of which could be attributed to time or trawl-intensity. The trawl impact appeared to induce greater assemblage dissimilarity and variability in space and time, perhaps by creating conditions that could be exploited by opportunistic species.

The factor consistently accounting for the greatest differences in these epibenthic assemblages was the depth strata. The strong depth signal indicated that there were strong compositional differences between the deep and shallow benthic assemblages — stronger than any observed temporal variation. Such strong effects can mask the effects of the benthic experiments like trawling if they area not removed or isolated from the analyses.

4.2 Recovery time frames

The project identified the taxa that appeared to have recovered within the 5-year period of the recovery monitoring, with an estimate of the uncertainty. The possible time frames for taxa that had not recovered at that time were also estimated. As can be expected however, the recovery extrapolations beyond the data had broad confidence intervals, sometimes as much as zero to infinity. The time frames were also uncertain because the data were adequate for only simple models for population recovery and there is no assurance that populations would follow such simple dynamics indefinitely into the future. If greater precision about recovery rates and time frames is considered necessary then further sampling, particularly of slower recovering, less common, more uncertain species would be required. The recovery time frames estimated for this experiment were independent of the extent of the initial impact, due to the use of the relatively simple Model 3 — where recovery was represented by the Time*Intensity term — again because the variability in the data did not support more detailed models. In reality, recovery may take longer where higher trawl intensity had caused greater depletions, and be faster where lower trawl intensity had caused less depletion.

From the Sled data, the taxa estimated to have recovered included: *Solenocaulon* sp (~0 yr to recover), Scleractinia (~0 yr), *Echinogorgia* sp (~0 yr), *Hypodistoma deeratum* (~1 yr), *Sarcophyton* sp (~2 yr), *Ctenocella pectinata* (~4 yr), *Junceella juncea* (~4 yr), *Dichotella divergens* (~4 yr), Nephtheidae (~4 yr), Alcyonacea (~4 yr), *Annella reticulata* (~4 yr), Porifera (~5 yr), and *Xestospongia testudinaria* (~5 yr). The taxa estimated to have not recovered included: *Ianthella flabelliformis* (~6 yr), *Turbinaria frondens* (~7 yr), *Cymbastela coralliophila* (~66 yr), and no recovery was observed for *Junceella fragilis*.

From the ROV data, the taxa estimated to have recovered included: Alcyonacea (~0 yr), *Solenocaulon* sp. (~1 yr), *Dichotella divergens* (~3 yr), Porifera (~5 yr), and *Annella reticulata* (~5 yr). The taxa estimated to have not recovered included: *Ellisella* sp. (~7 yr), *Junceella juncea* (~8 yr), Nephtheidae (~8 yr), *Ianthella basta* (~8 yr), *Ianthella flabelliformis* (~9 yr), Ascideacea (~10 yr), *Subergorgia* sp. (~11 yr), *Bebryce* sp. (~11 yr), *Semperina brunea* (~12 yr), *Ctenocella pectinata* (~15 yr), *Xestospongia testudinaria* (~16 yr), *Echinogorgia* sp. (~18 yr), *Turbinaria frondens* (~19 yr), Scleractinia (~59 yr), and no recovery was observed for *Junceella fragilis*, *Subergorgia suberosa*, *Cymbastela coralliophila*. The ROV timeframes estimated for *Sarcophyton* sp. (~158 yr) and *Hypodistoma deeratum* (~255 yr) are probably unreliable, as discussed in section 4.1.1, and the Sled estimates should be considered more realistic.

The estimates of impact and recovery rates, and hence recovery timeframes, from the Sled and ROV data were reasonably consistent for the 5 or so most frequently occurring taxa. However, for several other taxa, there were marked differences in the estimates from these different data sources. Several factors may have contributed to the discrepancies. The natural variability, generally, was substantial and led to large uncertainty in all mean estimates — and thus chance differences in estimates between devices. This aspect would have been exacerbated with less frequently occurring taxa. The area of seabed observed by the two methods had limited overlap. The Sled passed relatively quickly through ROV patches and would have observed only a small proportion of those patch animals observed by the ROV. The Sled also passed through other benthic patches and over larger areas of inter-patch habitat, which provided the potential opportunity to observe the impact and recovery of other meta-populations of sessile animals. Hence also the different relative frequencies of fauna from the two devices. The position of the ROV was known with greater accuracy and precision, consequently the associated estimate of trawl intensity for any measured individual seabed fauna would have had correspondingly greater accuracy and precision, leading to sharper actual contrasts on a gradient of

trawl intensity. Conversely, the Sled position was known less accurately and precisely, due to the dynamics of an underway vessel and the greater distance between the vessel and the camera, which would have blurred the trawl intensity contrast and potentially biased the impact and recovery estimates. On the other hand, the density of fauna observed by the Sled was estimated quantitatively due to more precise estimates of Sled swept area. However, the density of ROV fauna (with respect to trawl intensity) could only be approximated indirectly, even though the completeness of the surveys of benthic patches was known with some certainty. Videos from prior Sled surveys were available to be re-processed to estimate the before and 1 month after status, whereas quantitative ROV surveys began with this project starting at 10 months after the trawl experiment. Hence, the before and impact status was not observed by the ROV and could only be imputed from controls (different sites) and by back-extrapolation from months 10, 23 and 61. As a result, the impact and recovery rate estimates from either device were not necessarily better than the other, but both contribute to bounding the uncertainty of these estimates and time-frame projections.

A further observation is that these large sessile megabenthic fauna that form living patches of habitat appear to be much more dynamic than originally thought, both in this study and in the FRDC Megabenthos study (Pitcher *et al.* 2004). The ROV patches were originally selected due to their high quality dense aggregations of fauna and it is possible, given stochastic dynamics, that by chance the most likely future status of prime habitat patches, such as these, was something lower in quality and density. This appeared to be a possible scenario in the case of several ROV control patches and, potentially, impact patches also.

4.3 Faunal vulnerability to trawling

In the case that seabed fauna may be exposed to industry trawling, due to overlapping distributions, their vulnerability is dependent on their removal rate (or mortality per trawl) and their subsequent rate of recovery. For example, some species with good recovery rates might be vulnerable to trawling if they are not resistant to removal. Conversely, other species with low recovery rates might be relatively invulnerable to trawling if they are very resistant to removal and damage. Such species are unlikely to be driven down to low abundance, even though they would take a long time to recover from such a state. Accordingly, assessment of vulnerability considers resistance to removal and recovery in a combined way and hence is directly related to recovery timeframes. It is also subject to the same broad uncertainties discussed above.

Vulnerability was assessed by plotting survival per trawl (= 1 – depletion rate) against recovery rate on a background of recovery times for a range of depletion and recovery rates (Figure 4-1). It is apparent that at high recovery rates, recovery times are relatively less sensitive to depletion rates than at low recovery rates, where recovery times are critically sensitive to depletion rates. Vulnerability is oriented perpendicular to the contours of recovery time — the more vulnerable species are located closer to the red zone of Figure 4-1 and the less vulnerable towards the blue zone. Note that the species appear to be somewhat strung out along the recovery time contours, particularly for the Sled, and there are significant correlations between depletion and recovery rates (Sled: r^2=0.41; ROV: r^2=0.40).

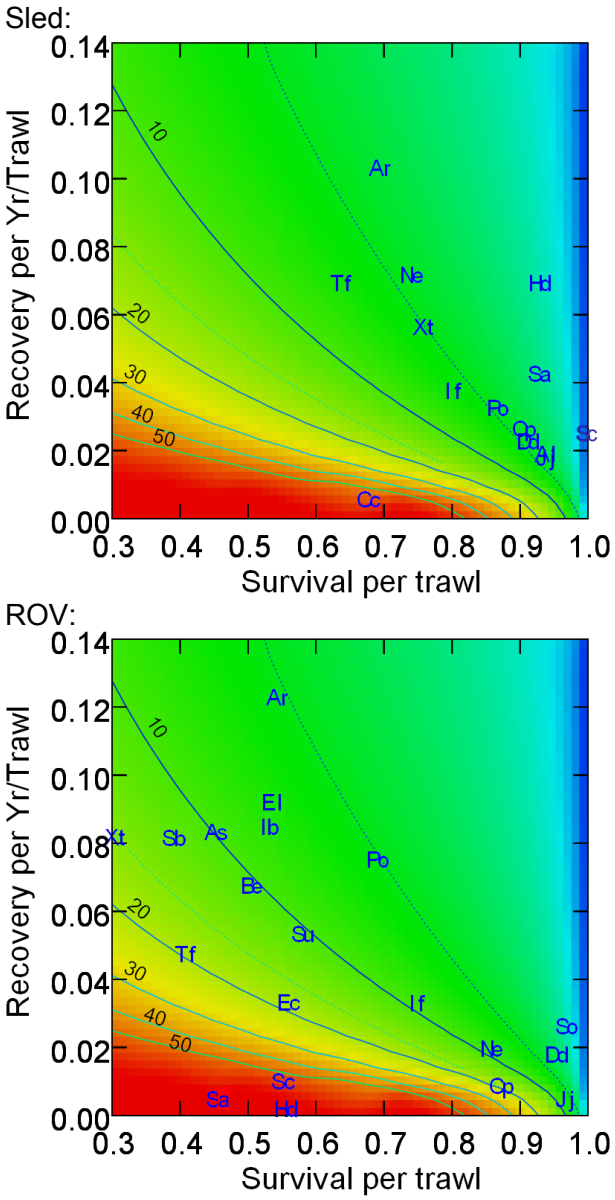

Label	Benthos Species
Al	*Alcyonacea*
Ar	*Annella reticulata*
As	*Ascideacea*
Be	*Bebryce* sp.
Cc	*Cymbastela coralliophila*
Cp	*Ctenocella pectinata*
Dd	*Dichotella divergens*
Ec	*Echinogorgia* sp.
El	*Ellisella* sp.
Hd	*Hypodistoma deeratum*
Ib	*Ianthella basta*
If	*Ianthella flabelliformis*
Jf	*Junceella.fragilis*
Jj	*Junceella juncea*
Ne	*Nephtheidae*
Po	*Porifera*
Sa	*Sarcophyton* sp.
Sb	*Semperina brunea*
Sc	*Scleractinia*
So	*Solenocaulon* sp.
Ss	*Subergorgia suberosa*
Su	*Subergorgia* sp.
Tf	*Turbinaria frondens*
Xt	*Xestospongia testudinaria*

Figure 4-1: Plots of estimated recovery rates against estimated survival rates (1-depletion) for megabenthos species as an indication of relative vulnerability. The coloured background indicates relative recovery time (dark blue = 0 years, through to red for longer time frames), and contour lines show recovery time in years.

The estimates for relative vulnerability from the Sled and ROV were in reasonable agreement for *Ianthella flabelliformis*, Porifera, *Annella reticulata* and *Dichotella divergens*. Some other species had marked differences between the Sled and ROV, including *Sarcophyton* and *Hypodistoma deeratum* (as discussed above) and Scleractinia. Different morphotypes of Scleractinian hard corals are likely to have different impact and recovery rates, eg. branching corals may be relatively easily broken but recover quickly whereas small massive corals maybe quite robust but take longer to recover and plate corals (eg. *Turbinaria frondens*) may be intermediate. If these morphotypes had different representation in the Sled and ROV observations for unidentified hard corals, such differences may contribute to this discrepancy. After considering the relative reliability of data from the Sled and ROV, the taxa were ranked in the following approximate order of vulnerability:

High vulnerability:

Cymbastela coralliophila (Sponge)
Scleractinia (Hard Corals)
Turbinaria frondens (Hard Coral)
Junceella fragilis (Gorgonian)

Moderate vulnerability:

Semperina brunea (Gorgonian)
Xestospongia testudinaria (Sponge)
Subergorgia suberosa (Gorgonian)
Subergorgia sp. (Gorgonian)
Bebryce sp. (Gorgonian)
Ianthella flabelliformis (Sponge)
Ctenocella pectinata (Gorgonian)
Echinogorgia sp. (Gorgonian)
Ellisella sp. (Gorgonian)

Low-moderate vulnerability:

Junceella juncea (Gorgonian)
Porifera (Sponges)
Annella reticulata (Gorgonian)
Dichotella divergens (Gorgonian)
Nephtheidae (Soft Corals)

Low vulnerability:

Alcyonacea (Soft Corals)
Sarcophyton sp. (Soft Corals)
Hypodistoma deeratum (Solitary ascidian)
Solenocaulon sp. (Gorgonian)

If these vulnerable seabed fauna are exposed to industry trawl effort of significant intensity, their populations are likely to be reduced in areas of overlap — and more substantially reduced for more vulnerable fauna.

4.4 Conclusions

Given the new information from this project on impact and recovery rates, recovery timeframes, and vulnerability of seabed habitat fauna, it can be expected that progress towards sustainable multiple use of the region would be facilitated by management measures that controlled spatial overlap of the distribution of trawl effort with the distribution of these vulnerable fauna, through zoning of habitats for appropriate sustainable use. Knowledge of the distribution and abundance of the types of seabed fauna identified as vulnerable here is the key to such approaches.

Recently, there was also a critical opportunity to undertake a much larger space/time scale recovery experiment, due to the 1 July 2004 re-zoning of the GBR Marine Park. The long term treatment part of the "experiment" was underway for many decades in the form of past trawling effort up until the time of the re-zoning. It was possile that carefully designed and replicated closures of a range of trawled areas, which take into account habitat strata, together with precise measurements of biotic changes within the closures over time that can be contrasted with measurements of similar areas that continue to be trawled, would deliver information on recovery at large scales that would be unique globally.

The major remaining impediment to assessing and developing management plans that would lead to a sustainable trawl fishery, was the lack of information on the distribution of seabed biota, particularly for the vulnerable megabenthos identified here, but also for other seabed fauna that may be affected by

trawling. The recently completed GBR Seabed Biodiversity Project (Pitcher *et al.* 2007) has made a major contribution to this knowledge gap. It has been only by combining this knowledge of biotic distributions with fine-scale data on the distribution and intensity of trawl effort, in dynamic impact-recovery models, that it was possible to fully assess the regional scale effects of trawling in the GBR Marine Park. Modelling approaches such as the Trawl Scenario MSE (Ellis and Pantus 2001) have adopted the recovery information provided by this project, as well as biotic distributions from the Seabed Biodiversity Project. The trawl model has assisted with assessment of the current sustainability of the trawl fishery by evaluating the series of management measures implemented between 1999 and 2005, in terms of benefits to vulnerable seabed fauna (Pitcher *et al.* 2007, section 2.4.8.). This showed that generalized depletion trends up until the late 1990s have all been arrested and reversed subsequently (Pitcher *et al.* 2007, section 3.8). The 2001 trawl effot buyback and the subsequent progressive penalties on licence transfers appeared to have made the biggest positive contributions; the 2004 rezoning of the GBR made a small positive contribution for some species. With information from this Recovery of Seabed Habitat Project and other projects, the Trawl Scenario MSE Model is now well placed to contribute to the development of any future management plans aiming to ensure future sustainability of seabed habitats and benthos, by evaluating the environmental benefits of those plans as well as their consequences for the fishery.

5 REFERENCES

Alino, P.M., Coll, J.C. (1989) Observations of the synchronized mass spawning and post-settlement activity of octocorals on the Great Barrier Reef, Australia: biological aspects. *Bull Mar Sci*, 45, 697–707.

Brazeau, DA, Lasker, HR (1989) Reproductive cycle and larval release of a Caribbean gorgonian. *Biol Bull* 176:l-7

Breslow, N.E., and D.G. Clayton. (199)3. Approximate inference in generalised linear mixed models. *Journal of the American Statistical Association* 88: 9-25.

Burridge C.Y., Pitcher C.R., Wassenberg T.J., Poiner I.R., Hill, B.J. (2003). Measurement of the rate of depletion of benthic fauna by prawn (shrimp) otter trawls: an experiment in the Great Barrier Reef, Australia. *Fisheries Research* 60: 237–253

Burridge C.Y., Pitcher C.R., Hill, B.J., Wassenberg T.J., Poiner I.R. (2006) A comparison of demersal communities in an area closed to trawling with those in adjacent areas open to trawling: a study in the Great Barrier Reef Marine Park, Australia. *Fisheries Research* 79: 64-74.

Clarke, K.R., and R.M. Warwick. (1994). *Change in marine communities: an approach to statistical analyses and interpretation.* Plymouth Marine Laboratory, Plymouth. 144 pp.

Collie J.S., Hall S.J., Kaiser M.J. & Poiner I.R. (2000). A quantitative analysis of fishing impacts on shelf-sea benthos. *Journal of Animal Ecology* 69: 785-798.

Committee on Ecosystem Effects of Fishing: (2002) Phase 1— *Effects of Bottom Trawling on Seafloor Habitats* Ocean Studies Board Division on Earth and Life Studies National Research Council National Academy Press, Washington, D.C.

Currie, D.R., and G.D. Parry. (1996). Effects of scallop dredging on a soft sediment community: a large-scale experimental study. *Mar. Ecol. Prog. Ser*. 134: 131–50

Duplisea, D. E., Jennings, S., Warr, K. J., Dinmore, T. A. (2002). A size-based model of the impacts of bottom trawling on benthic community structure. *Can J Fish Aquat Sci*, 59: 1785-1795.

Ellis, N., F. Pantus. (2001). *Management Strategy Modelling: Tools to evaluate trawl management strategies with respect to impacts on benthic biota within the Great Barrier Reef Marine Park area.* Final Report to the Great Barrier Reef Marine Park Authority, June 2001, 93 pp.

Fabricius, K., Alderslade, P. (2001) *Soft Corals and Sea Fans: A Comprehensive Guide to the Tropical Shallow-Water Genera of the Central-West Pacific, the Indian Ocean and the Red Sea*, Australian Institute of Marine Science, Townsville. Pp 264.

Freese, J.L. (2001). Trawl-induced damage to sponges observed from a research submersible. Marine Fisheries Review 63(3): 7-13.

Freese, L., P. J. Auster, J. Heifetz, and B. L. Wing. (1999). Effects of trawling on seafloor habitat and associated invertebrate taxa in the Gulf of Alaska. Mar. Ecol. Prog. Ser. 182: 119–126.

Fromont, J., Bergquist, P.R. (1994) Reproductive biology of three sponge species of the genus *Xestospongia* (Porifera: Demospongiae: Petrosiida) from the Great Barrier Reef. *Coral Reefs*, 13: 119–126.

Gibbs P.J., A.J. Collins, and L.C. Collett. (1980). Effect of otter prawn trawling on the macrobenthos of a sandy substratum in a New SouthWales estuary. Aust. J. Mar. Freshw. Res. 31: 509–16.

Harrison PL, Wallace CC (1990) Reproduction, dispersal, and recruitment of scleractinian corals. In: Dubinsky Z (ed) *Ecosystems of the world*. Elsevier, Amsterdam, p 133-207

Henry, L-A., Kenchington, E.L.R., Silvaggio, A. (2003) Effects of mechanical experimental disturbance on aspects of colony responses, reproduction, and regeneration in the cold-water octocoral Gersemia rubiformis. *Can. J. Zool.* 81: 1691–1701

Jennings S, Dinmore TA, Duplisea DE, Warr KJ, Lancaster JE. (2001). Trawling disturbance can modify benthic production processes. *J Anim Ecol* 70:459–75.

Kaiser, M.J., De Groot, S.J. (2000). *The Effects of Fishing on Non-Target Species and Habitats: Biological, Conservation and Socio-Economic Issues*. Blackwell Science, Oxford. 399 pp.

Kaiser, M.J., J.S. Collie, S.J. Hall, S. Jennings, and I.R. Poiner. (2003). Modification of marine habitats by trawling activities: prognosis and solutions. *Fish and Fisheries* 3: 114-136.

Lambert, C.C. (2005a). Historial introduction, overview, and reproductive biology of the protochordates. *Can. J. Zool*. 83(1): 1–7.

Lambert, G. (2005b). Ecology and natural history of the protochordates. *Can. J. Zool*. 83(1): 34–50.

Lambshead, P.J.D, H.M. Platt, and K.M. Shaw. (1983). The detection of differences among assemblages of marine benthic species based on an assessment of dominance and diversity. *Journal of Natural History*. 17: 859-874.

Legendre, P, and L. Legendre. (1998). *Numerical Ecology*. Second English Edition. Elsevier Science B.V., Amsterdam, 853 pp.

Maldonado, M. (2006) The ecology of the sponge larva *Can. J. Zool*. 84: 175–194

Mann K. H. (2000). *Ecology of Coastal Waters: with implications for management*. Blackwell Science, Massachusetts, USA, 432 pp.

Mann, K. H., and J. R. N. Lazier. (1991). *Dynamics of Marine Ecosystems*. Blackwell Scientific Publications, Oxford.

Pitcher, C.R., Burridge, C.Y., Wassenberg, T., Smith, G.P., O'Connor, R., Jones, P., Ellis, N. and G. Fry. (2000) *Recovery of seabed habitat from the effects of impact of prawn trawling in the far northern section of the Great Barrier Reef*: Final Report to GBRMPA on Year 1 Research. CSIRO Division of Marine Research Report, 180 pp.

Pitcher, C.R., Venables, W., Ellis, N., McLeod, I., Pantus, F., Austin, M., Cappo, M., Doherty, P. and N. Gribble. (2002) *GBR seabed biodiversity mapping project: Phase 1* Report to CRC-Reef. CSIRO/AIMS/QDPI Report, 192 pp.

Pitcher, C.R., Wassenberg, T.J., Cappo, M.C., Smith, G.P., Austin, M., Gordon, S.R., Bustamante, R.H., Moeseneder, C.H., Speare, P.J., Kennedy, J.A., Doherty, P.J., and J.N.A. Hooper (2004). *Dynamics of large sessile seabed fauna, important for structural fisheries habitat and biodiversity of marine ecosystems – and use of these habitats by key finfish species.* Final report to Fisheries Research & Development Corporation. CSIRO Marine Research. 308 pp.

Pitcher, C.R., Doherty, P., Arnold, P., Hooper, J., Gribble, N., Bartlett, C., Browne, M., Campbell, N., Cannard, T., Cappo, M., Carini, G., Chalmers, S., Cheers, S., Chetwynd, D., Colefax, A., Coles, R., Cook, S., Davie, P., De'ath, G., Devereux, D., Done, B., Donovan, T., Ehrke, B., Ellis, N., Ericson, G., Fellegara, I., Forcey, K., Furey, M., Gledhill, D., Good, N., Gordon, S., Haywood, M., Hendriks, P., Jacobsen, I., Johnson, J., Jones, M., Kinninmoth, S., Kistle, S., Last, P., Leite, A., Marks, S., McLeod, I., Oczkowicz, S., Robinson, M., Rose, C., Seabright, D., Sheils, J., Sherlock, M., Skelton, P., Smith, D., Smith, G., Speare, P., Stowar, M., Strickland, C., Van der Geest, C., Venables, W., Walsh, C., Wassenberg, T., Welna, A., Yearsley, G. (2007). *Seabed Biodiversity on the Continental Shelf of the Great Barrier Reef World Heritage Area.* AIMS/CSIRO/QM/QDPI Final Report to CRC Reef Research. 320 pp. ISBN 978-1-921232-87-9

Poiner, I.R., Glaister, J., Pitcher C.R., Burridge, C., Wassenberg, T., Gribble N., Hill B., Blaber, S.J. M., Milton, D.A., Brewer D., and N.Ellis. (1998) *The environmental effects of prawn trawling in the far northern section of the Great Barrier Reef Marine Park: 1991–1996.* Final Report to GBRMPA and FRDC. CSIRO Division of Marine Research and and Queensland Department of Primary Industries Report, 554 pp.

Sainsbury K.J. (1991) Application of an experimental approach to management of a tropical multispecies fishery with highly uncertain dynamics. ICES Marine Science Symposium 193:301-320

Sainsbury, K.J., Campbell, R. Whitelaw, A.W., (1993). Effects of trawling on the marine habitat on the north west shelf of Australia and implications for sustainable fisheries management In: Hancock DA (ed) *Sustainable fisheries through sustainable fish habitats*. Australian Society for Fish Biology Workshop. AGPS, Canberra, pp. 137-145.

Sainsbury, K.J., Campbell, R., Lindholm, R., Whitelaw, A.W., (1997). Experimental management of an Australian multispecies fishery: examining the possibility of trawl-induced habitat modification. In: Pikitch EK. Huppert DD and Sissenwine MP (eds). *Global trends: fisheries management.* American Fisheries Society, Bethesda, Maryland, pp. 107-112.

Thrush, S.F., and P.K. Dayton. (2002). Disturbance to marine benthic habitats by trawling and dredging: Implications for marine biodiversity. Annu. Rev. Ecol. Syst. 2002. 33: 449–73.

Tilmant, J. T. (1979). *Observations on the impacts of shrimp roller frame trawls operated over hard-bottom communities, Biscayne Bay, Florida*. U.S. Dep. Inter., Natl. Park Serv. Rep. Ser. P-553, 23 pp.

Van Dolah, R.F., Wendt, P.H., Nicholson, N. (1987). Effects of a research trawl on a hard-bottom assemblage of sponges and corals. Fish. Res. 5: 39–54.

Venables, W.N., and B.D. Ripley. (2002). *Modern Applied Statistics with S.* 4th edition. Springer-Verlag, New York

Walker, T.A., Bull, G.D. (1983) A newly discovered method of reproduction in gorgonian coral. *Mar. Ecol. Prog. Ser*. 12: 137-143

6 STAFF

CSIRO Marine & Atmospheric Research

C.R. Pitcher
M. Austin
R.H. Bustamante
A. Butler
T.M. Cannard
S.J. Cheers
N. Ellis
A.G. Koutsoukos
C.H. Moeseneder
G.P. Smith
T.J. Wassenberg

CSIRO Mathematical & Information Sciences

W. Venables
C.Y. Burridge
P.N. Jones

7 APPENDICES

7.1 Calibration of the Sled's video-image analysis system

7.1.1 Outline of calibration process

For each of ~17,000 benthic organisms, an image was captured from Sled video at the moment the organism base touched a baseline defined by preliminary photogrammetry. The video interpreter then selected the pixel coordinates of up to three pairs of features from that image:

1. *either* a selected pair of tick marks on the bar that were 10 cm apart and above the organism on the bar *or* the top and bottom of the ~4 cm deep bar (if tick marks could not be seen clearly, as on some of the pre-1996 video)
2. the base and the highest point of the organism (except for whips or organisms at the edge of the image, for which the height was estimated by eye only)
3. the furthest left and right parts of the organism (only if certain validity criteria were met).

For statistical analysis purposes, these pixel coordinates had to be transformed to three-dimensional real-world coordinates (measured in mm). This should have been straightforward to derive, given the precise geometry of the Sled setup and the exact distortion characteristics of the combination of camera and housing used in each survey, but information of the necessary precision was not available.

An alternative approach was developed that made use of the pixel coordinates of tick marks on the horizontal bar (the first pair above) and the knowledge that these tick marks are 100mm apart on a flat surface. A non-linear mathematical function was constructed to map from real-world coordinates to pixel coordinates (and back). It used non-linear optimisation (implemented in AD Model Builder via an interface in Splus) to estimate the values of geometry and camera parameters. The optimisation process minimised the sum of squares of the difference between actual and predicted pixel coordinates of the selected suite of tick marks deemed relevant to a particular set of organism images, after the tick marks were screened to remove statistical outliers.

The camera and housing set-ups changed a number of times over the six surveys (October 1994 to February 2001) as technology was improved. There was also some variation within surveys, attributed to minor changes in the position of the camera or to flexibility of the Sled frame. The full suite of ~17,000 organism images from the six surveys was therefore partitioned into 127 groups with a view to achieving within-group homogeneity in the mapping of the three-dimensional real world to the two-dimensional pixel coordinate system. For some parameters (e.g. optical radial distortion), the values were assumed constant for an entire survey. For other parameters (e.g. camera angles), the values were assumed constant for a group of consecutive transects.

7.1.2 Geometry of the Sled and camera set-up

The Sled consisted of two parallel D-shaped sides joined by horizontal bars (Figure 7-1). The horizontal bar joining the outermost part of the curve of the D at the front of the Sled had vertical tick marks equally spaced at 100 mm intervals. The bar was 500 mm above the seabed. A camera was mounted from the top of the Sled about half-way back. The camera was angled downwards (at angle

θ) so that the ground immediately below the bar (the baseline) and the bar itself were visible in the video monitor (Figure 7-3). The set-up was designed so that the camera lay square on to the bar, but the calibration allows for an error ϕ in this angle (Figure 7-2). The camera could also be twisted in its housing so that horizontals in the real world did not appear horizontal on the screen; this was accounted for by a twist angle ψ.

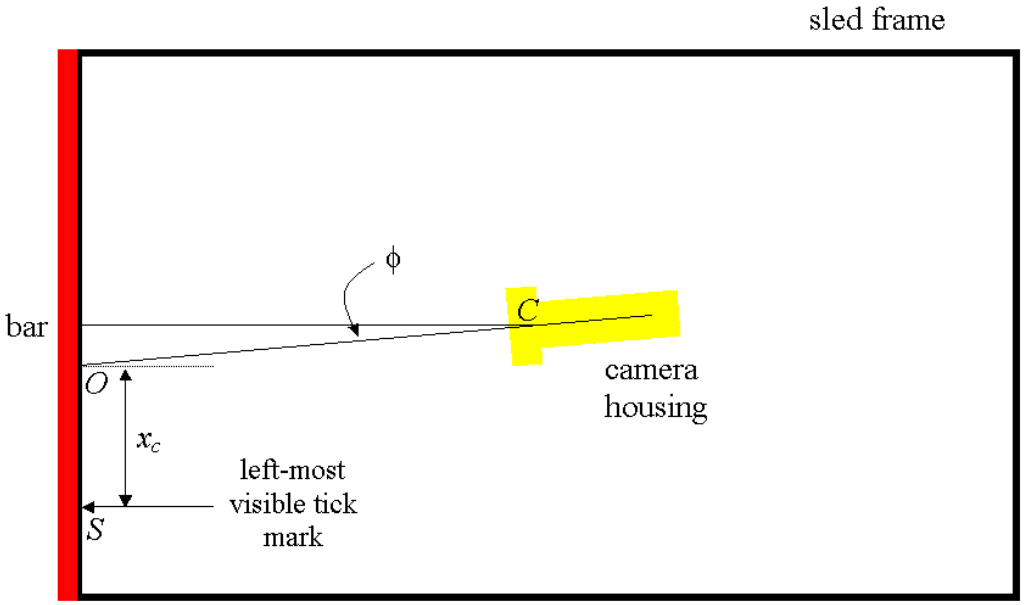

Figure 7-1: Sled: view from above. The axis of symmetry of the camera had an azimuth angle ϕ relative to the perpendicular to the bar. This was the angle between the vertical plane through the axis of symmetry of the camera and the vertical plane perpendicular to the bar through the nodal point of the camera *C*. By design ϕ should be zero, but the calibration allows for design error.

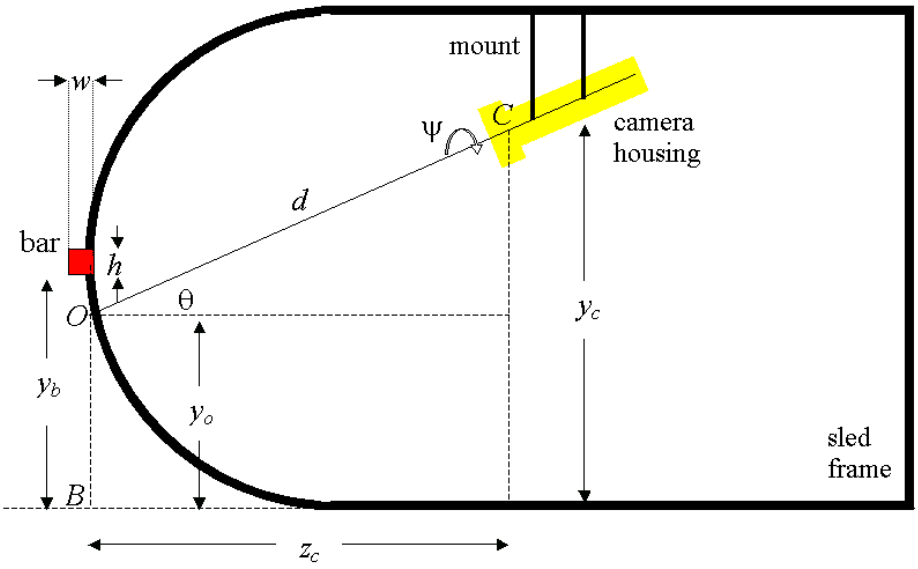

Figure 7-2: Sled: view from left-hand side. The pitch angle θ was the angle, measured in the vertical plane through the axis of symmetry of the camera, between that axis and the horizontal. The point *C* was the nodal point of the camera. The mount points are free to move forward or back along the Sled frame and the pitch angle

can be changed by adjusting the camera housing on the mount. The calibration allowed for a twist angle ψ of the camera about the axis of symmetry.

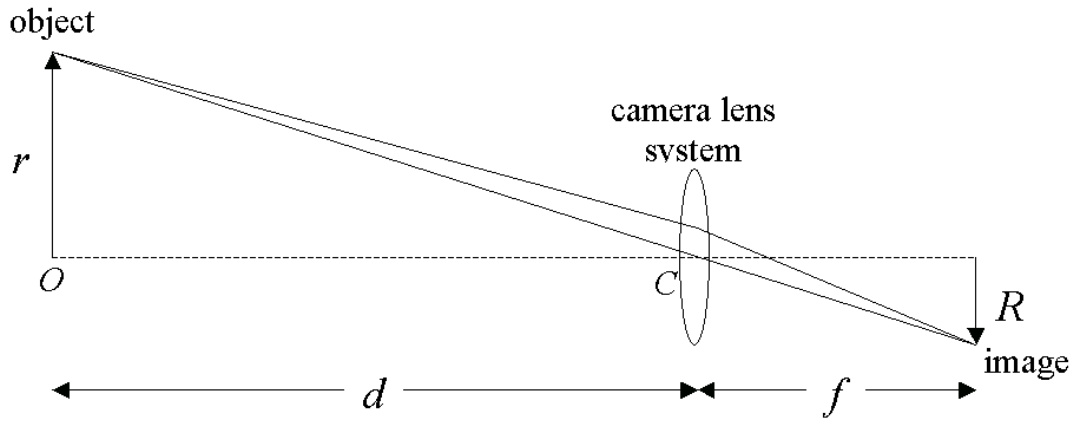

Figure 7-3: The camera lens system and mapping from object to image coordinates. The camera had a fixed focal length. The assumption was made that objects are sufficiently distant so that they are imaged at the focal length *f*. The nodal point *C* was the point through which objects appear to be projected onto the image plane. This was on the axis of symmetry inside the camera lens system; its exact location could be determined by camera calibration.

The camera had a fixed focal length and it was the assumed that all objects in the vicinity of the bar were in focus and imaged on the focal plane (Figure 7-4). It was also assumed that the lens system is radially symmetric, but there was an allowance for some radial distortion. For objects of height *r* near the axis of symmetry the image height *R* satisfies $R = rf/d$. For objects further away from the axis there was radial-lens distortion which was accounted for by a quintic correction:

$$R = \alpha r + \beta r^3 + \gamma r^5$$

where $\alpha = f/d$. The pixel (u_c, v_c) at the axis of symmetry (**Figure 7-5**) is an unknown and so, too, is the actual location of the camera.

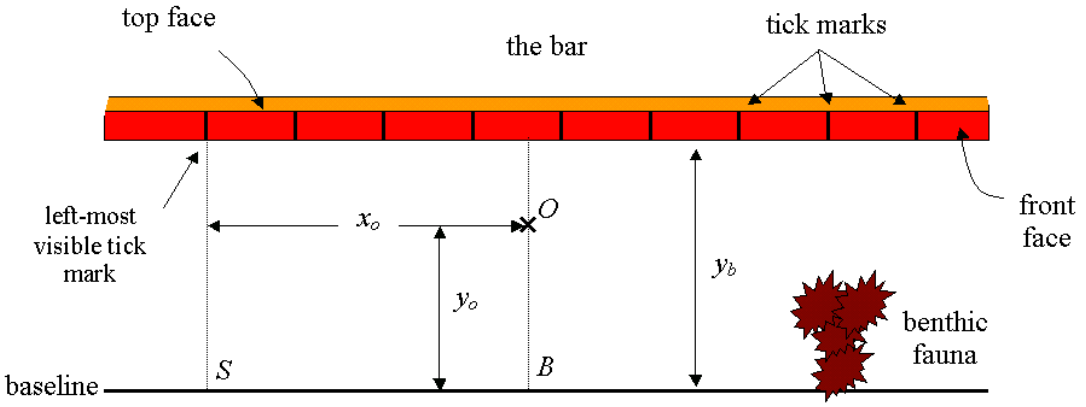

Figure 7-4: View from camera. The bar plane is the vertical plane through the front face, which is assumed to be vertical. The intersection of this plane with the ground is the baseline. The origin of coordinates *S* is at the baseline directly below the left-most visible tick mark. The tick-mark interval is 100 mm. The point *O* is the intersection of the bar plane with the axis of symmetry of the camera. It has location (x_o, y_o) in bar coordinates. The top face of the bar is visible from the camera, but it does not have any tick marks. During interpretation, the operator captures the video image when the benthic fauna straddles the baseline.

In all, the geometry can be described by 11 parameters:

- α, β and γ describe the properties of the lens system
- u_c, v_c describe the coordinates of the screen relative to the camera axis
- θ, ϕ and ψ describe the orientation of the camera relative to the bar
- x_o, y_o and d describe the position of the camera relative to the bar.

7.1.2.1 Conversion from real-world coordinates to screen coordinates

In order to perform the calibration, it was necessary to transform positions in space to positions on the screen. And in order to convert pixel measurements to physical dimensions, it was necessary to transform positions on the screen back into positions in space. We therefore needed to set up coordinates in space and on the screen.

The most convenient coordinate system in space has its origin in the bar plane on the baseline at point *S*: the *x* coordinate is distance to the right of the leftmost visible tick mark; the *y* coordinate is distance above the ground; and the *z* coordinate is the distance in front of the bar (see Figure 7-3). The pixel coordinate system has its origin at the bottom left of the screen at point O_s (Figure 7-4).

To pass easily between the two coordinate systems, an intermediate coordinate system based on the object plane was defined. This was the plane that was perpendicular to the axis of symmetry of the camera and such that the plane, the axis of symmetry and the bar plane intersect at a point *O* (see Figure 7-6). This was the origin of the coordinate system with coordinates (x', y', z'). From *O* the x' direction is horizontal within the object plane, the y' direction is perpendicular to the x' direction within the object plane, and the z' direction points straight at the camera.

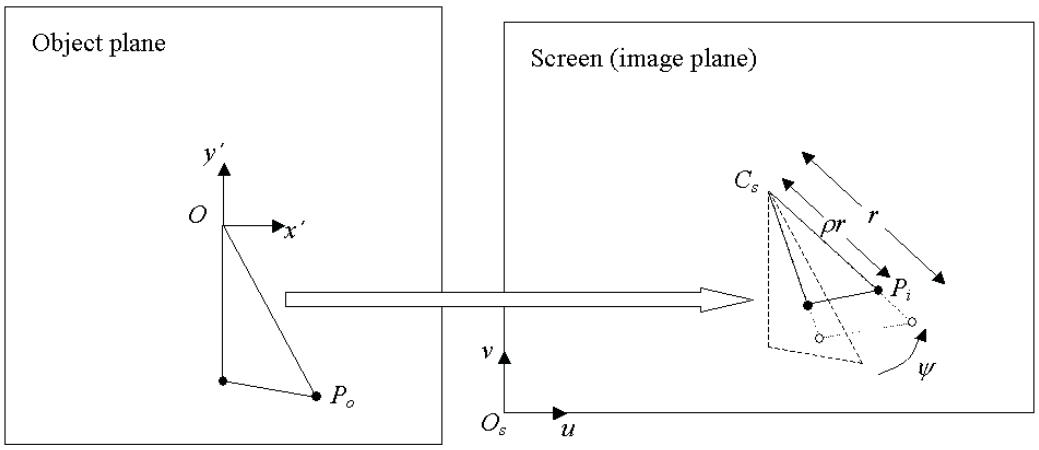

Figure 7-5: The mapping of the object plane to the screen. The origin *O* was imaged at pixel position C_s on the screen, which is likely to be close to the centre of the screen. The origin of pixel coordinates (u, v) is O_s at the bottom left corner. The coordinates of C_s are (u_c, v_c). The calibration allowed for the camera to be twisted clockwise by an angle ψ relative to the axes of the object plane. Therefore on the screen objects appeared rotated anti-clockwise by ψ. There was a change in scale of magnitude ρ going from object plane units to screen units, which depended mainly on the focal length *f*. Objects that are distance *r* from the origin in the object plane map to images that are distance ρr from C_s on the screen. Radial-lens distortion was taken into account, since ρ depends on *r*.

7.1.2.2 Estimating the parameters

The parameters were estimated by non-linear optimisation. The quantity to be optimised was the weighted sum of square deviations between the observed and predicted pixel locations of the 100 mm tick marks on the bar. Depending on the camera set-up (i.e. survey), between 7 and 18 ticks were visible on the screen at any one time. The tick marks were counted from the left, with tick number 1 being the leftmost visible tick mark and (in the case of survey EOT0101) tick number 18 being the rightmost (e.g. see Figure 7-4).

Formally, the objective function that minimised was

$$F(u,v,x,y;\mathbf{p}) = \sum_{i=1}^{n}\left[w_i^u \left(u_i - \hat{u}\left(x_{j_i}, y_{j_i}, 0, \mathbf{p}_{k_i}\right)\right)^2 + w_i^v \left(v_i - \hat{v}\left(x_{j_i}, y_{j_i}, 0, \mathbf{p}_{k_i}\right)\right)^2 \right]$$

where n is the number of measurements; (u_i, v_i) is the observed tick-mark pixel location; j_i is the tick-mark number; k_i is the calibration group number and $\left(w_i^u, w_i^v\right)$ are weights between 0 and 1 for the i-th measurement; $(x_j, y_j, 0)$ is the known position in bar plane coordinates of the the j-th tick mark; $\mathbf{p}_k = (\alpha^k, \beta^k, \gamma^k, \theta^k, \phi^k, \psi^k, x_o^k, y_o^k, u_c^k, v_c^k, d^k)$, is the vector of unknown parameters for the k-th calibration group; and $(\hat{u}(x, y, z, \mathbf{p}), \hat{v}(x, y, z, \mathbf{p}))$ the predicted pixel location of the point (x, y, z) in bar plane coordinates, given parameter vector $\mathbf{p}$. In principle, F could be minimised over all surveys simultaneously. However, since there were no parameters in common across surveys, it proved more convenient to split F up by survey, and estimate the parameters for each survey separately.

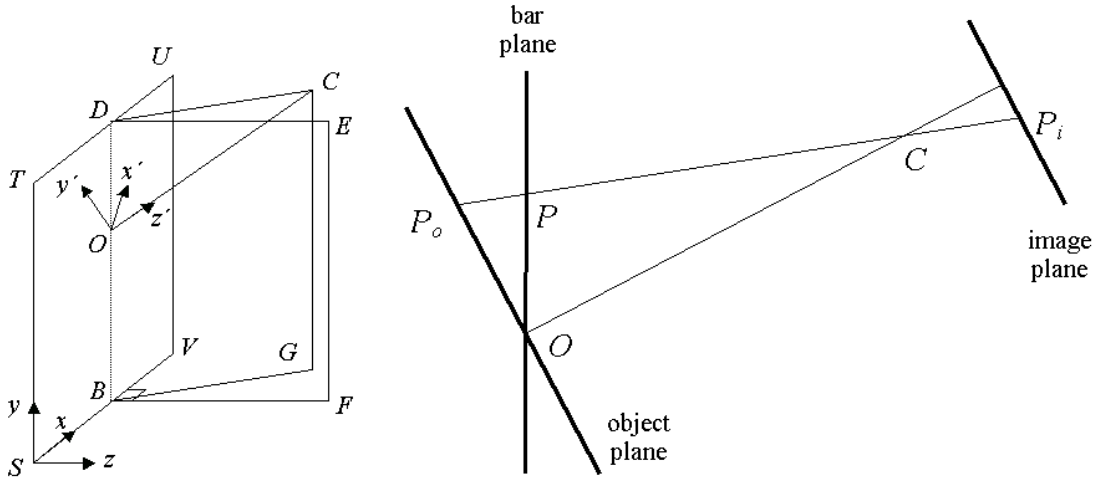

Figure 7-6: Geometry of the Sled camera set-up. *SBV* is the baseline and *STUV* is the bar plane. *OC* is the axis of symmetry of the camera and *BDCG* is the vertical plane through this axis. *BDEF* is the vertical plane through *O* perpendicular to the bar plane, $\angle CDE$ is the azimuth angle ϕ and $\angle OCD$ is the pitch angle θ. The object plane is the plane through *O* perpendicular to *OC*. A point *P* in the bar plane is projected onto P_o in the object plane, which has image P_i in the image plane. Two coordinate systems are defined: (x, y, z) with origin at *S* and (x', y', z') with origin at *O*. Both x and x' are horizontal. Directions x and y lie in the bar plane; directions x' and y' lie in the object plane.

7.1.2.3 Initial calibration to obtain camera pitch angle

In preliminary trials, the proposed method of calibration based on bar tick marks proved inadequate for estimating the pitch angle of the camera. To do this reliably required data providing a contrast between vertical pixel distances and horizontal pixel distances. Since the bar is mainly horizontal in extent, it was not possible to estimate pitch from the bar data alone.

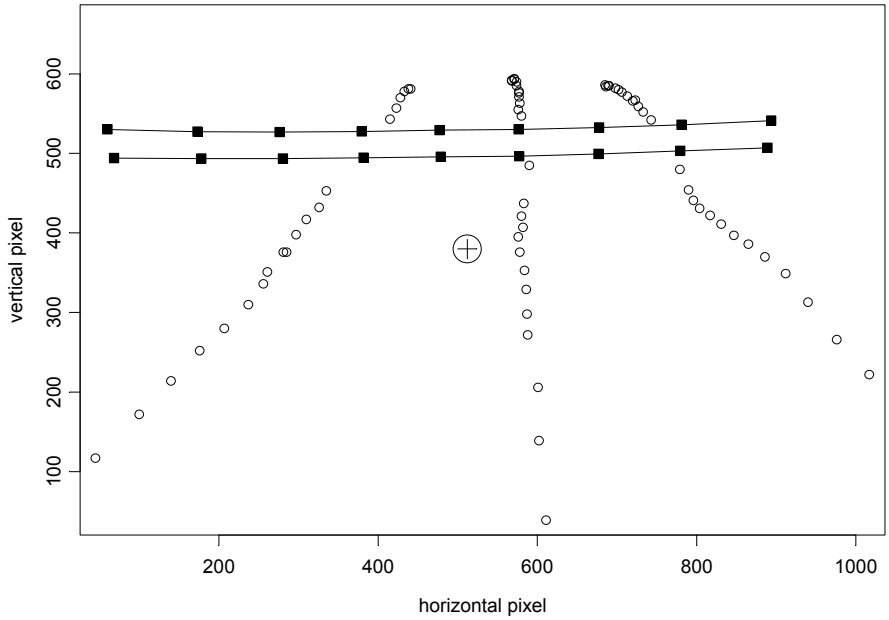

Figure 7-7: Obtaining vertical-contrast data from multiple images. The open circles denote picks of the bases of three objects tracked from when they first become visible at the top of the screen to when they disappear off the bottom or side. The filled squares are picks of the top and bottom of the bar. The lines represent the opaque bar behind which the objects become obscured. The large cross-hairs denote the camera axis.

Contrast in the vertical direction was obtained by building up vertical tracks from multiple images. This is most easily seen from Figure 7-7. The positions of selected objects trace lines that fan out as the objects approach the Sled. The rate at which the lines fan out and the apparent location of the horizon are strongly dependent on the pitch angle. For instance, as the pitch becomes steeper, the lines become more parallel. Therefore these lines were used, which we dubbed ‘snail trails’, as auxiliary information to estimate the pitch.

This was implemented as a two-stage iterative procedure:

1. given pitch, estimate the other calibration parameters from the bar pixel data, and
2. given the other calibration parameters, estimate pitch from the snail-trail data.

The steps were repeated until convergence.

The estimation of pitch requires some explanation. Given pitch and the other calibration parameters, the snail-trail pixels can be projected onto their estimated positions on the seabed, relative to the bar coordinates. The actual locations of the objects were not known, but it is known that they must move in parallel relative to the Sled. Therefore the unknown locations were estimated by fitting a linear B-spline model in video-frame time with an intercept term that depends on object. That is, for object i at time t, the world coordinates relative to the bar (x_{it}, y_{it}, z_{it}) are modelled by:

$$x_{it} = x_{0i} + BS(t)\cdot\mathbf{b}_x + \varepsilon_{it}; \quad y_{it} = 0; \quad z_{it} = z_{0i} + BS(t)\cdot\mathbf{b}_z + \eta_{it};$$

where x_{0i} and z_{0i} are the intercept terms, $BS(t)$ is a B-spline basis matrix on 7 degrees of freedom, $\mathbf{b}_x$ and $\mathbf{b}_z$ are the spline coefficients, and ε_{it} and η_{it} are independent normal variates. Height above the ground y_{it}, naturally, is zero.

Clearly, this model is an idealisation: it describes the situation where the ground is perfectly flat and the Sled remains pointing in a fixed direction while being pulled along a curving path. Real video data was somewhat noisier: the Sled tends to pitch, yaw and roll in response to ground that is often bumpy. Therefore segments of video where the ground appeared smooth and the Sled remained steady were searched for. In each segment, the bases of up to 6 clearly distinguishable objects (not necessarily biota) that were spread across the full width of the screen as they reached the bottom and were simultaneously visible for most of the segment were selected. By ensuring such overlap, the degree of replication to estimate the spline curve describing the Sled's path was improved. Typically, segments were 2 to 3 seconds long, which is the time from when the objects first became distinct to when an object moved out of the field of view.

The tops and bottoms of all visible bar ticks on the same video segment were also selected. It was not necessary to replicate these measurements, as the bar remained fixed in the screen over such a short segment.

For a given value of pitch, θ, the estimation was made by minimising the weighted sum of square distances between the spline model positions and the projected positions from the pixel data. Objects further away were downweighted because their projected position would have larger error. Then $R^2(\theta)$ was calculated, which is the ratio of residual sum of square distances *RSS* to sum of square distances about the mean projected position. Finally the estimate of θ chosen was the value that minimised $R^2(\theta)$. The reason for minimising R^2 and not simply *RSS* was that the scale of the projected positions depended on θ; the goal was to fit the projected points independently of this scale.

The snail-trail procedure was fairly labour-intensive. The data collection and analysis was restricted to a single representative plot from each of 13 calibration groups. Each group was chosen to span, within a survey, contiguous plots with broadly similar patterns of tick marks. For instance, in survey EOT0195, the bar ticks for plots 17 and 18 were distinctly higher than for the other plots, so this survey was split into two groups.

The results of the snail-trail calibration are shown in Table 7-1. These results were much more plausible than those of an earlier approach based on tick data alone, which gave angles that were too low. We also thought that the angles marked with an asterisk were too high, so these were discarded for alternative estimates. Finally, the estimated pitch angles were used as fixed parameters in the full calibration based on all the tick-mark data. All other parameters were re-estimated in the full calibration.

7.1.3 Survey-specific calibration

Each survey was calibrated separately, and each brought its own peculiarities. The procedure is summarised in Table 7-2, which shows how the parameters were grouped, and in Table 7-3, which shows the fixed and estimated values (or group averages thereof). Each calibration generally proceeded in a staged manner, with subsequent models a refinement of a model in the previous stage. Summary properties of each calibration are shown in Table 7-4.

Table 7-1: Estimated pitch for 13 representative plots from the snail-trail analysis. Also shown is the estimated α value, which is fairly constant within survey. The rows are ordered chronologically. The angles marked with an asterisk are unfeasibly high.

SurveyID	Plot	camera pitch °	mm to pixel scale
EOT0294	PL11TR02	28.3	0.90
EOT0195	PL18TR03	21.0	0.91
EOT0195	PL22TR03	23.4	0.92
EOT0196	PL01TR01	21.6	1.53
EOT0196	PL20TR02	21.1	1.53
EOT0296	PL01TR01	*32.8	0.67
EOT0296	PL04TR01	26.2	0.67
EOT0197	PL01TR02	25.5	0.67
EOT0197	PL04TR02	25.5	0.66
EOT0197	PL18TR02	*32.1	0.67
EOT0197	PL22TR01	26.3	0.66
EOT0101	PL15TR01	19.6	0.61
EOT0101	PL21TR01	19.9	0.61

Table 7-2: Model specifications for different stages of calibration. Each row represents a particular model and the cell contents indicate the unit for which separate parameters are specified. The units are survey (c), 'group' (g), plot (p), transect (t), 'smear' group (s) and minicluster (m). The symbols * and / denote crossing and nesting, respectively. Fixed parameters are indicated in bold, estimated parameters in *italic*. Notes: [a] second calibration group only; [b] horizontal bar-tick measurements only; [c] vertical bar-tick measurements only; [d] first half of data only; [e] second half of data only.

Survey	Stage	Parameter										
		d	α	β	γ	θ	ϕ	ψ	x_0	y_c or y_0	u_c	v_c
EOT0294	1	**c**	*c*	**c**	**c**	**c**	*c*	*p*	*p*	*p*	**c**	**c**
EOT0195	1	**c**	*c*	*c*	**c**	**g**	*g*	*p*	*g*	*p*	**c**	**c**
	2	*p*	**c**	**c**	**c**	**g**	*p*	*p*	*g*	*p*	**c**	**c**
EOT0196	1[a]	**c**	*c*	*c*	**c**	**c**	*c*	*c*	*c*	*c*	**c**	**c**
	2[b]	*g*	**c**	**c**	**c**	**c**	*c*	*g*	*c*	*g*	**c**	**c**
	3[b]	*g*	**c**	**c**	**c**	**c**	*c*	*g*	*m/g*	*p*	**c**	**c**
	4[c]	*p*	**c**	**c**	**c**	**c**	**c**	*p*	**c**	*p*	**c**	**c**
EOT0296	1	**c**	*c*	*c*	**c**	**c**	*c*	*c*	*c*	*c*	**c**	**c**
	2	*c*	**c**	**c**	**c**	**c**	*c*	*g*	*g*	*g*	**c**	**c**
	3	*g*	**c**	**c**	**c**	**c**	*c*	*p*	*m/g*	*g*	**c**	**c**
EOT0197	1	**c**	*c*	*c*	*c*	**c**	*c*	*t/p*	*m*	*c*	**c**	**c**
	2	*g*	**c**	**c**	**c**	**c**	*c*	*t/p*	*m*g*	*g*	**c**	**c**
EOT0101	1[d]	**c**	*c*	*c*	**c**	**c**	*g*	*s*	*s*g*	*s*g*	**c**	**c**
	2[e]	**c**	*c*	*c*	**c**	**c**	*g*	*s*	*s*g*	*s*g*	**c**	**c**

Table 7-3: Summary of estimation procedure for all surveys. Fixed parameters are indicated in bold, estimated parameters in *italic*. Most surveys were estimated incrementally in stages. The values are the averages within the

calibration groups as given by Table 7-2. For parameter y_0 the alternate parameterization y_c is used, except for survey EOT0101.

Survey	Stage	Parameter										
		d (mm)	α	$\beta \times 10^6$	$\gamma \times 10^{12}$	θ (º)	ϕ (º)	ψ (º)	x_0 (mm)	y_c (y_0*) (mm)	u_c (pixel)	v_c (pixel)
EOT0294	1	**830**	*0.90*	*0.26*	**0.00**	**28.3**	*1.0*	*–0.3*	*430*	*759*	**512**	**380**
EOT0195	1	**830**	*0.91*	*0.25*	**0.00**	**22.2**	*2.0*	*0.1*	*478*	*662*	**512**	**380**
	2	*830*	**0.91**	**0.25**	**0.00**	**22.2**	*1.0*	*0.0*	*477*	*662*	**512**	**380**
EOT0196	1	**830**	*1.53*	*0.21*	**0.00**	**21.1**	*–0.5*	*0.3*	*302*	*791*	**512**	**380**
	2	*830*	**1.53**	**0.21**	**0.00**	**21.1**	*–0.5*	*0.3*	*300*	*785*	**512**	**380**
	3	*829*	**1.53**	**0.21**	**0.00**	**21.1**	*–0.5*	*0.4*	*300*	*792*	**512**	**380**
	4	*850*	**1.53**	**0.21**	**0.00**	**21.1**	**–0.5**	*1.5*	**302**	*808*	**512**	**380**
EOT0296	1	**830**	*0.67*	*0.16*	**0.00**	**26.2**	*–1.7*	*–0.4*	*600*	*804*	**512**	**380**
	2	*757*	**0.67**	**–0.02**	**0.34**	**26.2**	*–1.5*	*–0.1*	*601*	*881*	**512**	*450*
	3	*757*	**0.67**	**–0.02**	**0.34**	**26.2**	*–1.5*	*–0.1*	*601*	*881*	**512**	*450*
EOT0197	1	**830**	*0.67*	*–0.02*	*0.34*	**25.9**	*–2.4*	*–2.4*	*598*	*807*	**512**	**380**
	2	*829*	**0.67**	**–0.02**	**0.34**	**25.9**	*–2.5*	*–2.4*	*598*	*806*	**512**	**380**
EOT0101	1	**830**	*0.61*	*–0.06*	**0.00**	**19.7**	*0.0*	*1.8*	*890*	*476**	**512**	**380**
	2	**830**	*0.61*	*–0.07*	**0.00**	**19.7**	*1.1*	*2.9*	*881*	*469**	**512**	**380**

Table 7-4: Summary properties of the calibration by survey. For survey EOT0101, 48 groups were used in the calibration, but only 16 (corresponding to the 'rest' position of the bar) were applied to animal data.

Year	Survey	Visible tick-marks (*n*)	RMS pixel error	Data points (*n*)	No. of calibration groups
1994	EOT0294	10	2.8	1397	5
1995	EOT0195	10	4.0	1111	7
1996	EOT0196	7	4.7	3885	19
1996	EOT0296	13	4.2	6592	21
1997	EOT0197	13	3.1	9266	27
2001	EOT0101	18	4.5	14616	(16) 48
			Total	36977	(95) 127

7.1.4 Applying the calibration to animal data

We applied the calibration to all animals with normal upright attached position (i.e. not edge on, lying flat, uprooted, floating or upside-down) for which measurement was feasible (generally non-whips). For these animals the operator digitised:

- *base*, the point in contact with the ground
- *top*, the highest part
- *left*, the leftmost part
- *right*, the rightmost part.

The purpose of applying the calibration was to assign coordinates for these four points in 3D space.

With a single video image, it is not possible to uniquely position the top, left and right points in space. This is because all points on a ray entering the camera map to a single pixel. In general one would require stereoscopic video to achieve unique positioning in space. However, the *base* is uniquely determined from a single video, because it lies at the intersection of the ray with the ground. By assuming that the ground is flat in the neighbourhood of the Sled, we can find the intersection of the ray with the plane $Y = 0$.

To position the top, left and right points in space, we needed to make further assumptions. One possibility was to assume that all the points lie in a plane Z = constant, i.e. a vertical plane through the base parallel to the bar (see Figure 7-8). However, there is no reason to suppose the animals would be so aligned, and, for animals measured at the edge of the screen, this would impose an artificial elongation parallel to the bar (the line l_1r_1 in Figure 7-8). More natural would be to use a plane perpendicular to the direction of the ray, which takes into account the aspect of the animal relative to the camera rather than to the bar. We adopted an idea similar to this: we chose the position to be the point on the ray that minimised the (horizontal) distance to the vertical line through the base. For fauna symmetric about a vertical axis, this approach gives the correct positioning in space. We used this criterion for both left and right points and for the top point.

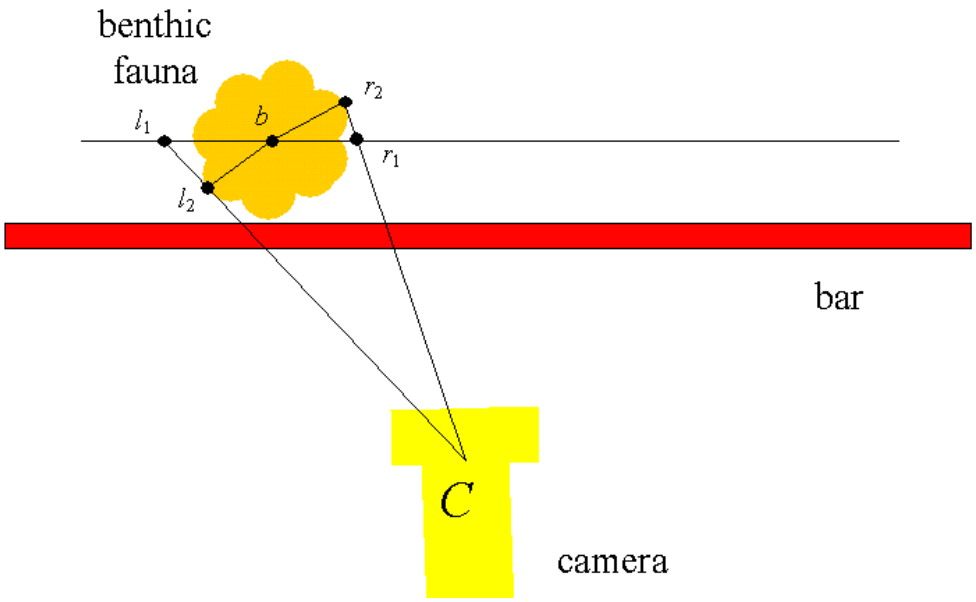

Figure 7-8: Resolving the non-uniqueness of positioning in space. The extreme left and right points are at l_2 and r_2. Projecting them onto a vertical plane through the base b would send them to l_1 and r_1, making the animal appear elongated.

For each animal, we had to determine which calibration to apply, since there were 127 sets of parameters in all (see last column of Table 7-4). For surveys EOT0294, EOT0195 and EOT0101, the parameters were determined by the plot or transect. But for the middle surveys, in which the tick marks showed sub-transect structure, the animal had to be assigned to the correct minicluter. This was straightforward for animals whose tick-marks had already been used in the calibration. Animals whose tick-marks had not been assigned to miniclusters, perhaps because they were outliers, were assigned the commonest minicluster for that transect.

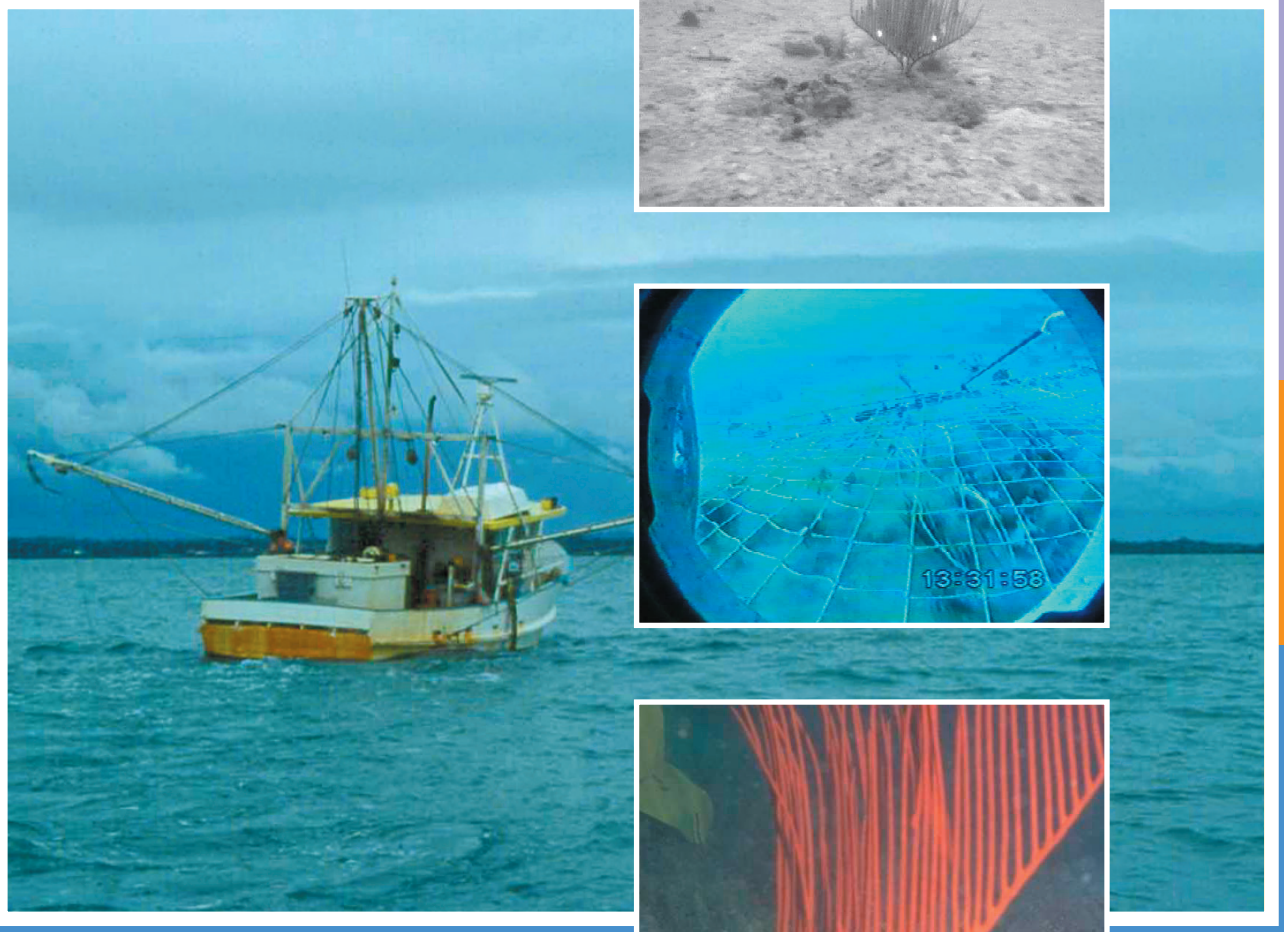

CSIRO Marine and Atmospheric Research
CSIRO Mathematical and Information Sciences
Marine Laboratories, P.O. Box 120,
Cleveland, QLD, Australia, 4163